Chemical modification and signalling of redox-sensitive transcription factors in the adaptive response to drug-induced liver injury

Thesis submitted in accordance with the requirements of the University of Liverpool for the degree of Doctor of Philosophy

Alvin Jia Liang Chia

February 2011

DECLARATION

This thesis is the result of my own work. The material contained within this thesis has not been presented, nor is currently being presented, either wholly or in part for any other degree or qualification.

Alvin Jia Liang Chia

This research was carried out in the Division of Molecular and Clinical Pharmacology, in the Institute of Translational Medicine, at The University of Liverpool.

CONTENTS

ABSTRACT

Drug induced liver injury (DILI) is one of the main causes of patient morbidity and mortality, and is an important factor in drug attrition during development. DILI is commonly associated with exposure to therapeutic agents or the formation of reactive metabolites from hepatic metabolism. These may cause redox perturbation within the cells which can result in oxidative stress as well as protein modification. These events can lead to the activation or inhibition of cellular defence responses. Although there are defence mechanisms present to counter this, if the chemical challenge is overwhelming and the defence is breached, a switch from cell defence to cell death is favoured. Two families of transcription factors, in particular, are the focus of much interest in determining the role of transcriptional adaptation to stress, namely Nrf2 and NF-kappa B (NF-κB). Nrf2 regulates the majority of cytoprotective genes and is regulated by its inhibitory protein Keap1. NF-κB is the master regulator of cell immunity, inflammation, proliferation and survival. The main aim of the investigations described within this thesis are to investigate 1) the co-regulation of the Keap1/Nrf2 and NF-κB pathways during cellular stress, 2) the molecular mechanisms underlying Nrf2 activation, and also 3) the basal status of cysteine residues present in Keap1 and how they serve as 'sensors' to cellular stress.

The first investigation in this thesis was to investigate Nrf2 and NF-κB, whose simultaneous regulatory functions during cellular stress remains unclear. Both transcription factors were known to be sensitive to electrophilic stress and redox perturbation in mouse liver cells. Molecular probes such as; N-acetyl-p-benzoquinineimine (NAPQI), the reactive metabolite of paracetamol (APAP); dinitrochlorobenzene (DNCB), a model electrophile; and buthionine (S,R)-sulfoximine (BSO), an inhibitor of glutamate cysteine ligase were used to induce cellular stress. NAPQI, DNCB and BSO can all cause glutathione (GSH) depletion; however only NAPQI and DNCB can covalently bind proteins. All three chemicals induced Nrf2 nuclear accumulation, but NF-κB binding activity was only increased after BSO treatment. In fact, NF-κB binding activity decreased after exposure to NAPQI and DNCB. The employment of RNAi to manipulate Keap1 (the inhibitor of Nrf2), Nrf2 itself and NF-κB-p65, was used to understand their roles in the response to drug stress. The RNAi depletion of Keap1 led to reduced toxicity following exposure to DNCB and also the depletion of Nrf2 and NF-κB augmented toxicity. Interestingly, increased Nrf2 caused by Keap1 depletion was reversed by co-depletion of NF-κB. We have demonstrated that Keap1/Nrf2 and NF-

kB respond differently to electrophiles which bind proteins covalently and also the redox perturbation associated with glutathione depletion. This suggests that cross-talk may enable NF-κB to partly influence Nrf2 expression during cellular stress.

One of the current hypotheses to explain Nrf2 activation centres on the key modification of Keap1 cysteine residues by chemical or oxidative stress. It has been suggested that Nrf2 activation can occur as a result of chemical modification of cysteine residues within Keap1, but also as a consequence of oxidative stress without concomitant chemical modification. In order to further elucidate the specific pre-requisites for Nrf2 activation, five molecules known to induce Nrf2 activation via cysteine modification and/or by GSH depletion were deployed. These five Nrf2-inducing molecules were chosen based on the following properties; (1) direct cysteine alkylation and GSH depletion – DNCB and Iodoacetamide (IA); (2) direct cysteine alkylation but no GSH depletion – dexamethosone-21-mesylate (Dex-mes) and 15-deoxy-Δ-(12,14)-prostaglandin J2 (15d-PGJ_2); or (3) GSH depletion but no direct cysteine alkylation - BSO. A control molecule trimellitic anhydride (TMA) which does not modify cysteine or deplete GSH was also used. This study has demonstrated that Nrf2 can be activated (1) by DNCB and IA, (2) by Dex-mes and 15d-PGJ_2, and (3) by BSO. TMA did not activate Nrf2. Therefore, these results have demonstrated that Nrf2 can be activated by either direct modification of Keap1, through a profound depletion of GSH alone or through a combination of both. Moreover, a toxicologically-relevant molecule such as TMA, that displays neither of these properties, is unlikely to induce Nrf2-dependent cell defence.

Following this, further investigations were planned to elucidate the Keap1 cysteine basal status and also further explore the molecular mechanisms underlying how Keap1 cysteine residues sense chemical or oxidative stress. An ectopic Keap1-expressing cell-based system and liquid chromatography electrospray ionisation tandem mass spectrometry (LC-ESI MS/MS) was used to analysis Keap1 cysteine modifications. A high concentration of N-ethylmalemide (NEM) (50mM) over 2min was used to alkylate Keap1-V5 cysteine residues in HEK293T cells. The aim of this was to achieve the maximum coverage of Keap1-V5 cysteines intracellularly within a short time frame without causing cellular damage. Interestingly, a proportion of the Keap1-V5 overexpressed protein displays all of its cysteine residues modified by NEM. This suggests that all Keap1 cysteine residues are available for modification by reactive chemicals, and can be found in a basally reduced state. Next, investigations were designed to determine if Keap1-V5 cysteine residues can undergo S-glutathionylation.

Immunoprecipitated Keap1-V5 from HEK293T cells was resolved on non-reducing and reducing gels following treatment with or without BSO and the subsequent addition of DMSO, IA and NEM. Gels were probed with anti-Keap1 and anti-GSH antibodies. Under non-reducing conditions, S-glutathionylation on Keap1-V5 proteins was detected in the control, BSO, IA and NEM treated samples but under reducing conditions S-glutathionylation, a form of reversible oxidation, on Keap1-V5 was removed. This suggested that S-glutathionylation on Keap1-V5 can occur constitutively under basal conditions or as a form of oxidative modification under cellular stress. Therefore, a proportion of Keap1 cysteines are found to be reduced basally and S-glutathionylation can occur under basal or stressed conditions. This further suggests that every Keap1 cysteine residue can serve as a 'sensor' to detect electrophiles or reactive oxygen species during cellular stress which will ultimately lead to Nrf2 activation.

In order to further improve the investigation into the role played by Keap1 cysteine modification in Nrf2 activation, the use of click-chemistry (CC) as a novel technique was tested. The common alkylating agents, IA and NEM, are incorporated with an alkyne group to form click compounds. These click compounds were tested in comparison with their parent compounds for their ability to induce Nrf2. Based on this study, NEM-Click and NEM were observed to have similar Nrf2-activating properties. However, when compared to IA and IA-click, NEM-click is more efficient in activating Nrf2 and causes less toxicity in cells. Hence, NEM-click and CC can be used as a novel approach for the analysis of the role of Keap1 cysteine modification in Nrf2 activation.

To summarise, the results presented in this thesis have demonstrated that chemical and oxidative stresses have a differential effect on the Keap1/Nrf2 and NF-κB pathway. Moreover, we have described the existence of a crosstalk mechanism between both pathways. Furthermore, Nrf2 inducing molecules have been observed to be able to activate Nrf2 by direct modification of Keap1 cysteine residues, depletion of cellular GSH without concomitant binding of Keap1 cysteines or both. The results of this investigation have also shown that all the cysteines on a proportion of Keap1 are reduced basally, and they are available for modification by chemical molecules or can be S-glutathionylated under basal and stressed conditions. For future work, it is important to further explore the crosstalk mechanism between both pathways, and to further elucidate the modifications of Keap1 cysteine residues either by chemical binding or oxidation and how this results in the activation of Nrf2 using novel approaches such as NEM-click.

ACKNOWLEGDEMENTS

I would like to thank my supervisors Dr Chris Goldring, Dr Neil Kitteringham and Prof Kevin Park for giving me this wonderful opportunity to do this PhD. I would not have gone this far in life without your encouragement, support and guidance that you have given me. Thank you for the kindness and friendship that you have shown me during my long and fantastic time here. You have my deepest gratitude! I would like to acknowledge the financial support from The University of Liverpool, ORSAS, Pfizer Ltd and the Wellcome Trust.

I would also like to thank Dr Roz Jenkins, Dr Vicki Elliot South, Dr Anahi Santoyo and Dr Caroline Earnshaw for their wonderful assistance and support with proteomics, Dr Laura Watkin for her support and interest with the Keap1/Nrf2 work, Dr Amy Mercer for her help in FACS analysis and my mentor, Dr Ian Copple for his tutoring and guidance throughout my PhD. To Alison, Jan, Luke, Phill R, Pete, Phil R, Les and Dave I am very grateful for the help that you have given me.

A very big thank you to everyone, who I have became good friends with in the department; Abh, Anahi, Ayman, Brian, Caroline, Cliff, Eva, Eunice, Hayley W, Hayley C, Jo W, John F, Lorna, Manal, Phil SL, Rowena Shaw, Sabah, Swale, Tom and Viv. To the BSS Crew for the camaraderie, fun and wicked time we had – Thank you. I am grateful to my homies Chris and Daniel for their everlasting friendship and this is why I am away from home for such a long time.

A super duper special thank you and big hugs to Rowena for being a fantastic friend giving me encouragement and support through my ups and downs, providing me a place to stay if not I would have been homeless, Rym for being a fantastic lab buddy and friend throughout our PhD, Adam for being my best buddy and brother there is no one else better I could have asked for, Dan for being my best mate and the great times we have with footy, coffee time and proofreading my thesis, Sophie for being a great friend, dancing buddy and proofreading my chapters, and to Luke, Craig, Rachel and Han for their friendship, all the fun and silly time we spent together. You guys made my time in Liverpool sound and boss! Ta La!

Finally, I would like to thank Pa, Ma, Uncle David, Andy and Martin for all their encouragement and support given to me, Jen for being there for me while I am writing up. I like to dedicate this PhD to my beloved grandma. I love all of you.

PUBLICATIONS

Papers

Megherbi, R.*, **Chia, A.J.***, Copple, I.M., Randle, L.E., Jenkins, R.E., Kitteringham, N.R., Goldring, C.E. & Park, B.K. DNCB activates the Keap1/Nrf2 cell defence independently of Keap1 covalent modification. *Manuscript in preparation*.

*Joint first authorship

Chia, A.J., Firman, J., Goldring, C.E., Randle, L.E., Kitteringham, N.R., Mercer, A.E., O'Neill, P. & Park, B.K. The use of click chemistry for the investigation of Nrf2 activation. *Manuscript in preparation*.

Chia, A.J., Goldring, C.E., Kitteringham, N.R., Randle, L.E. & Park, B.K. The generation, detection and effects of reactive drug metabolites: Evidence for cell defence in ADR (2010). *Manuscript submitted to Medicinal Research Reviews.*

Chia, A.J., Goldring, C.E., Kitteringham, N.R., Wong, SQ., Morgan, P. & Park, B.K. Differential effect of covalent protein modification and glutathione depletion on the transcriptional response of Nrf2 and NF-kappaB (2010). *Biochemical Pharmacology*, 80 (3), 410-421.

Copple, I.M., Goldring, C.E., Jenkins, R.E., **Chia, A.J.**, Randle, L.E., Kitteringham, N.R., Hayes, J.D. & Park, B.K. The hepatotoxic metabolite of acetaminophen directly activates the Keap1-Nrf2 cell defense system (2008). *Hepatology*, 48 (4), 1292-1301.

Abstract

Chia, A.J., Kitteringham, N.R., Park, B.K. & Goldring, C.E. Effect of chemical stress on basal and inducible redox sensitive transcription factors. *InVitro Toxicology Society Winter Meeting 2008*.

ABBREVIATIONS

αCHCA;	α-cyano-4-hydroxy-cinnamic acid
ACN;	acetonitrile
Ahr;	aromatic hydrocarbon receptor
ANOVA;	analysis of variance
AP-1;	activator protein 1
ARE;	antioxidant response element
BITC;	benzyl isothiocyanate
BSA;	bovine serum albumin
BSO;	buthionine (S,R)-sulfoximine
BTB;	broad complex /tram-track/ bric-a-brac
bZip;	basic leucine zipper
cAMP;	cyclic adenosine monophosphate
CBP;	CREB-binding protein
CDSS;	Centre for Drug Safety Science
CK-II;	casein kinase-II
CLIC;	chloride intracellular channel
CMV;	cytomegalovirus
CNC;	cap 'n' collar
CO_2;	carbon dioxide
Con;	control
CREB;	cAMP-responsive element binding protein
μCi	microCurie
Cul3;	Cullin 3
CYP450;	cytochrome P450
Cys;	cysteine
Dex-mes;	dexamethasone 21-mesylate
DGR;	double glycine repeat
dH_20;	distilled H_20
DILI;	drug induced liver injury
DMEM;	Dulbecco's modified Eagle's medium
DMSO;	dimethyl sulphoxide
DNCB;	2,4-dinitrochlorobenzene
15d-PGJ_2;	15-deoxy-Δ-(12,14)-prostaglandin J2
dsRNA;	double stranded RNA
DTNB;	5,5'-dithiobis(2-nitrobenzoic acid)
DTT;	dithiothrietol
ECH;	erythroid cell-derived protein with CNC homology

EDTA;	ethylenediaminetetraacetic acid
ERK-1;	extracellular signal-regulated kinase 1
FBS;	fetal bovine serum
GCL;	γ-glutamylcysteine ligase
GCLc;	GCL, catalytic subunit
GCLm;	GCL, regulatory sybunit
GSH;	glutathione
GSSG;	oxidised GSH
GST;	GSH S-transferase
H_2O;	water
H_2O	hydrogen peroxide
HEPES;	4-(2-hydroxyethyl)-1-piperazineethanesulfonic acid
HO-1;	heme oxygenase 1
HRP;	horseradish peroxidase
HNE;	4-hydroxylnonenal
HSE;	heat shock response element
HSF;	heat shock transcription factor
HSP;	heat shock protein
IA;	Iodoacetamide
IκB;	inhibitor of κB
IKK;	IκB kinase
IVR;	intervening region
Keap1;	Kelch-like ECH-associated protein 1
kDa;	kiloDalton
LC-ESI MS/MS;	liquid chromatography electrospray ionisation MS/MS
LDH;	lactate dehydrogenase
LPS;	lipopolysacharride
MALDI-TOF MS;	matrix-assisted laser desorption ionisation time-of-flight mass spectrometry
MAPK;	mitogen-activated protein kinase
Mn-SOD;	manganese-dependent SOD
MOPS;	3-(N-morpholino)propanesulfonic acid
mRNA;	messenger RNA
MS/MS;	tandem mass spectrometry
MUT;	mutant

m/z;	mass-to-charge ratio
NaCl	sodium chloride
NADPH;	nicotinamide adenine dinucleotide phosphate
NAPQI;	N-acetyl-*p*-benzoquinoneimine
Neh;	Nrf2-ECH homology
NEM;	N-ethylmaleimide
NES;	nuclear export signal
NF-κB;	nuclear factor κB
NLS;	nuclear localisation signal
NQO1;	NAD(P)H:quinine oxidoreductase 1
NO;	nitric oxide
Nrf2;	nuclear factor erythroid 2 related factor 2
PBS;	phosphate-buffered saline
PERK;	protein kinase R-like endoplasmic reticulum kinase
PI3k;	phosphatidyl inositol 3-kinase
PKC;	protein kinase C
PXR;	pregnane X receptor
Res;	Resveratrol
RIPA;	radioimmunoprecipitation assay
RNA;	ribonucleic acid
RNAi;	RNA interference
ROS;	reactive oxygen species
rpm;	revolutions per minute
RXR;	retinoid X receptor
SD;	standard deviation of mean
SDS;	sodium dodecyl sulphate
SH;	sulphydryl
siRNA;	short interfering RNA
SMX;	sulfamexthoxazole
SMX-NO;	nitroso sulfamexthoxazole
SOD;	superoxide dismutase
SOH;	sulphenic acid
SO_2H;	sulphinic acid
SO_3H;	sulphonic acid
S-S;	disulphide
ST;	sulphotransferase
Std;	standards
SV40;	simian virus 40

tBHQ;	*tert*-butylhydroquinone
TBS;	tris-buffered saline
TFA;	trifluoroacetic acid
TMA;	trimellitic anhydride
TNB;	5-thio-2-nitrobenzoic acid
TRE;	AP-1 binding response element
TRP;	transient Receptor Potential Channel
TRPA1;	transient Receptor Potential (TRP) ion channel
U;	Unit
UDPGA;	uridine diphosphate glucuronic acid
UGT;	UDP-glucuronosyltransferases
UK;	United Kingdom
v/v;	volume/volume
WT;	wild type
w/v;	weight/volume
XRE;	xenobiotics response element

CHAPTER 1

General Introduction

CONTENTS

1.1 INTRODUCTION

Adverse drug reactions (ADRs) are categorised as any detrimental effect outside the normal therapeutic use of a drug (Pirmohamed *et al.* 1998). They are one of the main causes of hospital admission (Pirmohamed *et al.* 2004), leading to morbidity and mortality among patients and play a significant role in drug attrition during development (Park *et al.* 2005a). Whilst many cell types may be damaged by off target effects of a drug molecule, the liver is clearly one of the most commonly affected organs. The main physiological role of the liver is to metabolise xeno- and endobiotics to aid their clearance. The main proteins involved in the metabolism of drugs are the cytochrome P450 (CYP450) enzymes which are found in abundance in the liver. These phase 1 enzymes can bio-inactivate drugs to form non-reactive metabolites. However, they are also largely recognised for formation of chemically reactive metabolites (CRMs), which may be a prerequisite for certain toxicities seen in ADRs. Hence, the liver is the main site of drug metabolism making it a major target for liver-specific toxicity or drug-induced liver injury (DILI) (Park *et al.* 1995). The generation of CRMs has been observed with paracetamol (Hinson *et al.* 1981), carbon tetrachloride (Recknagel *et al.* 1989), bromobenzene (Jollow *et al.* 1974) and furosemide (Williams *et al.* 2007) during hepatotoxicity and recent evidence, in the largest study of its kind, indicates the direct role of hepatic metabolism forming CRMs as a risk factor for hepatic adverse events (Lammert *et al.* 2010).

The impending ability for CRMs to bind to cellular proteins, alter their conformation and function, leading to drug-induced toxicity (Zhou *et al.* 2005) has been classified as "The Critical Protein Hypothesis". This hypothesis suggests that the covalent binding of liver proteins by CRMs, once glutathione (GSH), the most abundance intracellular non-protein

thiol molecule is depleted, leads to liver injury (Park *et al.* 2005a). Hence, these alterations to hepatic cellular proteins may elicit a hepatocellular defence response by initiating protein expression. The liver can produce a number of responses capable of bio-inactivating CRMs. These cellular defence responses are involved in the restoration of homeostasis and include GSH and GSH-dependent enzymes, Phase I and II proteins, transcription factors and heat shock proteins [Fig 1.1 illustrates this balance between defence (specifically for the defence elicited by the transcription factor Nrf2) and damage during exposure to paracetamol].

Whilst GSH and GSH-dependent enzymes form the vanguard of the cellular defence response against CRMs (DeLeve *et al.* 1991), phase I and II proteins also play a key role. Phase I enzymes catalyse oxidation, reduction and hydrolysis reactions to incorporate a functional group for subsequent Phase II conjugation reactions and elimination. The Phase I family is made up of the CYP450 superfamily, flavin-containing mono-oxygenase system, dehydrogenases, esterases and NADPH-cytochrome P450 reductases. Phase II enzymes include anti-oxidant and detoxification proteins that are either ubiquitously expressed or inducible in cells (Prestera *et al.* 1993b). These facilitate the removal of CRM from the body by increasing their polarity enabling their elimination into bile or urine. There are several transcription factors which can respond to CRM formation within cells (Primiano *et al.* 1997). These include: the Cap'n'Collar (CNC) family consisting of nuclear factor-erythroid 2 (NF-E2)-related factors; Nrf1, Nrf2 and Nrf3 (Motohashi *et al.* 2002), the Nuclear factor kappa-light-chain-enhancer-of activated B cells (NF-κB) family comprising of five members; p65 (Rel A), RelB, c-Rel, p50/p105 (NF-κB1) and p52/p100 (NF-κB2) (Hayden *et al.* 2004),

activating protein (AP-1) which is made up of a family of homo- and hetero- dimers of Jun, Fos or activating transcription factor basic region leucine zipper (bZIP) proteins (Karin *et al.* 1997), and the heat shock protein (HSP) family which is expressed basally at low levels under physiological conditions and consists of the small HSPs (16-30), HSP40, HSP60, HSP70, HSP90 and HSP110 (Freeman *et al.* 1996; Kalmar *et al.* 2009). Together, these factors act in concert to drive the transcription and translation of many cytoprotective genes to aid the detoxification of CRMs and the restoration of cellular and organ homeostasis.

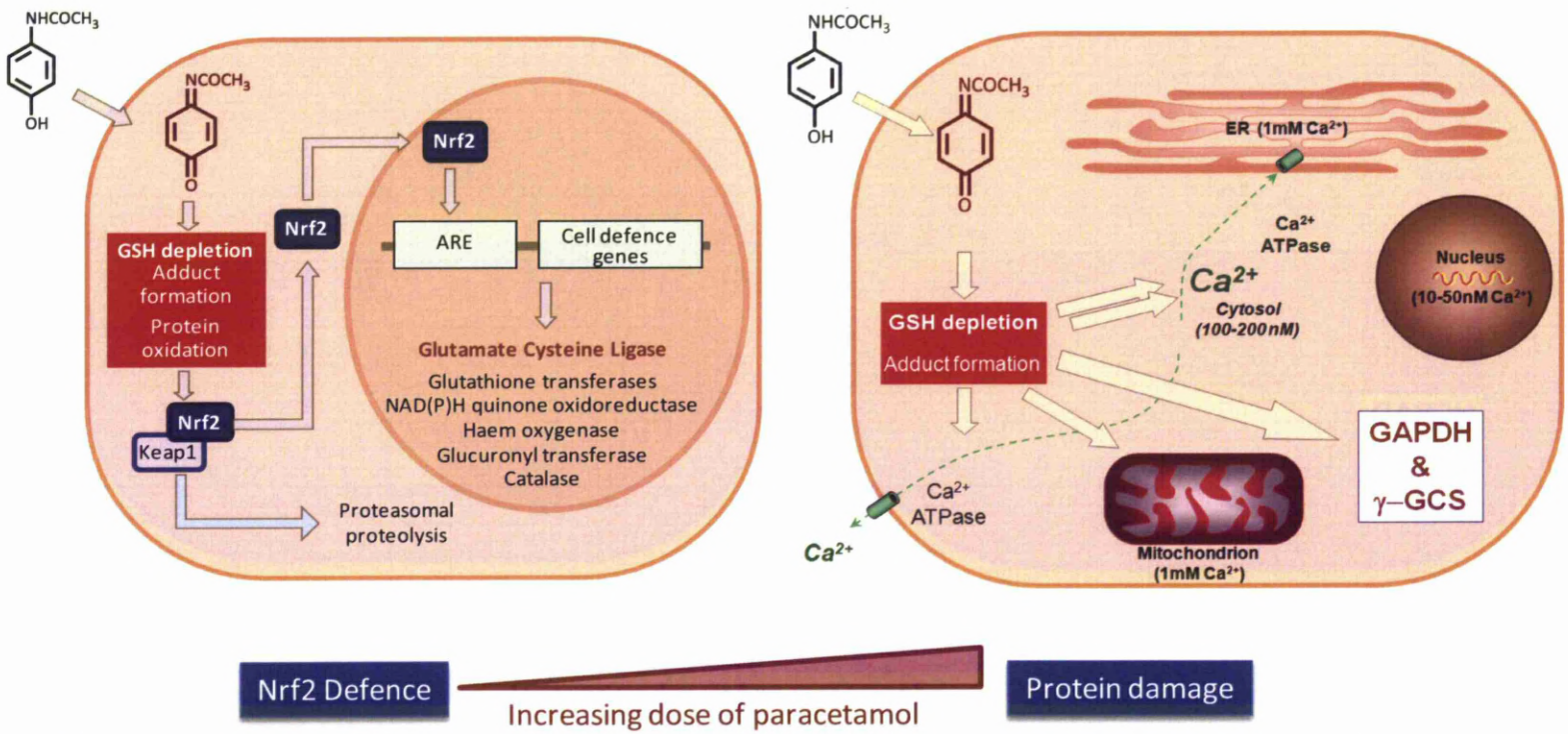

Figure 1.1: **The balance between Nrf2-dependent cellular protection and critical protein damage during exposure to paracetamol.** Formation of NAQPI leads to the depletion of GSH and adduct formation. Nrf2 activation and the transcription of cell defence genes occurs upon initial dose expose to paracetamol. However, with increasing doses of paracetamol, cell defence becomes overwhelmed and protein damage ensues [Adapted from (Park *et al.* 2005a)].

1.2 ADVERSE DRUG REACTIONS AND DRUG-INDUCED LIVER INJURY

A major cause of patient morbidity and mortality is adverse drug reactions. In the United States, it has been estimated that ADRs contributed to about 100,000 deaths alone in 1994 (Lazarou *et al.* 1998). A recent study in Sweden showed that ADRs comprised the 7th most common cause of death (Wester *et al.* 2008). This observation is in line with other studies in the United States and Canada where it has been described as the 4th and 19th most common cause of deaths, respectively (Lazarou *et al.* 1998; Bains *et al.* 1999). A recent analysis of 18,820 hospital admissions from two Merseyside hospitals in the UK, conducted from November 2001 to April 2002, showed that adverse drug reactions accounted for 1225 (6.5%) admissions. Twenty-eight people (2.3%) died directly from the reactions (Pirmohamed *et al.* 2004). Recently, a case study reported that 1 in 7 patients suffered from an ADR, and this was a significant cause of morbidity and increased hospital stay (Davies *et al.* 2009). Therefore, ADRs are a significant cause of hospital admission and patient morbidity and mortality.

ADRs can be classified into five main types in accordance with their chemical and pharmacological characteristics (Table 1.1) (Park *et al.* 1998). ADRs can affect many parts of the body. However, the liver represents the primary target for drug-induced liver injury (DILI) due to its main physiological role in drug metabolism and CRM formation (Park *et al.* 1995). DILI accounts for a significant cause of patient morbidity and mortality (Lee *et al.* 2005). Furthermore, DILI accounts for more than 50% of acute liver failure (Ostapowicz *et al.* 2002; Lee 2003) and is one of the main causes of drug attrition within development. More than 600 drugs have been shown to cause liver toxicity (Park *et al.* 2005a). Hence, the understanding of DILI is required to further improve drug

safety and reduce the occurrence of DILI in patient populations (Holt *et al.* 2010).

Type of Reactions	Characteristics	Examples
A-Augmented	1. Predictable from drug pharmacology 2. Exaggeration of pharmacological effect 3. Dose -dependent	1. Hypotension with anti-hypertensives drugs 2. Haemorrhage with anti-coagulants drug
B-Bizzare (Idiosyncratic)	1. Not predictable from the drug pharmacology 2. Dependent on the individual metabolic or immunological factors which may contribute to susceptibility 3. Not dose-dependent	1. Hepatitis with halothane 2. Hypersensitivity with anti-convulsants
C-Chemical	1. Predicted or rationalised from the chemical characteristic of the drug and its metabolite	1. Hepatotoxicity with paracetamol
D-Delayed	1. Reactions arises years after treatment	1. Tumours from chemotherapeutic agents 2. Phocomelia with thalidomide
E-End-of-treatment	1. Reactions arises when treatment stops or drug withdrawn	1. Withdrawal seizures upon stopping phenytoin 2. Withdrawal syndrome upon stopping paroxetine

Table 1.1: Classification of ADRs. Types of ADRs, A-E, with their characteristics and examples. (Adapted from Park *et al*, 1998).

1.3 PARACETAMOL HEPATOTOXICITY

Paracetamol (APAP) is an easily available, over the counter analgesic and antipyretic drug. Its mechanism of action is thought to be through the inhibition of cyclooxygenase activity, leading to the reduction of pro-inflamatory prostaglandin synthesis (Hinz *et al.* 2008). However, a novel mechanism of action has been proposed that suggest thats active paracetamol metabolites have an analgesic and antipyetic effect indirectly through the cannabinoid receptors by activating transient receptor potential vanilloid 1 (Zygmunt *et al.* 2000; Ottani *et al.* 2006; Mallet *et al.* 2010). The consumption of paracetamol taken at therapeutic doses is safe, but it is associated with hepatotoxicity when taken in overdose (Lee 2004).

The cause of paracetamol-induced hepatotoxicity is through the direct result of the formation of a reactive metabolite, NAPQI (Hinson *et al.* 1981). The bioactivation and excretion of paracetamol is represented schematically in Fig 1.2. Therapeutic doses of paracetamol are metabolised and excreted, around 55% and 30% by UDP-glucuronosyltransferase (UGT) and sulphotransferase (ST), as the glucuronide and sulphate conjugates, respectively (Howie *et al.* 1977). However, the Phase I enzymes, CYP2E1, CYP3A4 and CYP1A2 can metabolise 5% of a therapeutic dose of APAP to NAPQI (Dahlin *et al.* 1984; Raucy *et al.* 1989; Thummel *et al.* 1993). NAPQI is then rapidly detoxified by GSH or glutathione S-transferase (GST)-mediated conjugation with GSH and excreted in the urine as a cysteine or mercapturate product (Mitchell *et al.* 1973). During paracetamol overdose, sulphation by ST and glucuronidation by UGT rapidly become saturated and excess paracetamol will become bioactivated by CYP450 (Bessems *et al.* 2001). The production of NAPQI will be quenched by GSH

but when the GSH system becomes overwhelmed, NAPQI will accumulate within hepatoctyes. This could lead to NAPQI binding covalently to proteins which may result in the modification of their function and structure. The accumulation of NAPQI has been shown to modify and inhibit 17 proteins in the livers of rodents [for a review, see (Park *et al.* 2005a)]. The covalent modification of proteins and the oxidation of protein thiols are believed to correlate with paracetamol-induced toxicity (Davis *et al.* 1974; Potter *et al.* 1974; Roberts *et al.* 1987; Bartolone *et al.* 1988). This cellular protein modification has been suggested to be associated with mitochondrial dysfunction, decreased ATP synthesis and the disruption of calcium homeostasis (Jaeschke *et al.* 2006). The disruption of calcium homeostasis can alter cell permeability, leading to the formation of blebs on the cell membrane, causing lost of membrane integrity (Lee 2003). Nevertheless, the depletion of GSH and the covalent binding of proteins by NAPQI will not only result in cellular toxicity (David Josephy 2005) but also activate the cellular adaptive defence response during drug exposure (Park *et al.* 2005a), for a summary see Fig 1.3.

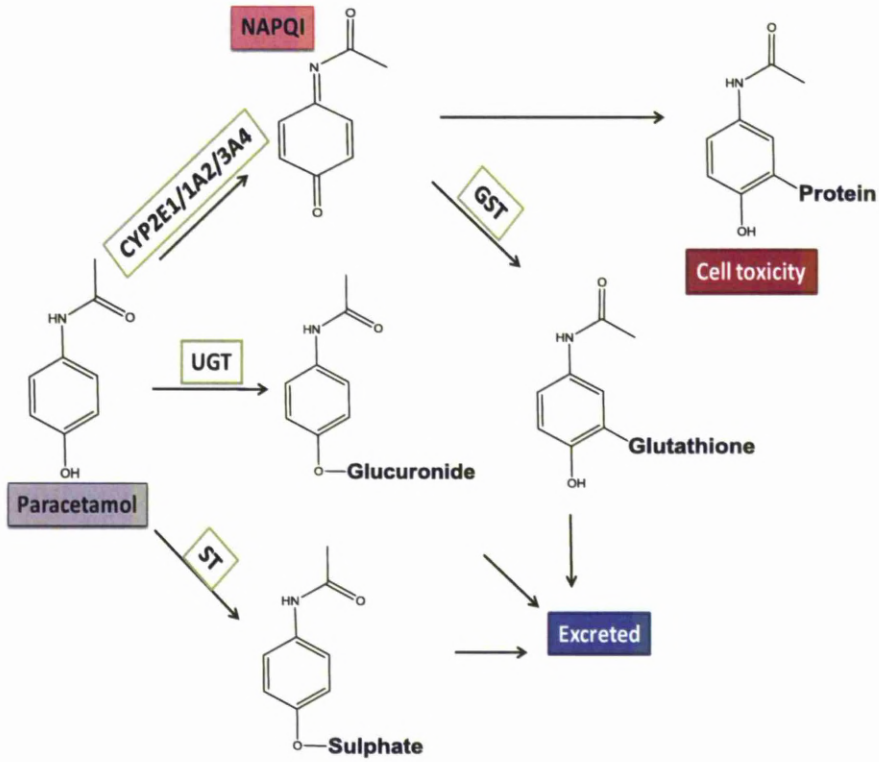

Figure 1.2: Paracetamol Metabolism. The therapeutic dose of paracetamol is mainly excreted through the formation of glucuronide and sulphate conjugates by UGT and ST, respectively. About 5% of paracetamol is bioactivated by CYP450 enzymes to form the reactive metabolite NAPQI. During a therapeutic dose, NAPQI is detoxified by GSH constitutively or through GST-mediated conjugation. However, during overdose, the main conjugation pathway is saturated and NAPQI formation increases. This results in NAQPI accumulation and depletion of GSH. The accumulated NAPQI can bind to proteins which is believed to be the primary initiating event during drug-induced liver toxicity (Zhou *et al.* 2005).

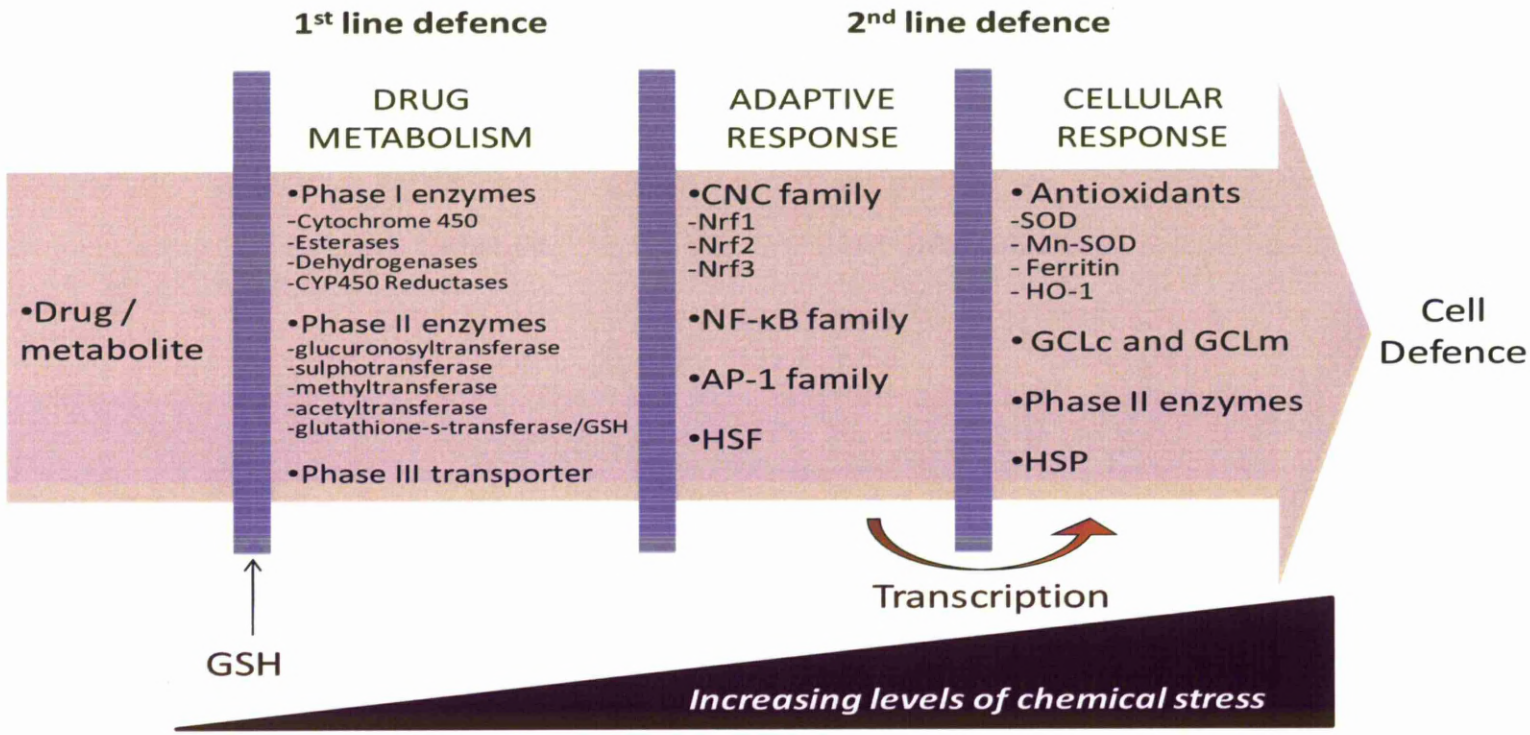

Figure 1.3: **The tiers of cellular defence against chemically reactive drug metabolites.** The first tier of defence involves GSH and drug metabolism enzymes. The second tier of defence involves transcription factors which induce the transcription of cytoprotective proteins in response to CRMs to promote cellular defence.

1.4 CELLULAR DEFENCE AGAINST CELLULAR STRESS

1.4.1 Glutathione and glutathione-dependent enzymes

Glutathione (GSH) is at the front line in cellular defence as it is the most abundant (up to 10mM) non-protein tripeptide thiol (Meister 1988; DeLeve *et al.* 1991). GSH serves as a primary defence mechanism by acting as a redox buffer for chemical and oxidative stress (DeLeve *et al.* 1991). The synthesis of GSH involves two steps: 1) the rate-limiting conjugation step of L-glutamate conjugation to cysteine via the γ-glutamylcysteine ligase catalytic subunit (GCLc) to form γ-glutamylcysteine and 2) the conjugation of glycine to γ-glutamylcysteine, via glutathione synthetase to yield GSH (Kaplowitz *et al.* 1985). The reactive cysteine thiol of GSH serves as a nucleophilic group which permits the major function of GSH, the detoxification of reactive oxygen species and conjugation of reactive electrophiles which help maintain the thiol status of other proteins (DeLeve *et al.* 1991). The detoxification and conjugation of CRMs can be spontaneous, partially with "soft" electrophiles, or enzymatically via the activity of glutathione S-transferase (GST) with "hard" electrophiles (DeLeve *et al.* 1991; Hayes *et al.* 1999). GSTs are highly diverse enzymes and their primary role is the conjugation of GSH to electrophiles and peroxidation of lipid hydroperoxides (DeLeve *et al.* 1991). During APAP toxicity, NAPQI is formed from the metabolism of APAP by CYP450, particularly 2E1, 1A2 or 3A. NAPQI is rapidly quenched by GSH spontaneously or via GST mediation. Hence, GSH and GSTs play in an important role in cellular defence by quenching CRMs by forming GSH-conjugates.

1.4.2 Phase I, II drug metabolism and III drug transporters

The first tier in cellular defence against drugs and xenobiotics, once GSH levels have been depleted, is comprised of the phase I, II drug metabolising enzymes and III transporters. Phase I drug metabolism enzymes include the CYP450 enzymes which are found in high abundance in the liver. The CYP450 superfamilies are membrane-bound microsomal enzymes (Meyer 1996; Guengerich 2003). There are five families of CYP450 involved in drug metabolism, CYP1, CYP2, CYP3, CYP4 and CYP7 (Wrighton *et al.* 1996; Xu *et al.* 2005). The primary role of CYP450 enzymes is to act as a detoxification pathway and to metabolise endogenous and exogenous compounds. However, the process may actually generate compounds that are more reactive than the parent compounds, a process known as bioactivation, which is important in the initiation of some adverse drug reactions (Park *et al.* 2005b; Antoine *et al.* 2008).

Phase II drug metabolising enzymes consist of a diverse group of enzymes varying in abundance within the liver. UDP-glycosyltransferases, UGT, ST, methyltransferases, acetyltransferases, and GSTs make up the majority of the phase II enzymes. The main functional role of phase II enzymes is the addition of a polar group onto a functionalised molecule (the result of phase I metabolism). This enables the excretion of drugs and xenobiotics into the bile and urine. With respect to the formation of CRMs from phase I reactions, phase II serves as a detoxification pathway to bioinactivate these and facilitate their subsequent removal from the cell (Timbrell *et al.* 2000; Gibson *et al.* 2001).

The removal of bioinactivated metabolites also involves phase III transporters. These transporters play a role in the transportation and

removal of endogenous and exogenous compounds (Borst *et al.* 2002). The liver expresses the following drug transporters: the multi-drug resistance protein (MDR) 1 and 2 (P-glycoprotein); the multi-drug resistance associated protein (MRP) 1, 2, 3, and 4; breast cancer resistance protein (BCRP); organic anion (OAT) 2; and bile salt export pump (BSEP). These transporters are all involved in the transportation of drugs, drug conjugates, glutathione conjugates, glucuronide conjugates and bile (Klaassen *et al.* 2010).

The role of phase I, II and III proteins in cellular defence during drug exposure can be illustrated by the detoxification pathway of paracetamol (APAP) using Nrf2 knockout and wild type mouse. Nrf2 knockout mice have been demonstrated to be compromised in their cellular defence systems, they appears to have a lower basal and/or inducible expression of cytoprotective proteins in the liver (Itoh *et al.* 1997; Chan *et al.* 2000; Kwak *et al.* 2001; Ramos-Gomez *et al.* 2001; Chanas *et al.* 2002; Iida *et al.* 2004). Furthermore, Nrf2 knockout mouse have been observed to be highly susceptible to APAP induced toxicity due to the lack of expression of Nrf2-dependent genes (Enomoto *et al.* 2001; Reisman *et al.* 2009). Therefore, a comparison of phase I, II and III pathways between the wild type mouse liver against the Nrf2 knockout mouse liver was used in the illustration (Fig 1.4).

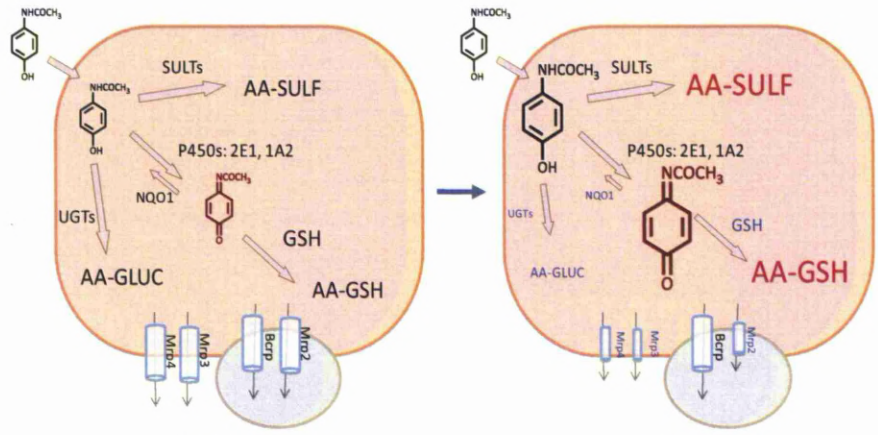

- AA-SULF and AA-GLUC are major metabolites
- AA-GSH is a minor metabolite

- Increased AA-SULF in plasma, bile, liver
- Decreased AA-GLUC in plasma, increased in liver

Figure 1.4: Control of disposition of paracetamol by phase I, II and III proteins in wild type and Nrf2-null murine hepatocytes. In wild type hepatocytes, the majority of paracetamol is metabolised by UGT and ST and excreted as glucuronide and sulphate conjugates. A minor amount of acetaminophen is metabolised to NAPQI and rapidly quenched by GSH. Glucuronide and sulphate conjugates are transported out of the hepatocyte by phase III transporters. In Nrf2-null hepatocytes there is a decrease in UGT. Therefore the majority of paracetamol is either metabolised by STs or to NAPQI by CYP450s and excreted as sulphate or GSH conjugate. There is also a decreased efflux of conjugates from the decrease in expression of Nrf2 dependent phase III transporters. (Maher *et al.* 2007; Aleksunes *et al.* 2008; Reisman *et al.* 2009)

1.4.3 The redox-sensitive transcription factors implicated in the cellular response to chemically reactive metabolites

For a schematic overview of this section, specifically with respect to APAP exposure, and which, to some extent, can be considered a paradigm for the response to other CRMs, see Figure 1.3.

1.4.3.1 The cap 'n' collar (CNC) family

Cells are constantly challenged with harmful endogenous compounds, reactive oxygen species, lipid hydroperoxides or exogenous compounds such as UV radiation or environmental pollutants. In order to deal with constant exposure to such stresses, mammalian cells have evolved a number of second tier adaptive cellular defence mechanisms. The adaptive defence response involves the CNC family of transcription factors, amongst which Nrf2 is now considered to be the most important member, which are able to rapidly respond to a range of different forms of oxidative and chemical stress [for reviews, see (Hayes *et al.* 2009; Copple *et al.* 2010a)]. The Nrf1, Nrf2 and Nrf3 proteins are part of the CNC family, which heterodimerise with small Maf proteins via the bZip domain (Andrews *et al.* 1993; Marini *et al.* 1997; Kobayashi *et al.* 1999). This heterodimerisation between Nrf subunits and Maf proteins can enable recognition and binding to the antioxidant response element (ARE), a *cis*-acting enhancer with a sequence motif of 5'-gagTcACaGTgAGtCggCAaaatt-3'. Critical nucleotides are annotated in capital letters (Nioi *et al.* 2003). The ARE sequence motif is found in the promoter region of anti-oxidant and phase II genes. Activation of the ARE leads to the transcription of these cytoprotective proteins (Rushmore *et al.* 1991; Prestera *et al.* 1995; Blank *et al.* 1997).

Nrf1

Nrf1 is a member of the CNC family and shares several similarities with Nrf2; mainly the highly conserved CNC domain, a 43 amino acid sequence found between the N-terminal and the basic domain (Blank *et al.* 1997). Nrf1 is able to heterodimerise with small Maf proteins to bind to ARE motifs and it is abundantly expressed in major organs (Marini *et al.* 1997; Motohashi *et al.* 2002). There are two forms of Nrf1, a 120kDa and 65kDa isoform which could be formed through alternative translation initiation (Chan *et al.* 1993). The larger Nrf1 isoform is expressed ubiquitously in the cytoplasm. However, unlike Nrf2, Nrf1 is not sequestered by Keap1, even though it can interact with Keap1. It has been suggested that Nrf1 is localised to the cytoplasm by its interaction with the endoplasmic reticulum (ER) and the 65kDa isoform of Nrf1 (Nrf1-p65) is found in the nucleus (Wang *et al.* 2006). It has been identified in monkey kidney cells in the ER membrane- and nuclear envelope- enriched fractions (Zhang *et al.* 2009b). The N-terminal domain of Nrf1 contains a transmembrane domain which is absent in Nrf2. This targets Nrf1 to the ER (Wang *et al.* 2006; Zhang *et al.* 2006) and is glycosylated at the NST domain, a seven asparagine (-Asn-X-Ser/Thr) - glycosylation consensus site (Zhang *et al.* 2007b). Hence, the glycosylation may play a part in the localisation of Nrf1 in the cell.

Nrf1 has been shown to play an essential role in sustaining liver development (Chen *et al.* 2003) as the Nrf1 knockout mouse shows embryonic lethality (Chan *et al.* 1998). Although the role of Nrf1 in cellular defence remains unclear, Nrf1 knockout primary hepatocytes have been shown to be more susceptible to oxidative stress (Chen *et al.* 2003). Furthermore, Nrf1 has been shown to be involved in the control of several cytoprotective genes, i.e. GCL catalytic subnit (GCLc) and the

GCL modifier subunit (GCLm) (Kwong *et al.* 1999; Chen *et al.* 2003; Zhao *et al.* 2010), Heme oxygenase-1 (HO-1), glutathione peroxidase 1 (Chen *et al.* 2003), metallothionein (MT) 1 and 2 (Chen *et al.* 2003; Ohtsuji *et al.* 2008), NAD(P)H: quinone oxidoreductase 1 (NQO1) (Venugopal *et al.* 1996; Zhao *et al.* 2010) and the sulfotransferase family 3A member 1 (Ohtsuji *et al.* 2008). The Nrf1-p65 was suggested to be able to compete with Nrf2 for small Maf proteins by also binding to the ARE and inhibiting the oxidative stress response (Wang *et al.* 2007). Nrf1 have also been shown to dimerise with MafG proteins which bind to consensus sequences that are identical to ARE sequence. The evidence for the involvement of Nrf1 in the regulation of cell defence genes is based on either Nrf1 knockout or conditional Nrf1 knockout animals or hepatocytes. Until recently there has been little compelling evidence of the direct induction of Nrf1 by chemically reactive compounds or oxidative stress. Zhang and colleagues demonstrated that *tert*-butyl hydroquinone (tBHQ) increases Nrf1 activity and that mutations in amino acids 31-90 of the NTD domain disrupt the activity (Zhang *et al.* 2009b). The increase in Nrf1 activity has been postulated to be a consequence of the chemical stress caused by the formation of the tBHQ reactive metabolite, 2-t-butyl-1, 4 benzoquinone from bioactivation by CYP1A1 (Gharavi *et al.* 2007). Activation may also occur through the depletion of GSH by tBHQ (Nakamura *et al.* 2003) leading to the induction of oxidative stress. Furthermore, inorganic arsenic has also been shown to result in the activation of Nrf1 and the induction of GCLc, GCLm and NQO1 through ARE binding (Zhao *et al.* 2010). In summary, Nrf1 may be activated by the presence of CRMs and the depletion of GSH but its mechanism remains elusive and more work needs to be done in this area.

Nrf2

The most studied member of the CNC family is Nrf2. This protein is expressed in most tissues but especially those involved in detoxification and/or constant exposure to the external environment (Motohashi *et al.* 2002). In a homeostatic environment, Nrf2 is sequestered by its inhibitor protein, Kelch-like erythroid cell-derived protein with CNC homology (ECH)-associated protein1 (Keap1), in the cytosol (Itoh *et al.* 1999b). A Keap1 homodimer interacts with Nrf2 and targets it for ubiquitination and subsequent proteosomal degradation by functioning like a substrate adaptor for a Cullin-dependent E3 ubiquitin ligase complex (Cul3 ligase) (Cullinan *et al.* 2004b; Kobayashi *et al.* 2004a; Zhang *et al.* 2004; Furukawa *et al.* 2005). This accounts for the relatively short half life of Nrf2 (10-30min) (Alam *et al.* 2003; Itoh *et al.* 2003; McMahon *et al.* 2003; Nguyen *et al.* 2003; Stewart *et al.* 2003; Yamamoto *et al.* 2007). Under chemical or oxidative stress, Keap1 is unable to repress Nrf2, allowing Nrf2 nuclear accumulation leading to the transcription of ARE-regulated genes (Itoh *et al.* 1999a; Dhakshinamoorthy *et al.* 2001). Classical examples of Nrf2-ARE dependent gene transcription and their functions are NQO1 (Dhakshinamoorthy *et al.* 2000), which catalyses two electron reduction and detoxification of quinones (Venugopal *et al.* 1996), HO-1 (Prestera *et al.* 1995) which catabolises heme to yield biliverdin, free iron and carbon monoxide (Alam *et al.* 1999; Ishii *et al.* 2000), the aldo-keto reductase family 1 (AKR1) (Kwak *et al.* 2003) which reduces aldehydes and ketones to primary and secondary alcohols (Nishinaka *et al.* 2005; Lou *et al.* 2006), GSTs (Itoh *et al.* 1997) which catalyse the conjugation of GSH to electrophiles (Hayes *et al.* 2000; McMahon *et al.* 2001), GCLc and GCLm (McMahon *et al.* 2001) and UDP-glucuronosyltransferases (UGTs) (Enomoto *et al.* 2001; Thimmulappa *et al.* 2002), which catalyse the

conjugation of UDPGA to lipophilic substrates (Shelby *et al.* 2006; Yueh *et al.* 2007). Fig 1.4 illustrates the role of Nrf2 in the control of genes involved in defence, specifically with respect to APAP exposure. Together these proteins comprise much of the second tier of the defence response. The mechanism of Nrf2 activation by drug or xenobiotics-induced stress has not been fully clarified but there are currently two major hypotheses proposed, which are not necessarily mutually exclusive, i.e. the modification of cysteine residues in Keap1 and the phosphorylation of Nrf2, which will be discussed in detail in section 1.6.

Therefore, the generation of CRMs by phase I enzymes can have a direct effect on the cellular defence mechanism via the Nrf2/Keap1 pathway as shown by NAPQI formation during acute APAP-induced hepatotoxicity. Even at a sub-toxic level of exposure to APAP, NAPQI causes GSH depletion and can covalently bind to Keap1. This has been postulated to lead to the induction of an Nrf2 mediated cellular defence response and the transcription of Nrf2-ARE dependent genes (Goldring *et al.* 2004; Copple *et al.* 2008a; Randle *et al.* 2008).

Nrf3

The newest member of the CNC family is Nrf3, discovered and characterised by Kobayashi and colleagues (Kobayashi *et al.* 1999). Nrf3, in common with other Nrf family members, shares structural similarity in its CNC domains and can heterodimerise with small Maf proteins to bind to ARE motifs (Kobayashi *et al.* 1999). It is expressed in major organs but is most abundant in the placenta (Kobayashi *et al.* 1999). Recent work has suggested that Nrf3 is localised and bound to the ER membrane, and

like Nrf1, it is glycosylated (Nouhi *et al.* 2007; Zhang *et al.* 2009a; Pepe *et al.* 2010).

The role of Nrf3 remains unknown but it has been suggested recently that the upregulation of Nrf3 plays an important role in smooth muscle cell differentiation (Pepe *et al.* 2010). The Nrf3 knockout mouse has no noticeable phenotype when compared to the wild type and there is no effect on phase 2 gene expression (Derjuga *et al.* 2004; Kobayashi *et al.* 2004b). There is currently no direct evidence of chemical or oxidative stress activating Nrf3. However, there is contradicting evidence as to the role of Nrf3 in activating ARE gene expression. Sankaranarayanan and Jaiswal suggested that human Nrf3 negatively regulates the expression of NQO1 (Sankaranarayanan *et al.* 2004). These authors noted that Nrf3 overexpression depressed the expression and induction of NQO1 in response to tBHQ. Interestingly, RNA interference directed against Nrf3 reversed these effects. This is in line with a current report that overexpression of Nrf3 also negatively regulates the expression of NQO1 (Pepe *et al.* 2010). However, Zhang and colleagues have shown that mouse Nrf3 activity is only slightly induced by tBHQ and sulforaphane when analysing an ARE reporter construct gene. The authors noted that the ARE reporter gene used by Sankaranarayanan and Jaiswal was different to their, by the absence of an AP-1 binding motif. Hence, they postulated that the presence of the AP-1 binding motif allowed Nrf3 to be recruited, forming a heterodimer with c-Fos or Fra1 to compete out Nrf2 (Zhang *et al.* 2009a).

1.4.3.2 NF-κB family

NF-κB exists in the cytoplasm of unstimulated cells as homo- or hetero-dimers, bound to a family of inhibitory proteins known as Inhibitor of κB (IκB), via non-covalent interactions. There are five

members belonging to the mammalian NF-κB family [p65 (RelA), RelB, c-Rel, p50/p105 (NF-κB1) and p52/p100 (NF-κB2)] which may form part of the second tier of the cellular defence response. They are characterised by a conserved 300 amino acid N-terminal region called the Rel-homology domain (RHD) which is required for dimerisation between NF-κB family subunits and also for interaction with the IκB inhibitory proteins (May *et al.* 1998; Hayden *et al.* 2004). This interaction conceals the nuclear localisation signal (NLS) of p65 in the p65/p50 dimer which can prevent the NF-κB:IκB complex from translocating to the nucleus, thereby maintaining NF-κB in an inactive state (Jacobs *et al.* 1998). Although the complex is predominantly localised to the cytoplasm, the NLS of p50 is not concealed by the binding of IκB. The nuclear export sequence (NES) found on IκB allows the shuttling of the complex between the nucleus and the cytoplasm (Johnson *et al.* 1999; Huang *et al.* 2000b; Hayden *et al.* 2004).

Activation of NF-κB requires the dissociation and degradation of IκB from the NF-κB:IκB complex, allowing unbound NF-κB to be released. Upon the release of NF-κB from the NF-κB:IκB complex, NF-κB can translocate to the nucleus. The RHD binds to κB elements with a consensus sequence of 5'-GGGRNYYYCC-3' (N=any base, R=purine and Y=pyrimidine) (Chen *et al.* 1999) and can trigger gene transcription. After binding to the κB elements, the promotion and enhancement of gene transcription requires the presence of a transactivation domain (TAD). This domain is located on the C-terminal region of p65, RelB and c-Rel. The homodimers of p52 and p50 therefore lack this domain. This can be seen in the transcriptional activity of p65, RelB, c-Rel and the repressive activity of p52 and p50 homodimers (Zhong *et al.* 2002; Chen *et al.* 2004; El Gazzar *et al.* 2007).

NF-κB transcriptional activity can trigger inflammatory responses, cell proliferation, cell survival and anti-oxidant responses. NF-κB achieves cell survival by initiating the transcription of anti-apoptotic proteins such as XIAP (Stehlik *et al.* 1998; Braeuer *et al.* 2006; Kairisalo *et al.* 2007), cIAPs (Chu *et al.* 1997; Wang *et al.* 1998), c-FLIP (Kreuz *et al.* 2001; Micheau *et al.* 2001), A1 (Zong *et al.* 1999), A20 (Malewicz *et al.* 2003) and BCL-xL (Chen *et al.* 2000). It initiates cell proliferation by initiating the transcription of cell cycle regulators and cyclins (Kucharczak *et al.* 2003), and causes inflammation by the induction of expression of inflammatory proteins such as tumour necrosis factor-α (TNF-α), interleukins (IL), interferon-β, macrophages colony stimulating factor (M-CSF), granulocyte macrophages colony stimulating factor (GM-CSF), cyclooxygenase II (COX-II), inducible nitric oxide synthase (iNOS) (Pahl 1999) and several anti-oxidant proteins such as manganese-dependent SOD (Mn-SOD) (Delhalle *et al.* 2002; Tanaka *et al.* 2002; Djavaheri-Mergny *et al.* 2004) and ferritin (Pham *et al.* 2004).

NAPQI and its parent compound APAP can abrogate NF-κB binding activity in cells (Blazka *et al.* 1995; Boulares *et al.* 1999) and attenuate TNF-α induction of NF-κB in *vivo* (Matsumaru *et al.* 2003). Blazka has previously demonstrated that mice treated with APAP show a rapid decrease in NF-κB binding associated with an increase in damaged hepatocytes. The induction of NF-κB-dependent genes, iNOS and IAP-1 by TNF-α was also reduced after exposure to APAP *in vivo*. Moreover, this effect was not observed when repeated in Huh7 cells which lack P450 activity. Therefore, these studies show that the reactive metabolite of APAP can inhibit NF-κB and its dependent genes.

Recently, it has been suggested that NF-κB plays a role in the expression of cytochrome P450 proteins (Ishibe *et al.* 2009). The

interleukin-1 receptor antagonist (IL-1ra) knockout mouse has a higher level of expression of NF-κB and suppressed CYP450 enzymes. This observation is also associated with reduced levels of APAP toxicity. Also, the induction of NF-κB activity by IL-1α suppresses the expression of CYP450 in wild type mouse hepatocytes (Ishibe *et al.* 2009). NF-κB and its inducers, TNF-α and LPS, have also been shown to repress the activity of the aromatic hydrocarbon receptor (Ahr). It has been hypothesed that RelA is able to associate with Ahr, forming an inactive complex capable of inhibiting the transcription of CYP1A1 and CYP1A2 (Tian *et al.* 1999; Ke *et al.* 2001). Suppression of CYP2E1 enzymes by LPS was abrogated with the co-administration of curcumin, a NF-κB inhibitor, which suggests that NF-κB plays a critical role (Sewer *et al.* 1996; Cheng *et al.* 2003). Another CYP450 family involved in the bioactivation of APAP to NAPQI is the CYP3A family. CYP3A4 and CYP3A11 are partly regulated by the pregnane X receptor (PXR)-retinoid X receptor (RXR) complex and are affected by NF-κB. It has been suggested that NF-κB can bind to RXR forming a NF-κB-RXR-PXR complex. This inactive complex can lead to the inhibition of CYP3A enzyme transcription (Gu *et al.* 2006; Zhou *et al.* 2006). In summary, NF-κB can play a role in the suppression of CYP450 enzymes by inhibiting their transcription through the formation of inactive complexes amongst various nuclear receptors. Therefore, it is possible that NAPQI may augment APAP toxicity by inhibiting NF-κB binding activity which may ultimately lead to the loss of CYP450 suppression mediated by NF-κB. This increased expression of CYP450 would be expected to lead to an enhanced formation of NAPQI from APAP, further increasing toxicity. However, more investigation is required to test this hypothesis.

1.4.3.3 Activating protein-1

Activating protein-1 (AP-1) is comprised of a family of transcription factors made up of homo- and hetero-dimers of Jun (v-Jun, c-Jun, JunB, JunD), Fos (v-Fos, c-Fos, FosB, Fra1, Fra2) or activating transcription factor (ATF2, ATF3/LRF1, B-ATF) basic region leucine zipper (bZIP) proteins. AP-1 may serve as an additional secondary cellular defence mechanism. Jun, Fos and ATF2 can heterodimerise with each other. Jun and ATF2 can form homodimers amongst themselves but Fos cannot homodimerise. The major isoform of AP-1 is the c-Jun and c-Fos heterodimer (Karin *et al.* 1997). The activity of AP-1 is dependent on the regulation of AP-1 gene transcription and post-translational modifications (Karin 1995). Whilst the constitutive expression of c-Jun and c-Fos is very low in the nucleus of many cells, they are very rapidly and transiently transcribed upon induction by extracellular signals (Abate *et al.* 1991). The binding to the AP-1 binding response element (TRE) initiates transcription of proteins that are involved in cell proliferation, differentiation, cell survival and death. Thus, AP-1 mediates cell proliferation and differentiation by the regulation and expression of cell cycle regulators such as cyclin D, cyclin A, cyclin E, p53, p21 and p16. It also mediates cell death by the expression of TNF-α, Fas Ligand (FasL) and its receptor (Fas), and also controls cell survival by inhibition of the tumour suppressor gene p53 (Hess *et al.* 2004). Although induction of AP-1 DNA binding activity may, to some as yet unknown degree, be involved in the regulation of anti-oxidant proteins such as HO-1, CuZn SOD (Chiu *et al.* 2003), GCLc and GCLm (Kitteringham *et al.* 2000), this activity is not now considered to be as critical in the transcriptional defence response as that observed with Nrf2. Furthermore, whilst the other roles of AP-1 described above may be

important in defining how the liver responds to CRM formation, there is still no definitive evidence for this.

1.4.3.4 Heat Shock Proteins

The HSPs are a family of molecular chaperone proteins that are highly conserved and basally expressed at low levels under normal physiological conditions. They assist protein folding, protein synthesis and prevent protein aggregation or direct poorly-folded proteins for degradation (Freeman *et al.* 1996; Kalmar *et al.* 2009). During chemical stress, protein adduction can occur, and HSPs are postulated to enhance the solubility of denatured proteins and eventual degradation of these proteins (Beckmann *et al.* 1992; Ciocca *et al.* 1993). The HSP family consists of small HSPs (16-30), HSP40, HSP60, HSP70, HSP90, HSP110 and mitochondrial HSP. By increasing their expression, HSPs can respond to different forms of cellular stress such as hyperthermia and oxidative or chemical stress. This process is known as the heat shock response (Lindquist 1986) and is mediated by Heat Shock transcription Factors (HSFs) which bind to consensus sequences known as heat shock response elements (HSE) on the promoter region of HSP genes (Whitesell *et al.* 2009). HSF-1, HSF-2 and HSF-3 have been identified as regulators of HSPs transcription in humans, where HSF-1 plays the dominant role in the expression of inducible HSP during the heat shock response (Pirkkala *et al.* 2001; Whitesell *et al.* 2009).

The upregulation of HSPs during cellular cytoprotection has been shown to diminish the effect of hepatotoxicity (Salminen *et al.* 1996). The induction of HO-1, which is also known as HSP32, during perturbations in cellular redox such as GSH depletion or oxidative stress demonstrates that HSPs are redox sensors (Ewing *et al.* 1993; Motterlini *et al.* 1996). Heat stress has been shown to upregulate the inducible

form of HSP70 (HSP70i) in HEPG2 cells which can protect against hepatotoxicity (Salminen *et al.* 1996). The HSPs' cellular defence capability can be illustrated for APAP toxicity. HSP25 and HSP70i have been shown to be induced by hepatotoxic doses of APAP (Salminen *et al.* 1997a; Sumioka *et al.* 2004). Furthermore, prior upregulation of HSP25 and HSP70i by heat stress reduces the hepatotoxicity from an acute dose of APAP in *vivo* (Salminen *et al.* 1997b). The overexpression of HSP25 in cells has been shown to increase the level of GSH (Baek *et al.* 2000). In a HSP70i knockout murine model, there is evidence of APAP-induced toxicity compared to wild-type animals, thus indicating an important role of HSP70i in APAP toxicity (Tolson *et al.* 2006). From the literature there is evidence to suggest that HSPs can be upregulated by cellular stress and can protect cells and reduce APAP cellular toxicity. In summary, the HSPs probably play an important role in the cellular response and defence against APAP toxicity.

1.5 PROTEIN THIOL MODIFICATIONS

The thiol-containing cysteine amino acid is one of the most reactive among all amino acids (Davies 2005), allowing them to readily undergo oxidation (Paulsen *et al.* 2010) or alkylation by electrophiles (Marnett *et al.* 2003). The modification of cysteine can alter the function or the conformation of the protein via the oxidation or reduction of electrons at the thiol group (Cooper *et al.* 2002). The cysteine thiol group (-SH) can be oxidised to the sulphenic acid (-SOH), which is unstable and reversible, and can be further oxidised to the irreversible sulphinic ($-SO_2H$) and sulphonic acids ($-SO_3H$). The –SH group can also form a disulphide linkage (S-S), either within a single protein or with other proteins. Thiol groups can also undergo S-glutathionylation (-SSG) with GSH. In the presence of nitric oxide, the –SH group can be modified

to form S-nitrosothiol (-SNO). Electrophiles can also alkylate the cysteine thiol group resulting in the formation of cysteine-electrophile adducts (Fig 1.5) (Rudolph *et al.* 2009; Paulsen *et al.* 2010). Therefore, the concept that protein function can be regulated by a change in cysteine chemical state is important. This is exemplified by the activation of apoptosis signal-regulating kinase 1 and the inhibition of protein tyrosine phosphatase 1B by cysteine modification (Spickett *et al.* 2010). A more detailed discussion of the regulation of protein function by cysteine modification is in section 1.6.

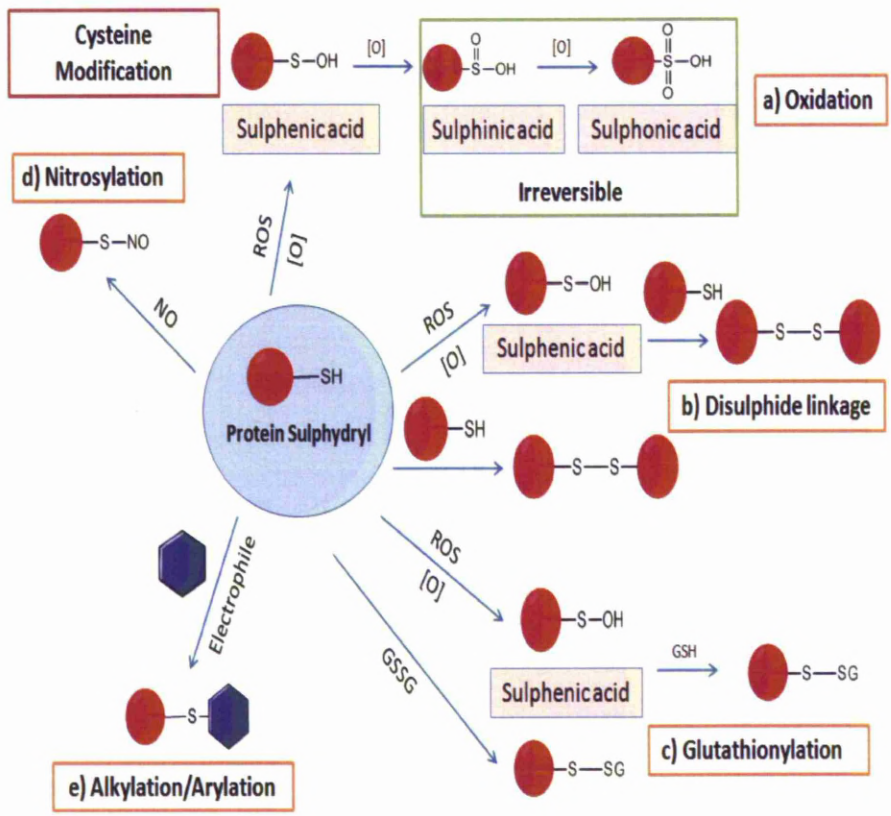

Figure 1.5: Schematic overview of cysteine post-translational modifications. The thiol group within cysteine can be (a) oxidised to different oxidation states, oxidation, (b) formed disulphide linkages, (c) glutathionylated and (d) nitrosylated. (e) Alkylation/Arylation can also occurred on the thiol group by reactive intermediates. (Rudolph *et al.* 2009; Paulsen *et al.* 2010).

1.6 THE REDOX-TRANSCRIPTION FACTOR PATHWAYS

This section emphasises in detail the signalling pathways of NF-κB and Keap1/Nrf2.

1.6.1 NF-κB Pathways

The NF-κB pathway is characterised by three pathways, the classical, alternative and atypical pathways. The three pathways are activated by different stimuli such as pro-inflammatory cytokines, the immune response and by oxidative stress (Gloire *et al.* 2009).

1.6.1.1 The classical Pathway

The classical NF-κB pathway is commonly stimulated by a pro-inflammatory cytokine such as tumour necrosis factor-α (TNF-α), lipopolysaccharide (LPS) and interleukin-1 (IL-1) (Fig 1.6a). The initiation of the classical pathway by these pro-inflammatory compounds relies on the dissociation of IκB from the NF-κB, which is initiated by the phosphorylation of serine residues 32 and 36 on IκB-α, by IκB kinase (IKK) (Brockman *et al.* 1995; Brown *et al.* 1995). This then directs IκB-α for ubiquitination by the members of the Skp1-Culin-Roc1/Rbx/Hrt-1-Fbox (SCF or SCRF) family of ubiquitin ligases, leading to the proteosomal degradation of IκB (Scherer *et al.* 1995; Ben-Neriah 2002). IKK is a dimer consisting of two different subunits, IKKα and IKKβ, which is held in an IKK complex with a regulatory subunit called NF-κB essential modifier (NEMO) (Scherer *et al.* 1995; Mercurio *et al.* 1997; Mercurio *et al.* 1999; Ben-Neriah 2002). IKKα and IKKβ are serine/theronine kinases which are able to phosphorylate members of the IκB family (DiDonato *et al.* 1997). The classical pathway controls the transcription of genes involved in cell proliferation, survival/death, differentiation and the inflammatory response (Perkins 2007).

1.6.1.2 The alternative pathway

The alternative pathway can be initiated by LPS, lymphtoxin receptors and CD40. This is triggered when the IKKα subunit is activated by NF-κB inducing kinase (NIK) instead. The p100 of the NF-κB family is phosphorylated by IKKα, leading to the ubiquitination and processing of p100 to p52. This allows the newly processed p52 and its associated partner, RelB, to translocate into the nucleus. The alternative pathway activates the transcription of genes involved in lymphoid organ development and adaptive immunity (Fig 1.6b) (Bonizzi *et al.* 2004).

1.6.1.3 The atypical pathway

The atypical pathway activates NF-κB by an IKK-independent mechanism. Stimuli such as ultraviolet light, reactive oxygen species and hydrogen peroxide can result in the phosphorylation of IκB-α (Gloire *et al.* 2006; Perkins 2006; Lluis *et al.* 2007). Expression of the HER2 oncogene results in the phosphorylation of the IκB-α's PEST domain by casein kinase-II (CK-II) (Schoonbroodt *et al.* 2000; Kato *et al.* 2003). The phosphorylated IkB-α is either degraded or dissociated from NF-κB (Fig 1.6c) (Perkins 2006). Alternatively, the depletion of GSH has been suggested to activate the NF-κB pathway (Fig 1.6) (Rahman *et al.* 2000; D'Alessio *et al.* 2004; Filomeni *et al.* 2005), but the mechanisms remain unclear. However, there are suggestions that this could involve the formation of oxidised GSSG from hydrogen peroxide stimulation (Droge *et al.* 1994) or that it may occur through the formation of reactive oxygen species and hydrogen peroxide (Gloire *et al.* 2006; Lluis *et al.* 2007).

1.6.1.4 The role of cysteine in NF-κB activity

The NF-κB pathway can be inhibited by protein cysteine modification. Both endogenous and exogenous compounds have been shown to inhibit this pathway. It has been suggested that cysteine 179 in the activation loop of IKKβ is involved in the activation of the NF-κB pathway. Therefore, endogenous compounds like 15-Deoxy-Δ12,14-prostaglandin J2 (15d-PGJ_2) (Rossi *et al.* 2000; Straus *et al.* 2000), 4-hydroxynonenal (Ji *et al.* 2001) and exogenous compounds such as triterpenoids; 2-cyano-3,12-dioxooleana-1,9,-dien-28-oic acid (CDDO), the C-28 methyl ester of CDDO (CDDO-Me), 1-[2-cyano-3,12-dioxooleana-1,9(11)-dien-28-oyl]imidazole (CDDO-Im), xanthohumol (a prenylated chalcone) and N-Tosyl-L-phenylalanine chloromethyl ketone (TPCK) (a serine/cysteine protease inhibitor), can inhibit the NF-κB pathway by covalent modifications of cysteine 179 within IKKβ (Ahmad *et al.* 2006; Yore *et al.* 2006; Ha *et al.* 2009; Harikumar *et al.* 2009). Hence, this modification will block the phosphorylation of IκBα by IKKβ and will inhibit the activation of NF–κB. NF-κB DNA binding can also be inhibited by cysteine modification by exogenous and endogenous compounds. For example, endogenous compounds such as 15d-PGJ_2 and ethyl pyruvate (Straus *et al.* 2000; Cernuda-Morollon *et al.* 2001; Han *et al.* 2005) have been shown to covalently modify cysteine 38 and 62 of p65 and p50, respectively. In addition, exogenous compounds such as TPCK, xanthohumol and organoselenium compounds (Chen *et al.* 2007; Ha *et al.* 2009; Harikumar *et al.* 2009) also show similar cysteine modification on p65 and p50.

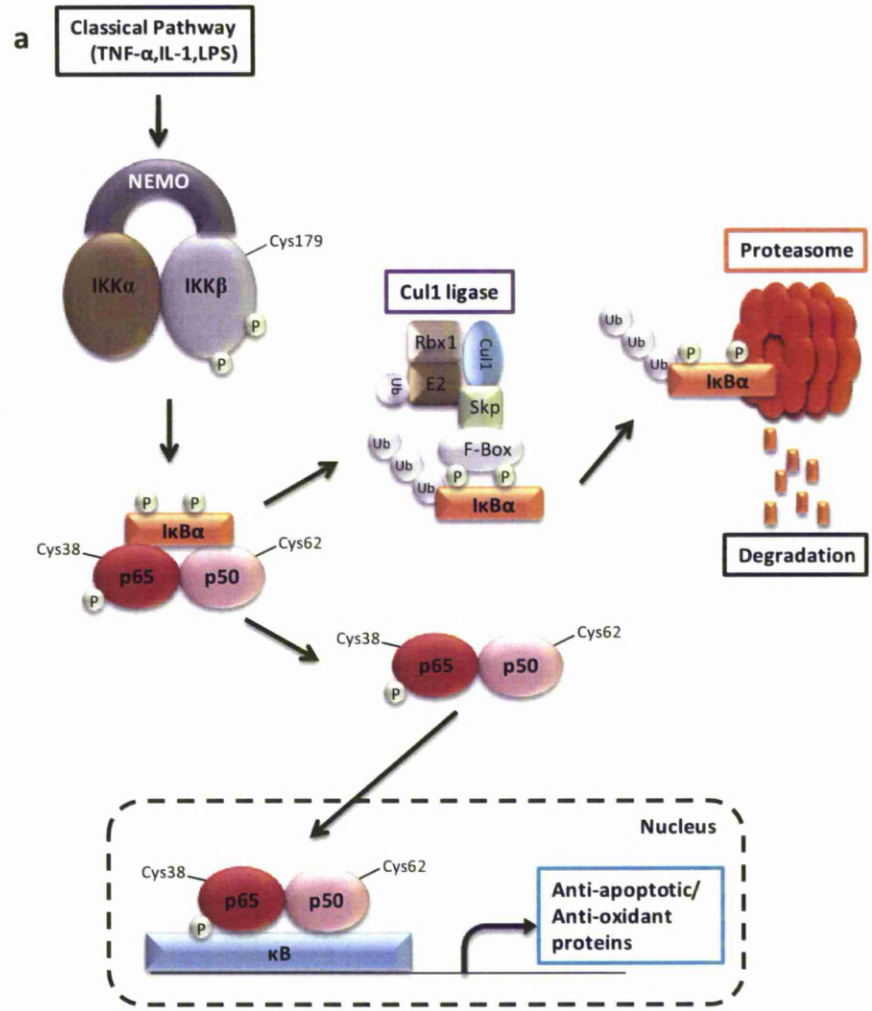

Figure 1.6: The classical NF-κB activation pathway (a). The classical pathway depends on the activation of IKKβ to phosphorylate IκB-α to allow p65/p50 NF-κB complex nuclear translocation. Adapted from (Perkins 2007).

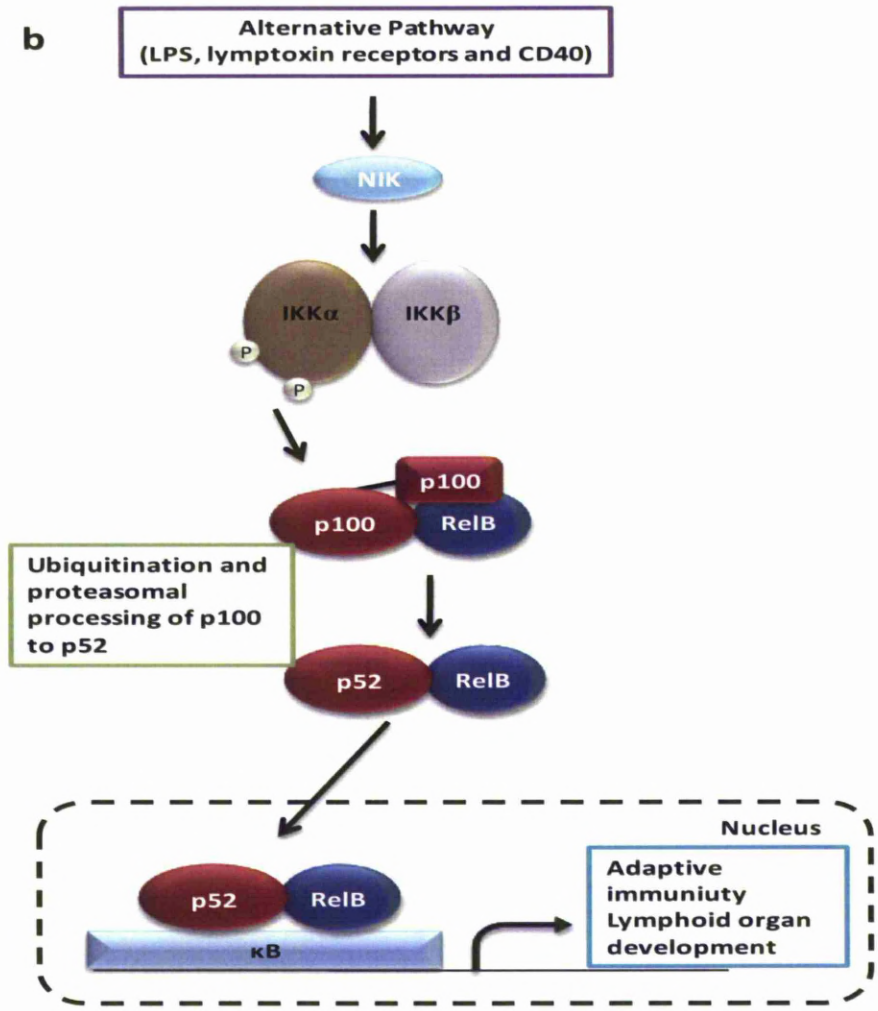

Figure 1.6: The alternative NF-κB activation pathway (b). The alternative pathway depends on the activation of IKKα by NIK to phosphorylate p100 NF-κB subunit and subsequent ubiquitination and processing to p52. This can lead to the activation of p52/RelB NF-κB complex nuclear translocation. Adapted from (Perkins 2007).

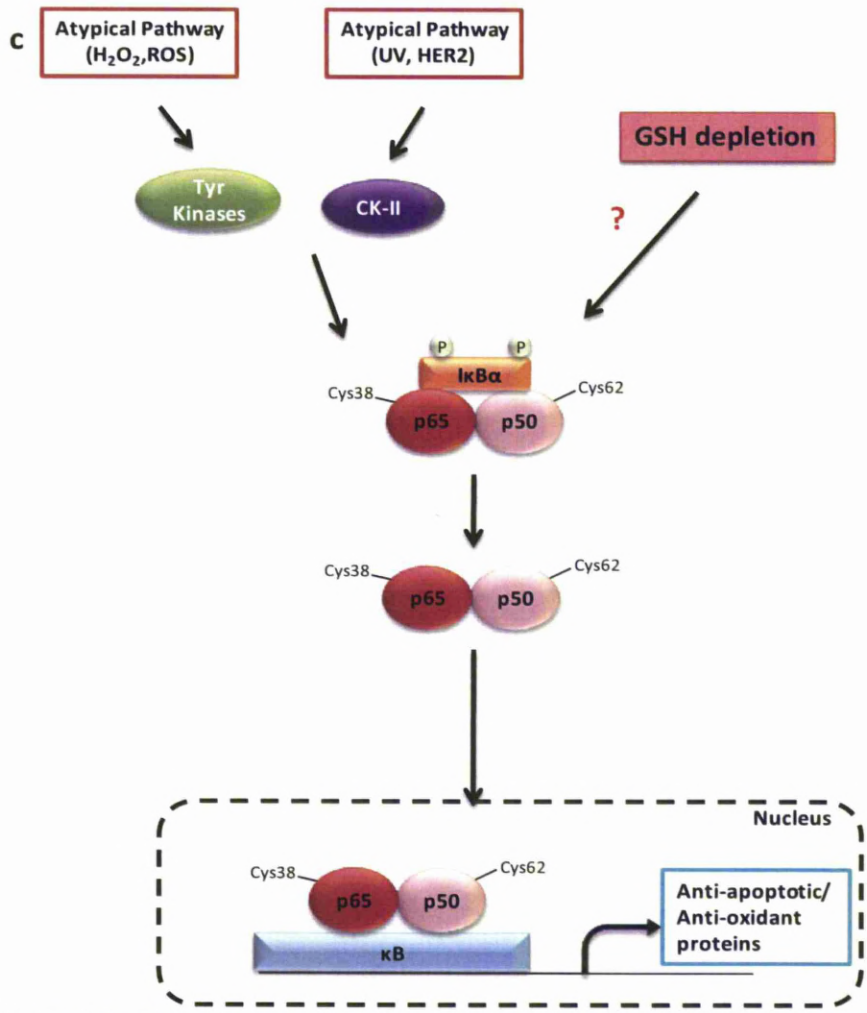

Figure 1.6: The atypical NF-κB activation pathway (c). The atypical pathway involves kinases to phosphorylate IκB-α and may be involved in the mechanism of p65/p50 NF-κB complex activation from GSH depletion. Adapted from (Perkins 2007).

1.6.2 The Keap1/Nrf2 pathway

1.6.2.1 The structure of Nrf2

Nrf2 is a member of the CNC family (see 1.4.3.1). Mouse and human Nrf2 contains six Nrf2-ECH homology (Neh) domains (Table 1.2) (Itoh *et al.* 1997) which are highly conserved among vertebrates (Fig 1.7) (Kobayashi *et al.* 2002). Nrf2 binding to the ARE involves a highly conserved cysteine residue (C506) in the Neh1 domain which leads to the transcription of Nrf2-dependent genes (Bloom *et al.* 2002). The binding of Nrf2 to the ARE results in the recruitment of coactivators of transcription such as the cAMP response element binding protein (CREB) - binding protein (CBP) and BRG1 (Brahma-related gene 1) through the Neh4 and Neh5 domains (Zhang *et al.* 2007a). Therefore, the interaction between Nrf2 and the transcriptional activators enables Nrf2 to regulate the transcription of its cytoprotective genes described in 1.4.3.1. Nrf2 also contains cysteine residues that are conserved through evolution. The mouse and rat Nrf2 contain 7 cysteines whilst the human Nrf2 contains 6 cysteines. The mouse Nrf2 which contains 7 cysteines is shown schematically in Fig 1.7 (He *et al.* 2009).

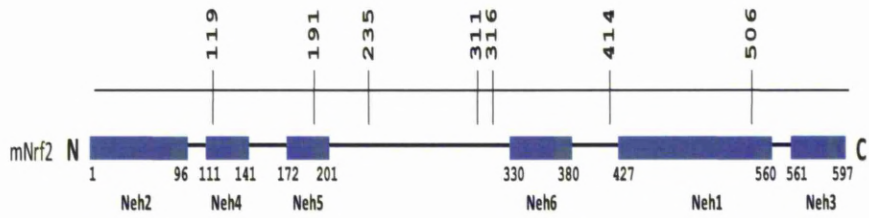

Figure 1.7: Schematic representation of the Nrf2 Neh domains. The six Neh domains are represented by blue boxes with each domain labelled. The line above represents the numbered Nrf2 cysteine residue.

Domain	Location in mouse Nrf2	Functions	References
Neh2	1-96	Contains DLG /DIDLID and ETGE motifs which binds to Keap1 Lysine-rich region for ubiquitinations Contain nuclear import signal (NLS) (amino acids 42-53)	(Itoh *et al.* 1999b; McMahon *et al.* 2004; Katoh *et al.* 2005; McMahon *et al.* 2006; Tong *et al.* 2006a; Theodore *et al.* 2008)
Neh4	111-141	Transactivation Interactions with transcription coactivator, CBP	(Katoh *et al.* 2001)
Neh5	172-201	Transactivation Interactions with transcription coactivators. CBP and BRG1 Contain nulcear export signal (NES) (amino acids 175-186)	(Katoh *et al.* 2001; Li *et al.* 2006; Zhang *et al.* 2007a)
Neh6	330-380	Regulate Nrf2 degradation in the nucleus of cell under oxidative stress	(McMahon *et al.* 2004)
Neh1	427-560	Contains the CNC and bZip regions Allows dimerisation with other bZip proteins Binds to ARE Contains NLS (amino acids 494-511 & 587-593) and NES (amino acids 545-554)	(Itoh *et al.* 1999b; Bloom *et al.* 2002; Jain *et al.* 2005; Theodore *et al.* 2008)
Neh3	561-597	Transactivation	(Nioi *et al.* 2005)

Table 1.2: Functions of Nrf2 Neh domains.

1.6.2.2 The role of phosphorylation in the regulation of Nrf2 activity

The activation of Nrf2 upon cellular stress is mainly based on the hypothesis of Keap1 cysteine covalent modification. This will be discussed in detail in 1.6.2.5. However, there are suggestions that the phosphorylation of Nrf2 can activate Nrf2 activity and the induction of its downstream cellular defence genes. There are many studies which have suggested that the phosphorylation of Nrf2 can act as a regulatory pathway for Nrf2 activation. These studies used pharmacological inhibitors of specific protein kinases and showed reduced Nrf2 activation by known activating molecules (Nguyen *et al.* 2000; Lee *et al.* 2001; Johnson *et al.* 2002; Bloom *et al.* 2003; Numazawa *et al.* 2003; Lee-Hilz *et al.* 2006). The potential role of protein kinase C in the phosphorylation of Nrf2 has been shown (Huang *et al.* 2000a; Huang *et al.* 2002; Bloom *et al.* 2003; Niture *et al.* 2009), as well as other protein kinases such as extracellular signal-regulated kinase1 (ERK-1) (Papaiahgari *et al.* 2006), phosphoinositide-3-kinase (PI3K) (Kang *et al.* 2002), c-Jun N-terminal kinase 1 (JNK1) (Keum *et al.* 2003), glycogen synthase kinase-3β (GSK-3β) (Salazar *et al.* 2006), protein kinase R (PKR)-like endoplasmic reticulum kinase (PERK) (Cullinan *et al.* 2003; Cullinan *et al.* 2004a), Mitogen-activated protein kinases (MAPK) (Cullinan *et al.* 2003; Zipper *et al.* 2003; Keum *et al.* 2006) and CK-II (Pi *et al.* 2007; Apopa *et al.* 2008) . Therefore, phosphorylation of Nrf2 may play an important regulatory step in Nrf2 activation.

1.6.2.3 The role of cysteines in Nrf2 activity

The regulation of Nrf2 activity is thought to be not solely governed by phosphorylation. The modification of Nrf2 cysteine residues can play a role in Nrf2 activity. A recent report by He and Ma suggested that Nrf2 cysteine residues can function as sensors in response to cellular stress (He *et al.* 2009). The report shows that known ARE inducers, arsenic and phenylarsine oxide (PAO), are able to induce Nrf2 activation by binding to Nrf2 cysteine residues. The mutation of Nrf2 cysteines to alanine (C235A, C311A-C316A, C414A or C506A) also shows an inhibition of the binding of PAO. Furthermore, arsenic induction of Nrf2 and NQO1 proteins was reduced by introducing mutation at C191A, C235A, C311A/C316A, C414A and C506A (He *et al.* 2009). However, more work has to be done to fully consolidate these findings and elucidate how Nrf2 cysteine residues play a role in the Nrf2 response to cellular stress.

1.6.2.4 The role and structure of Keap1

Keap1 is the inhibitory protein of Nrf2. It binds to the Neh2 domain of Nrf2, sequestering it in the cytoplasm under homeostatic conditions (Itoh *et al.* 1999b), and has similar sequence motifs found on the actin-binding Kelch protein in *Drosophila* (Xue *et al.* 1993). By binding to the actin cytoskeleton, Keap1 is located in the cytosol of the cells (Kang *et al.* 2004). The Keap1 protein, similar to Nrf2, is highly conserved in vertebrates (Fig 1.8) (Kobayashi *et al.* 2002) and it contains five domains, but only three of which are functional (Table 1.3). The human and mouse Keap1 proteins are cysteine-rich, consisting of 27 and 25 cysteines, respectively. The ratio of cysteines to other amino acids is 4.3% and 4.0% in human and mouse Keap1 respectively. This is above the average of 2.3% across all human and mouse proteins (Miseta *et al.*

2000). Furthermore, many Keap1 cysteine residues are flanked by one or more basic amino acids (arginine, lysine, histidine), resulting in them having low predictive pKa values and therefore making them highly reactive (Snyder *et al.* 1981). Keap1 has not only been suggested to serve as the regulator of Nrf2 but also to act as a 'sensor' for chemical and oxidative stresses (Prestera *et al.* 1993a; Talalay *et al.* 1995). The 25 Keap1 cysteines within the mouse protein are represented schematically in Fig 1.8.

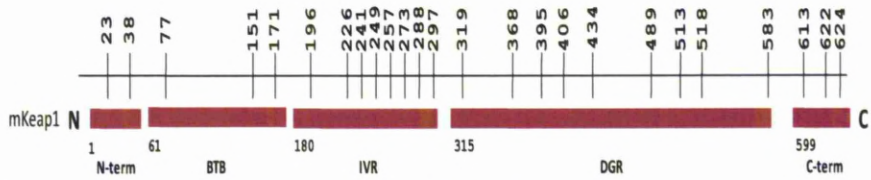

Figure 1.8: Schematic representation of Keap1 domains. The five domains are represented by red boxes with each domain labelled. The line above represents the numbered Keap1 cysteine residue.

Domain	Location in mouse Keap1	Functions	References
BTB (Broad complex/Tramtrack/Bric-a-brac)	67-178	Keap1 homodimerisation Cul3 ligase interaction	(Zipper *et al.* 2002; Cullinan *et al.* 2004b)
IVR (Intervening region)	179-321	Cysteine-rich region (8 cysteine residues in 102 amino acids)	
DGR (double glycine repeats)	322-608	Contains 6 double glycine repeats Interactions with Nrf2 Neh2 domain Binds to actin cytoskeleton	(Itoh *et al.* 1999b; Kang *et al.* 2004; Li *et al.* 2004; McMahon *et al.* 2006; Tong *et al.* 2006a)

Table 1.3: Keap1 functional domains.

1.6.2.5 The evidence for the chemical modification of Keap1 cysteine residues in the regulation of Nrf2 activity

There has been compelling evidence that shows reactive chemicals are able to modify sulphydryl groups resulting in the activation of the Keap1/Nrf2 pathway. This evidence was provided through the use of biotinylated Nrf2 inducing compounds (Itoh *et al.* 2004; Levonen *et al.* 2004), spectroscopic binding experiments and mass spectrometry (Dinkova-Kostova *et al.* 2002). These chemicals have been shown to react with the recombinant Keap1 by binding to cysteine residues, leading to activation of Nrf2 in *vitro* (Dinkova-Kostova *et al.* 2002; Dietz *et al.* 2005; Eggler *et al.* 2005; Hong *et al.* 2005a; Hong *et al.* 2005b; Liu *et al.* 2005; Luo *et al.* 2007; Copple *et al.* 2008a). Chemically-reactive compounds can also bind to Keap1 cysteines selectively in living cell-based models (Hong *et al.* 2005a; Copple *et al.* 2008a; Rachakonda *et al.* 2008).

Amongst all of the Keap1 cysteine residues that can be modified by chemicals, there are four cysteines (Cys257, Cys273, Cys288 and Cys297) located in the IVR domain, that have been consistently suggested to be highly sensitive and to be the ultimate effector of Nrf2 response (Dinkova-Kostova *et al.* 2002). Two out of these, Cys273 and Cys288, have been demonstrated to be important for the repressive activity of Keap1 under basal conditions (Zhang *et al.* 2003; Levonen *et al.* 2004; Wakabayashi *et al.* 2004; Kobayashi *et al.* 2006a; Yamamoto *et al.* 2008). Mutatgenesis studies *in vitro* show that the mutation of cysteines 273 or/and 288 to serine or alanine does not affect the association between Keap1 and Cul3 ligase (Kobayashi *et al.* 2004a) but it does abrogate the ubiquitination of Nrf2 by Cul3 ligase and subsequent proteasomal degradation, which is also observed by us in

the Centre for Drug Safety Science (CDSS) (unpublished data). This therefore permits Nrf2 accumulation and transcription of cytoprotective genes (Zhang *et al.* 2003; Levonen *et al.* 2004; Wakabayashi *et al.* 2004; Kobayashi *et al.* 2006a) and *in vivo* (Yamamoto *et al.* 2008). Another cysteine, Cys151, which has not been identified as part of the highly sensitive cysteine group mentioned previously, has also been postulated to be highly sensitive as well (Eggler *et al.* 2005). Cys151, which is located within the BTB domain of Keap1, also appears to play an important role in the repression of Nrf2 during chemical and oxidative stresses (Zhang *et al.* 2003; Zhang *et al.* 2004; Eggler *et al.* 2005). The Cys151 mutation to serine causes the abrogation of Nrf2 stabilisation to the presences of Nrf2 inducers (Zhang *et al.* 2003; Gao *et al.* 2007). It has been suggested that the inhibition of Nrf2 ubiquitination during cellular stress was due to the covalent modification of Cys151 which resulted in the dissociation of Cul3 ligase from Keap1 (Rachakonda *et al.* 2008). Hence, the evidence shown suggests strongly that the chemical modification of Keap1 cysteine residues, especially Cys151, Cys273 and Cys288, may be important in the activation of Nrf2. However, there is also the possibility that oxidative stress without drugs/electrophiles/reactive intermediates binding to cysteines can also activate Nrf2. It has been postulated that the oxidation of one or more cysteines in Keap1 can lead to the formation of sulphenic acid and the eventual formation of cysteine disulphide linkages (Wakabayashi *et al.* 2004). It has been shown that the depletion of GSH, without covalent binding to Keap1, can also lead to Nrf2 activation (Copple *et al.* 2008a). Therefore, the generation of CRMs may either form covalent adduct with Keap1 or induce cysteine oxidation within Keap1 by GSH depletion to activate Nrf2.

1.6.2.6 Keap1 regulation and the interaction with Nrf2

A two-site substrate recognition 'hinge and latch' model was recently proposed to be a key regulatory mechanism of Nrf2 regulation under homeostatic or stressed conditions (Tong *et al.* 2006a; Tong *et al.* 2006b). Keap1 has been suggested to exist as a homo-dimer intracellularly (McMahon *et al.* 2006), and that this binds to Nrf2 at a 2:1 ratio (Wakabayashi *et al.* 2004; Lo *et al.* 2006; Tong *et al.* 2006a). Keap1 binds to Nrf2 through the Neh2 domain. This interaction is permitted via the strong affinity ETGE motif (Kobayashi *et al.* 2002), the 'hinge' that allows Nrf2 to move freely in space (McMahon *et al.* 2006), and via the weaker affinity DLG motif, the 'latch' that positions Nrf2 for the ubiquitination of lysine residues (McMahon *et al.* 2006; Tong *et al.* 2006a). In line with this, the deletion or mutation of the ETGE motif attenuates the binding between Keap1 and Nrf2, resulting in an abrogated degradation of Nrf2 and subsequent accumulation (Kobayashi *et al.* 2002; Kobayashi *et al.* 2004a; Furukawa *et al.* 2005). On the contrary, the deletion or mutation of the DLG motif does not affect the binding between Keap1 and Nrf2 but it still abolishes Nrf2 degradation which also results in the accumulation of Nrf2 (McMahon *et al.* 2004; McMahon *et al.* 2006).

Nrf2 inducers can also activate the Keap1/Nrf2 pathway by promoting the accumulation of Nrf2 in the cytoplasm and nucleus. However, there is currently no evidence to suggest that they cause the complete disruption between Keap1 and Nrf2 binding which results in the release of Nrf2 (Zhang *et al.* 2003; Zhang *et al.* 2004; Eggler *et al.* 2005; Kobayashi *et al.* 2006a). Indeed, evidence suggests that these Nrf2 inducers may actually increase the interaction between Keap1 and Nrf2, probably through the reduction of Keap1-bound Nrf2 degradation (Hong

et al. 2005b; Hu *et al.* 2006; Kobayashi *et al.* 2006a). This is noticeable when protein synthesis is inhibited by cyclohexamide. Nrf2 nucleus accumulation is inhibited when cells are exposed to tBHQ, suggesting that de novo Nrf2 protein synthesis and not Nrf2 released from Keap1 accumulates in the nucleus (Kobayashi *et al.* 2006a). Under conditions of cellular stress, the ubiquitination of Nrf2 is attenuated through the disruption of the Nrf2/Keap1/Cul3 ligase complex in the 'hinge and latch' model (Zhang *et al.* 2004; Hu *et al.* 2006; Kobayashi *et al.* 2006a). The disruption of the complex is suggested to occur via the loss of the DLG motif interaction from Keap1 resulting in a conformational change via cysteine modification (McMahon *et al.* 2006; Tong *et al.* 2007). Due to the disruption of the Nrf2/Keap1/Cul3 ligase complex, Nrf2 is no longer targeted for ubiquitination and is therefore degraded. However, in this situation, Nrf2 is still bound to Keap1 via the ETGE motif. Thus, Keap1 is saturated and newly synthesised Nrf2 proteins are allowed to accumulate within the nucleus and induce the transcription of Nrf2-dependent genes (Fig 1.9) (Tong *et al.* 2006b). The evidence presented in this chapter support the major role played by the Keap1/Nrf2 pathway activated during cellular stress as part of a targeted cellular defence response.

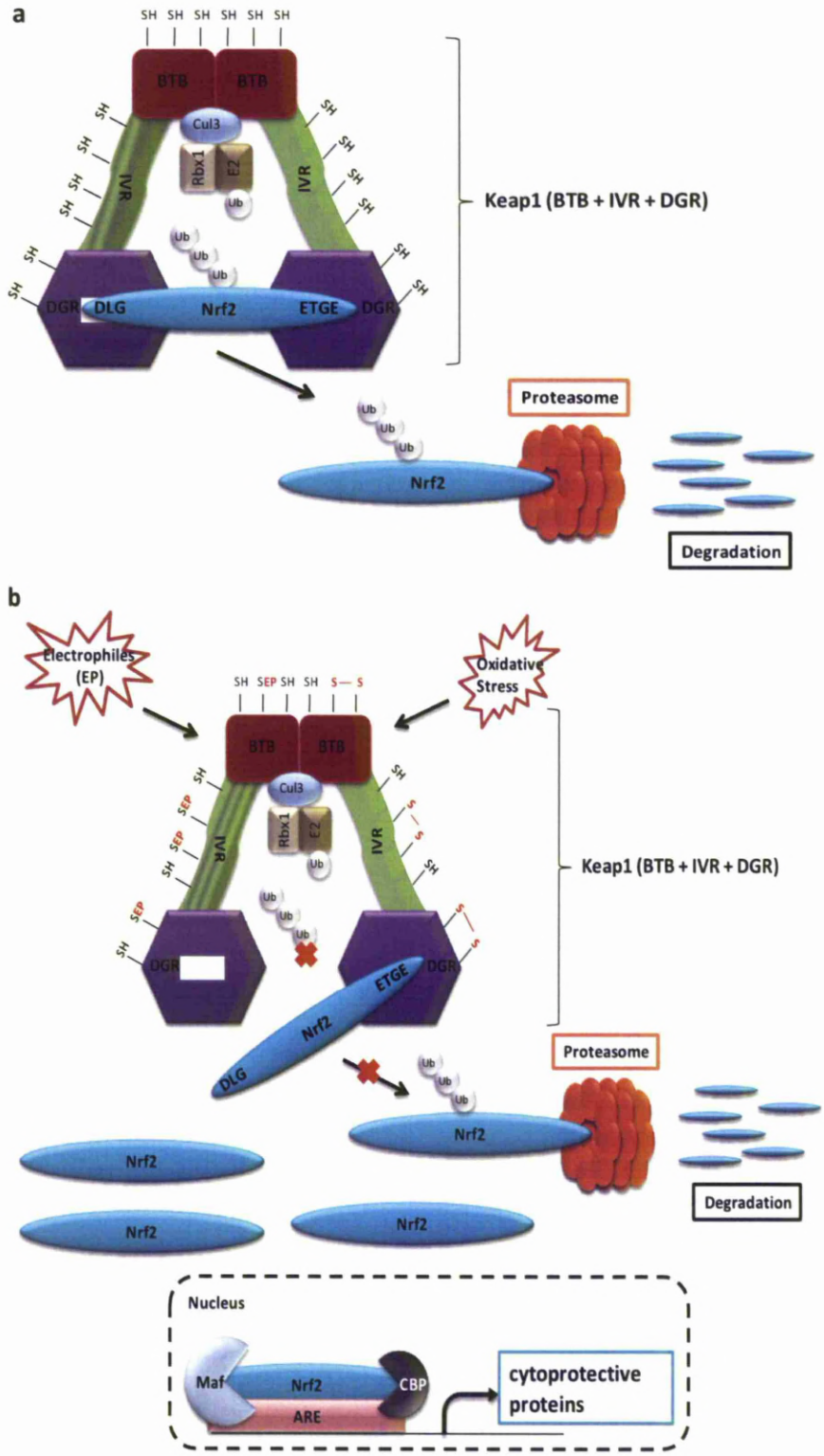
a
SH SH SH SH SH SH
BTB BTB
Cul3
Rbx1
E2
Ub
IVR
IVR
Keap1 (BTB + IVR + DGR)
Ub Ub Ub
DGR
DLG
Nrf2
ETGE
DGR
Proteasome
Ub Ub Ub
Nrf2
Degradation
b
Electrophiles (EP)
Oxidative Stress
SH SEP SH SH S— S
BTB BTB
Cul3
Rbx1
E2
Ub
IVR
IVR
Keap1 (BTB + IVR + DGR)
Ub Ub Ub
DGR
ETGE
DGR
Nrf2
DLG
Proteasome
Ub Ub Ub
Nrf2
Degradation
Nrf2
Nrf2
Nrf2
Nucleus
Maf
Nrf2
CBP
ARE
cytoprotective proteins

Figure 1.9: The 'hinge and latch' model of Nrf2 activation. Under basal conditions, the Keap1 homodimer, consists of BTB, IVR and DGR domains, binds to the ETGE and DLG motifs within the Nrf2 molecule, allowing Nrf2 ubiquitination and proteasomal degradation (a). In the presence of cellular stress, the modification of cysteines by electrophiles or from oxidative stress causes the disruption of the weaker affinity DLG motif (latch), probably through the induced conformational change in Keap1, while the binding of the stronger affinity ETGE motif (hinge) remains. The Nrf2 protein is still able to bind to Keap1 but is no longer being ubiquitinated and degraded. Hence, Keap1 is saturated with Nrf2 and newly synthesised Nrf2 can accumulate within the nucleus and lead to the transcription of cytoprotective genes (b). Adapted from (Tong *et al.* 2006b).

1.7 THE SYNCHRONIZED CELLULAR DEFENCE RESPONSE AGAINST CELLULAR TOXICITY

The cellular defence response consists of a variety of proteins such as the GSH biosynthetic enzymes, phase I and II enzymes, transcription factors and heat shock proteins (see Fig 1.10). Phase I or CYP450 enzymes form part of the cellular detoxification pathway. However, the generation of CYP450-dependent CRMs may still occur, as seen with the formation of NAPQI from APAP. These can be quenched by GSH and GSTs, or metabolised by Phase II enzymes, which also serve as a cellular detoxification pathway. Both pathways are part of the first line of cellular defence. If both pathways are overwhelmed, the transcription factors involved in cellular defence will be activated. These are the CNC family, NF-κB family, AP-1 family and HSF. The CNC family is made up of Nrf1, Nrf2 and Nrf3. Nrf2 in particular plays a major role in cellular defence by inducing the transcription of phase II metabolising enzymes and anti-oxidant proteins. The NF-κB family may play a role in cellular defence through the induction of anti-oxidant proteins, although its activity has been shown to be inhibited by CRMs. The AP-1 family has also been observed to protect cells by inducing the transcription of anti-

oxidant and GSH synthesis proteins. Heat shock proteins have been shown to be upregulated by cellular stress and to protect cells. HO-1 (HSP32), HSP25 and HSP70i have been reported to be induced during cellular stress and decrease cellular toxicity.

In conclusion, to respond to reactive drug metabolites, cells possess both basal and inducible layers of cell defence (Fig 1.3). Both forms of cellular defence play an important role in the cytoprotection of cells against the generation of reactive metabolites that may cause cell damage with the potential for ultimately triggering adverse effects.

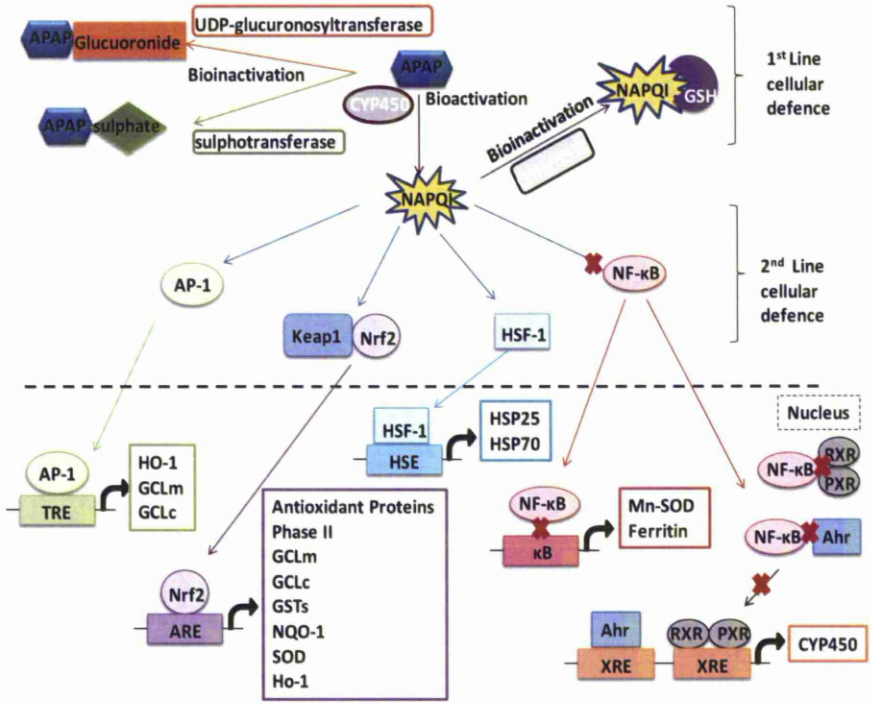

Figure 1.10: Schematic overview of the proteins involved in cellular defence, with an emphasis on redox-sensitive transcription factors involved in the APAP mechanism of hepatotoxicity. The first line of defence: APAP is bioinactivated by UDP-glucuronosyltransferase and sulphotransferase to the glucuronide and sulphate conjugates. Some of the APAP dose will be bioactivated by CYP450 to NAPQI. The generation of NAPQI is normally rapidly quenched by GSH/GSTs. During GSH depletion, where APAP reaches high levels, excess NAPQI generated can either activate or inhibit second line defence. Second line of defence: activated transcription factors include Nrf2, AP-1 and HSF which enable the transcription of cytoprotective proteins, antioxidants, GCLc, GCLm phase II enzymes and HSPs. NF-κB is inhibited by NAPQI which may lead to the inhibition of antioxidant transcription but may also down-regulate the anti-apoptotic role of NF-κB. However, this remains to be proven. Furthermore, inhibited NF-κB may not be able to bind to CYP450 nuclear receptors and suppress the transcription of CYP450. This could potentially result in an increase in CYP450 and an elevated formation of reactive drug metabolites, although, again this mechanism is still unproven (Blazka *et al.* 1995; Salminen *et al.* 1997a; Boulares *et al.* 1999; Tian *et al.* 1999; Kitteringham *et al.* 2000; Ke *et al.* 2001; Chiu *et al.* 2003; Goldring *et al.* 2004; Sumioka *et al.* 2004; Zhou *et al.* 2005; Gu *et al.* 2006; Zhou *et al.* 2006; Copple *et al.* 2008a; Randle *et al.* 2008).

1.8 THESIS AIMS

The liver can defend itself against chemical or oxidative stress triggered by drugs or their reactive metabolites, through the upregulation of its defence response. In order to remove the toxic insult as a result of cellular stress, the hepatic defence response will trigger a series of different tiers of defence. The adaptive defence tier is partly regulated by a group of transcription factors which play a critical role in the defence response against cell stress. Hence, understanding the molecular mechanisms that underlie the activation of these transcription factors is important in elucidating the events leading to the progression and consequences of cell damage, liver injury and possibly DILI. Two of the key pathways involved in these regulations are Keap1/Nrf2 and NF-κB.

A limited degree of inter-individual variability in the Keap1/Nrf2 pathway has been observed within the human population. Polymorphisms in the promoter region of *NRF2* gene in humans (Yamamoto *et al.* 2004; Arisawa *et al.* 2007; Marzec *et al.* 2007; Arisawa *et al.* 2008; Hua *et al.* 2010) and mice (Cho *et al.* 2002) have been identified, and these mutations are linked with an increase in susceptibility to some diseases (Cho *et al.* 2002; Arisawa *et al.* 2007; Marzec *et al.* 2007; Arisawa *et al.* 2008; Hua *et al.* 2010), such as hypoxia, chronic obstructive pulmonary and peptic ulcer diseases. Currently, there is no evidence of predisposing polymorphisms in the human or mouse *KEAP1* genes. On the other hand, cancer development related to somatic Nrf2 mutations have been observed in lung, laryngeal, oesophageal and skin carcinomas (Kim *et al.* 2010b), and loss-of-function somatic mutations in *KEAP1* resulting in uncontrolled Nrf2 activation have been identified in lung, breast and bile duct cancer cell lines, bile duct and gall bladder primary tumours and also in lung cancer

patients (Padmanabhan *et al.* 2006; Singh *et al.* 2006; Nioi *et al.* 2007; Shibata *et al.* 2008). Hence, variability can influence cellular defence and it is important to determine how the Keap1/Nrf2 pathway is activated, as well as how its threshold is set for prevention of cellular damage. By understanding how cells defend themselves, we may ultimately begin to explore the question as to whether individuals are more prone to damage if this normal pathway is perturbed.

Furthermore, little is known regarding the control of this pathway in the context of the key transcription pathway NF-κB, crucial to how hepatocytes respond to chemical injury. Therefore, the aims of this thesis are to: 1) Explore the simultaneous regulation of transcription factors Nrf2 and NF-κB under cellular stress, and therefore the balance between cell protection and cell death. 2) To explore further the mechanism(s) of Nrf2 activation, either by (i) cysteine modifications within Keap1 or (ii) GSH depletion without concomitant Keap1 cysteine modification, through the usage of a panel of chemicals. 3) To evaluate novel click compounds in the investigation of Nrf2 activation. 4) To establish the Keap1 thiol status during basal conditions and 5) to begin to address the question do the Keap1 cysteines undergo oxidation as well as covalent modification during chemical or oxidative stress?

Addressing these aims will improve the understanding of the role of both pathways regulated during chemical stress and may gain further insight into the role of cellular protection during DILI.

CHAPTER 2

Differential effect of covalent protein modification and glutathione depletion on the transcriptional response of Nrf2 and NF-κB

CONTENTS

2.1 INTRODUCTION

Man is constantly exposed to chemical stress which can be exacerbated by the increasing use of therapeutic drugs. However, under extreme level of exposure, such as an overdose, manifestation of toxicity may occur. The mechanisms underlying the toxicity associated with exposure to these therapeutics agents are not clearly defined but are likely to involve chemical stress and/or oxidative stress. Chemical stress comprises the generation of a reactive drug metabolite from its parent compound and subsequent covalent modification of critical proteins (Zhou *et al.* 2005). Oxidative stress is the generation of reactive oxygen species from the metabolism of drugs by cytochrome P450 enzymes and through mitochondrial uncoupling, but it may also arise from mitochondria permeability transition. (Jaeschke *et al.* 2002). Hence, both chemical and oxidative stress can evoke cellular defence response via transcription factors during drug induced liver injury (DILI).

DILI is a major cause of hospital admissions (Pirmohamed *et al.* 2004), and one of the principal reasons for attrition of new chemical entities (Park *et al.* 2005a). For example, acetaminophen (APAP), a commonly used analgesic known to induce liver injury on overdose, accounts for the most common form of acute liver failure in the United States (Ostapowicz *et al.* 2002). A proportion of the pathogenesis of DILI may occur through the generation of chemically reactive metabolites (CRMs), usually formed through oxidative metabolism of drugs by phase 1 enzymes (Park *et al.* 2005a). CRMs can covalently modify critical proteins, and bind to and deplete glutathione (GSH), the predominant cellular redox buffer. This causes disturbance to the cellular redox potential yielding a more oxidising environment (DeLeve *et al.* 1991). Although there are defence mechanisms present to counter such

disturbances (Prestera *et al.* 1995), if the chemical challenge is overwhelming and the defence is breached, a switch from cell defence to cell death is favoured either by apoptosis or necrosis [for a review, see (Park *et al.* 2005a)]. Thus, a cell will defend itself where possible, but under extreme conditions it may allow itself to die. The ability of a cell to respond to chemical stress occurs at least partially through the activation of transcription factors. These transcription factors are constitutively present in the cell or are rapidly synthesised when required, facilitating the upregulation of proteins implicated in cell defence or cell death. Nuclear factor-erythroid 2 (NF-E2)-related factor (Nrf2) and NF-kappa B (NF-κB) are two redox-sensitive transcription factors, which have been extensively investigated with aim to determine the role of transcriptional adaption to chemical stress.

Nrf2 plays a crucial role in cellular defence, and is the major regulator of antioxidant response elements (AREs) present in the regulatory region of the majority of cytoprotective genes (Itoh *et al.* 1997). Under basal conditions, Nrf2 is sequestered by Keap1 in the cytoplasm (Itoh *et al.* 1999b), and is constitutively targeted for ubiquitination by the Cullin3-dependent E3 ubiquitin ligase complex, which results in its subsequent proteasomal degradation (Zhang *et al.* 2004). Under certain stress conditions, such as exposure to electrophiles or an increase in reactive oxygen species (ROS), cysteine residue on Keap1 are readily modified. This suggests that Keap1 undergoes a conformational change, blocking Nrf2 ubiquitination and enabling nuclear accumulation of Nrf2 and transactivation of ARE-dependent genes (Dinkova-Kostova *et al.* 2002; Zhang *et al.* 2003).

Nuclear factor kappa-light-chain-enhancer-of activated B cells (NF-κB) comprises five members belonging to the mammalian NF-κB

family, i.e., p65 (Rel A), RelB, c-Rel, p50/p105 (NF-κB1) and p52/p100 (NF-κB2). NF-κB exists in the cytoplasm of unstimulated cells as homo- or hetero-dimers, bound to a family of inhibitory proteins known as IkappaB (IκB) via non-covalent interactions. The predominant hetero-dimer present in cells is p65/p50 dimer (Hayden *et al.* 2004). Upon stimulation, the IκB kinase (IKK) complex which consists of a complex with two subunits, IKKα and IKKβ, and a regulatory subunit, NF-κB essential modifier (NEMO) (Mercurio *et al.* 1999), phosphorylates IκB-α (Brockman *et al.* 1995). Upon phosphorylation, IκB-α is targeted for ubiquitination and directed for proteasomal degradation (May *et al.* 1998). This allows the release of NF-κB and its nuclear accumulation resulting in the transcription of genes involved in the inflammatory response, cell proliferation, cell survival and to a limited degree, the anti-oxidant response.

To date, there is little evidence for simultaneous regulation of Nrf2 and NF-κB within cells and little is known about the cellular consequences of such co-regulation. It may be valuable to understand what is happening to both transcription factors simultaneously to begin to understand the likely mechanisms that occur when a cell is exposed to chemical stress. I have attempted to begin to explore the role of simultaneous regulation of these two transcription factors through the experiments presented in this chapter, which are designed to investigate the functional outcome of chemical stress/protein modification on the transcription factors as well being informative of how the cells actually detect these stresses. In this study, I hypothesised that the balance between both transcription factors might serve as a key cytoprotective mechanism to detect and respond to cell stress, where activation or

inhibition of NF-κB, or Nrf2, or both transcription factors, may dictate the cellular response to stress.

2.2 MATERIALS AND METHODS

2.2.1 Materials

The mouse hepatoma cell line, Hepa-1c1c7 was obtained from American Type Culture Collection (Manassas, VA, USA). The rabbit anti-mouse Nrf2 primary antibody was kindly donated by Professor John Hayes (Biomedical Research Centre, University of Dundee, UK). The recombinant mouse His-tagged Nrf2 was kindly donated by Dr Ian Copple (MRC Centre of Drug Safety Science, University of Liverpool, UK) Rabbit anti-mouse NF-κB p50, monoclonal anti-mouse NF-κB p65, Goat anti-mouse Keap1 primary antibodies were from Santa Cruz Biotechnology (Heidelberg, Germany). Rabbit anti-goat HRP-conjugated secondary antibody was from Dako UK (Ely, UK). DMEM and trypsin/versene were from Lonza Biologics (Slough, UK). The Wilovert D6330 light microscope was from Will-Wetzlar (Wetzlar, Germany). The SP2 AOBS confocal microscope was from Leica Microsystems (Milton Keynes, UK). Nunclon Δ cell culture flasks, dishes, multi-well plates and LabTek II chamber slides were from Nalge-Nunc International (c/o VWR international, Lutterworth, UK). Vectashield was from Vector Laboratories (Peterborough, UK). Protein assay dye reagent, Precision Plus protein Kaleidoscope standards, non-fat dry milk, Mini Trans-Blot Cell and the GS-710 calibrated imaging densitometer were from Bio-Rad (Hemel Hempstead, UK). FBS, NuPAGE Novex 4-12% Bis-Tris gels, NuPAGE LDS sample buffer, sample reducing agent and antioxidant, XCell Surelock mini-cell, Hoechst 33258, Lipofectamine 2000, NF-κB p65 and control RNAi duplexes were from Invitrogen (Paisley, UK). The Nrf2, Keap1 and control RNAi duplexes were from Dharmacon (Lafayette, USA). The Cytotoxicity Detection Kit was from Roche Diagnostics (Burgess Hill, UK). The MRX microplate reader was from Dynatech Laboratories (Billingshort, UK). The TotalLab 100 software was from

Nonlinear Dynamics (Newcastle, UK). Western Lightening Enhanced Chemiluminescence reagents and adenosine 5'-triphosphate, [γ-32P] ATP were from Perkin Elmer (Seer Green, UK). The Hybond nitrocellulose membranes, Hyperfilm HCL, Hoefer SE600 Ruby electrophoresis system and Polydeoxy(Inosinate-Cytidylate) Acid, Sodium Salt were from GE Healthcare Life Sciences (Little Chalfont, UK). Storage Phosphor Screen, Phosphor Imager and ImageQuant software were from Molecular Dynamics (Sunnyvale, CA). Consensus NF-κB oligonucleotide, T4 Polynucleotide Kinase and buffer were from Promega (Southampton, UK). Penicillin-streptomycin solution, Trypan Blue solution, NAPQI, DNCB, DMSO, BSO, BSA, MOPS, DTNB, GSH, NADPH, GSH reductase, β-mercaptoethanol, Triton X-100, spermidine, spermine, protease inhibitor cocktail, the rabbit anti-actin primary antibody, the goat-anti rabbit HRP-conjugated secondary antibody, anti-rabbit IgG (whole molecule)–FITC antibody produced in goat, anti-mouse IgG (whole molecule)–FITC antibody produced in goat, the Kodak BioMax MS intensifying screen, Kodak developer and fixer solution, Ponceau S solution, Tween 20, PBS tablet, paraformaldehyde, sulphosalicyclic acid, HEPES and Coomassie Brilliant Blue G-250 dye were from Sigma-Aldrich (Poole, UK). All other reagents were of analytical or molecular grade and were from Sigma-Aldrich.

2.2.2 Cell Culture and Cell Count

The mouse hepatoma cell line, Hepa-1c1c7, which has been employed by others in previous studies of the Keap1/Nrf2 pathway (Jowsey *et al.* 2003; Natsch *et al.* 2008; He *et al.* 2010; Nguyen *et al.* 2010) and NF-κB pathway (Korashy *et al.* 2008), was maintained at 37°C in a 5% CO_2 atmosphere in conventional growth medium Dulbecco's modified Eagle's medium (DMEM) supplemented with 584mg/L L-

gutamine, 10% fetal bovine serum (FBS), 100 U/ml penicillin, and 100ug/ml streptomycin. Cells were grown in 75cm^2 Nunclon Δ culture flasks and routinely passaged every 2-3 days, at around 80% confluency. Following a wash with unsupplemented DMEM, cells were incubated with 5ml of trypsin/versene for 1min at room temperature. Removal of trypsin/versene and the cells were returned to the incubator for 5min allowing sufficient time to enable complete detachment of cells from the flask surface. Cells were then resuspended in 10ml growth medium and homogenised five times through a 21-gauge needle, using a 10ml syringe to break up any cell clumps. For continuation, cells were re-seeded at a cells:growth medium ratio of 1:4.

Cells were counted using Trypan Blue solution (0.4% weight/volume; w/v) and a haemocytometer to ensure that an accurate numbers of cells were seeded. Cells were detached as mentioned above, 45μl aliquot of cells was combined with 5μl Trypan Blue solution. 10μl of this mixture was transferred to the edge of a haemocytometer. Cells were visualised using 20X objective of a Wilovert D6330 light microscope. Viable cells (no Trypan Blue dye up take) within the central 5 x 5 square (equivalent to 0.1mm^3) were counted and the original cell density was calculated as follows: Number of cells counted x 1.1 (to correct for dilution with Trypan Blue solution) = cells per 0.1mm^3 x 10,000 = cells per 1cm^3 = cells per 1ml

2.2.3 Cell Treatment

Hepa-1c1c7 cells were seeded onto 96-well plates, 24-well plates, 56.7cm^2 Nunclon Δ culture dishes at 2 x 10^4 cells/well, 2 x 10^5 cells/well, 5 x 10^6 cells/dish respectively on the previous day. Cells were washed once with unsupplemented DMEM and then 99μl, 495μl and 9.99ml of unsupplemented DMEM was added to 96-well plates, 24-well

plates and culture dish, respectively. N-acetyl-*p*-benzoquinoneimine (NAPQI) and dinitrochlorobenzene (DNCB) were dissolved in dimethyl sulfoxide (DMSO) except for buthionine sulfoximine (BSO), which was dissolved in dH_2O, at 100x the final concentration. To each dish, 10µl of the dissolved compounds or DMSO were added (1:1000 dilutions). For 96-well plates and 24-well plates, all compounds or DMSO were further diluted 10-fold in unsupplemented DMEM, and then 1µl and 5µl were added to each well (1:100 dilution) respectively. The overall concentration of DMSO in the cell culture medium was 0.1% (volume/volume; v/v). The cells were then placed back in the incubator for the indicated time.

2.2.4 Preparation of cytosolic and nuclear extracts and whole cell lysates

After treatment, cells were washed once with unsupplemented DMEM, removed from the surface of the culture dish by scraping and resuspended in 1 ml buffer A (lysis; 50mM NaCl, 10mM 4-(2-hydroxyethyl)-1-piperazineethanesulfonic acid (HEPES), 1mM ethylenediaminetetraacetic acid (EDTA), 0.5mM sucrose, 0.5mM spermidine, 0.15mM β-mercaptoethanol, 0.2% (v/v) protease inhibitor cocktail, 0.2% (v/v) Triton X-100). Lysates were centrifuged at 3500rpm, 4°C, for 5min, and the supernatant was retained as the cytosolic fraction. For nuclear protein extraction, the pellet was washed in 0.5ml buffer B (wash; 25% (v/v) glycerol, 50mM NaCl, 10mM HEPES, 1mM EDTA, 0.5mM spermidine, 0.15mM spermine, 10mM β-mercaptoethanol, 0.2% protease inhibitor cocktail) and centrifuged at 3500rpm, 4°C, for 5min. Following removal of the supernatant, the pellet was resuspended in 0.1ml buffer C (extraction; 0.35M NaCl, 25% (v/v) glycerol, 10mM HEPES, 1mM EDTA, 0.5mM spermidine, 0.15mM

spermine, 10mM β-mercaptoethanol, 0.2% protease inhibitor cocktail) and incubated on ice for 30min, to facilitate the osmotic extraction of nuclear proteins, which was clarified with a final centrifugation at 3500rpm, 4°C, for 5min (Dignam *et al.* 1983). All subcellular fractions were stored at -80°C before analysis.

For whole cell lysate preparation, cells were lysed with 0.1ml radioimmunoprecipitation assay (RIPA) buffer (0.15M NaCl, 1% (v/v) NP-40, 0.5% (v/v) sodium deoxycholate, 0.1% (v/v) SDS, 25mM Tris-Cl, 0.2% (v/v) protease inhibitor cocktail) and incubated on ice for 5min before storing at -80°C to quick freeze cells. Clarification before analysis was necessary as freeze-thaw cycles may denature protein aggregates. Cell lysates were clarified with centrifugation at 3500rpm for 10min to pellet cell debris.

2.2.5 Measurement of protein content

The total protein content of cytosolic and nuclear fractions was determined using Protein Assay Dye Reagent based on the method of Bradford (Bradford 1976). This assay relies on the binding of Coomassie Brilliant Blue G-250 dye to basic and aromatic amino acids, that results in a change in dye colour from red to blue, and a consequent change in absorbance maximum from 465 to 595nm. Hence, the increase in absorbance at 570nm, measured using a MRX microplate reader, is proportional to the amount of dye and to the amount of protein present. A standard curve, ranging from 0.0125 – 0.25μg bovine serum albumin (BSA) was used to calculate the protein content.

2.2.6 Western immunoblotting

Cytosolic (15μg) or nuclear extracts (5μg) or whole cell lysates(10μg) were added to 5μl loading buffer (70% (v/v) NuPAGE sample loading buffer, 30% (v/v) Nupage reducing agent) and denatured

by incubating at 80°C for 5min. Samples were loaded onto pre-cast 4-12% NuPAGE Novex bis-tris ployacrylamide gels, alongside PrecisionPlus Protein Kaleidoscope standards. Samples were resolved by electrophoresis in a XCell Surelock mini-cell, using a 3-(N-morpholino)propanesulphonic acid (MOPS) running buffer (50mM MOPS, 50mM tris base, 3.5mM sodium dodecyl sulphate, 1mM EDTA, 0.25% (v/v) NuPAGE antioxidant), running at 90V for 10min, followed by 60min at 170V. Separated proteins were transferred to Hybond nitrocellulose membranes using Bio-Rad Mini Trans-Blot cell, in accordance with the manufacturer's instructions. To determine that the transfer process was successful, membranes were stained with Ponceau S solution for 10sec. Membranes were blocked for 15min with 10% (w/v) non-fat dry milk (Bio-Rad) in tris-buffered saline (TBS; 0.15M NaCl, 25mM Tris base, 3mM KCl, pH 7.0) containing 0.1% (v/v)Tween 20. Blocked membranes were probed with rabbit anti-mouse Nrf2 (1:5000 in TBS-Tween containing 2% (w/v) BSA) or anti-goat Keap1 (1:2000 in TBS-Tween containing 2% (w/v) BSA) for 1hr. After several washes, membranes were probed with goat anti-rabbit or rabbit anti-goat (1:10000 in TBS-Tween containing 2% (w/v) non-fat dry milk) horseradish peroxidise (HRP)-conjugated secondary anti-IgG for 1hr. Western blots were visualised using Western Lightening Enhanced chemiluminescence reagent and exposed to Hyperfilm ECL under darkroom conditions, using a Kodak BioMax MS intensifying screen and developed using Kodak developer and fixer solutions. All blots were also probed with rabbit anti-β-actin primary (1:5000 in TBS-Tween containing 2% (w/v) BSA) and goat anti-rabbit HRP-conjugated secondary anti-IgG for 1hr to ensure equal loading. Recombinant mouse His-tagged Nrf2 (+ con) was loaded as a standard to confirm antibody specificity. Western blot films were scanned using a GS-710 calibrated imaging densitometer,

western blot band volumes were quantified using TotalLab 100 software and normalised against actin.

2.2.7 NF-κB Electrophorectic mobility shift assay (EMSA)

A consensus NF-κB wild type (WT) oligonucleotide probe 5' to 3' strand: (5'-AGT TGA GGG GAC TTT CCC AGG C-3') (Lenardo *et al.* 1989) was 5' end-labelled with adenosine 5'-triphosphate, [γ-32P] ATP. The oligonucleotide labelling was prepared by addition of 20% (v/v) NF-κB WT probe (1.75pmol/μL) to 10% (v/v) T4 Polynucleotide Kinase 10X buffer, 10% (v/v) [γ-32P] ATP (250μCi), 50% (v/v) water and 10% (v/v) T4 Polynucleotide Kinase (5-10U/ul). The labelled oligonucleotide was incubated for 20min at 37°C; the reaction was terminated by the addition of 10% (v/v) 0.25M EDTA and reconstituted in 90% (v/v) 1X Tris-EDTA buffer. The radiolabelled oligonucleotide was stored at -20°C.

EMSA loading samples consisted of; 5X binding buffer (20% (v/v) Ficoll, 100mM HEPES, 175mM NaCl, 300mM KCl, 0.05% (v/v) NP40 and 10mM dithiothreitol (DTT)), poly dI.dc (0.1ug/ul), nuclear extracts and water. The EMSA loading samples were prepared in order indicated in table 2.1 and were incubated at room temperature for 10min.

5x Binding Buffer	2μl
Poly dI.dc	1μl
Distilled Water	make up to volume of 10μl
Nuclear extracts	5μg (volume not greater than 4μl)

Table 2.1: Preparation of EMSA loading samples as indicated.

To the EMSA loading samples, 1μl of radiolabelled oligonucleotide was added and incubated at room temperature for 20min. The definition of a NF-κB specific shift was made according to the following criteria; supershift assays using NF-κB specific antibodies, addition of 1μl of

mouse anti-p65 and/or anti-p50 (Santa Cruz) and a control non-specific antibody was added to the loading sample. For competition assays, 1µl of unlabelled wild-type (WT) or mutant (MUT) (5'-AGT TGA GGC GAC TTT CCC AGG C-3') oligonucleotides were added to the loading sample. The antibodies, or unlabelled WT and MUT oligonucleotides, were added 10min prior to addition of labelled oligonucleotide. Samples were loaded onto a 5% polyacrylamide gel, which was pre-run for 30min at 160V. The protein-DNA complexes were resolved by non-denaturing electrophoresis using a Hoefer SE 600 Ruby vertical electrophoresis system for 1.5hr at 200V in 0.5x Tris-Borate-EDTA buffer. After electrophoresis, the gel was fixed in 10% (v/v) methanol/10% (v/v) acetic acid for 30min. The fixed gel was transferred onto a sheet of filter paper, covered with Saran wrap and vacuum-dried. Dried gels were subsequently exposed to a Storage Phosphor Screen for 12hr, before being scanned by a Phosphor Imager. The gels were visualised and bands were quantified using ImageQuant software.

2.2.8 Confocal Microscopy

Hepa-1c1c7 cells were plated out on Lab-Tek II chamber slides at 2.5 x 10^5 cells/chamber for 24hr before treatment. Following treatment, cells were washed 2 x 3min with 0.5ml 1X phosphate-buffered saline (PBS; 0.137M NaCl, 10mM NA_2HPO_4, 1.8mM KH_2PO_4, 2.7mM KCl, pH7.4) and fixed in 0.5ml fresh 4% (w/v) paraformaldehyde at 4°C for 30min, and cells were then washed 4 x 3min with 0.5ml 1X PBS. Fixed cells were then permeabilised with 0.5ml of 0.2% (v/v) Triton X-100, quenched with 0.5ml 100mM glycine and blocked with 0.5ml of 10% (v/v) FBS, for 10min each. Cells were then incubated with 0.2ml of rabbit anti-mouse Nrf2 or monoclonal anti-mouse NF-κB p65 (1:500) in 2% (v/v) FBS at 37°C for 1hr. Following 3 x 3min washes with 0.5ml 1X PBS, cells were

incubated with 0.2ml of FITC-conjugated goat anti-rabbit or FITC-conjugated goat anti-mouse (1:250) in 2% FBS at 37°C for 1hr. Cells were washed 3 x 3min again with 0.5ml 1X PBS and nuclei DNA were counter-stained with 0.2ml of Hoechst 33258 (2ug/ml) in PBS at room temperature for 10min. Cells were then washed 3 x 3min with 0.5ml 1X PBS. Chambers were detached from the slides using the splitting tool provided by manufacturer, and allowed to dry at room temperature for 5min. Coverslips were mounted using Vectashield hard-set medium in accordance with the manufacturer's instructions. Slides were covered with aluminium foil and stored at 4°C before confocal analysis. Immunofluoresence was visualised using a Leica SP2 AOBS confocal microscope.

2.2.9 RNA interference

Short interfering RNA (siRNA) has been used as an analytical tool for the study of genes function in mammalian cells. Hence, depletion of Nrf2, Keap1 and NF-κB in Hepa-1c1c7 cells was achieved using RNAi, which works on the process of post-transcriptional gene silencing by cleavage and degradation of the messenger RNAs (mRNAs) with complementary sequences (Leung *et al.* 2005). RNAi is triggered when a cell encounters a long double stranded RNA (dsRNA) molecule (Fire *et al.* 1998). The dsRNA is cleaved by an enzyme called Dicer into shorter fragments known as small interfering RNAs (siRNA) consisting of 21-22 nucleotide. The cleaved siRNAs will produce "sense" and "antisense" strand siRNA. The "sense" strand will be degraded and "antisense" strand will be incorporated in a RNA-inducing silencing complex (RISC). RISC will be activated upon the binding of the "antisense" siRNA and degradation of targeted complementary mRNAs (Elbashir *et al.* 2001; Novina *et al.* 2004; Preall *et al.* 2005)(Fig 2.1).

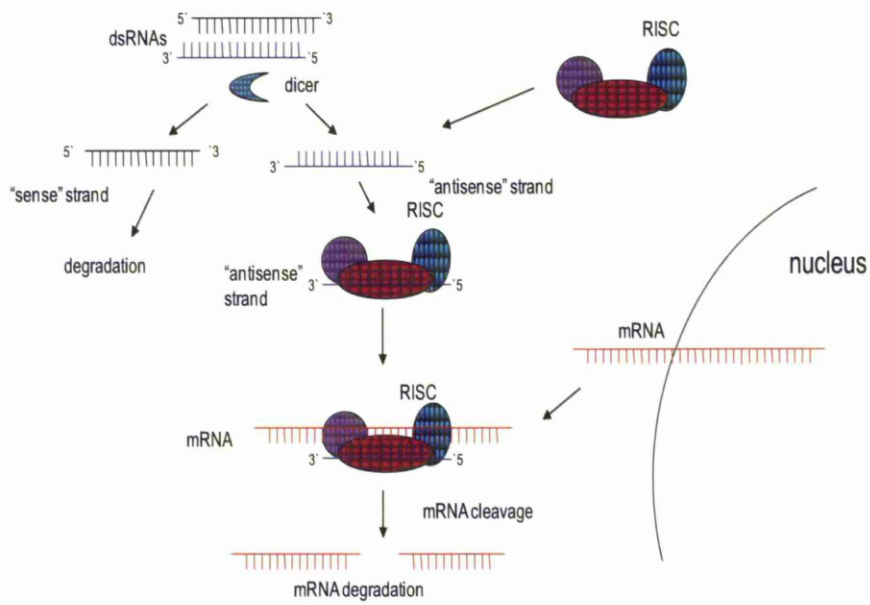

Figure 2.1: Mechanism of RNAi pathway. The RNAi pathway is triggered when the cell encounters a dsRNA molecule. The dsRNA is cleaved into siRNA by the enzyme, dicer. The sense strand siRNA will be degraded. The antisense strand siRNA will be incorporated into RISC which will be activated and triggers cleavage of targeted mRNA complementary sequence resulting in degradation of mRNA. As a result of this mRNA degradation, no protein was translated and gene expression is effectively silenced post-transcriptionally. (Adapted from Leung and Whittaker, 2005)

Short interfering RNA (siRNA) duplexes targeting mouse Keap1, Nrf2 and NF-κB, p65 were used. The siRNA duplexes were as follows; si-Nrf2 sense 5'- GCA AGA AGC CAG AUA CAA A-3', antisense 5'- U UUG UAU CUG GCU UCU UGC- 3', si-Keap1 sense 5'- GCU AUG ACC CGG ACA GUG A -3', antisense 5'- U CAC UGU CCG GGU CAU AGC – 3', si-p65#1 sense 5'- UUC AUC UCC GGA GAG ACC AUU GGG A – 3', anti-sense 5' – U CCC AAU GGU CUC UCC GGA GAU GAA – 3', si-p65#2 sense 5'- AGG UUC UGG AAG CUA UGG AUA CUG C – 3', anti-sense 5' – UCC AAG ACC UUC GAU ACC UAU GAC G – 3', si-p65#3 sense 5'- AUA CAC CUC AAU GUC UUC UUU CUG C – 3', anti-sense 5' – UAU GUG GAG UUA CAG AAG AAA

GCA G – 3'. Hepa-1c1c7 were plated out onto 96 well plates at 1 x 10^4 cells/well for NF-κB siRNA validation, 96 well plates at 7 x 10^3 cells/well for LDH assay, 24 well plates at 5 x 10^4 cells/well for GSH assays and 10-cm dishes at 4 x 10^6 cells/dish for nuclear extractions. Cells were transfected with 10nM of siRNA directed against Keap1 or Nrf2, and 3nM siRNA against p65 for 48hrs, using Lipofectamine 2000 according to the manufacturer's instructions.

2.2.10 Measurement of Lactate Dehydrogenase Leakage

Measurement of cellular cytotoxicity was determined by measuring the leakage of the cytoplasmic enzyme lactate dehydrogenase (LDH) into the cell culture media. This involves a two-step enzymatic process; in the first step, LDH reduces NAD+ to NADH + H+ by the oxidation of lactate to pyruvate. The second step is the transfer of 2H from NADH + H+ to the yellow tetrazolium salt 2-[4-iodophenyl]-3-[4-nitrophenyl]-5-phenyltetrazolium chloride by a catalyst (diaphorose) which yields a red formazan dye with an absorbance maximum of 500nm. Hence, the amount of the red formazan formed over time is directly proportional to the LDH activity in the culture media, and therefore correlates to the degree of cell death. The amount of LDH leakage corresponds to the degree of membrane damage and it is normally used as a marker for cellular necrosis.

Hepa-1c1c7 cells were plated out on 96-well plates at 2 x 10^4 cells/well for 24 hrs or as stated in the RNAi treatment section (section 2.2.6). Following treatment, the plates were centrifuged briefly at 3000rpm to pellet cells, and cell-free culture media was removed to a new 96-well plate. Cells were lysed with 40µl of DMEM containing 2% (v/v) Triton X-100, followed by centrifuged at 3000rpm for 5min. To a new 96-well plate, 50µl of cell-free culture media (diluted 1:4 in DMEM)

and cell lysate (diluted 1:20 in DMEM) were transferred separately. LDH leakage was measured using a Cytotoxicity Detection Kit; 50µl assay reagent (1µl catalyst per 45µl dye solution) was then added to each well. The plate was incubated in the dark for 30min and air bubbles were removed by brief centrifugation of the plates at 3000rpm. Formation of red formazan salt was measured at 490nm on a MRX microplate reader. Blank readings were obtained from wells containing 50µl DMEM and subtracted from the sample readings. LDH leakage from cells into the culture medium (extracellular) is expressed as a percentage of total LDH (intracellular plus extracellular).

2.2.11 Measurement of Glutathione

Total glutathione (GSH) content was quantified using the 5,5 O-dithiobis(2-nitrobenzoic acid) -GSH reductase recycling method, as previously described by Vandeputte et al (Vandeputte *et al.* 1994). In this method, GSH is oxidised by DTNB to yield GSSG and the 5-thio-2-nitrobenzoic acid (TNB) chromophore (1), which has an absorbance maximum of 412nm. GSSG is reduced to GSH by the action of GSH reductase in the presence of NADPH (2). Thus, the rate of formation of TNB was measured at 405nm, which is proportional to the sum of GSH and GSSG present in each sample.

$$2GSH + DTNB \longrightarrow GSSG + TNB \quad (1)$$

$$GSSG + NADPH + H^{+} \longrightarrow 2GSH + NADP^{+} \quad (2)$$

Hepa-1c1c7 cells were plated out on 24-well plates at 2 x 10^5cells/well for 24hr. Following treatment, cells were scraped and resuspended in 0.125ml of 10mM HCl. An aliquot was used to measure total protein content as described in section 2.2.5. 6.5% of sulphosalicylic acid was added to the remaining samples to a final concentration of 1.3% (w/v),

and protein precipitation was facilitated by incubating on ice for 10min. Protein was pelleted by centrifugation at 18,000g for 5min. 20µl supernatant was transferred to a clear 96-well plate, and combined with 20µl of assay buffer (0.143M NaH_2PO_4, 6.3mM EDTA, pH 7.4) for 5min. The enzymatic reaction was initiated by the addition of 0.35U GSH reductase and measured kinetically at 405nm for 5min on a MRX microplate reader. The rate of TNB formation was calculated as the change in absorbance min^{-1}. Sample GSH concentrations were calculated via reference to a standard curve ranging from 0-50 mol/mL GSH. The GSH concentration for each sample was normalised to total protein content.

2.2.12 Data Analysis

Data are expressed as mean ± standard deviation of the mean. Normality was assessed by the Shapiro-Wilk Test. The significance of differences within the data was assessed by a One-way ANOVA or Student's t-test for normally distributed data, and Kruskal-Wallis analysis of variance (ANOVA) for non-parametric data. A difference was considered significant at $p<0.05$.

2.3 RESULTS

2.3.1 NAPQI and DNCB activate Nrf2 but inhibit NF-κB activity

In common with all mammalian hepatoma cell lines, Hepa-1c1c7, lacks metabolic competence and therefore cannot directly bioactivate acetaminophen. Consequently, NAPQI, the chemically reactive metabolite of acetaminophen (Dahlin *et al.* 1984), was used in these studies along with DNCB, a model alkylating agent and contact sensitizer (Lowney 1971). Both have been previously shown to deplete GSH and covalently bind cellular proteins (Potter *et al.* 1974; Potter *et al.* 1986; Huang *et al.* 2001; Aleksic *et al.* 2007; Copple *et al.* 2008a). Following a 1hr exposure, nuclear accumulation of Nrf2 increased with increasing concentrations of NAPQI (Fig 2.2a) and DNCB (Fig 2.2b); an increase in Nrf2 after exposure to NAPQI or DNCB has been demonstrated previously in the CDSS (Copple *et al.* 2008a). Immunochemical analysis of Nrf2 and NF-κB-p65 cellular localisation shows an increase in NF-κB-p65 cellular abundance (Fig 2.8a, second panel) and a clear increase in Nrf2 (Fig 2.8b, second panel) accumulation in the nucleus after 1 hr of DNCB treatment. These cells consistently express low but detectable levels of NF-κB DNA binding activity (Fig 2.3), however on the contrary to Nrf2 expression, NF-κB DNA binding decreased with increasing concentrations of NAPQI (Fig 2.3a) and DNCB (Fig 2.3b). Both chemicals caused a depletion of total GSH, which fell to 20% of the control at the highest dose of NAPQI (Fig 2.4a) and to undetectable levels at the highest dose of DNCB (Fig 2.4b). Lactate dehydrogenase (LDH) leakage assays show limited leakage after exposure of cells to test compounds for 1hr, although this is significant at 300μM of NAPQI (Fig 2.4c). The assay demonstrates substantial toxicity at 24hr following exposure to

concentration of NAPQI at 100μM and 300μM, and with DNCB at all concentration between 10μM to 100μM (Fig 2.4d).

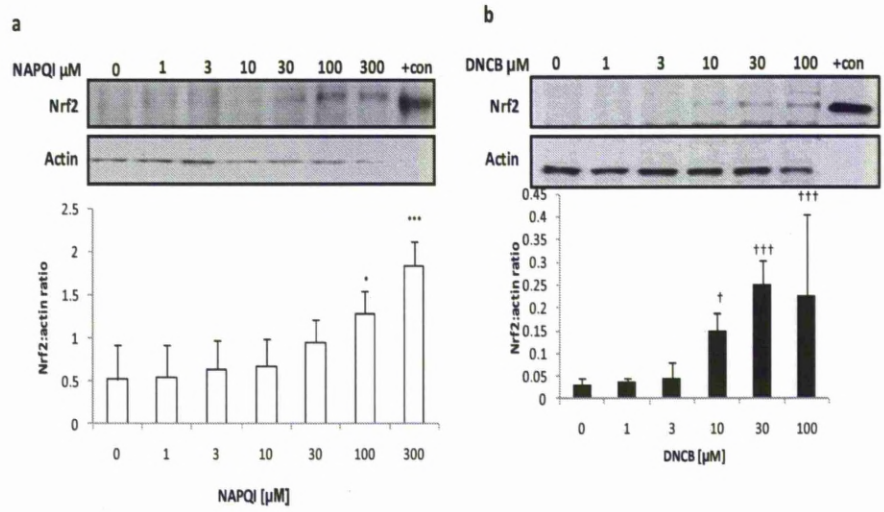

Figure 2.2: Chemical stress activates Nrf2. Hepa-1c1c7 cells were treated for 1hr with NAPQI (a) or DNCB (b) and nuclear protein resolved on SDS-PAGE and probed for Nrf2. NAPQI (a) and DNCB (b) activates Nrf2 nuclear accumulation dose-dependently. Actin is shown as loading control. Recombinant mouse His-tagged Nrf2 was loaded as a positive control on the blot (+con). The bottom panel shows the densitometric analysis of Nrf2 positive bands normalised against actin. One-way ANOVA, *p<0.05, ***p<0.001. Kruskal Wallis, †p<0.05, †††p<0.001. The control cells were treated with 0.1% DMSO. Representative gel from n=3 is shown. Error bars = Standard deviation of mean, n=3.

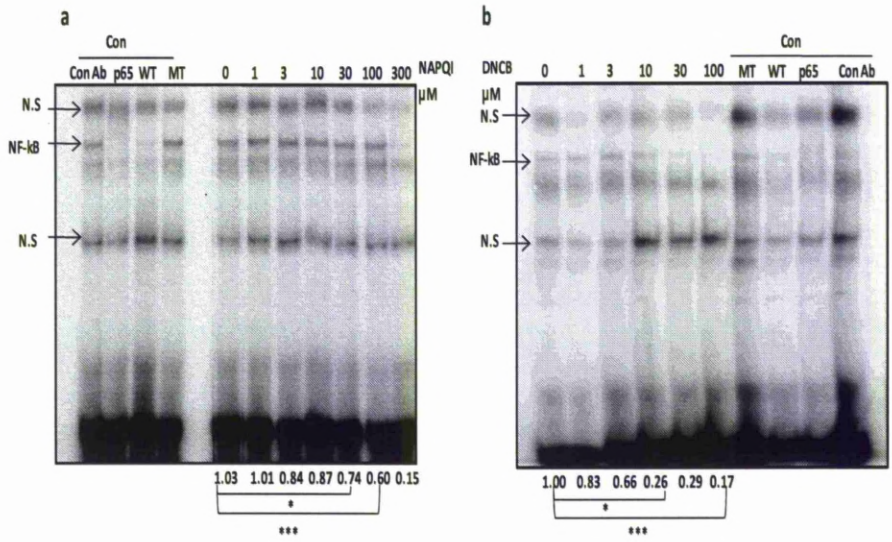

Figure 2.3: Chemical stress inhibits NF-κB. Hepa-1c1c7 cells were treated for 1hr with NAPQI (a) or DNCB (b) and nuclear protein was assayed using EMSA for NF-κB activity. NAPQI (a) and DNCB (b) inhibits NF-κB binding activity dose-dependently.The EMSA assay was specific for the NF-κB protein as addition of a 50-fold excess of wild-type oligonucleotide (wt) to the control reaction (Con) displaced the bound protein from the radiolabelled oligonucleotide, while this was not observed with the addition of excess mutant (Mut) oligonucleotide. The addition of specific anti-NF-κB antibody (p65), as opposed to non-specific antibody (con Ab) to the binding control reaction (Con) caused a supershift in the NF-κB band confirming the composition of the NF-κB complex. The data demonstrate the densitometric analysis of NF-κB normalised against control treatment since normalisation to an internal control in EMSA is not possible. Kruskal-Wallis, $*p<0.05$, $***p<0.001$. The control cells were treated with 0.1% DMSO. Representative gels from n=3 is shown. N.S; non-specific binding.

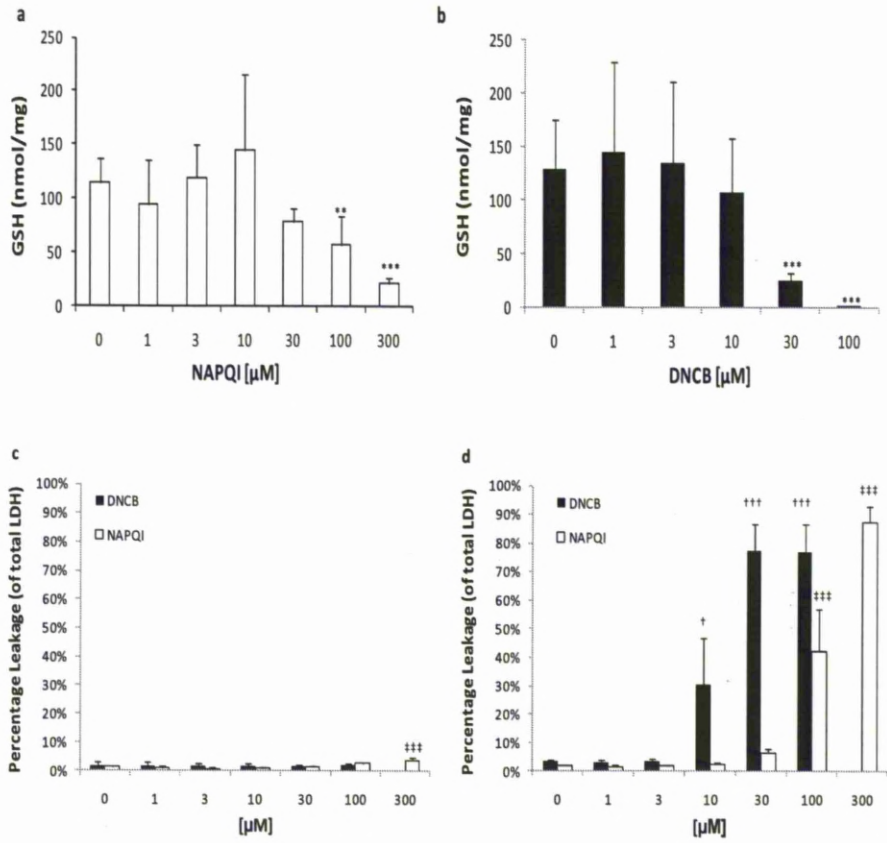

Figure 2.4: Chemical stress depletes GSH and induces toxicity over 24hr. Hepa-1c1c7 was treated for 1hr with NAPQI (a) or DNCB (b) and lysed with 10mM HCL. GSH depletion reaches 80% of control with highest dose of NAPQI (a) and 100% of control with highest dose of DNCB (b). Total GSH normalised against total protein content. Kruskal Wallis, $^{**}p<0.01$, $^{***}p<0.001$. Cells were treated for 1hr with NAPQI or DNCB (c) and 24hr with NAPQI or DNCB (d). LDH assay shows minimal leakage upon treatment with NAPQI or DNCB for 1hr (c). LDH assay shows substantial leakage upon treatment with NAPQI or DNCB (d) after 24hr. Extracellular LDH activity is expressed as a percentage of total (extracellular plus intracellular) LDH activity. One-way ANOVA, $^{\dagger}p<0.05$, $^{\dagger\dagger\dagger}p<0.001$, $^{\ddagger\ddagger\ddagger}p<0.001$. The control cells were treated with 0.1% DMSO. Error bars = Standard deviation of mean, n=3.

2.3.2 Glutathione depletion activates both Nrf2 and NF-κB activities

I then examined whether GSH depletion and/or the protein covalent modification due to the electrophilic nature of these compounds was responsible for the different effects observed on these pathways. We therefore used L-buthionine (S,R)-sulfoximine (BSO), which depletes intracellular GSH efficiently by irreversible inhibition of the rate limiting enzyme of GSH synthesis, GCLc (Griffith 1982). It is now well-accepted that depletion of GSH due to exposure of cells to BSO leads to redox perturbation in a variety of cell models, for recent examples see (Zhou *et al.* 2005; Cristofanon *et al.* 2009). BSO concentrations of 3μM to 30μM depletes GSH after 24hr exposure (Fig 2.5a), but does not induce NF-κB binding activity (Fig 2.5b). However, 100μM to 500μM of BSO increased NF-κB binding activity (Fig 2.6b) and increased nuclear accumulation of Nrf2 (Fig 2.7a), which correspond with GSH levels being depleted to below 20% of the basal level (Fig 2.6a); a BSO-mediated increase in Nrf2 has been seen previously in the CDSS (Copple *et al.* 2008a). Immunochemical analysis of Nrf2 and NF-κB cellular localisation after 24hr of BSO exposure indicates some cellular accumulation of NF-κB (Fig 2.8a, third panel) and substantial nuclear accumulation of Nrf2 (Fig 2.8b, third panel). After a 24hr exposure to BSO there was no evidence of cytotoxicity (Fig 2.7b).

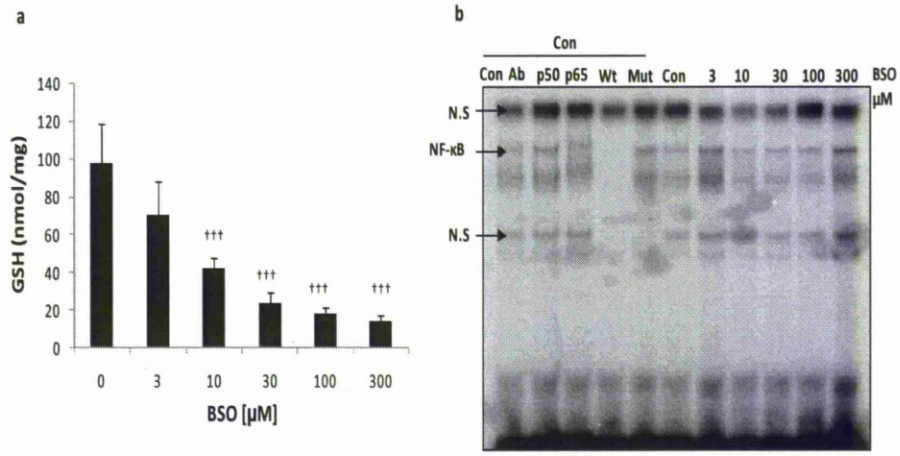

Figure 2.5: Depletion of GSH activates NF-κB at high dose only. Hepa-1c1c7 cells were treated for 24hr with BSO and lysed with 10mM HCL. GSH was depleted dose-dependently (a). Total GSH normalised against total protein content. Kruskal-Wallis, †p<0.05, †††p<0.001. Cells were treated for 24hr with BSO and nuclear protein was assayed for NF-κB activity. BSO activates the translocation and binding of NF-κB at 300uM only (b). The EMSA assay was specific for the NFkB protein as addition of a 50-fold excess of wild-type oligonucleotide (wt) to the control reaction (Con) displaced the bound protein from the radiolabelled oligonucleotide, while this was not observed with the addition of excess mutant (Mut) oligonucleotide. The addition of specific anti-NF-κB antibody (p65), as opposed to non-specific antibody (con Ab) to the binding control reaction (Con) caused a supershift in the NF-κB band confirming the composition of the NF-κB complex. The control cells were treated with dH_2O. Error bars = Standard deviation of mean, n=3. Representative gel from n=3 is shown. N.S; non-specific binding.

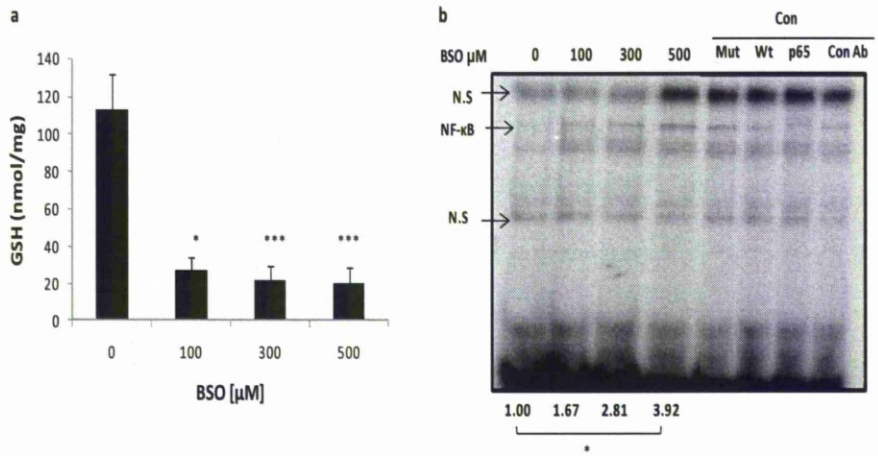

Figure 2.6: Severe depletion of glutathione activates NF-κB . Hepa-1c1c7 cells were treated for 24hr with BSO and lysed with 10mM HCL. GSH was depleted by a maximum of 80% of control (a). Total GSH normalised against total protein content. Kruskal-Wallis, *p<0.05, ***p<0.001. Cells were treated for 24hr with BSO and nuclear protein was assayed for NF-κB activity. BSO activates the translocation and binding of NF-κB dose-dependently (b). The EMSA assay was specific for the NFkB protein as addition of a 50-fold excess of wild-type oligonucleotide (wt) to the control reaction (Con) displaced the bound protein from the radiolabelled oligonucleotide, while this was not observed with the addition of excess mutant (Mut) oligonucleotide. The addition of specific anti-NF-κB antibody (p65), as opposed to non-specific antibody (con Ab) to the binding control reaction (Con) caused a supershift in the NF-κB band confirming the composition of the NF-κB complex. The data shows the densitometric analysis of NF-κB normalised against control treatment since normalisation to an internal control in EMSA is not possible. Kruskal-Wallis, *p<0.05. The control cells were treated with dH_2O. Error bars = Standard deviation of mean, n=3. Representative gel from n=3 is shown. N.S; non-specific binding.

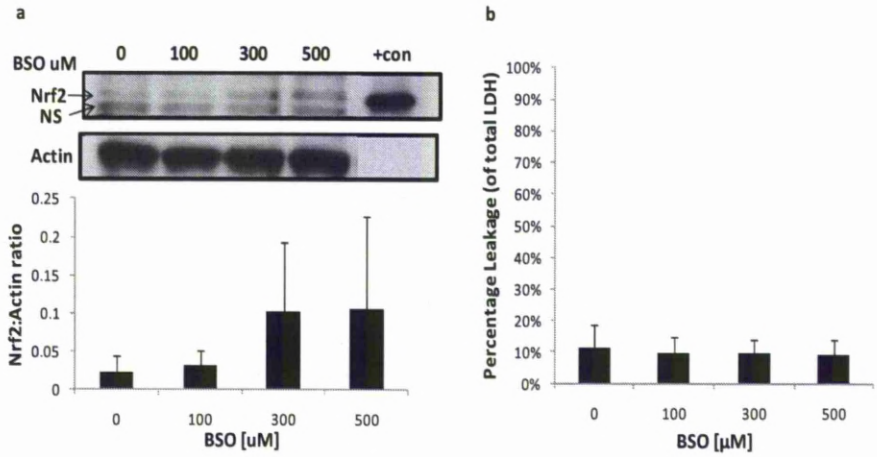

Figure 2.7: Depletion of glutathione activates Nrf2. Hepa-1c1c7 was treated for 24hr with BSO and nuclear protein resolved on SDS-PAGE and probed for Nrf2. BSO activates Nrf2 nuclear accumulation dose-dependently (a). Actin is shown as loading control. Recombinant mouse His-tagged Nrf2 was loaded as a positive control on the blot (+con). The bottom panel shows densitometric analysis of Nrf2 normalised against actin. Cells were treated for 24hr with BSO. LDH assay shows minimal leakage upon treatment with BSO (b). Extracellular LDH activity is expressed as a percentage of total (extracellular plus intracellular) LDH activity. The control cells were treated with dH_2O. Error bars = Standard Deviation of mean, n=3. Representative gel from n=3 is shown. N.S; non-specific binding.

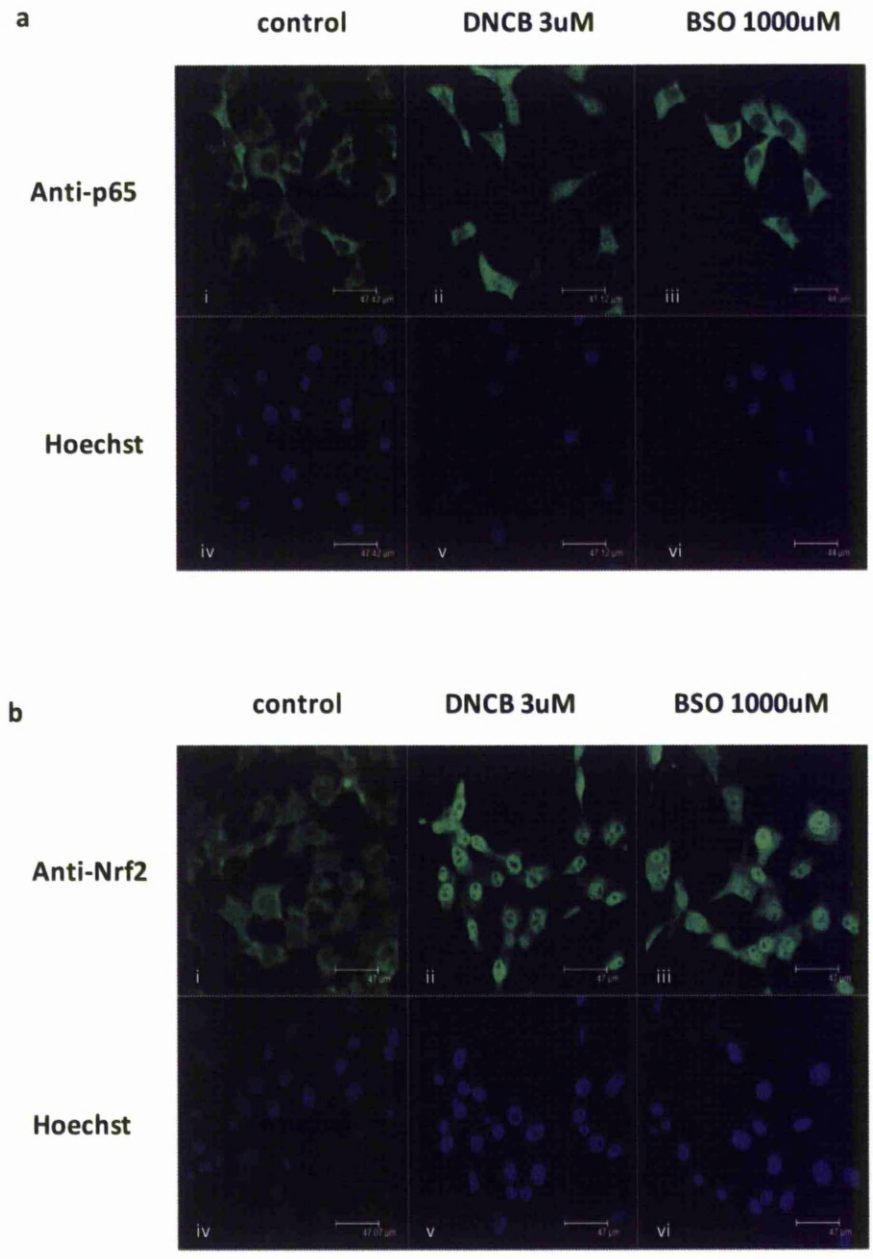

Figure 2.8: Subcellular localization of p65 (a) and Nrf2 (b) in Hepa-1c1c7 cells exposed to control and DNCB or BSO for 1hr and 24hr, respectively. FITC-conjugate goat anti-p65 (a)(i, ii and iii), FITC-conjugate goat anti-Nrf2 (b)(i, ii and iii) and Hoechst 33258 (A)(B)(iv, v and vi) immunofluorescence were visualised by confocal microscopy.

2.3.3 Comparison of Nrf2 and NF-κB regulation by NAPQI, DNCB and BSO

The effect of treatment with NAPQI, DNCB or BSO on Nrf2 and NF-κB activity can be seen clearly in figure 2.9. NAPQI (Fig 2.9a) and DNCB (Fig 2.10a), which can covalently bind proteins and deplete GSH, increased Nrf2 activity and decreased NF-κB binding activity, whilst the GSH-depleting agent, BSO (Fig 2.10b), increased both Nrf2 and NF-κB activity.

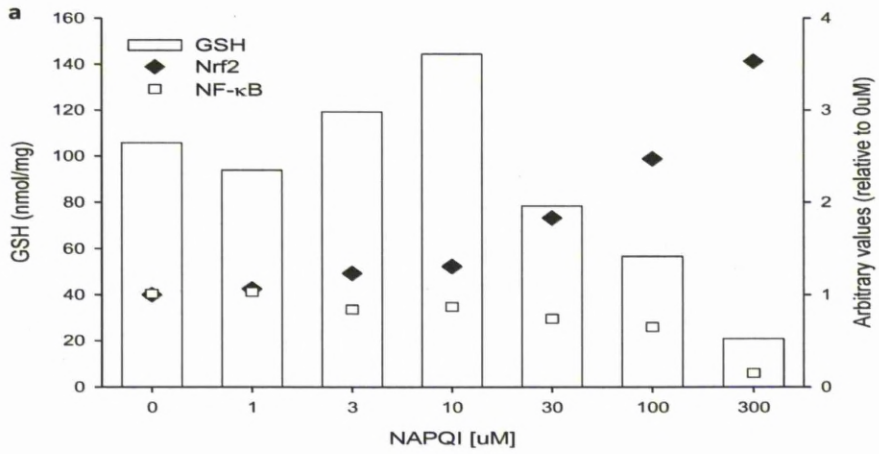

Figure 2.9: The effect of NAPQI treatment on Nrf2, NF-κB and GSH in Hepa-1c1c7 cells. NAPQI increased Nrf2 nuclear accumulation and decreased NF-κB binding activity in parallel with GSH depletion. Error bars have been omitted from the graph for visual clarity, n=3.

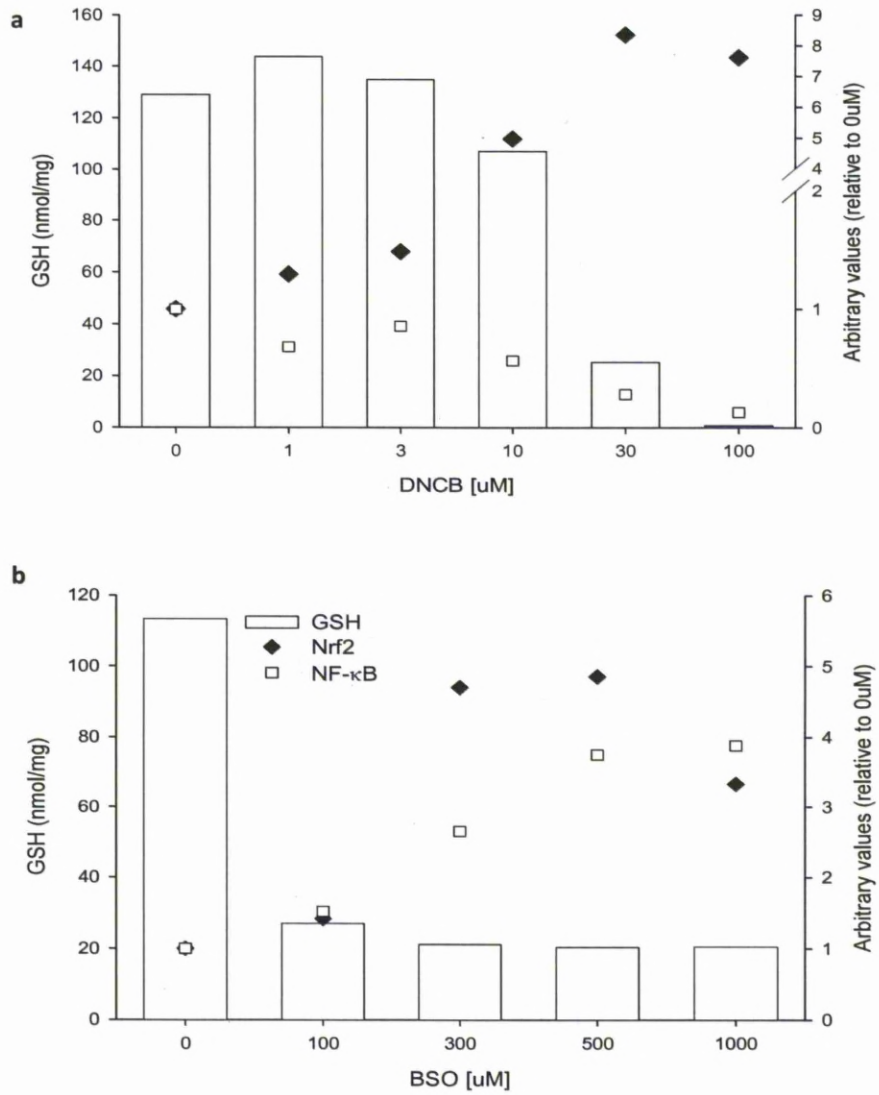

Figure 2.10: The effect of DNCB and BSO treatment on Nrf2, NF-κB and GSH in Hepa-1c1c7 cells. DNCB (a) increased Nrf2 nuclear accumulation and decreased NF-κB binding activity in parallel with GSH depletion. BSO (b) increased both Nrf2 nuclear accumulation and NF-κB binding activity in parallel with GSH depletion. Error bars have been omitted from graphs for visual clarity, n=3.

2.3.4 RNA interference modulates Keap1, Nrf2 and NF-κB, p65 subunit expression

RNAi is a conserved mechanism of specific gene silencing through post-translational degradation of mRNA (Dykxhoorn *et al.* 2005). In this study, RNAi was used to investigate the physiological and molecular effects of Keap1, Nrf2 and p65 silencing on cellular cytoprotection. This single dose of siRNA molecules against Keap1 was an initiate screening to validate which siRNA molecule was the most effective against Keap1 at 10nM. The basal Keap1 protein depletion is below 35% when compared to mock transfection and negative control (Fig 2.11a). The RNAi depletion of Keap1 resulted in a concomitant increase in the nuclear Nrf2 level (Fig 2.11b and c). The use of Keap1 and Nrf2 RNAi have been shown, against the proteins respectively, which resulted in 80% silencing of each protein (Copple *et al.* 2008a). RNAi directed against NF-κB, p65 subunit expression was also successful. A 70% reduction in basal NF-κB p65 expression was detected in cells treated with p65 RNAi (Fig 2.12a) concurrently with a decrease in nuclear NF-κB DNA binding activity (Fig 2.12b). The co-transfection of two RNAi molecules against p65 was compared to single transfection – this did not silence NF-κB any further. Therefore, there was no synergistic effect from the co-transfection (Fig 2.13).

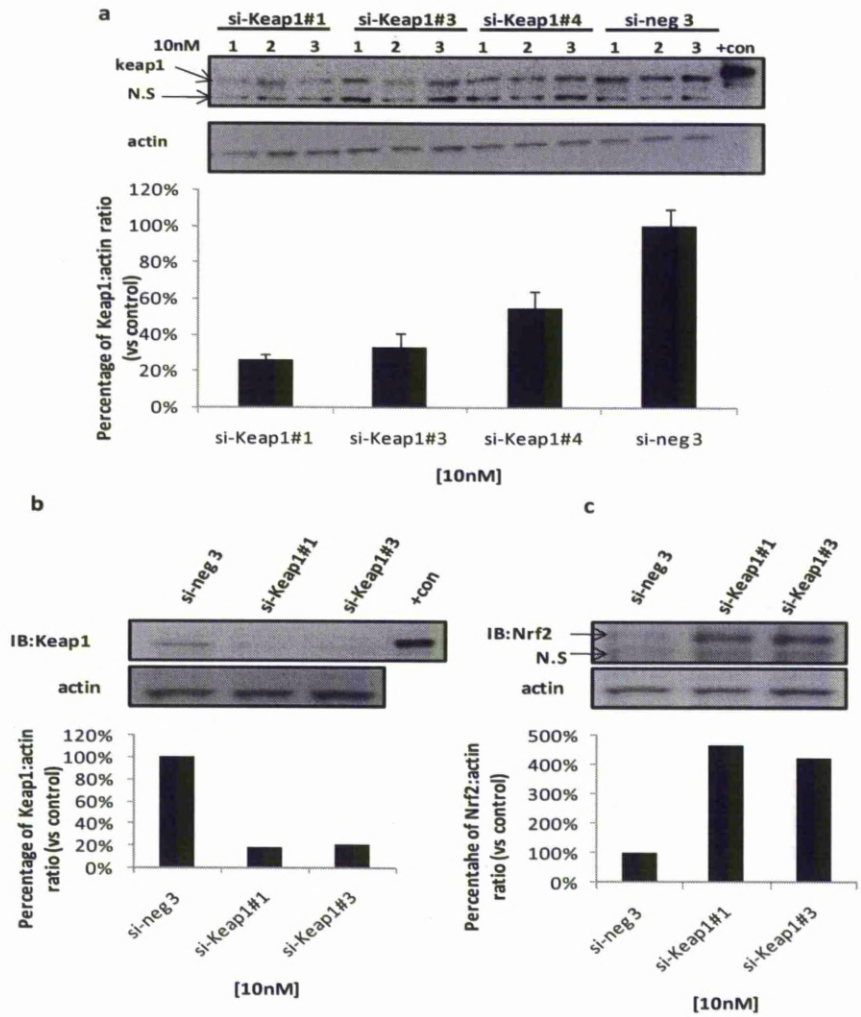

Figure 2.11: RNAi modulates Keap1 subunit expression. Hepa-1c1c7 cells were transfected with Keap1 siRNA for 48hr (Copple *et al.* 2008a) and cytosolic extracts resolved on SDS-PAGE and probed for Keap1. Keap1 siRNA depleted Keap1 protein expression to approximately 70% of control for si-Keap1#1, si-Keap1#3 and 50% of control for si-Keap1#4 (a). Correspondingly, 70% Keap1 protein depletion (b) caused an approximately 50% increased in nuclear Nrf2 (c). Actin is shown as loading control.Actin is shown as loading control. Recombinant mouse HIS-tagged Nrf2 was loaded as positive control on the blot (+con). si-neg 3 is control for all 3 Keap1 siRNA. (a) Percentage of Nrf2:actin ratio from triplicate measurements, n=1. Representative gel from n=1 is shown. Densitometry value from n=1. N.S; non-specific binding. IB; immunoblotting.

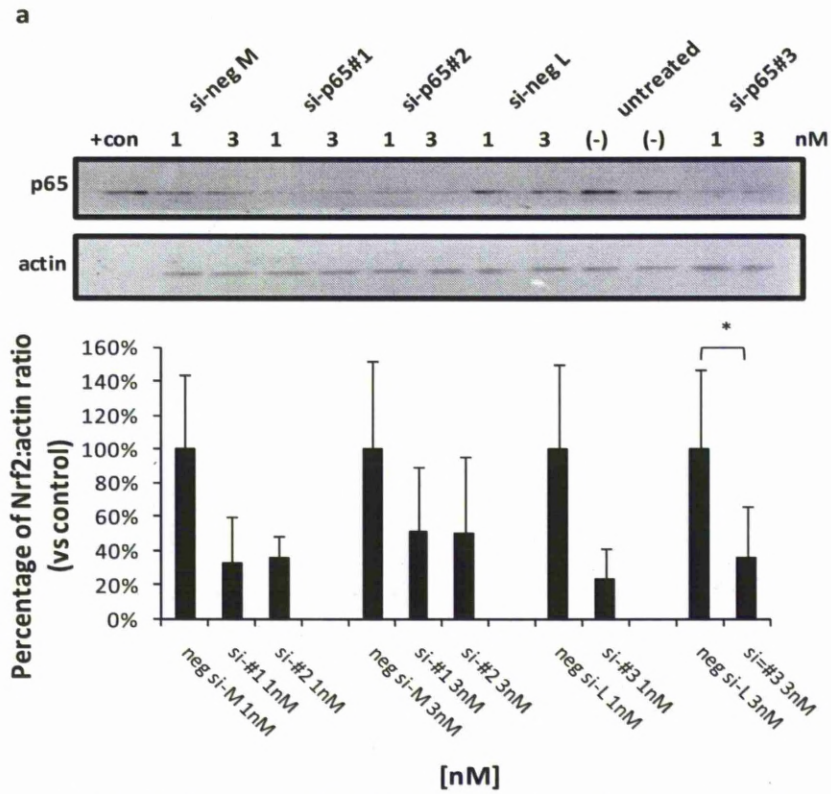

Figure 2.12a: RNAi modulates NF-κB, p65 subunit expression. Hepa-1c1c7 cells were transfected for 48hr with NF-κB siRNA. Cytosolic extracts resolved on SDS-PAGE and probed for NF-κB. NF-κB siRNA deplete NF-κB protein expression to approximately 70% of control. Actin is shown as loading control. Cell lysates from HepG2 overexpressed p65 was loaded as positive control on the blot (+con). si-negM and si-negL are controls for si-p65#1/si-p65#2 and si-p65#3 respectively. The bottom panel shows densitometric analysis of NF-κB positive bands normalised against actin. Paired t-test, $*p<0.05$. The data shows the densitometric analysis of NF-κB normalised against control. Error bars = Standard deviation of mean, n=3. Representative gel from n=3 is shown.

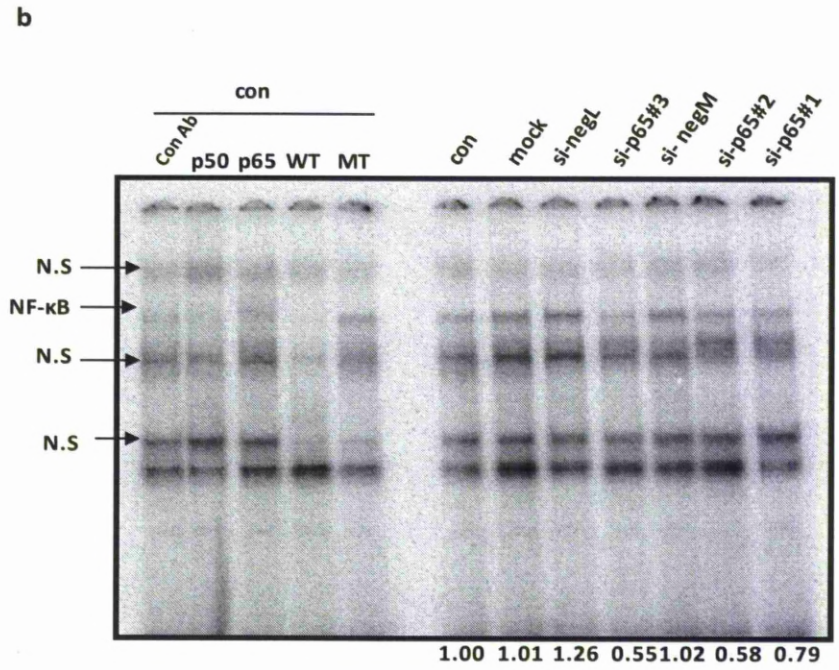

Figure 2.12b: RNAi modulates NF-κB, p65 subunit expression. Hepa-1c1c7 cells were transfected for 48hr with NF-κB siRNA. Nuclear protein was assayed for NF-κB activity. NF-κB siRNA decreased constitutive binding compared to control. The assay was specific for the NFkB protein as addition of a 50-fold excess of wild-type oligonucleotide (wt) to the reaction displaced the bound protein from the radiolabelled oligonucleotide, while this was not observed with the addition of excess mutant (Mut) oligonucleotide. The addition of specific anti-NF-κB antibody (p50, p65), as opposed to non-specific antibody (con Ab) to the binding reaction caused a supershift in the NF-κB band confirming the composition of the NF-κB complex. The data shows the densitometric analysis of NF-κB normalised against control treatment since normalisation to an internal control in EMSA is not possible. Representative gel from n=3 is shown. Densitometry value = mean, n=3. N.S; non-specific binding.

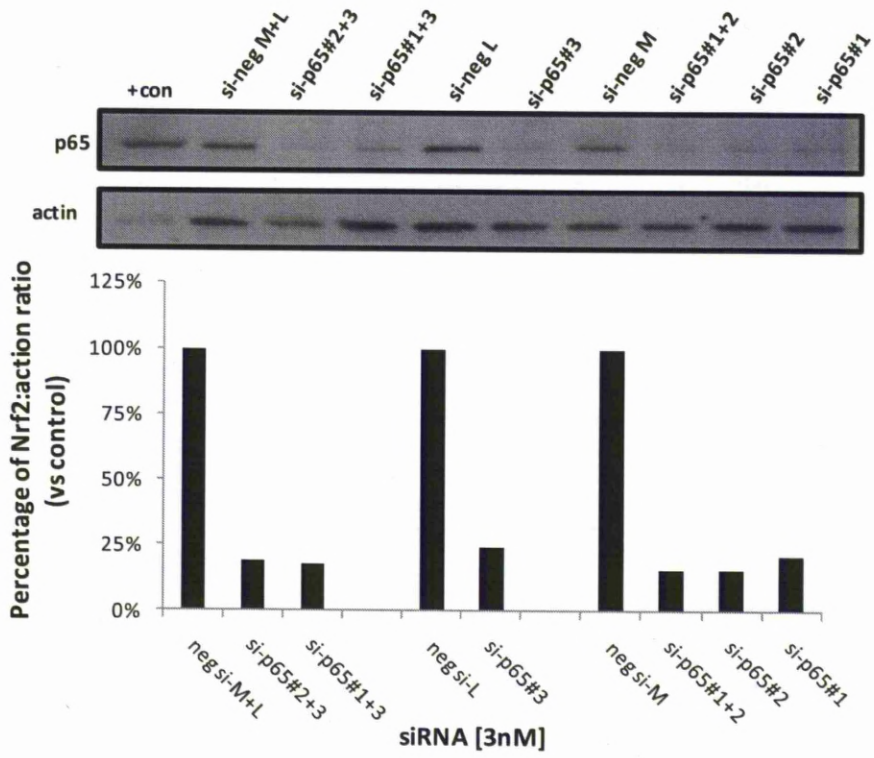

Figure 2.13: RNAi modulates NF-κB, p65 subunit expression. Hepa-1c1c7 cells were transfected for 48hr with either one or two NF-κB siRNA. The cytosolic extracts were then resolved on SDS-PAGE and probed for NF-κB. NF-κB siRNA deplete NF-κB protein expression to approximately 75% of control, the co-transfection of two siRNA had no additional effect on depleting NF-κB. Actin is shown as loading control. Cell lysates from HepG2 overexpressed p65 was loaded as positive control on the blot (+con). si-neg M+L , si-negM and si-negL are controls for si-p65#1+3/si-p65#2+3, si-p65#1/si-p65#2/si-p65#1+2 and si-p65#3 respectively. The bottom panel shows densitometric analysis of NF-κB positive bands normalised against actin. Percentage of Nrf2:actin ratio is the mean of two independent experiments, n=2. A representative gel from n=2 is shown.

2.3.5 RNAi modulation of Nrf2, Keap1 and p65 influences cell defence in Hepa-1c1c7 cells

Modulation of Nrf2, Keap1 and NF-κB, p65 had a profound effect on the ability of Hepa-1c1c7 cells to elicit a defence response against chemical stress. DNCB was again used as a model electrophile to induce chemical stress. LDH assays indicated that RNAi knockdown of Keap1 (Fig 2.14a) protects the cells against DNCB toxicity. DNCB toxicity was augmented when Nrf2 was depleted with RNAi directed against Nrf2 (Fig 2.14b) and p65 was depleted (Fig 2.14c) individually. Interestingly, the phenotypic effect of the Keap1 knock down was reversed when both Keap1 and p65 (Fig 2.14d) were depleted simultaneously. The comparison of toxicity for each RNAi modulation should be made against their respective controls and should not be compared with other RNAi treatments.

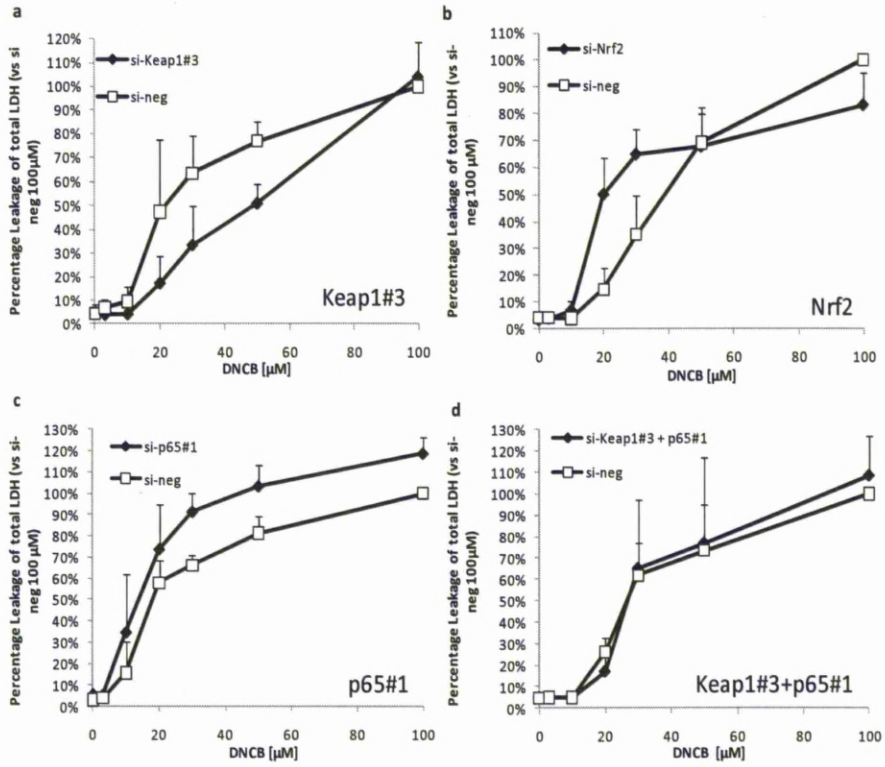

Figure 2.14: RNAi modulation of Nrf2, Keap1 and p65 influences cell defence. Hepa-1c1c7 cells were transfected for 48hr with RNAi and treated for 6hrs with DNCB. Keap1 depletion decreased DNCB toxicity (a). Nrf2 (b) depletion increased DNCB toxicity. Increased in DNCB toxicity was seen with p65 depletion (c). Keap1 and p65 co-depletion shows the effect of Keap1 knockdown alone is reversed by depletion of p65 (d). All data compared to their respective negative controls (si-neg). The control cells were treated with 0.1% DMSO. Error bars = Standard deviation of mean, n=3-4.

2.3.6 RNAi depletion of Nrf2 and Keap1, but not p65, influences the basal level of GSH in Hepa-1c1c7 cells

The effect of modulation of Nrf2, Keap1 and p65 on the basal level of GSH was then assessed, to determine whether the GSH level has an influence on the toxicity seen with DNCB. Keap1 silencing increased the basal level of GSH by approximately 40% and at 10μM of DNCB, the GSH level increased by an additional 20% (Fig 2.15a). Nrf2 silencing decreased the basal level of GSH by approximately 20% and at 20μM of DNCB, there is a clear decrease in GSH levels to less than 20% of total GSH (Fig 2.15b). p65 RNAi did not affect the basal level of GSH or levels after treatment with DNCB (Fig 2.15c). Interestingly, in the presence of Keap1 and NF-κB-p65 RNAi, there was no increase in the basal GSH level (Fig 2.15d).

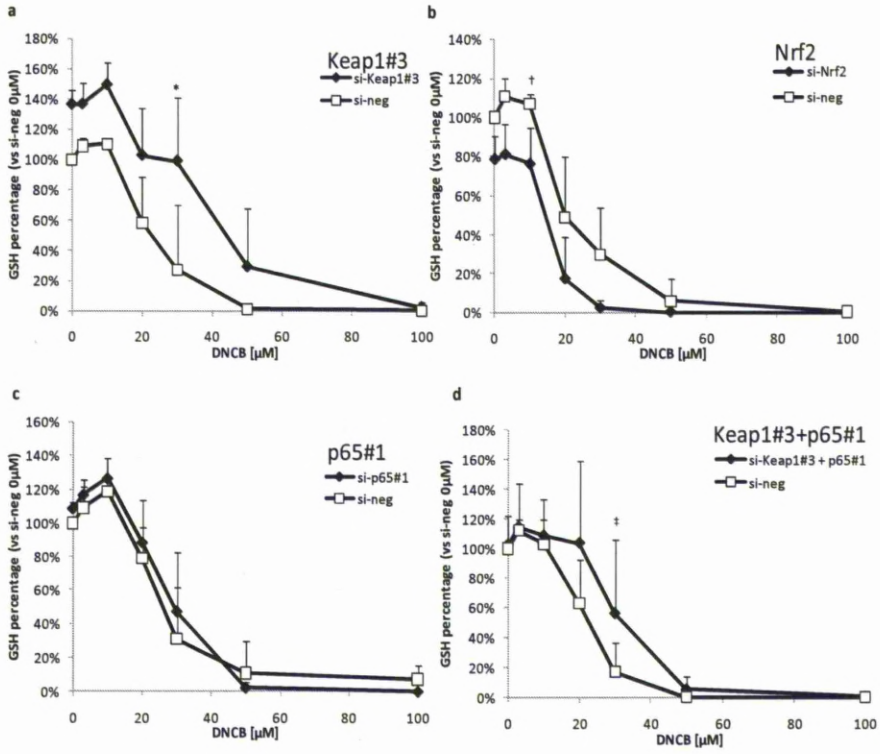

Figure 2.15: RNAi modulation of Nrf2, Keap1 and p65 influences the level of GSH. Hepa-1c1c7 cells were transfected for 48hr with RNAi and treated for 6hrs with DNCB. Keap1 depletion increased basal GSH levels (a). Nrf2 depletion caused a decrease in basal GSH level (b). With p65 depletion there is no change in basal GSH level (c). Where both Keap1 and p65 are depleted simultaneously, there is no increase in basal GSH levels (d). Total GSH was normalised to total protein content versus si-neg control untreated. All data are compared to their respective negative controls (si-neg). Kruskal-Wallis, *p<0.05 si-keap1#3 versus si-neg, †p<0.05 si-Nrf2 versus si-neg. Kruskal-Wallis, ‡p<0.05 si-Keap1#3 + p65#1 versus si-neg. The control cells were treated with 0.1% DMSO. Error bars = Standard deviation of mean, n=3-4.

2.3.7 Simultaneous depletion of Keap1 and NF-κB-p65 by RNAi influences the basal level of Nrf2 in Hepa-1c1c7 cells

In order to investigate the possible influence of NF-κB-p65 on the activity of Nrf2, the effect of RNAi depletion of NF-κB-p65 on Nrf2 expression was determined in Hepa-1c1c7 cells. p65 RNAi alone had no effect on the cellular expression of Nrf2, however, when co-transfected with Keap1 RNAi, p65 depletion reversed the induction of Nrf2 caused by Keap1 depletion (Fig 2.16). This suggests that p65 may play a role in the modulation of Nrf2 expression.

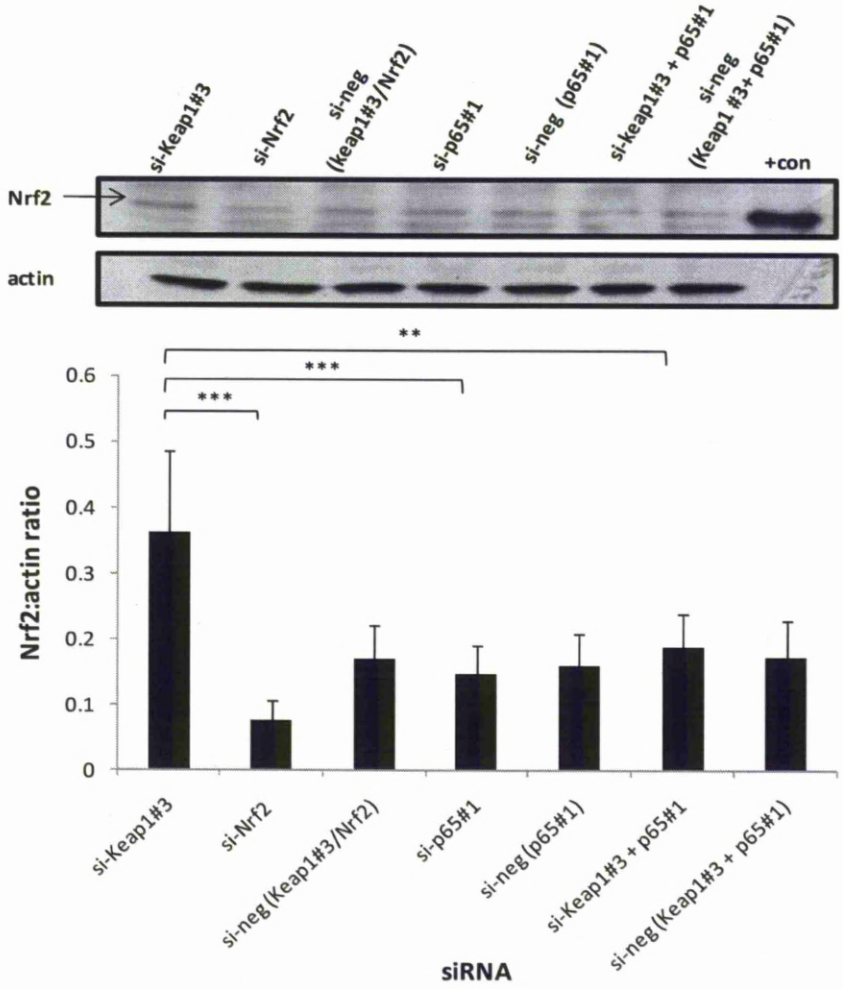

Figure 2.16: Simultaneous RNAi modulation of Keap1 and p65 influences the level of Nrf2 protein. Hepa-1c1c7 cells were transfected for 48hr with RNAi. Whole cell lysates were resolved on SDS-PAGE and probed for Nrf2 protein. Keap1 depletion increases Nrf2 and the depletion of Nrf2 decreases Nrf2. p65 depletion had no effect on basal Nrf2 levels in Hepa-1c1c7 cells. The depletion of Keap1 and p65 simultaneously reduced the expression of Nrf2 basally. All data are compared to their respective controls. Actin is shown as loading control. Recombinant mouse His-tagged Nrf2 was loaded as a positive control on the blot (+con). The bottom panel shows the densitometric analysis of Nrf2 normalised against actin. One-way ANOVA, $**p<0.01$, $***p<0.001$. Representative gel from n=4. Error bars = Standard deviation of mean, n=4.

2.4 DISCUSSION

The importance of the NF-κB pathway in cellular survival, proliferation and the inflammatory response are well documented, along with the role of the Nrf2/Keap1 pathway in the cellular defence. However, it is still unclear as to how both pathways simultaneously respond to chemical stress and redox perturbation. In this study, both chemical stress and GSH depletion induced Nrf2, detected as nuclear accumulation observed by confocal microscopy (Fig 2.8) and western blotting. DNCB induced chemical stress caused a decrease in NF-κB binding activity (Fig 2.2d) despite the cellular accumulation of NF-κB-p65 (Fig 2.3b). On the other hand, redox perturbation that ensues from the GSH-depleting action of BSO activates nuclear translocation of Nrf2 as well as causing increased DNA-binding activity of NF-κB (Figs 2.7a and 2.6b). This is consistent with the notion that Nrf2 can be activated through covalent modification as well as GSH depletion. In the case of NF-κB, activity can either be enhanced by GSH depletion, or inhibited by reactive chemical exposure, through cysteine modification by covalent binding to one or more subunits in NF-κB, or to other factors that regulate NF-κB. Here we have observed that NAPQI and DNCB inhibit NF-κB DNA activity. However, whether both chemicals control NF-κB through an upstream effect such as, IKK complex or IκB or by directly interfering with its activity remains unclear and hence further investigation is needed. For both transcription factors, nevertheless, it should be noted that a definitive link between critical cysteine(s) modification, which may be irreversible or reversible, as a consequence of covalent binding or GSH depletion, still remains to be determined experimentally.

Our observations are in agreement with previous studies in animal and cell-based models indicating that NAPQI induces the activation of Nrf2 (Goldring *et al.* 2004; Copple *et al.* 2008a) and inhibits NF-κB DNA-binding activity (Blazka *et al.* 1995). BSO depletes GSH by binding to the active site of GCLc non-covalently, inhibiting the activity of GCLC (Griffith 1982). In the cell-based model, I have shown that depletion of GSH by BSO induces the nuclear accumulation of Nrf2 and increases NF-κB binding concurrently (Fig 2.6 and Fig 2.7a). The depletion of GSH over 24hrs by BSO does not elicit cytotoxicity (Fig 2.7b). This is in agreement with the previous finding in which BSO induced nuclear accumulation of Nrf2 (Copple *et al.* 2008a) and findings by others in which BSO induced NF-κB activity (D'Alessio *et al.* 2004; Filomeni *et al.* 2005). It should be emphasized that the induction of Nrf2 and NF-κB by BSO only occurs if the depletion of GSH is below 20% of total cellular GSH content at 100μM, which may be the threshold level to induce both transcription factors. In addition, both of the Nrf2 and NF-κB responses to NAPQI, DNCB and BSO occurred in the absence of toxicity, highlighting their ability to detect and respond to either chemical or GSH depletion before toxicity emerges.

It has been shown previously that 15-deoxy-Δ12, 14-prostaglandin J2 (15d-PG J2), an endogenous cyclopentenone prostaglandin molecule which can exert a powerful anti-inflammatory activity, is able to induce Nrf2/Keap1 and inhibit NF-κB (Straus *et al.* 2000; Hosoya *et al.* 2005). Whilst 15d-PGJ2 has been reported to directly bind to Keap1 thiol residues and induce Nrf2, without the depletion of GSH (Itoh *et al.* 2004; Copple *et al.* 2008a), NF-κB binding activity can be inhibited by 15d-PGJ2 through the direct modification of the p65 subunit (Straus *et al.* 2000). Therefore, it is becoming clear that exogenous and

endogenous compounds possessing the potential for protein covalent binding display very different effects on the Nrf2/Keap1 and NF-κB pathways. In contrast, agents such as BSO, which deplete GSH may have similar effects on both redox-sensitive transcription factors. Hence, these factors may serve as sensors to different types of stress, allowing cells to adapt and respond accordingly.

An important issue that needs to be considered regarding the validity of experiments such as those in the present study, is the fact that a reactive metabolite (in this case NAPQI) is added exogenously to cells rather than being generated endogenously. The necessity to add a reactive metabolite outside of the cell, remains a major hurdle in attempting to study the molecular pathways elicited by exposure of cells to drugs that require bioactivation. Nevertheless, data from this laboratory addressing the reactivity of residues in several proteins (i.e. GST-P and Keap1 – the regulator of Nrf2) show that these proteins demonstrate similar profiles of cysteine reactivity, as assessed by mass spectrometry, whether the protein is present at endogenous levels (GST-P) or is over-expressed (Keap1), to the profile of NAPQI binding to the recombinant proteins *in vitro* (Copple *et al.* 2008a; Jenkins *et al.* 2008). Therefore, whilst there are certainly limitations that need to be considered when a reactive metabolite is added exogenously to a cell rather than generated intracellularly, for certain reactive metabolites the profiles of modification outside and inside a cell may be similar.

Both Nrf2 and NF-κB play important roles in cellular defence, by inducing antioxidant enzymes, phase II enzymes and anti-apoptotic proteins. Co-regulation has not been shown before, therefore I have attempted to explore the consequences of such co-regulation by studying the effect of modulating the level of each transcription factor

pathway both separately and simultaneously. Using RNAi with DNCB as a model electrophile, I have shown here that an increase in cellular Nrf2, caused by Keap1 silencing, shifts the DNCB toxicity curve to the left, demonstrating increased resistance to DNCB toxicity when compared to its negative control. Conversely, decreased Nrf2 protein expression resulted in an increased susceptibility to DNCB toxicity when compared to its negative control. These findings support previous reports (Copple *et al.* 2008a) and emphasise the importance of Nrf2 in cellular defence. From these data, p65 does not appear to play a significant role in cell protection since si-p65 reduced the DNCB IC_{50} by only 4uM (Fig 2.14c). To better understand the role of each transcription factor individually and in concert with respect to cell defence and protection, we used RNAi simultaneously against Keap1 and p65, in order to: monitor how changes in one transcription factor pathway alters the response mediated by the other pathway and to attempt to model previous responses of Nrf2 and NF-κB observed in the cell during DNCB induced chemical stress. As predicted, depletion of Keap1, the inhibitor of Nrf2, increased cellular defence. The co-transfection of RNAi against Keap1 and p65 reversed the phenotypic effect seen with individual Keap1 knock-down (Fig 2.14d). The protective effect of Nrf2 induction caused by the loss of Keap1 was reduced when p65 was depleted, implying a role for p65 as a modulator of Nrf2-dependent cell protection. This therefore suggests that modulation of p65 has an effect on the ability of the cell to defend against toxicity via the Nrf2/Keap1 pathway, and that the Nrf2 and NF-κB pathways are linked.

GSH is a major antioxidant that quenches reactive xenobiotics and endogenous oxidative stress. Therefore, I examined if the depletion of Keap1, Nrf2 and p65 has any effect on the basal level of GSH, further

influencing the cells' ability to defend against electrophile reactive metabolite. I have demonstrated that the depletion of Keap1 increases the basal level of GSH (Fig 2.15a), and depletion of Nrf2 decreases the basal level of GSH (Fig 2.15b). This is consistent with previous investigation indicating that Nrf2 is one of the main regulators of GSH synthesis (Enomoto *et al.* 2001; McMahon *et al.* 2001; Copple *et al.* 2008a; Copple *et al.* 2008b). RNAi depletion of p65 has no effect on the level of GSH basally or in the presence of DNCB (Fig 2.15c). I have also shown that co- modulation of Keap1 and p65 affects the cell's ability to defend against DNCB toxicity. Interestingly, the simultaneous depletion of p65 and Keap1 prevented the increase in basal levels of GSH (Fig 2.15d) seen with Keap1 knockdown only. In line with this I have shown that the expression of Nrf2 was reduced by the co-depletion of Keap1 and p65 (Fig 2.16). The decrease in basal Nrf2 protein expression may explain the reverse in DNCB toxicity protection and the reduction of basal GSH by Keap1 depletion. Consequently, these observations imply that p65 may play an important role in the expression and the function of Nrf2.

The results of this study, indicating crosstalk between the Nrf2 and NF-κB pathways support evidence from other groups demonstrating that the GSH rate-limiting synthetic enzyme, GCLc, is regulated by Nrf2 indirectly through NF-κB (Yang *et al.* 2005a; Yang *et al.* 2005b; Kimura *et al.* 2009). Recently, it has also been shown that Keap1 is able to interact directly with IKKβ and the overexpression of Keap1 was seen to repress TNF-α induced NF-κB activity (Lee *et al.* 2009; Kim *et al.* 2010a), whilst the depletion of Keap1 by RNAi induced the nuclear accumulation and activity of NF-κB (Lee *et al.* 2009). However, the mechanism of how Keap1 regulate IKKβ remains unknown, but there are suggestions that

Keap1 regulates IKKβ either by promoting its proteasomal degradation via ubiquitination in human cells (Lee *et al.* 2009) or suppression through autophagic degradation and phosphorylation inhibition (Kim *et al.* 2010a). This suggests that Keap1 not only plays an important role in regulating Nrf2 but may also be a key regulator of the NF-κB pathway.

In conclusion, I have demonstrated that the transcription factors, Nrf2/Keap1 and NF-κB, respond differently to arylating and GSH-depleting agents. During chemical stress, it is likely that the cell attempts to protect itself by activating Nrf2, inducing a pleotropic transcriptional response of cytoprotective proteins. However, when this protective mechanism is overwhelmed and cellular damage is too great, it may be more beneficial for the cells to undergo apoptotic cell death due to the inhibition of NF-κB. During redox perturbation, to which the cell is constantly exposed under physiological conditions, activation of both Nrf2 and NF-κB may occur to protect the cells and prevent further damage (Fig 2.17). Protein modification by chemical arylation or oxidation as a consequence of GSH depletion on other signal transduction pathways involved in cellular protection or toxicity needs to be examined. Also, the use of GSH modulators such as N-acetylcysteine and GSH ester, or GSH depletors such as diethylmaleate and phorone, and the measurement of oxidative stress using chemical probes should be considered in future investigations. Our results also suggest a cross-talk between Nrf2/Keap1 and NF-κB pathways, where p65 was shown to modulate the expression and functionality of Nrf2. More work is required to fully define the emerging links between the Nrf2/Keap1 and NF-κB pathways, and how these impact on cellular response to drug exposure.

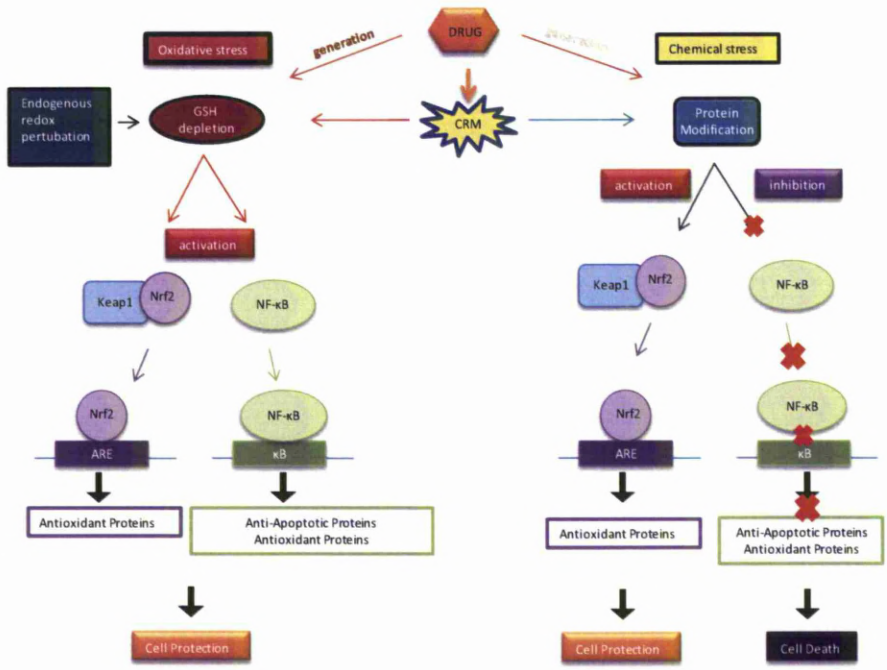

Figure 2.17: Proposed regulation of Nrf2 and NF-κB by protein modification or GSH depletion. Protein covalent modification associated with exposure to chemically-reactive metabolites activates Nrf2 inducing the transcription of cytoprotective proteins. However, protein covalent modification inhibits NF-κB, thereby reducing the transcription of anti-apoptotic and anti-oxidant proteins. This leads to cellular protection through the Nrf2 pathway, but if the protection is overwhelmed, cell death may ensue due to inhibition of NF-κB. GSH depletion without covalent modification will cause intracellular redox perturbation, activation of both Nrf2 and NF-κB, inducing the transcription of cytoprotective proteins, and anti-apoptotic and anti-oxidant proteins, respectively. This may lead to cellular protection against the potentially damaging effects of redox perturbation. [This scheme is based upon data derived in this study and other work (Blazka *et al.* 1995; D'Alessio *et al.* 2004; Goldring *et al.* 2004; Filomeni *et al.* 2005; Copple *et al.* 2008a; Ghosh *et al.* 2009)].

CHAPTER 3

Mechanism of Nrf2 activation – via chemical adduct formation and/or glutathione depletion

CONTENTS

3.1 INTRODUCTION

Keap1/Nrf2 pathway plays an important role in cellular protection during DILI. Keap1 controls the regulation of Nrf2 physiologically; Keap1 represses Nrf2 level in the cell by subjecting Nrf2 to ubiquitination and proteosomal degradation (Zhang *et al.* 2004). Alternatively, during chemical or oxidative stress, the repression of Nrf2 by Keap1 is disrupted, leading to the Nrf2 nuclear accumulation and transactivation of ARE-dependent genes (Itoh *et al.* 1997; Itoh *et al.* 1999b). However, the molecular mechanism underlying the Nrf2 activation by chemical or oxidative stress has not been fully clarified.

The current hypothesis of Nrf2 activation mechanism centres on the modification of Keap1 cysteine residues by chemical or oxidative stress. There is compelling evidence postulating that chemicals and reactive metabolites are able to chemically modify cysteine residues on Keap1, thereby biochemically triggering the Nrf2 pathway (Dinkova-Kostova *et al.* 2002; Zhang *et al.* 2003; Hong *et al.* 2005a). Specific cysteine residues have been shown to be modified by these chemicals on recombinant Keap1 in cell free *in vitro* systems associated with Nrf2 activation (Dinkova-Kostova *et al.* 2002; Dietz *et al.* 2005; Eggler *et al.* 2005; Hong *et al.* 2005b; Liu *et al.* 2005; Sakurai *et al.* 2006; Luo *et al.* 2007; Yamamoto *et al.* 2008) and can also bind to ectopic Keap1 in cell based models (Hong *et al.* 2005a; Rachakonda *et al.* 2008). Glutathione (GSH) is the most abundant non-protein tripeptide thiol, serving as the primary defence mechanism by playing a role in redox buffer against chemical and oxidative stress (DeLeve *et al.* 1991). The depletion of GSH has been shown to activate Nrf2 and the induction of ARE-dependent genes (Shertzer *et al.* 1995; Lee *et al.* 2008), but the mechanism of how GSH depletion activates Nrf2 remains to be clarified. It has been shown

that treatment with Nrf2 inducers lead to the formation of a disulphide bond within Keap1 in cells via the formation of an intermediate cysteine oxidation product, sulphenic acid (Wakabayashi *et al.* 2004). Cysteine residues can be readily oxidised, forming different intermediates. In many proteins, cysteine residues are able to be oxidised to cysteine sulphenic acid (R-SOH) which is considered unstable and can undergo further rapid oxidation to form a disulphide bond with either GSH or another protein cysteine. The formation of both cysteine sulphenic acid and the disulphide bond are reversible, and can be reduced back to former cysteine (Claiborne *et al.* 1999). The cysteine sulphenic acid can also be further oxidised to irreversible oxidations; sulphinic acid (R-SO_2H) and sulphonic acid (R-SO_3H) (Hamann *et al.* 2002; Wang *et al.* 2004). Therefore, modification of cysteine on Keap1 by oxidation from GSH depletion may lead to the activation of Nrf2 (Fig 3.1).

It has previously been indicated that Nrf2 activation can occur as a result of covalent modification of cysteine residues on Keap1 but also as a consequence of GSH depletion without concomitant chemical modification. Investigations in this chapter have focused on further exploring the specific pre-requisites for Nrf2 activation. Therefore, a panel of known Nrf2 inducing molecules were used. This panel of probe molecules is known to induce Nrf2 activation via the cysteine modification and/or by GSH depleting (Fig 3.2 and Fig 3.3). From this panel, molecules which expressed the following properties were chosen to investigate this: Cysteine modification and GSH depletion; cysteine modification but no GSH depletion; or GSH depletion but no cysteine modification. The three molecules chosen which exhibit the above mentioned three properties are iodoacetamide (IA), dexamethasone 21-mesylate (Dex-mes) and buthione (S,R)-sulfoximine (BSO) respectively.

These chosen molecules were investigated alongside three other molecules which exhibit different chemistries in binding proteins (Fig 3.2). Hence, the aim of this chapter is to further our understanding as to whether it is cysteine covalent modification, or oxidative stress by GSH depletion without concomitant chemical modification that is a prerequisite for Nrf2 activation, or in fact whether these properties of an Nrf2 inducer are not mutually exclusive. Hence, this study may give further insight on the mechanism of Nrf2 activation.

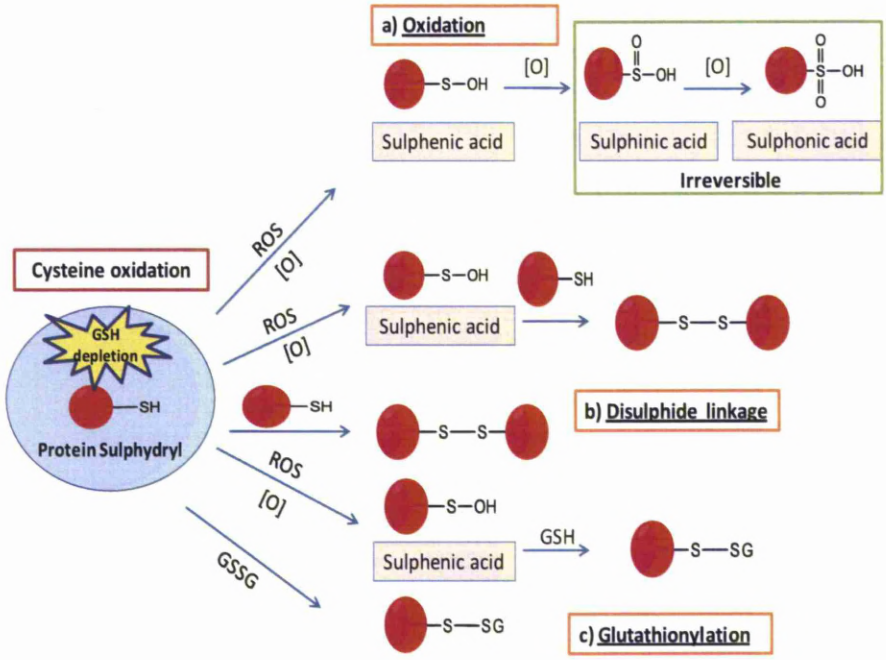

Fig 3.1: Schematic diagram of protein cysteine oxidation. Protein sulphydryl can be oxidised to sulphenic acid which can be further oxidised to (a) irreversible oxidation sulphenic and sulphonic acids. Sulfenic acid can also react with another protein sulphydryl or GSH to form (b) disulphide linkage or be (c) s-glutathionylated.

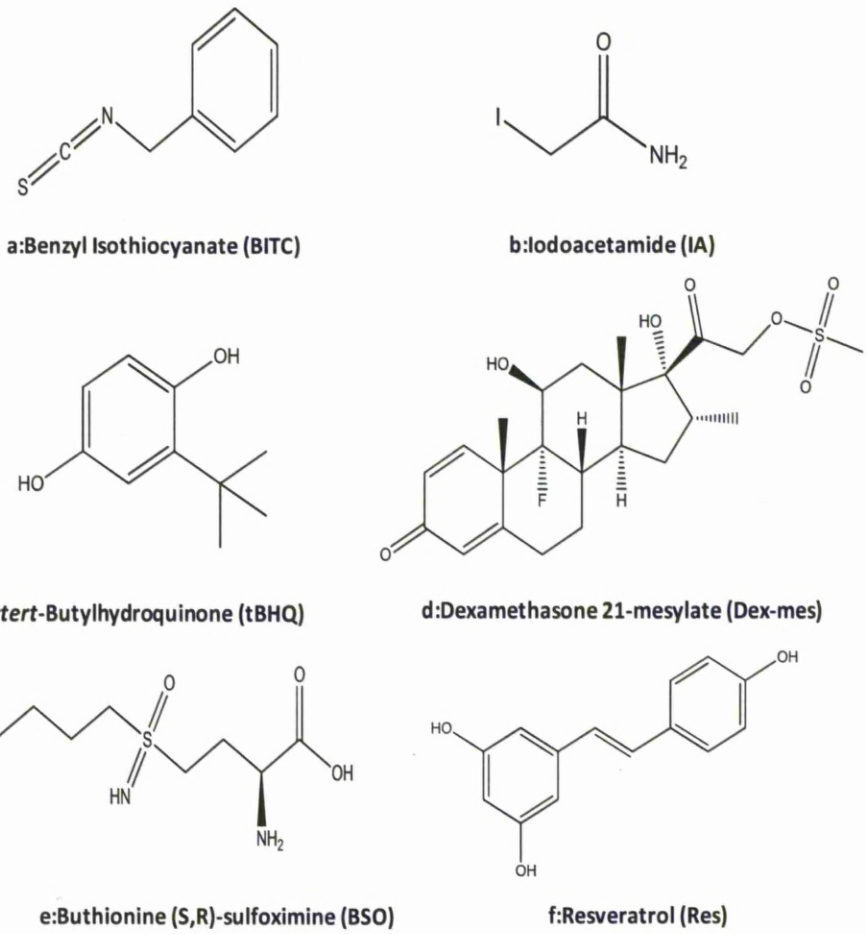

Figure 3.2: Chemical structure of the Nrf2-inducing molecules chosen for investigation in this chapter

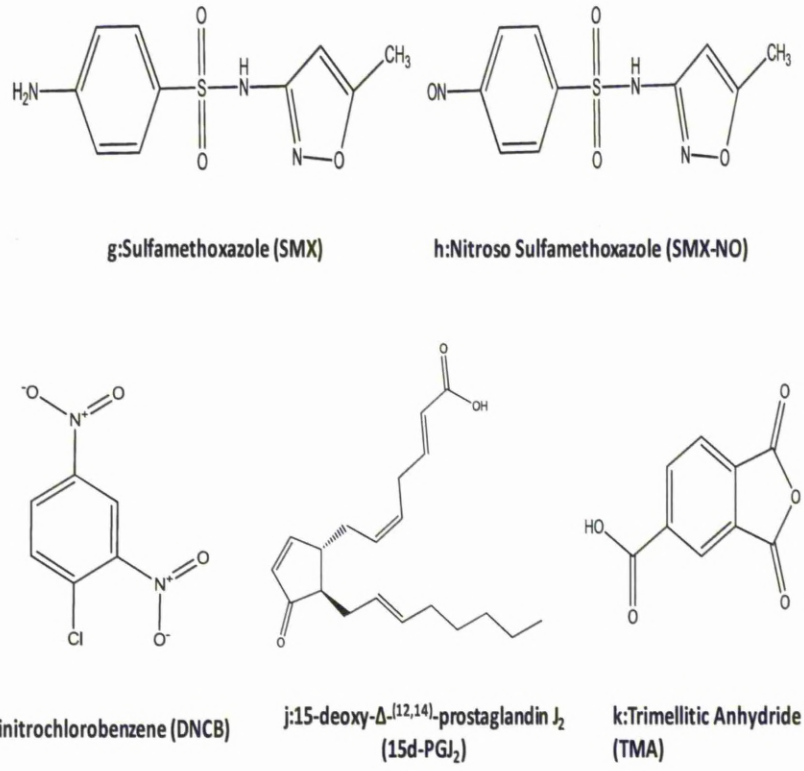

Figure 3.3: Chemical structure of the Nrf2-inducing molecules chosen for investigation in this chapter

3.2 MATERIALS AND METHODS

3.2.1 Materials

The pGL3B-1016/*nqo5'-luc* reporter plasmids was kindly donated by Professor John Hayes (Biomedical Research Centre, University of Dundee, UK). Reporter lysis 5X buffer, the β-galactosidase Enzyme Assay System, the Bright-Glo Luciferase Assay System and QuantiLum recombinant luciferase were from Promega (Southampton, UK). The FL600 fluorescence microplate reader was from BioTek instruments (Winooski, USA). GeneJuice was from Novagen (Nottingham, UK). The nitroso sulfamethoxazole was kindly donated by Dr Dean Naisbitt (MRC Centre of Drug Safety Science, University of Liverpool, UK). Dexamethasone 21—mesylate was obtained from Steraloids (Newport, RI, USA). 15-deoxy-Δ-(12,14)-prostaglandin J2 was from Alexis Biochemicals (Lausen, Switzerland). The benzyl Isothiocyanate, iodoacetamide, tert-butylhydroquinone, resveratrol, buthionine (S,R)-sulfoximine, dinitrochlorobenzene, trimellitic anhydride and sulfamethoxazole were from Sigma-Aldrich (Poole, UK).). All other reagents were of analytical or molecular grade were from Sigma-Aldrich.

3.2.2 Cell Culture and Cell Count

Hepa-1c1c7 cells were maintained and counted as detailed in section 2.2.2.

3.2.3 Cell Treatment

Hepa-1c1c7 cells were seeded onto 96-well plates, 24-well plates and 56.7cm^2 Nunclon Δ culture dishes at 2 x 10^4 cells/well, 2 x 10^5 cells/well and 5 x 10^6 cells/dish respectively on the previous day. All compounds (Fig 3.2) were dissolved in dimethyl sulfoxide (DMSO) except for buthionine sulfoximine (BSO), which was dissolved in distilled water, at 100x the final concentration. 15d-PGJ_2 was supplied pre-dissolved in

methyl acetate, the solvent was removed by evaporation, under a gentle stream of nitrogen gas. The solute was reconstituted in DMSO, at 100x the final concentration, before each treatment. Cells treatment was prepared as detailed in section 2.2.3.

3.2.4 Preparation of cytosolic and nuclear extracts and whole cell lysates

For cytosolic and nuclear extracts and whole cell lysate preparation was detailed as in section 2.2.4.

3.2.5 Measurement of protein content

The total protein content was determined as detailed in section 2.2.5.

3.2.6 Western immunoblotting

Nrf2 western immunoblotting was prepared as detailed in section 2.2.6.

3.2.7 Measurement of Glutathione

Total GSH content was quantified as detailed in section 2.2.11.

3.2.8 Analysis of Mouse Nqo1 ARE Reporter Activity

Hepa-1c1c7 were seeded onto 96-well plates at 2 x 10^4 cells/well and transfected for 24hr with 100 ng of either pGL3B-1016/nqo5'-luc wild-type reporter plasmid or a mutant plasmid containing an entirely scrambled ARE sequence, as previously described by Nioi et al (Nioi *et al.* 2003). pGL3B-1016/*nqo5'-luc* represents the pGL3 basic luciferase vector into which a 1016 bp 5'-upstream region of the mouse Nqo1 gene has been subcloned, enabling ARE-mediated regulation of modified firefly luciferase gene expression. Transfections were performed using GeneJuice reagent (Novagen, Nottingham, UK), in accordance with the manufacturer's instructions. Treatment of cells is as followed in section

3.2.3. Following treatment, media was removed and cells were lysed *in situ* using 0.1ml 1X Reporter Lysis Buffer (Promega, Southampton, UK). Lysates (20µl) were transferred to a white 96-well plate and 20µl Bright-Glo Luciferase assay reagent was added. 15µg QuantiLum recombinant firefly luciferase was used as a positive control for the assay. Air bubbles were removed by centrifuging briefly at 3000rpm. Firefly luciferase activity was measured immediately on BioTek FL600 fluorescence microplate reader, adapted to measure luminescence (BioTek Instruments, Winooski, VT). Blank readings were obtained from wells contain in 1X Reporter Lysis Buffer and Bright-Glo Reagent, and subtracted from sample readings. Blank readings were obtained from wells containing 1X Reporter Lysis Buffer and 1X Assay Buffer, and subtracted from sample reading.

3.2.9 Data Analysis

Data are expressed as mean ± standard deviation of the mean. Normality was assessed by the Shapiro-Wilk test. The significance of differences within the data was assessed by a one-way analysis of variance (ANOVA) or Student's t-test for normally distributed data, and Kruskal-Wallis ANOVA for non-parametric data. A difference was considered significant at $p<0.05$.

3.3 RESULTS

3.3.1 Nrf2 activation and GSH depletion by a panel of Nrf2 inducing molecules

Hepa-1c1c7 cells were exposed to a number of Nrf2 inducing molecules with the aim to determine which of these are the most potent Nrf2 inducers and whether they also result in GSH depletion. This was an initial screen that was carried out to select probe Nrf2-inducing chemicals with different properties for further detailed study. Consequently, only single dose ranging studies for each chemical were carried out, although triplicate measurements were made on all of the samples. Therefore statistical analysis was not appropriate for these sample sets but is carried out on the endpoints generated from the smaller selected chemical panel used in the subsequent experiments in this thesis. Within this panel, the molecules that increased Nrf2 activation and causes GSH depletion were BITC, tBHQ and IA. Those molecules that increased Nrf2 activation and had no effect on GSH content were Dex-mes, 15d-PGJ_2 and SMX-NO. Res and SMX had no effect on both Nrf2 activation and GSH depletion (Fig 3.3a-f). From this panel of Nrf2 inducers, three molecules with the greatest Nrf2 activation from dose range used in this investigation were selected; IA, a sulphydryl alkylating agent which covalently modified cysteine and depleted GSH (Fig 3.2b); Dex-mes, a sulphydryl reactive steroid, which covalently modified cysteine but did not deplete GSH (Fig 3.2d) and finally BSO, an inhibitor of GCLc which depleted GSH but did not result in covalent modification of cysteine (Fig 3.2e).

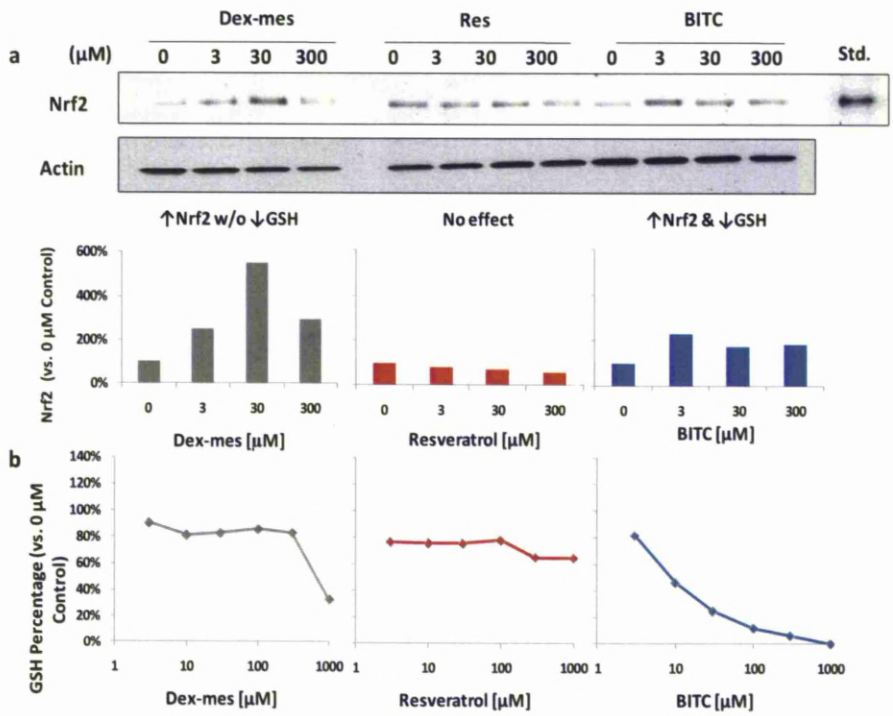

Figure 3.3: Effects of probe molecules on Nrf2 and GSH in Hepa-1c1c7 cells. (a) Western blot analysis of whole cell Nrf2 content in Hepa-1c1c7 cells exposed to the indicated concentrations of Dex-mes, Res and BITC (1hr exposure). Actin was probed as a loading control. The bottom panel shows the densitometric analysis of Nrf2 positive bands normalised against actin. Recombinant mouse Nrf2-His was loaded onto the gels as a standard (Std.). (b) Total GSH, normalised to total protein content, following exposure of Hepa-1c1c7 cells to the indicated concentrations of Dex-mes, Res and BITC (1hr exposure). Results are expressed as the change in GSH level relative to control cells. The control cells are treated with 0.1% DMSO. Representation gels from n=1 is shown. Total GSH level from triplicate measurements, n=1.

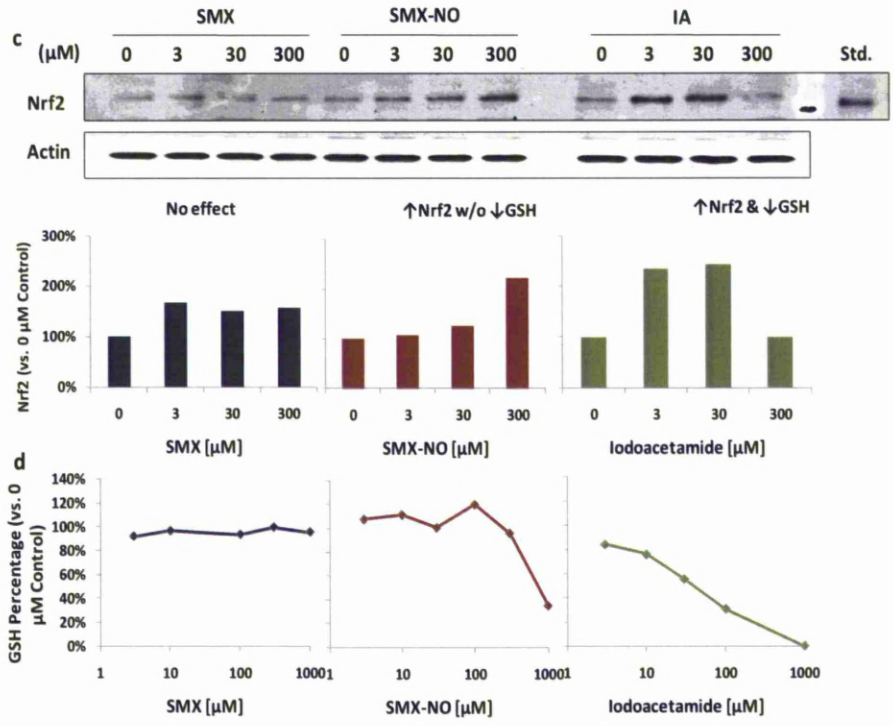

Figure 3.3: Effects of probe molecules on Nrf2 and GSH in Hepa-1c1c7 cells. (c) Western blot analysis of whole cell Nrf2 content in Hepa-1c1c7 cells exposed to the indicated concentrations of SMX, SMX-NO and IA (1hr exposure). Actin was probed as a loading control. The bottom panel shows the densitometric analysis of Nrf2 positive bands normalised against actin. Recombinant mouse Nrf2-His was loaded onto the gels as a standard (Std.). (d) Total GSH, normalised to total protein content, following exposure of Hepa-1c1c7 cells to the indicated concentrations SMX, SMX-NO and IA (1hr exposure). Results are expressed as the change in GSH level relative to control cells. The control cells are treated with 0.1% DMSO. Representation gels from n=1 is shown. Total GSH level from triplicate measurements, n=1.

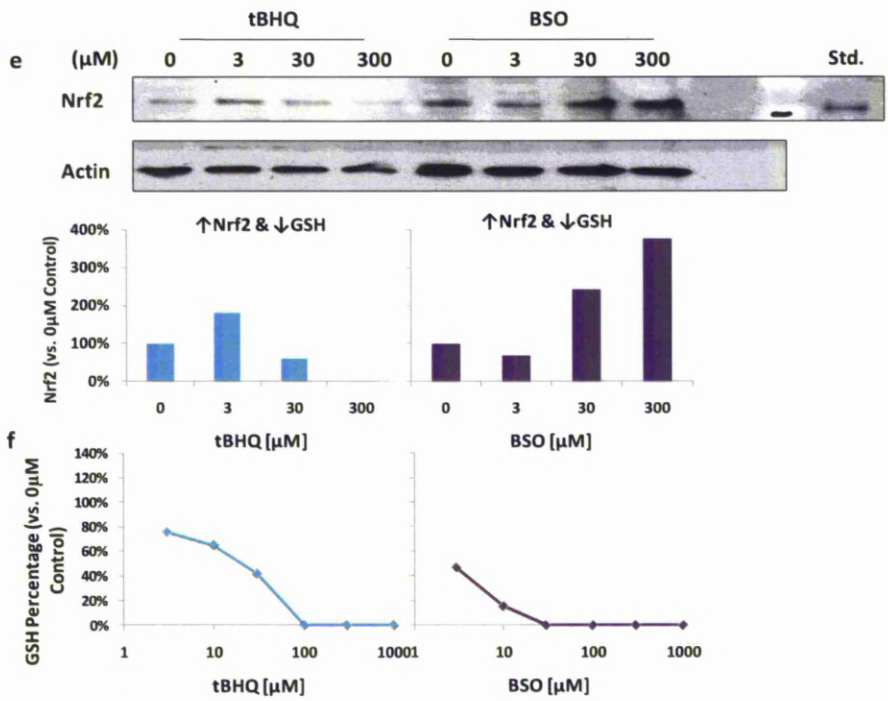

Figure 3.3: Effects of probe molecules on Nrf2 and GSH in Hepa-1c1c7 cells. (e) Western blot analysis of whole cell Nrf2 content in Hepa-1c1c7 cells exposed to the indicated concentrations of tBHQ (1hr exposure) and BSO (24hr exposure). Actin was probed as a loading control. The bottom panel shows the densitometric analysis of Nrf2 positive bands normalised against actin. Recombinant mouse Nrf2-His was loaded onto the gels as a standard (Std.). (f) Total GSH, normalised to total protein content, following exposure of Hepa-1c1c7 cells to the indicated concentrations of tBHQ (1hr exposure) and BSO (24hr exposure). Results are expressed as the change in GSH level relative to control cells. The control cells are treated with 0.1% DMSO except for BSO which is treated with water. Representation gels from n=1 is shown. Total GSH level from triplicate measurements, n=1.

3.3.2: Mouse Nqo1 ARE-regulated reporter assay by panel of Nrf2 inducing molecules

The activity of a reporter assay controlled by the promoter region of the mouse *Nqo1* gene, which contains a functional ARE motif, was used to assess if the increases in cellular Nrf2 are functionally relevant. The wildtype (WT) and mutant (MUT) ARE reporter constructs have been described previously (Nioi *et al.* 2003). Hepa-1c1c7 cells were transfected with wild WT and MUT ARE construct for 24hr, and exposed to Nrf2 inducing molecules for 1hr, the media was then replaced with treatment-free media and allowed to incubate for a further 15hr. This is also an initial screen that was carried out as another test to investigate effect of Nrf2 inducing molecules on Nrf2 activation via ARE binding. The molecules selected from the panel were, BITC (Fig 3.2a), Dex-mes (Fig 3.2d), tBHQ (Fig 3.2d) and Res (Fig 3.2g) with the addition of DNCB (Fig 3.2i).There was no increase in ARE reporter activity with the wild type and no difference was evident in ARE reporter activity between the WT and MUT construct, when exposed to Nrf2 inducing molecules (data not shown).

3.3.3. Activation of Nrf2 by Iodoacetamide, Dexamethasone 21-mesylate and Buthionine (S,R) sulphoximine

The aim of this experiment was to further validate the three selected Nrf2 inducing molecules for their ability to activate Nrf2 with/without cysteine covalent modification or GSH depletion. Larger dose ranges of BSO, Dex-mes and IA, spanning from 0μM to 300μM, were applied to the Hepa-1c1c7 cells. All three molecules induced Nrf2 activation (Fig 3.4). BSO depleted GSH dose-dependently, resulting in 80% depletion in comparison to the control at 300μM (Fig 3.4b). Nrf2 activation was induced to a greater extent when GSH was depleted to approximately 20% of control after 24hr (Fig 3.4a). Dex-mes was able to induce Nrf2 activation at 3μM to 100μM (Fig 3.4c) in the absence of GSH depletion (Fig 3.4d). IA activated Nrf2 dose-dependently (Fig 3.4e) and depleted GSH to undetectable levels within 1 hr at 100μM (Fig 3.4f).

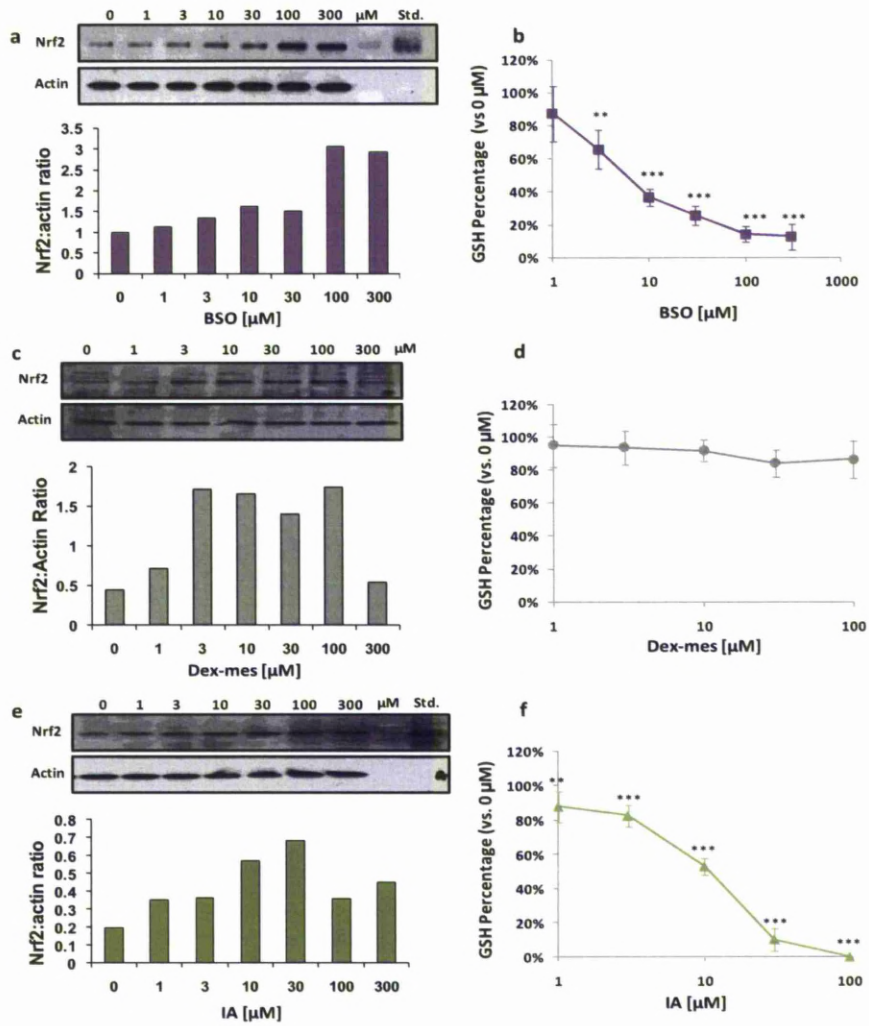

Figure 3.4: Effects of selected molecules on Nrf2 and GSH in Hepa-1c1c7 cells. Western blot analysis of whole cell Nrf2 content in Hepa-1c1c7 cells exposed to the indicated concentration of BSO(a) (24hr exposure), Dex-mes (c) or IA (e) (1hr exposure). β-actin was probed as a loading control. Recombinant mouse Nrf2-His was loaded onto the gels as a standard (Std.).Total GSH, normalised to total protein content, following exposure of Hepa-1c1c7 cells to the indicated concentrations of BSO (b) (24hr exposure, Dex-mes (d) or IA (f) (1hr exposure). Results are expressed as the change in GSH level relative to control cells. The control cells are treated with 0.1% DMSO except for BSO which is treated with water. Kruskal Wallis, $**p<0.01$, $***p<0.001$. Representative gel from n=1 is shown. Error bars = Standard Deviation of Mean, n=3

3.3.4 The role of cysteine adduct formation and GSH depleting molecules Nrf2 activation and its nuclear translocation

To investigate our hypothesis, and explore if either Keap1 cysteine adduct formation, GSH depletion or both mechanisms can trigger Nrf2 activation, we employed a panel of selected molecules with different chemical properties and measured their effects on Nrf2 in Hepa-1c1c7 cells. The probe molecules selected were 15d-PGJ_2, TMA, Dex-mes, DNCB, IA and BSO (Fig 3.5). These molecules were incubated with Hepa-1c1c7 cells and their ability to deplete cellular GSH was measured. Within this panel of molecules, the thiol-reactive steroid Dex-mes, the cyclopentenone 15d-PGJ2 and the lysine-reactive respiratory allergen TMA did not affect GSH levels in Hepa-1c1c7 cells over the concentration range of 0.3μM to 100μM (Fig 3.6). In contrast, the alkylating agents DNCB, IA and BSO caused the concentration-dependent depletion of GSH, with maximal depletion observed with 100μM DNCB and IA, with 100% depletion within 1hr exposure. BSO resulted in 87% ± 8% depletion at 300μM over a 24hr exposure period (Fig 3.6). The probe molecules were then further investigated, assessing their Nrf2 activation potency and subsequent Nrf2 accumulation in Hepa-1c1c7 cells. Cells were exposed to 15d-PGJ_2 (10μM), Dex-mes (30μM), IA (30μM), DNCB (30μM), TMA (30μM) (1hr exposure) or BSO (300μM) (24hr exposure). With the exception of TMA, all of the molecules caused the stabilisation and nuclear translocation of Nrf2 in Hepa-1c1c7 cells (Fig 3.7).

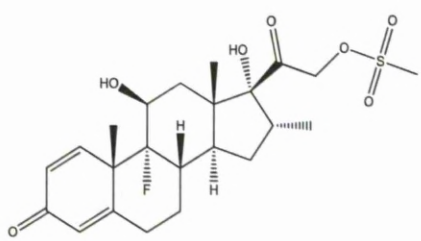

Dexamethasone 21-mesylate (Dex-mes)

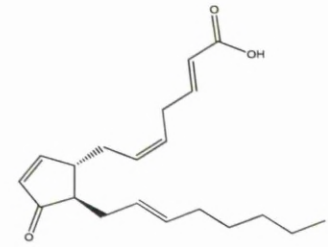

15-deoxy-Δ-$^{(12,14)}$-prostaglandin J_2 (15d-PGJ_2)

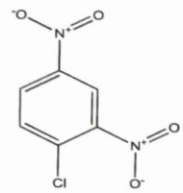

Dinitrochlorobenzene (DNCB)

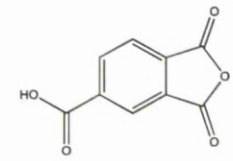

Trimellitic Anhydride (TMA)

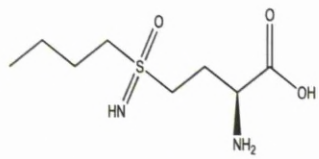

Buthionine (S,R)-sulfoximine (BSO)

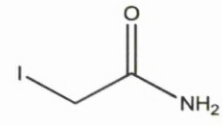

Iodoacetamide (IA)

Figure 3.5: Chemical structures of panel of selected molecules for further investigation of GSH depletion, Nrf2 activation and Nrf2 nuclear accumulation.

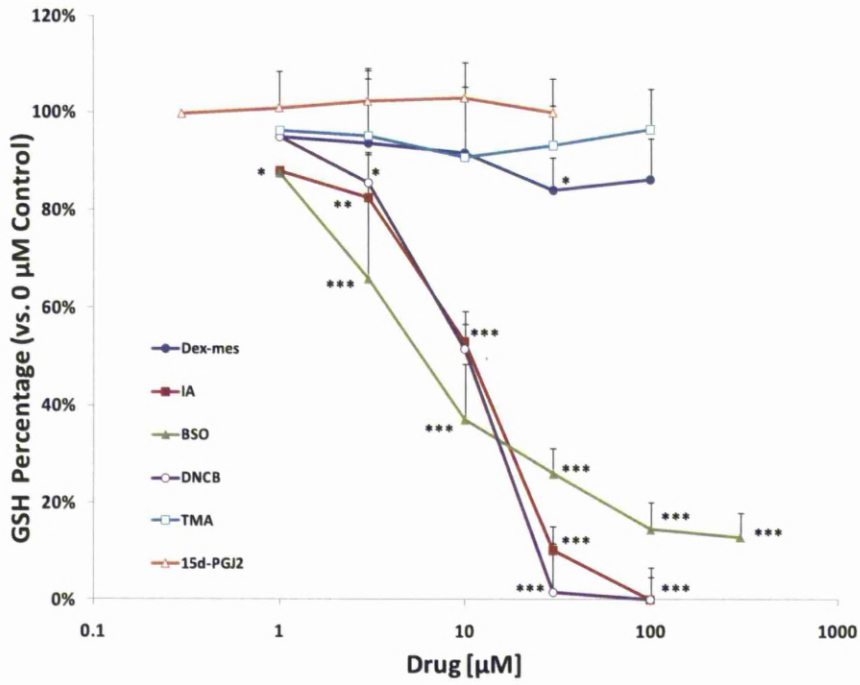

Figure 3.6: Effects of probe molecules on total GSH content in Hepa-1c1c7 cells. Total GSH, normalized to total protein content, following exposure of Hepa-1c1c7 cells to the indicated concentrations of 15d-PGJ_2, Dex-Mes, DNCB, IA, TMA (1hr exposure) or BSO (24-hour exposure). Results are expressed as the change in GSH level relative to control cells, in which GSH content was 37.3 ± 5.4 nmol/mg. One-way ANOVA, *p<0.05, **p < 0.01, ***p <0.001 versus vehicle control. Error bars = Standard deviation of mean, n=3.

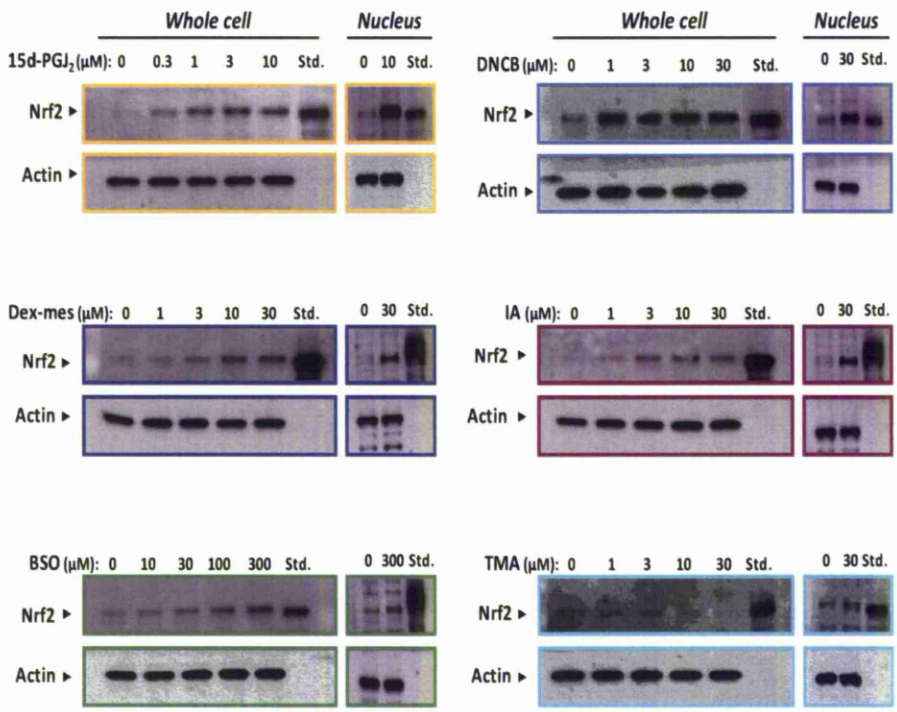

Figure 3.7: Effects of probe molecules on Nrf2 in Hepa-1c1c7 cells. Hepa-1c1c7 cells were exposed to the indicated concentrations of 15d-PGJ_2, Dex-mes, DNCB, IA, TMA (1hr exposure) or BSO (24hr exposure). Western blot analysis of whole cell and nuclear Nrf2 fractions was then performed. β-actin was probed as a loading control. Recombinant mouse Nrf2-His was loaded onto the gels as a standard (Std). Untreated cells were treated with 0.1% DMSO except for BSO which is treated with water. A representative gel from n=3 is shown.

3.4 DISCUSSION

Previously work in the CDSS in Liverpool has shown that the Keap1/Nrf2 pathway, which serves to protect mammalian cells against chemical/oxidative stress, is activated in mouse liver following the administration of acetaminophen *in vivo* (Goldring *et al.* 2004). Others have shown that chemical modification of Keap1's cysteine residues by chemically reactive metabolites lead to the activation of Nrf2 (Dinkova-Kostova *et al.* 2002; Zhang *et al.* 2003; Hong *et al.* 2005a). The possibility exists of formation of disulphide linkage or glutathionylation within Keap1 cysteines by redox perturbation (Holland *et al.* 2008), and that this can lead to the activation of Nrf2 (Wakabayashi *et al.* 2004; Fourquet *et al.* 2010). Although there are several mechanisms that have been proposed to explain the ability of Keap1/Nrf2 to respond to a diverse range of chemical and oxidative stress (Giudice *et al.* 2006; Giudice *et al.* 2010), the molecular mechanisms remain unclear. From functional studies, three cysteines in particular, namely Cys151, Cys273 and Cys288, have been identified to play an important role in Keap1 function. The mutation of Cys151, Cys273 or Cys288 leads to Keap1 being unable to repress Nrf2 basally; mutation of Cys151 have been shown to cause the dissociation of Cullin3-based E3 ubiquitin ligase (Cul3 ligase) from Keap1 leading to the abrogation of Nrf2 ubiquitination (Zhang *et al.* 2003; Zhang *et al.* 2004; Rachakonda *et al.* 2008; Eggler *et al.* 2009); mutation of either Cys273 or Cys288 have been suggested to abrogate the ubiquitination of Nrf2 and subsequent proteosomal degradation (Zhang *et al.* 2003; Levonen *et al.* 2004; Kobayashi *et al.* 2006a; Yamamoto *et al.* 2008). In fact modification studies have also shown that Keap1 cysteines including Cys151, Cys273 and Cys288, are highly reactive and are easily modified by chemicals and electrophiles – in vitro and in vivo? (Dinkova-Kostova *et al.* 2002; Dietz *et al.* 2005; Hong

et al. 2005a; Hong *et al.* 2005b; Eggler *et al.* 2007; Luo *et al.* 2007; Kobayashi *et al.* 2009). Therefore these data provide strong evidence to support the hypothesis that modification of certain cysteine residues within Keap1 may form a mechanism for the activation of Nrf2 (Dinkova-Kostova *et al.* 2002; Dietz *et al.* 2005; Eggler *et al.* 2005; Hong *et al.* 2005b; Liu *et al.* 2005; Luo *et al.* 2007; Yamamoto *et al.* 2008).

Within this study, comprehensive analysis of the panel of Nrf2 activating molecules, I found that molecules known to alkylate cysteine residues, Dex-mes, IA, DNCB and 15d-PGJ_2 do, as expected, induce Nrf2. The induction of Nrf2 leads to a subsequent downstream effect, which leads to the transcription and induction of cytoprotective genes. These cytoprotective genes involved are; phase II detoxify enzymes (Talalay *et al.* 1995), GSH and its synthesis proteins (McMahon *et al.* 2001), NQO1 (Dhakshinamoorthy *et al.* 2001), heat shock proteins and DNA repair enzymes (Kwak *et al.* 2003; Hu *et al.* 2006). Unfortunately, it is unclear whether Nrf2 activation by Dex-mes and DNCB induces that subsequent downstream effect, as our *Nqo1* ARE reporter activity investigation was unsuccessful. The possibilities that *Nqo1* ARE reporter activity being unsuccessful may either be because of poor transfection of the reporter plasmid into the cells or the poor expression of reporter plasmid in the cells, as the luciferase values emitted from the WT treatment correspond to the luciferase values emitted from the MUT treatment. The other reason may be that the cells are undergoing cytotoxicity, where treatment of Hepa-1c1c7 with molecules for 15hr may induce toxicity. Improvments can be made for the ARE reporter transfections; by co-transfecting with pCMV SPORT-β-galactosidase plasmid as an internal control, in which the E.Coli β-galactosidase gene is under the control of the upstream cytomegalovirus (CMV) promoter. The β-

galactosidase measured in the cells can serve to ensure that the transfection is successful; cellular cytotoxicity can be assessed to ensure that the treatment with molecules does not cause toxicity. Furthermore, the reporter plasmid could only increase luciferase activity by 40% after treatment when compared to untreated cells (Copple *et al.* 2008a). Therefore, the induction of luciferase is not high so nuclear accumulation of Nrf2 by Western blotting was used to determine Nrf2 activation was used instead. On the other hand, with the exception of Dex-mes and 15d-PGJ_2, all the other molecules depleted cellular GSH. Hence, given that Dex-mes and 15d-PGJ_2 exposure results in Nrf2 activation in the absence of GSH depletion, it can be concluded that GSH depletion is not a prerequisite for Nrf2 activation. BSO, when phosphorylated, inhibits the activity of GCLc by binding tightly but non-covalently in the enzyme active site (Griffith 1982). BSO activated Nrf2 only when cellular GSH was depleted to 20% of basal levels, a finding which is consistent with previous reports that only substantial depletion of GSH activates the Nrf2/Keap1 pathway (Levonen *et al.* 2004; Maher *et al.* 2007) and previous work from this laboratory showed that a more modest depletion of GSH by BSO to 40% of basal levels *in vivo* is not sufficient to activate Nrf2 (Goldring *et al.* 2004). There was no evidence for direct chemical modification of Keap1 by BSO (data not shown), which is consistent with its known biochemical mechanism of action and chemical structure (Griffith 1982). Therefore, it is possible that from the ability of BSO to deplete GSH and causing cellular redox perturbation, which could lead to the activation of Nrf2 by Keap1 cysteines oxidation. These oxidations may be either R-SOH and disulphide bonds or R-SO_2H and R-SO_3H, which are reversible oxidation or irreversible oxidation respectively (Ghezzi *et al.* 2003). Alternatively, the changes in cellular oxidative status that is provoked by the depletion of GSH may also

induce alternative signalling pathways that are involved in the activation of Nrf2 [for a review, see (Giudice *et al.* 2006; Giudice *et al.* 2010)]. The alternative signalling pathways that are induced by oxidative stress involved kinases; protein kinase C (PKC), mitogen-activated protein kinase (MAPK) cascades and casein kinase II (CK-II). The hypothesis is that these kinases are involved in the possible phosphorylation of Nrf2 leading to the Nrf2 activation. PKC (Bloom *et al.* 2003; Niture *et al.* 2009), MAPK (Cullinan *et al.* 2003; Zipper *et al.* 2003; Keum *et al.* 2006) and CK-II (Pi *et al.* 2007; Apopa *et al.* 2008) have been suggested to be involved in the phosphorylation of Nrf2, and this would alter the association of Nrf2 and Keap1; either allowing or inhibiting the nuclear translocation of Nrf2.

Through the utilisation of this panel of molecules with different electrophilic properties to test the possibility that Nrf2/Keap1 pathway can be induced through a mechanism other than the direct modification of Keap1's cysteine residues, the results in this chapter demonstrated that Nrf2 can be activated (1) by Dex-mes and 15d-PGJ_2 in the absence of GSH depletion but where cysteine residues are alkylated, (2) by DNCB and IA that deplete GSH and are able to alkylate cysteine residues, and (3) by BSO, which depletes GSH but is not able to alkylate cysteine residues. The modification of Keap1 cysteines have been well described in the literature but activation Nrf2 by GSH depletion and its mechanism is not so well described yet. Therefore, future experiments need to be performed to determine the mechanism behind Nrf2 activation through GSH depletion; i.e. is this via the oxidation of cysteines in Keap1, in other associated proteins, through the phosphorylation of Nrf2 by kinases, or through other as yet unidentified mechanisms?

In summary, this study has demonstrated that Nrf2 can be activated by either direct modification of Keap1 or through a profound depletion of GSH alone, and that other toxicologically-relevant molecules such as TMA that display neither of these properties are unlikely to induce Nrf2-dependent cell defence. For molecules that are capable of alkylating Keap1 and depleting GSH, it is likely that the differential contribution of both these mechanism underlies the activation of Nrf2 in a molecule-specific manner. Therefore, it is possible that both direct modification of Keap1 and depletion of GSH are involved in the activation of Nrf2. Such multiple mechanisms for detecting chemical/oxidative stress might explain the well-established versatility of Nrf2/Keap1 pathway.

Chapter 4

Thiol status of Keap1, the regulator of the cell defence transcription factor Nrf2, in the cellular environment

CONTENTS

4.1 INTRODUCTION

Cellular defence against chemical and oxidative stress is largely controlled through the specific activation of the Keap1/Nrf2 pathway and the transcription of Nrf2 dependent genes (Copple *et al.* 2008b). Through the action of Nrf2 at AREs, Keap1 and Nrf2 control cellular defence by regulating the expression of phase II detoxification, antioxidant and phase III transport proteins (Itoh *et al.* 1997; Ishii *et al.* 2002; Aleksunes *et al.* 2009). Currently, the most widely accepted model of the Nrf2 activation mechanism induced by chemical and oxidative stress is the concurrent oxidation or alkylation of key cysteine residues within Keap1 (Holtzclaw *et al.* 2004; Kobayashi *et al.* 2006b).

The human and mouse Keap1 proteins are both cysteine-rich, containing 27 and 25 cyteines, respectively. They therefore have a very high ratio of cysteine to other amino acids, at 4.3% and 4.0 % when compared to other human or mouse proteins, respectively (Miseta *et al.* 2000). The cysteines are distributed throughout the Keap1 protein in four distinct domains; BTB, IVR, DGR and CTR. The role of the cysteine residues within Keap1 has been the main focus of the Nrf2 activation hypothesis. The significant role played by the cysteine residues within Keap1 has been proposed based on cysteine functional, mutagenesis and covalent modification studies. From these investigations, three critical cysteine residues (Cys151, Cys273 and Cys288) have been attributed to play a significant role in the mechanism leading to Nrf2 activation (Zhang *et al.* 2003; Levonen *et al.* 2004; Wakabayashi *et al.* 2004; Kobayashi *et al.* 2006a; Yamamoto *et al.* 2008). Cys273 and Cys288, which are located within the IVR region, have been suggested to maintain the Keap1-dependent repression of Nrf2 under basal conditions in cell-based assays (Zhang *et al.* 2003; Levonen *et al.* 2004;

Wakabayashi *et al.* 2004; Kobayashi *et al.* 2006a) and *in vivo* (Yamamoto *et al.* 2008). Hence, it is believed that the mutation of both cysteines causes Keap1 not to be in a position to correctly bind Nrf2 for targeted ubiquitination and proteosomal degradation. The BTB-located cysteine, Cys151, has been shown to maintain the binding of Cul3 ligase to Keap1. The chemical covalent modification of Cys151 results in the dissociation of Cul3 ligase from Keap1, abrogating the ubiquitination of Nrf2 and the mutation of Cys151 can disrupt this dissociation (Zhang *et al.* 2003; Zhang *et al.* 2004; Rachakonda *et al.* 2008; Yamamoto *et al.* 2008; Eggler *et al.* 2009; Kobayashi *et al.* 2009).

In support of functional and mutagenesis studies of the model, covalent modification studies further support the concept that the cysteine residues within Keap1 play an important role in Nrf2 activation. Many reactive chemicals or electrophiles that are able to react and covalently modify or adduct Keap1 cysteine resisdues, are also able to activate Nrf2 (Dinkova-Kostova *et al.* 2002; Dinkova-Kostova *et al.* 2005; Copple *et al.* 2008a; Rachakonda *et al.* 2008). Electrophiles such as N-iodoacetyl-N-biotinylhexylenediamine (IAB), 1-biotinamido-4-4(4'-[maleimidiethylcyclohexane]-carboxamido)butane (BMCC) and DEX-MES have been shown to covalently modify cysteines present in recombinant mouse or human Keap1 *in vitro* (Dietz *et al.* 2005; Eggler *et al.* 2005; Hong *et al.* 2005a; Hong *et al.* 2005b; Liu *et al.* 2005; Liebler *et al.* 2006; Luo *et al.* 2007). Moreover, recent work has demonstrated that Keap1 cysteines are selectively modified by direct covalent modification in cells which over-express Keap1 in culture (Hong *et al.* 2005b; Copple *et al.* 2008a; Rachakonda *et al.* 2008). The panel of electrophiles studied and reported in the literature do not target a specific cysteine, instead each targets cysteine residues randomly across the Keap1 protein (Fig 4.1).

However, Cys151, Cys273 and Cys288 are targeted by electrophiles at a higher occurrence than the rest of the cysteines. This has lead to the hypothesis that these residues act as key sensors of chemical stress (Fig 4.1). The hypothesis of covalent modification of key sensor cysteines has been proposed previously (Kobayashi *et al.* 2009). However, the exact mechanism of how Keap1 senses the large number of different Nrf2-inducing electrophiles and their reactivity is still not clear.

Therefore, it is also possible that oxidative stress without the formation of chemical adducts on Keap1 can trigger Nrf2 activation. As mentioned previously in chapter 3, substantial depletion of cellular glutathione (GSH) can elicit Nrf2 activation in the absence of covalent modification. The mechanism by which this occurs is currently unclear, however oxidation of cysteine residues has been suggested (Wakabayashi *et al.* 2004). The different forms of cysteine oxidations are shown in Fig 3.1. Currently, there is no direct evidence that the cysteine residues within Keap1 cysteines undergo oxidation *in vivo*. However, Keap1 cysteines oxidation have been suggested from the identification of inter- or intra-disulphides between cysteines residues and S-glutathionylation of cysteine residues using mass spectrometry on recombinant Keap1 and immunoblotting of Keap1 from over-expressing cultured cells (Wakabayashi *et al.* 2004; Holland *et al.* 2008; Fourquet *et al.* 2010; Zhang *et al.* 2010).

Despite the extensive mechanistic studies on Keap1 cysteine residues, the basal thiol status of numerous cysteines in Keap1 is yet to be determined. With the exception of the eight cysteines located within the DGR domain of the human protein appear to be reduced basally, as the study has indicated that they do not appear to participate in disulphide bonds, at least in the absence of cellular stress (Li *et al.* 2004).

Using a cell based model and LC-MS/MS analysis, we have previously described in the CDSS (Copple *et al.* 2008a) are used as experimental methods in this chapter. The aims of this chapter are to investigate what the Keap1 thiol/cysteines status is under basal conditions and to further explore the molecular mechanisms underlying the ability of Keap1 cysteine residues to sense electrophile or oxidative stress.

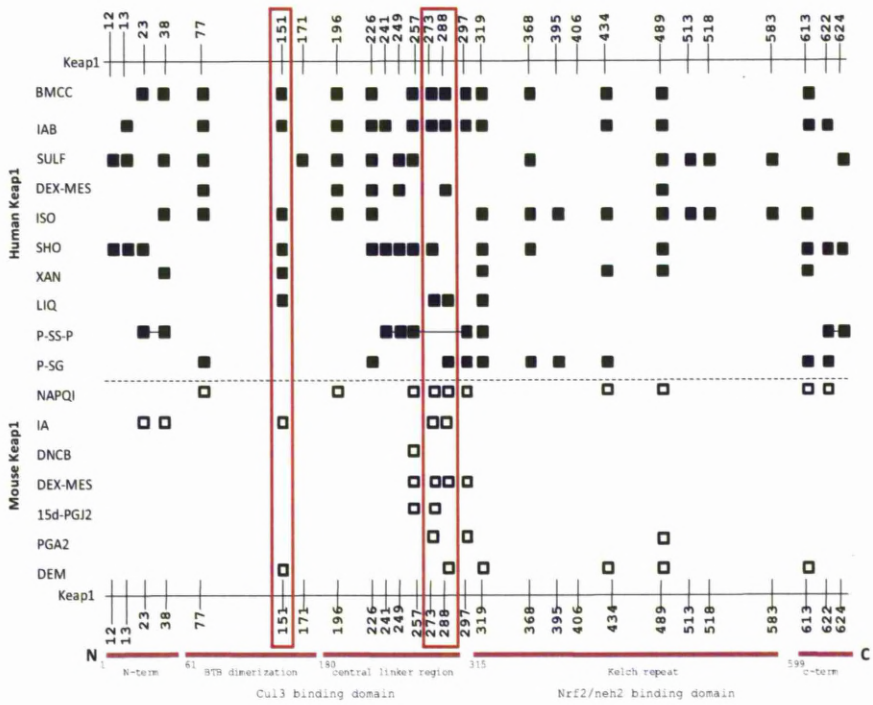

Figure 4.1: Schematic overview of human and mouse Keap1 cysteine residues and their modification by electrophiles. Electrophile modification of human Keap1 cysteine residues (black box) and mouse Keap1 cysteine residues (white box). The red box outlines the three critical cysteines of Keap1 (Cys151, Cys273 and Cys288). The domains of Keap1 are outlined at the bottom of the figure and the cysteine numbers are annotated at the top and bottom of the figure. The abbreviations of the electrophiles are as follows: BMCC; 1-biotinamido-4-4(4'-[maleimidiethylcyclohexane]-carboxamido)butane (Hong *et al.* 2005b; Luo *et al.* 2007), IAB; N-iodoacetyl-N-biotinylhexylenediamine (Hong *et al.* 2005b; Eggler *et al.* 2007), SULF; sulforaphane (Hong *et al.* 2005a), DEX-MES; dexamethasone-21-mesylate (Liebler *et al.* 2006), ISO; isoliquiritigenin, SHO; 10-Shogaol, XAN; xanthohumol (Luo *et al.* 2007), LIQ; liqustilide (Dietz *et al.* 2008), P-SS-P; protein disulphide, P-SG; s-glutathionlyation (Holland *et al.* 2008), NAPQI; N-acetyl-p-benzoquinoneimine, IA; iodoacetamide, DNCB; dinitrochlorobenzene (Copple *et al.* 2008a), DEX-MES (Dinkova-Kostova *et al.* 2002; Copple *et al.* 2008a), 15d-PGJ2; 15-deoxy-$\Delta^{12,14}$-prostaglandin J2 (Copple *et al.* 2008a; Kobayashi *et al.* 2009), PGA2; prostaglandin A2, DEM; diethylmaleate (Kobayashi *et al.* 2009). [Adapted from (Holland *et al.* 2008)].

4.2 MATERIALS AND METHODS

4.2.1 Materials

The Mouse Keap1-V5 encoding plasmid was kindly donated by Dr Ian Copple (CDSS, University of Liverpool, UK). The pcDNA3.1/V5-His-TOPO and Lipofeactamine 2000 were purchased from Invitrogen (Paisley, UK). The XL10-Gold ultracompetent *E. coli.* were purchased from Agilent Technologies (Stockport, UK). Sequencing grade modified trypsin was from Promega (Southampton, UK). The QIAfilter Plasmid Midi Kit was from Qiagen (Crawley, UK). The anti-GSH monoclonal antibody was from Virogen (Massachusetts, USA). The deuterated-5-NEM was from Qmx Laboratories (Essex, UK). The Series 200 HPLC was from Perkin Elmer (Massachusetts, USA). The C18 Uptisphere column was from Interchim, Cheshire Sciences Ltd (Chester, UK). The MALDI target plate, Voyager-DE PRO MALDI-TOF Biospectrometry Workstation, AB Sciex API3000 triple-quadrapole mass spectrometer, API QSTAR Pulsar I MS/MS spectrometer, Analyst QS and ProteinPilot software packages were from Applied Biosystems (Warrington, UK). The αCHCA matrix was from Laserbio Labs (Valbonne, France). The intergrated LCPackings System and C18 PepMap column were from Dionex (Camberley. UK). PicoTip emitters were from New Objective (Woburn, USA). The NanoDrop 1000 UV-spectrophotometer was from Labtech International (East Sussex, UK). The Concentrator 5301 was from Eppendorf (Cambridge, UK). The Nucleofector® was from Lonza (Slough, UK). All other reagents were of analytical or molecular grade and purchased from Sigma-Aldrich (Poole, UK).

4.2.2 Cell Culture and Cell Count

Hepa-1c1c7 cells were maintained and counted as detailed in section 2.2.2. The human embryonic kidney (HEK293T) cells were transformed with the large T antigen of Simian virus 40 (SV40), which enables the episomal replication of transfected plasmids that contain the SV40 origin of replication (DuBridge *et al.* 1987). HEK293T cells were maintained at 37°C in a 5% CO_2 atmosphere in conventional growth medium DMEM supplemented with 584mg/L L-gutamine, 10% FBS, 100 U/ml penicillin, and 100ug/ml streptomycin and cultured as described for Hepa-1c1c7 in section 2.2.2.

4.2.3 Mouse Keap1-V5 plasmid culture

The mouse Keap1-V5-encoding plasmid (Keap1-V5) was generated by Dr Ian Copple (Copple *et al.* 2008a). A mouse Keap1 full coding sequence with no stop codon was inserted into the TOPO cloning site of pcDNA3.1/V5-His-TOPO and transformed into XL10-Gold ultracompetent *E. coli*. A 15% (v/v) glycerol stock of pcDNA3.1/Keap1-V5 XL10-Gold E. *coli* was cultured in 600ml of LB broth supplemented with 50μg/ml ampicillin and incubated for 24hr at 37°C, 250rpm. The pcDNA3.1/Keap1-V5 plasmid was purified using QIAfilter Plasmid Midi Kit and eluted into 1X TE buffer (10mM Tris base, 1mM EDTA, pH 7.5). 1μl of the plasmid was assessed using a NanoDrop 1000 UV-spectrophotometer for DNA concentration and purity. An absorbance of 1.0 at 260nm is equivalent to 50μg/ml of DNA. The purity of DNA in each sample was determined via reference to the 260nm:280nm ratio. DNA samples with a 260nm:280nm ratio of below 1.8 were deemed as impure.

4.2.4 Transfection of cells with Keap1-V5

4.2.4.1 Lipofectamine transfection of cells with Keap1-V5

HEK293T or Hepa-1c1c7 cells were seeded onto 56.7cm^2 Nunclon Δ culture dishes at 4 X 10^6 cells/dish, on the day previously. Cells were transfected with pcDNA3.1/Keap1-V5 plasmid using Lipofectamine 2000. For each dish of cells, 1ml DMEM was combined with 40µl of Lipofectamine 2000 in a 20ml tube. 1ml DMEM was combined with 16µg of plasmid in a 20ml tube. The contents of both tubes were mixed and incubated at room temperature for 20min. All of the mixture was added, dropwise, to the dish. Cells were returned to a humidified incubator, at 37°C in a 5% CO_2 atmosphere for 24hr.

4.2.4.2 Nucleofector® transfection (nucleofection) of cells with Keap1-V5

The Nucleofector® method was attempted for the Keap1-V5 transfection. Hepa-1c1c7 cells were harvested and 1 X 10^6 or 2 X 10^6 cells were counted. Counted cells were centrifuged at 1500rpm for 5min and the supernatant was discarded. The cell pellet was resuspended at room temperature in Nucleofector® Solution provided by the manufacturer to a final concentration of 1 X 10^6 - 2 X 10^6 cells/100µl. 1µg or 5µg of DNA plasmid was then added to the 100µl cell suspension. The mixture was transferred into a certified cuvette provided by the manufacturer, while making sure that the sample covers the bottom of the cuvette, avoiding air bubbles and cuvette closed with a blue cap. The appropriate Nucleofector® program (H022 or T028) was selected with the cuvette inserted into the cuvette holder in the Nucleofector® and the programmed transfection was started. The cuvette was taken out after the programmed transfection, cells were transferred from the cuvettes into prepared 6-well plates. Cells were returned to a humidified

incubator, at 37°C in a 5% CO_2 atmosphere for 16hr and 19hr. All preparations were done under sterile conditions.

4.2.5 Cell Treatment

Hepa-1c1c7 cells were seeded onto 96-well plates and 6-well plates at 2 x 10^4 cells/well and 1 x 10^6 cells/well respectively on the previous day. Diamide was dissolved in water. Cell treatment was prepared as detailed in section 2.2.3.

4.2.6 Preparation of whole cell lysates

Whole cell lysate preparation was conducted as in section 2.2.4.

4.2.7 Measurement of Protein content

The total protein content was determined as detailed in section 2.2.5.

4.2.8 Immunopurification of Keap1-V5 after cell treatment

HEK293T cells were seeded onto 56.7cm^2 Nunclon Δ culture dishes at 4 X 10^6 cells/dish. BSO and diamide were dissolved in water and IA, NEM and DNCB were dissolved in DMSO. For BSO, diamide and DNCB, cell treatment was prepared as detailed in section 2.2.3. IA and NEM were dissolved in DMSO at 20x the final concentration. To each dish, 500µl of the dissolved compound or a DMSO control were added (1:20 dilutions) for 2min. The cells were lysed for immunopurification of Keap1-V5.

Keap1-V5 was immunopurified from whole cell lysate prepared in RIPA buffer. 1ml of lysate was incubated with 60µl anti-V5 agarose beads on a mechanical roller for 2hr at 4°C. The beads were collected by centrifugation at 5000g for 1min and washed three times with 500µl 1X PBS.

4.2.9 Western Immunoblotting

4.2.9.1 Whole cell lysates immunoblotting

Whole cell lysates (10μg or 25μg) were immunoblotted for Nrf2 and Keap1 as detailed in section 2.2.6.

4.2.9.2 Immunopurified Keap1-V5 immunoblotting

Immunopurified Keap1-V5 was immunobloted for Keap1 and S-glutathionylation as detailed in section 2.2.6. Proteins were eluted from anti-V5 agarose beads by resuspending in an equal volume of NuPage loading buffer. The slurry was heated at 80°C for 5min and the beads pelleted by centrifugation for 5min at 5000g. The supernatant was loaded onto a pre-cast 4-12% NuPage Novex bis-tris polyacrylamide gel. For non-reducing condtions, NuPage reducing sample was replaced with distilled water in the loading buffer and NuPage antioxidant was removed from the MOPS running buffer. Immunoblotting for S-glutathionylation were performed with mouse monoclonal anti-mouse glutathione (1:1000 in TBS-Tween containing 2% (w/v) BSA) and mouse anti-mouse (1:5000 in TBS-Tween containing 2% (w/v) BSA) HRP-conjugated secondary anti-IgG for 1hr.

4.2.10 Coomassie Brilliant Blue Staining and in-gel trypsin digestion

After immunopurification of Keap1-V5 as detailed in 4.2.8, proteins were eluted from anti-V5 agarose beads and loaded onto a gel as detailed in 5.2.9. After electrophoresis, the gel was fixed for 1hr in 40% (v/v) methanol containing 7% (v/v) glacial acetic acid. Coomassie staining solution was prepared by mixing 4 parts Coomassie stain (0.1% (w/v) Coomassie Brilliant Blue G-250 in 2% (w/v) phosphoric acid, 16% (w/v) ammonium sulphate) with 1 part 100% methanol. The gel was then stained with Coomassie staining solution for 1-2hr with gentle

agitation. The gel was destained with 10% (v/v) glacial acetic acid in 25% (v/v) methanol for 1min with gentle agitation. The gel was rinsed in 25% (v/v) methanol, and detained further in 25% (v/v) methanol for up to 24hr and stored at 4°C. The stained gel was placed on a light box and bands of interest were excised using a scalpel. The gel pieces were individually destained, in 0.1ml of 50mM ammonium bicarbonate (AmBic) in 50% (v/v) acetonitrile (ACN) for 15min at room temperature with occasional agitation. The destaining solution was removed and gel pieces were dried in a Concentrator 5301 for up to 15min. The gel pieces were rehydrated with 30µl 50mM AmBic containing 5ng/µl sequencing-grade modified trypsin and incubated overnight at 37°C. After tryptic digestion, 30µl of 60% (v/v) ACN, 1% (v/v) trifluoroacetic acid (TFA) was added and the samples were placed in a sonicating water bath for 5min at room temperature. The gel pieces were pelleted by centrifugation for 30s at 1000g, and the supernatant transferred to a new microfuge tube. A further 30µl of 60% (v/v) ACN, 1% (v/v) TFA was added to gel pieces, and the gel pieces were placed in the sonicating water bath for 5min at room temperature. The gel pieces were pelleted by centrifugation for 30s at 1000g, and supernatant was combined with that from the previous spin. The sample was dried in a Concentrator 5301 and the solute was reconstituted in 10µl of 5% (v/v) ACN/0.05% (v/v) TFA.

4.2.11 MALDI-TOF mass spectrometry

Following overnight tryptic digestion, peptide mixtures (0.5µl) were combined with an equal volume of α-cyano-4-hydroxy-cinnamic acid (αCHCA) matrix (10mg/ml αCHCA in 50% (v/v) ACN, 0.1% (v/v) TFA) and spotted onto a MALDI-TOF target plate alongside ProteoMass MALDI-MS standards (angiotensin II, adrenocorticotropic hormone fragment 18-39, oxidised insulin chain B, 0.5pmol each), using the dried-

droplet method. Peptide mass fingerprints were obtained on a Voyager DE Pro MALDI time-of-flight (TOF) Biospectrometry Workstation, in linear positive ion mode, and used in a MASCOT protein database search (http://www.matrixscience.com) to enable identification present within the sample.

4.2.12 LC-MS/MS methods

Samples were prepared by adding the following in a ratio of 1:5, diamide:GSH in water for 30min. The formation of the conjugate was measured using a Perkin Elmer Series 200 HPLC, 50µL of sample was injected on to a reversed-phase C18 Uptisphere column, 100 x 2.1 mm, 5µm and AB Sciex API3000 triple-quadrapole mass spectrometer was used for detection. The gradient solvent system used to separate the sample compounds consisted of 95% H2O + 0.1% formic acid (A) and 5% methanol (B) held for 2min, then increased to 95% (B) linearly for 9mins and increased back to 95% (A) held for 2min. The flow rate was 0.2ml/min, and column temperature was set at 30°C. Mass spectrometric data acquisition was performed using the following conditions: positive ionisation mode, ionisation voltage 5500V, ion source 350°C, nebuliser gas and curtain gas was maintained at settings of 12 and 10, respectively. The declustering potential was 51V and collision energy was 15V for all MS/MS scan. The mass transitions monitored were m/z 173 (diamide), m/z 380 (diamide + GSH), m/z 308 (GSH), m/z 613 (GSSG) and m/z 175 (hydrazine).

4.2.13 Preparation of NEM-modified human serum albumin for mass spectrometry

Human serum albumin (HSA) (2nmol) was dissolved in phosphate buffer was incubated with increasing ratios of NEM (1:1, 1:10, 1:100 and 1:500) dissolved in DMSO or DMSO as control for 2min at room

temperature. The HSA (20µl) was precipitated with 9 volumes of ice-cold methanol and was recovered by centrifuging at 14000g, 4 °C for 10 min. This was repeated three times to yield the maximum precipitation of HSA. The pellet were reduced by the addition of 20µl of 10mM DTT at 50 °C for 15min and unmodified cysteines were alkylated with 20µl of 55mM IA at room temperature for 15min. The HSA was precipitated again after treatment and pellet resuspended with 50µl of 50mM AmBic and was digested with 3 µg trypsin at 37 °C overnight. For LC-ESI-MS/MS analysis, the supernatant containing the peptides were dried in a Concentrator 5301. The solute was then reconstituted in 40µl of 5% (v/v) ACN, 0.05% TFA.

4.2.14 Preparation of Keap1-V5 for mass spectrometry

After incubation and washing, PBS was removed from Keap1-V5-bound anti-V5 agarose beads after centrifugation. The resulting beads (40µl dry volume) were reduced by resuspending in 59µl of PBS and 1µl of 100mM DTT. The mixture was incubated on a mechanical roller at 4°C for 15min. The beads were washed three times with 500µl of PBS after incubation to remove residual DTT. The unmodified cysteines were alkylated by resuspending beads in 50µl of PBS and 10µl of 550mM of IA or 200mM of NEM/d_5NEM, and incubated on a mechanical roller at 4°C for 15min. The beads were washed three times in 500µl of PBS to remove residual IA, NEM or d_5NEM after incubation. Prior to tryptic digestion, beads were washed once with 200µl of 25mM AmBic and then resuspended in 20µl of 25mM AmBic. A 400µg/ml stock solution of sequencing-grade modified trypsin was diluted 1 in 10 with 25mM AmBic and 5µl was added to the beads mixture. Trypsin digestion of the protein was performed overnight at 37°C. For LC-ESI-MS/MS analysis, the beads were pelleted after trypsin digestion by centrifuging for 30sec

at 5000g. The resulting supernatant containing the peptides was transferred to a new microfuge tube and dried in a Concentrator 5301 set at 30°C. The solute was reconstituted in 40µl of 5% (v/v) ACN, 0.05% TFA.

4.2.15 LC-ESI-MS/MS methods

The reconstituted solute (40µl) prepared from section 4.2.13 was loaded using a 0.1ml loop. The sample was delivered into an API QSTAR Plusar i system by automated in-line reversed phase liquid chromatography (LC) using an integrated LCPackings System (Famos autosampler, Ultimate LC pump, Switchos microcolumn switching module) and a 75µm x 15cm C18 PepMap Column via a nano-electrospray source head with a 10µm inner diameter PicoTip emitter. LC conditions were as follows; 15min at 5% (v/v) ACN, 0.05% (v/v) TFA, a gradient 5-48% (v/v) ACN, 0.05% (v/v) TFA over 60min, 10min at 99% (v/v) ACN, 0.05% (v/v) TFA and 10min at 5% (v/v) ACN, 0.05% (v/v) TFA, with a flow rate of 0.35µl/min throughput. Across a mass range of 300-2000 Dalton (Da), MS and MS/MS spectra were acquired automatically in positive ion mode using information-dependent acquisition powered by Analyst QS software. With an above threshold of 5 counts per sec, the three most intense ions in each MS spectrum were subjected to MS/MS analysis for 1.5sec and subsequently excluded from further analysis for 40sec. Amino acid modifications were detected with ProteinPilot software v2.0 using the Paragon™ algorithm and the most recent version of SwissProt database. Carboxyamidomethyl (+57.0Da), NEM (+126.0Da), d_5NEM (+131.0Da) and dinitrophenyl (DNP; +166.0Da) were selected as variable modifications. All adducts were confirmed by visual inspection of the MS/MS spectra.

4.3 RESULTS

4.3.1 Validation of Keap1-V5 transfection in HEK293T and Hepa-1c1c7 cells as models for investigating the thiol status of Keap1

Two methods were employed for the transient expression of Keap1-V5 in HEK293T and Hepa-1c1c7 cells. Firstly, both cell lines were transiently transfected for 16hr with Keap1-V5 via Lipofectamine 2000. The expression of Keap1-V5 in HEK293T and Hepa-1c1c7 cells by Lipofectamine were showed in Dr Ian Copple's thesis and separately here (Fig 4.2a). Keap1-V5 was well expressed in HEK293T but no expression was seen in the Hepa-1c1c7. A time-range investigation was used to compare Keap1-V5 transient transfection with Lipofectamine between HEK293T and Hepa-1c1c7. The Keap1 expression by time-range transfection at 19hr, 24hr and 28hr with lipofectamine in Hepa-1c1c7 was still not as efficient as in HEK293T at 24hr (Fig 4.2b). Since Lipofectamine was effective in transfecting Keap1-V5 into HEK293T, a range of Keap1-V5 DNA to Lipofectamine ratios were investigated to determine which ratio gave the optimum transfection. From the range of ratios investigated, a DNA to Lipofectamine ratio of 1:2.5 was determined to be the most efficient (Fig 4.2c). Longer transfection periods of 48hr improved the levels of Keap-V5 expression in HEK293T (4.2d). Next, a second method of transfection, nucleofection was used to try to improve the expression of Keap1-V5 in Hepa-1c1c7 cells. The cells were transiently transfected for 16hr with Keap1-V5 by nucleofection with 5μg of plasmid. These methods were shown to improve the expression (Fig 4.3a). Following this, increasing the amount of cells used for transfection and increasing the incubation period after nucleofection were tested to further improve and optimise the Keap1-V5 expression. However, neither increasing the amount of cells nor the longer

incubation period had any additional improvement on the expression of Keap1-V5 (Fig 4.3b and c). In fact, the results shown by nucleofection suggested that this method was inconsistent as the expression of Keap1-V5 varied with different transfections done. Therefore, Hepa-1c1c7 cells could not express Keap1-V5 efficiently with both transfection methods used. HEK293T transiently expressing Keap1-V5 remained the best model for the investigation of the thiol status of cysteine residues within Keap1 in living cells.

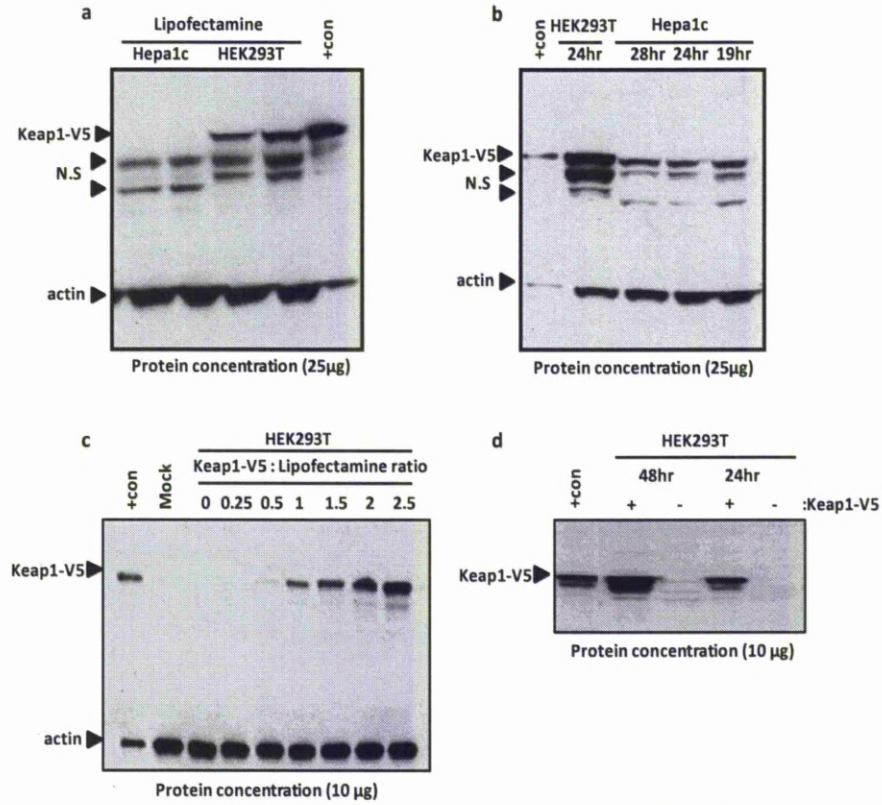

Figure 4.2: Transient expression of Keap1-V5 in HEK293T and Hepa-1c1c7 cells. HEK293T and Hepa-1c1c7 cells were transfected with Keap1-V5, using lipofectamine (a-d). Cell lysates were resolved using SDS-Page and the blots were probed for Keap1. Keap1-V5 was only expressed in HEK293T and not Hepa-1c1c7 with Lipofectamine (16hr) (a). Time-range transfections in Hepa-1c1c7 were not as effective as when compared to HEK293T (b). A Keap1-V5 DNA:Lipofectamine ratio of 1:2.5 was the optimised ratio for efficient expression of Keap1-V5 in HEK293T (c). A 48hr transfection increased the expression of Keap1-V5 compared to 24hr transfection (d). Recombinant Keap1-V5 was loaded as a positive control on the blot (+con). A representative gel is shown from n=2-3.

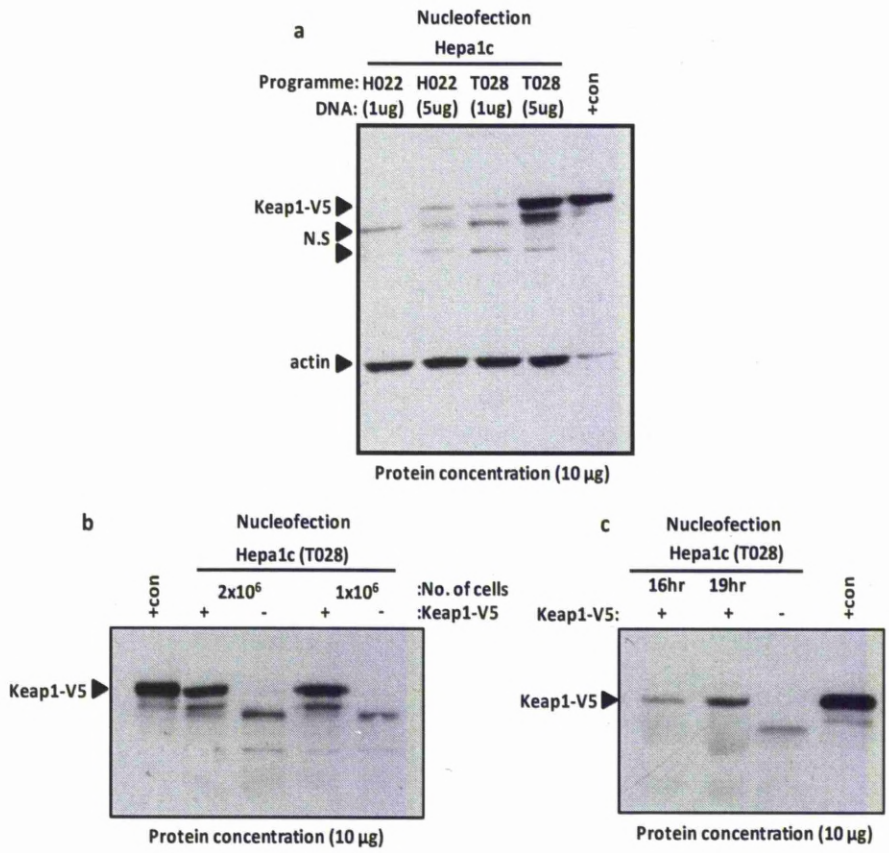

Figure 4.3: Transient expression of Keap1-V5 in HEK293T and Hepa-1c1c7 cells. HEK293T and Hepa-1c1c7 cells were transfected with Keap1-V5, using nucleofection (a-c). Cell lysates were resolved using SDS-Page and the blots were probed for Keap1. Nucleofection dependent transfection improved Keap1-V5 expression in Hepa-1c1c7 (a). The number of cells did not increase the amount of expression of Keap1-V5 with nucleofection after 16hr (b). Both 16hr and 19hr incubation periods could not reproduce consistent expression (c). Recombinant Keap1-V5 was loaded as a positive control on the blot (+con). A representative gel is shown from n=2-3.

4.3.2 MALDI-TOF MS identification of expressed and purified Keap1-V5 in HEK293T

The expression of Keap1-V5 in HEK293T was identified by MALDI-TOF. HEK293T cells were transfected with Keap1-V5 for 24hr and cells were lysed with RIPA buffer. The cell lysates were incubated with anti-V5 agarose beads. Following incubations with cell lysates, proteins bound to beads were resolved using SDS-PAGE and Coomassie Brilliant Blue G-250 (CCB) staining. Sections of the protein-stained gel were excised; bands 1-4 (Fig 4.4) were subjected to tryptic digestion and analysed by MALDI -TOF MS analysis. Bands 1 and 2 were identified as having mouse Keap1 as the major constituent protein. Bands 3 and 4 are the mouse immunoglobulin (IgG) heavy and light chains which were fragments of the anti-V5 IgG released from the anti-V5 agarose beads (Fig 4.4). Mouse Keap1 appeared as two bands on the gel, however, a MALDI–TOF MS analysis and MASCOT database search did not identify any oxidised cysteines on both Keap1-V5 bands (Fig 4.5-4.8).

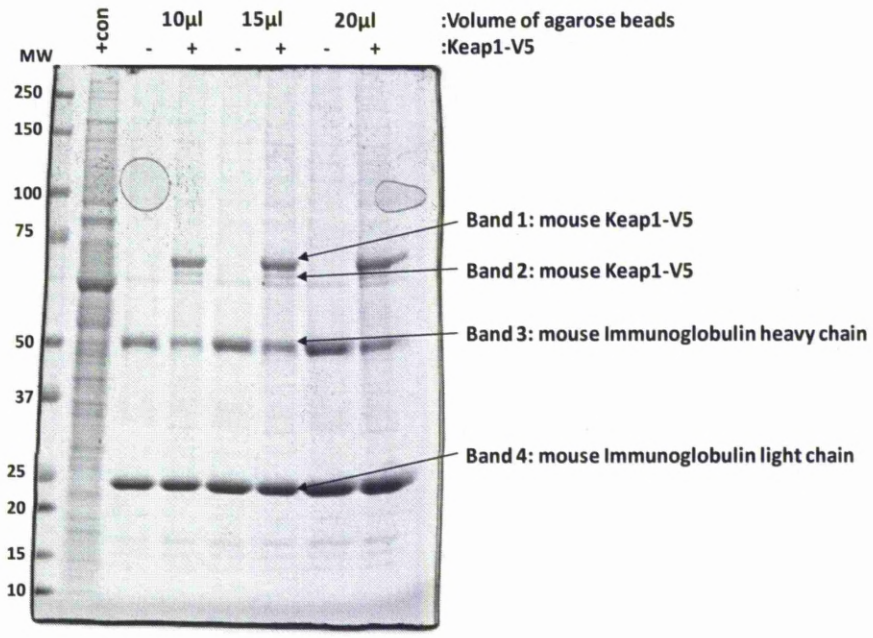

Figure 4.4: Identification of anti-V5 immunoprecipitated proteins with anti-V5 agarose beads. HEK293T cells were transfected with or without Keap1-V5 for 24hr. Whole cell lysates were prepared and incubated with anti-V5 agarose beads for 2hr at 4°C. Protein bound anti-V5 agarose beads were resolved by SDS page and CCB stained for protein visualisation. Stained protein bands were excised, digested with trypsin and analysed by MALDI-TOF. The data obtained from the MALDI-TOF MS spectra were used in a MASCOT protein database search to identify the major protein constituent(s) for each band Proteins with the highest degree of confidence were shown.

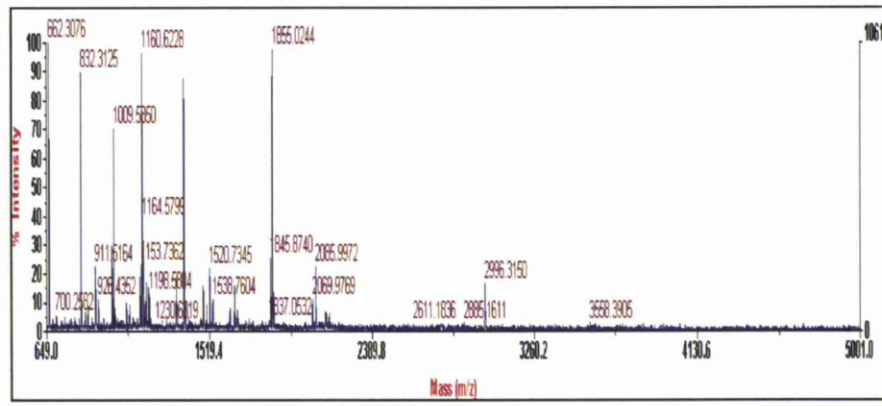

Figure 4.5: MALDI-TOF mass spectrum of the tryptic digests from proteins present in band 1. Band 1 as depicted in Fig 4.4 was excised, digested with trypsin and analysed by MALDI-TOF. The resulting peptide mixture was visualised on a Voyager DE Pro MALDI-TOF Biospectrometry Workstation, in linear positive ion mode.

	Accession	Mass	Score	Description
1.	KEAP1_MOUSE	69508	294	Kelch-like ECH-associated protein 1 - Mus musculus (Mouse)
2.	KEAP1_RAT	69354	261	Kelch-like ECH-associated protein 1 - Rattus norvegicus (Rat)
3.	KEAP1_PIG	69771	144	Kelch-like ECH-associated protein 1 - Sus scrofa (Pig)
4.	KEAP1_HUMAN	69621	122	Kelch-like ECH-associated protein 1 - Homo sapiens (Human)
5.	KEAP1_PONAB	69663	112	Kelch-like ECH-associated protein 1 - Pongo abelii (Sumatran orangutan)

Match to: **KEAP1_MOUSE Kelch-like ECH-associated protein 1 - Mus musculus (Mouse)**
Sequence Coverage: **57%**

1 MQPEPKLSGA PRSSQFLPLW SKCPEGAGDA VMYASTECKA EVTPSQDGNR
51 TFSYTLEDHT KQAFGVMNEL RLSQQLCDVT LQVKYEDIPA AQFMAHKVVL
101 ASSSPVFKAM FTNGLREQGM EVVSIEGIHP KVMERLIEFA YTASISVGEK
151 CVLHVMNGAV MYQIDSVVRA CSDFLVQQLD PSNAIGIANF AEQIGCTELH
201 QRAREYIYMH FGEVAKQEEF FNLSHCQLAT LISRDDLNVR CESEVFHACI
251 DWVKYDCPQR RFYVQALLRA VRCHALTPRF LQTQLQKCEI LQADARCKDY
301 LVQIFQELTL HKPTQAVPCR APKVGRLIYT AGGYFRQSLS YLEAYNPSNG
351 SWLRLADLQV PRSGLAGCVV GGLLYAVGGR NNSPDGNTDS SALDCYNPMT
401 NQWSPCASMS VPRNRIGVGV IDGHIYAVGG SHGCIHHSSV ERYEPERDEW
451 HLVAPMLTRR IGVGVAVLNR LLYAVGGFDG TNRLNSAECY YPERNEWRMI
501 TPMNTIRSGA GVCVLHNCIY AAGGYDGQDQ LNSVERYDVE TETWTFVAPM
551 RHHRSALGIT VHQGKIYVLG GYDGHTFLDS VECYDPDSDT WSEVTRMTSG
601 RSGVGVAVTM EPCRKQIDQQ NCTC

Figure 4.6: MASCOT protein database search results for a peptide mass fingerprint obtained from the MALDI-TOF MS analysis of band 1. The peptide mass fingerprint was applied to a MASCOT protein database search which identified the band 1 tryptic digest as mouse Keap1 without any post-translational modification. The top five proteins identified with the highest score of confidence are shown. The amino acid sequence coverage for mouse Keap1 was 57% and specific peptides covered by the MALDI-TOF MS analysis are underlined and in bold letters.

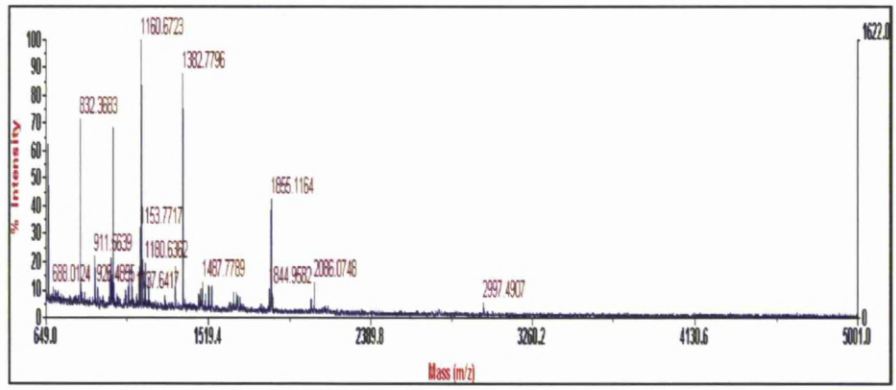

Figure 4.7: MALDI-TOF mass spectrum of the trypsin digests from proteins present in band 2. Band 2 as depicted in Fig 4.4 was excised, digested with trypsin and analysed by MALDI-TOF. The resulting peptide mixture was visualised on a Voyager DE Pro MALDI-TOF Biospectrometry Workstation, in linear positive ion mode.

	Accession	Mass	Score	Description
1.	KEAP1_MOUSE	69508	141	Kelch-like ECH-associated protein 1 - Mus musculus (Mouse)
2.	KEAP1_RAT	69354	104	Kelch-like ECH-associated protein 1 - Rattus norvegicus (Rat)
3.	KEAP1_PIG	69771	71	Kelch-like ECH-associated protein 1 - Sus scrofa (Pig)
4.	KEAP1_HUMAN	69621	62	Kelch-like ECH-associated protein 1 - Homo sapiens (Human)

Match to: **KEAP1_MOUSE Kelch-like ECH-associated protein 1 - Mus musculus (Mouse)**
Sequence Coverage: **28%**

1 M**QPEPKLSGA PR**SSQFLPLW SKCPEGAGDA VMYASTECKA EVTPSQDGNR
51 **TFSYTLEDHT KQAFGVMNEL R**LSQQLCDVT LQVK**YEDIPA AQFMAHKVVL**
101 **ASSSPVFK**AM FTNGLR**EQGM EVVSIEGIHP K**VMERLIEFA YTASISVGEK
151 CVLHVMNGAV MYQIDSVVRA CSDFLVQQLD PSNAIGIANF AEQIGCTELH
201 QRAR**EYIYMH FGEVAK**QEEF FNLSHCQLAT LISRDDLNVR CESEVFHACI
251 DWVKYDCPQR R**FYVQALLR**A VRCHALTPR**F LQTQLQK**CEI LQADARCKDY
301 LVQIFQELTL HKPTQAVPCR APKVGR**LIYT AGGYFR**QSLS YLEAYNPSNG
351 SWLR**LADLQV PR**SGLAGCVV GGLLYAVGGR NNSPDGNTDS SALDCYNPMT
401 NQWSPCASMS VPRNRIGVGV IDGHIYAVGG SHGCIHHSSV ERYEPERDEW
451 HLVAPMLTR**R IGVGVAVLNR LLYAVGGFDG TNR**LNSAECY YPERNEWR**MI**
501 **TPMNTIR**SGA GVCVLHNCIY AAGGYDGQDQ LNSVER**YDVE TETWTFVAPM**
551 **R**HHR**SALGIT VHQGK**IYVLG GYDGHTFLDS VECYDPDSDT WSEVTRMTSG
601 RSGVGVAVTM EPCRKQIDQQ NCTC

Figure 4.8: MASCOT protein database search results for a peptide mass fingerprint obtained from the MALDI-TOF MS analysis of band 2. The peptide mass fingerprint was applied to a MASCOT protein database search which identified the band 2 tryptic digest as mouse Keap1 without any post-translational modification. The top four proteins identified with the highest score of confidence are shown. The amino acid sequence coverage for mouse Keap1 was 28% and specific peptides covered by the MALDI-TOF MS analysis are underlined and in bold letters.

4.3.3 Alkylation of Keap1-V5 cysteine residues with a high concentration of alkylating agents, iodoacetamide and N-ethylmaleimide

The cell based model, previously described to investigate the formation of chemical adducts on Keap1-V5 cysteines (Copple *et al.* 2008a), was used to study the basal thiol status of Keap1 in the cellular environment. The common alkylating agents, IA and NEM were used to investigate the Keap1-V5 cysteine status in HEK293T cells by LC-ESI-MS/MS. A high concentration of IA and NEM (50mM) was used to treat the cells for 2mins. This was used as a freezing technique to attempt to alkylate all available reduced cysteine residues. Successful cysteine alkylation would indicate that the alkylated cysteine exists in a reduced form under basal conditions. Following alkylation, Keap1-V5 was immunoprecipitated from whole cell lysates with anti-V5 agarose beads and DTT was used to reduce any potential by reversible oxidation. Afterwards, NEM or IA was added to alkylate the newly reduced cysteines to differentiate the modification of cysteines before and after DTT reduction.

IA could not adduct some of Keap1-V5 cysteine residues despite the high concentration used (Fig 4.9a) but conversely, NEM was able to adduct every cysteine on the recombinant Keap1-V5 (Fig 4.9b). This is with exception of cysteine 622 and 624, which might not be released from the V5-agarose beads after tryptic digest due to their close proximity to the V5 tag of Keap1-V5. Cysteines 395 and 406, for example, were not alkylated by IA but could be alkylated by NEM. NEM was therefore considered to be a more efficient alkylating agent compared to IA and was used in subsequent investigations. Furthermore, the ability of NEM to adduct all of the Keap1-V5 cysteines suggests that all of these residues are reduced basally and are available

for alkylation in cells (Fig 4.10). To further confirm this observation, human serum albumin (HSA) was treated with NEM to determine whether or not NEM had the potential to break any disulphide bonds that form between cysteines. HSA contains 35 cysteines, 34 of which are involved in disulphide bond formation leaving one cysteine (Cys34) as a free thiol (Oettl *et al.* 2010). At a range of HSA to NEM ratios, NEM was only able to adduct the single reduced Cys34 (Table 4.1 and Fig 4.11). This indicates that NEM is unable to break disulphide bonds in HSA.

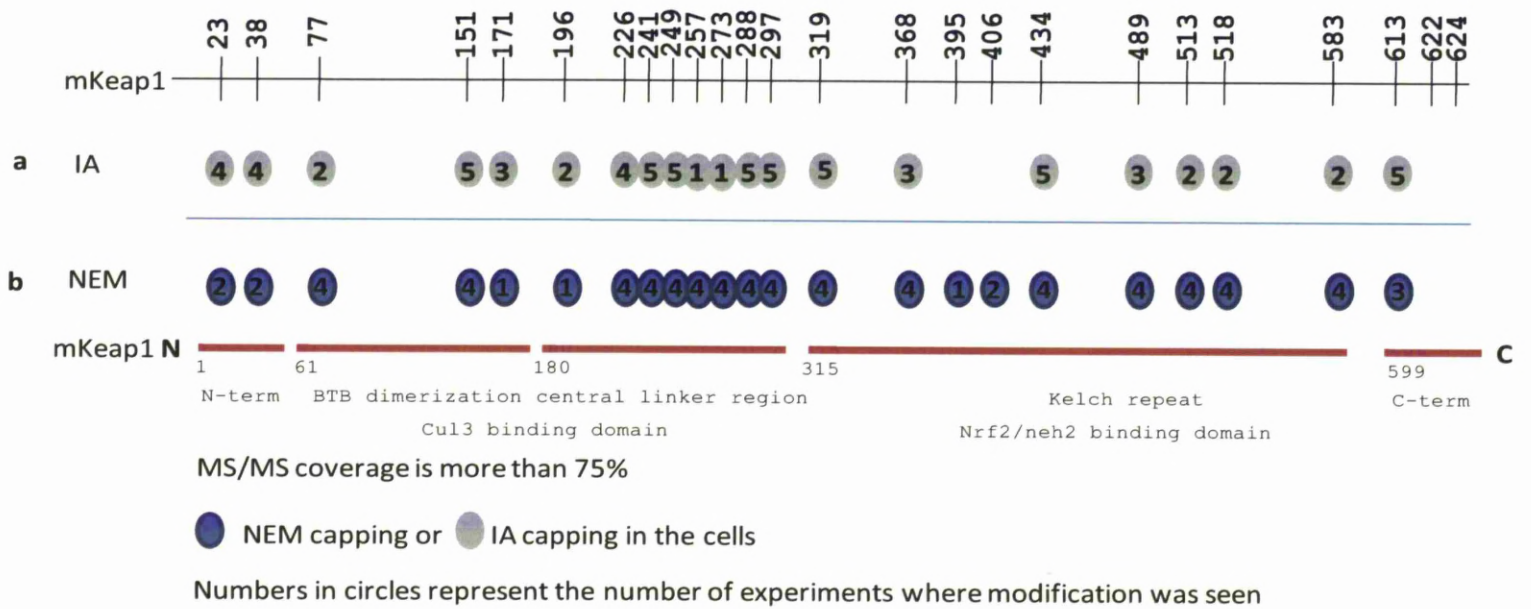

Figure 4.9: Schematic overview of mouse Keap1 cysteine residues expressed using HEK293T cells and their in-cell modification by IA and NEM. Cysteines modified in HEK293Tcells by IA (a) and NEM (b) are represented by grey and blue circles respectively. Numbers in the circles represent the number of experiments where the modification was seen. Cysteines 622 and 624 were not detected as modified cysteines. IA modification, n=5. NEM modification, n=4.

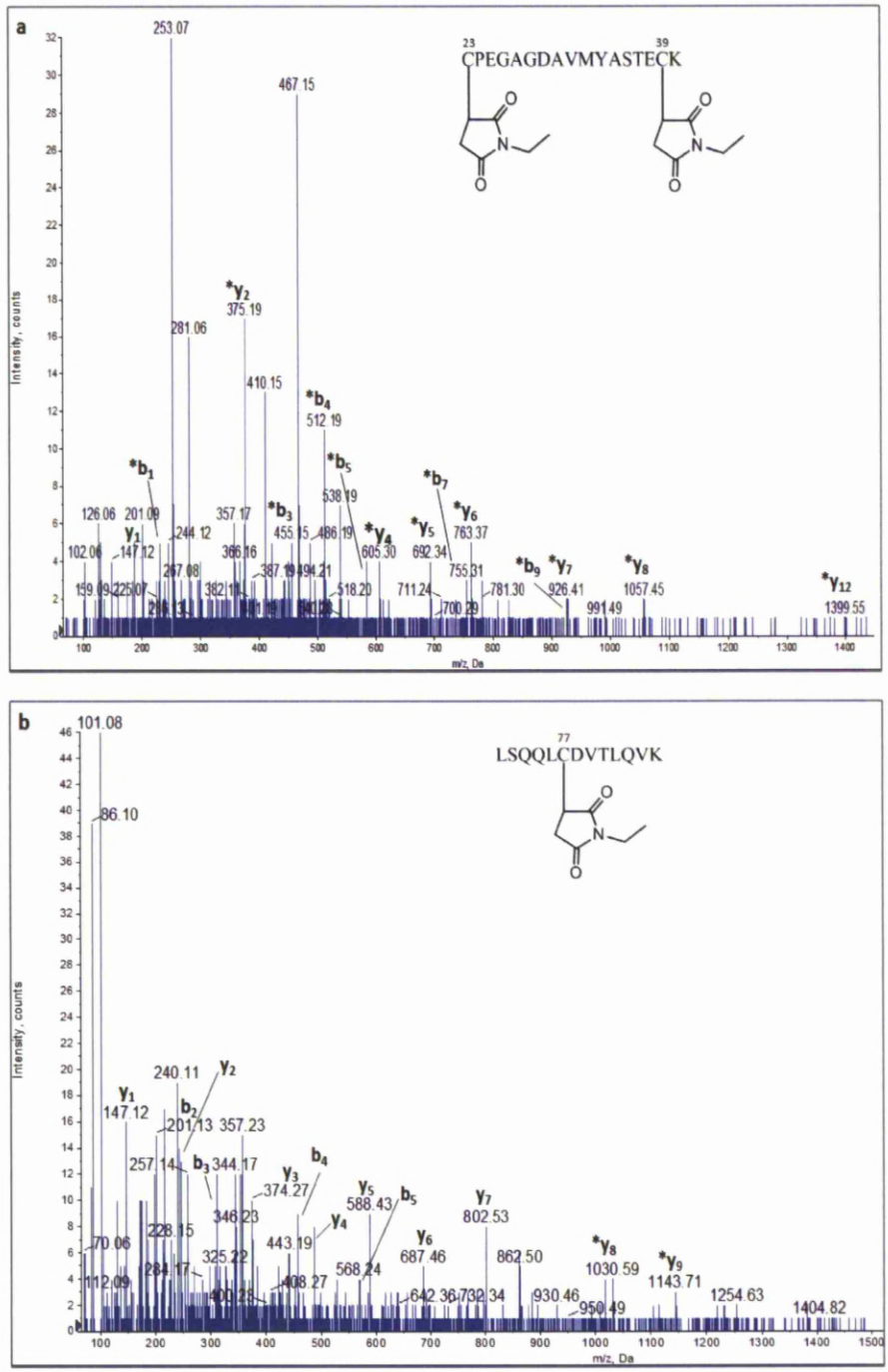

Figure 4.10: MS/MS spectrum indicating modification of Keap1-V5 (a) Cys-23/38 and (b) Cys-77 by NEM in HEK293T cells. y- and b-ions are labelled where present. * represents ions for which a mass shift of +126.0Da indicates modification by NEM.

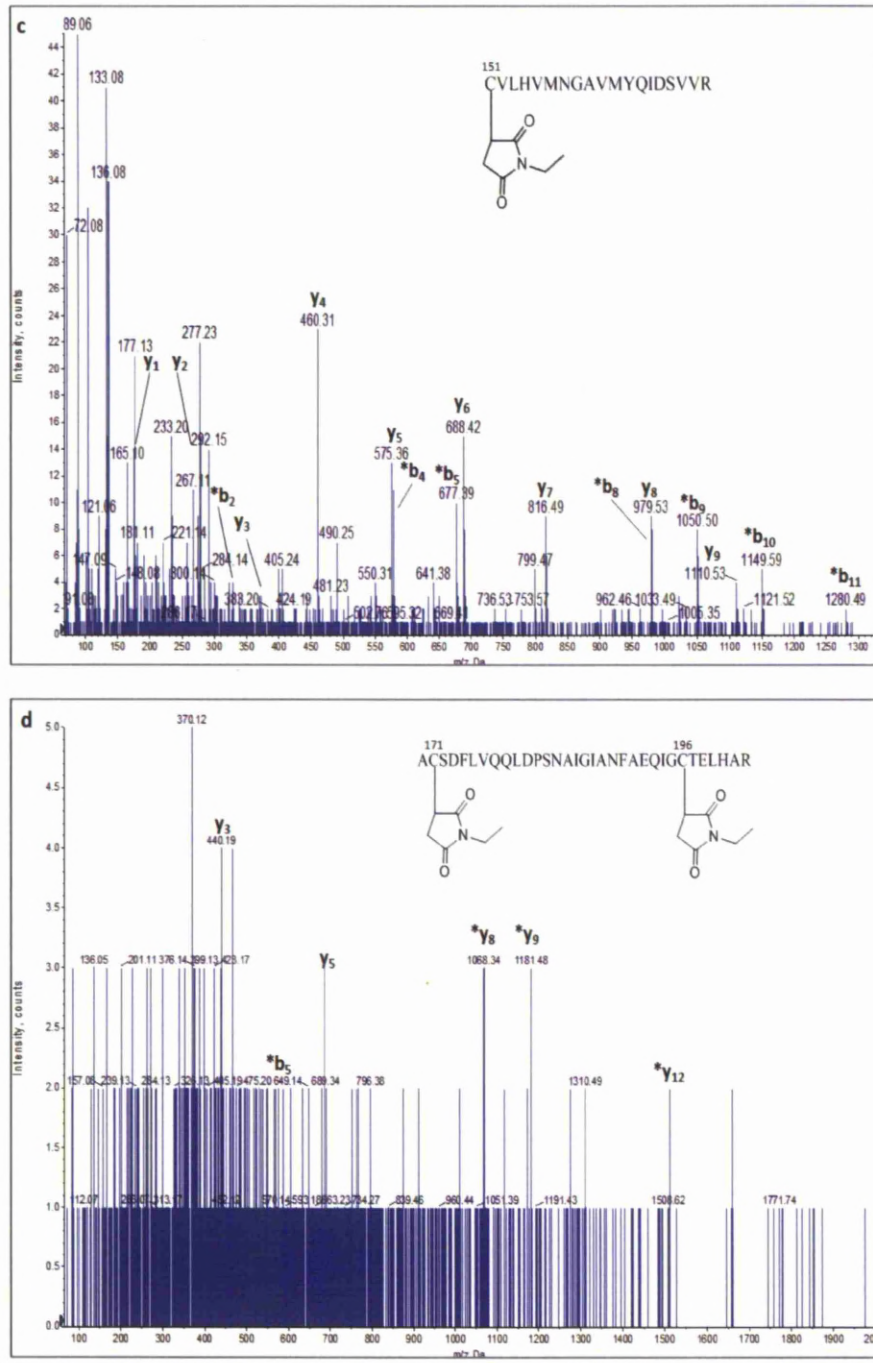

Figure 4.10: MS/MS spectrum indicating modification of Keap1-V5 (c) Cys-151 and (d) Cys-171/196 by NEM in HEK293T cells. y- and b-ions are labelled where present. * represents ions for which a mass shift of +126.0Da indicates modification by NEM.

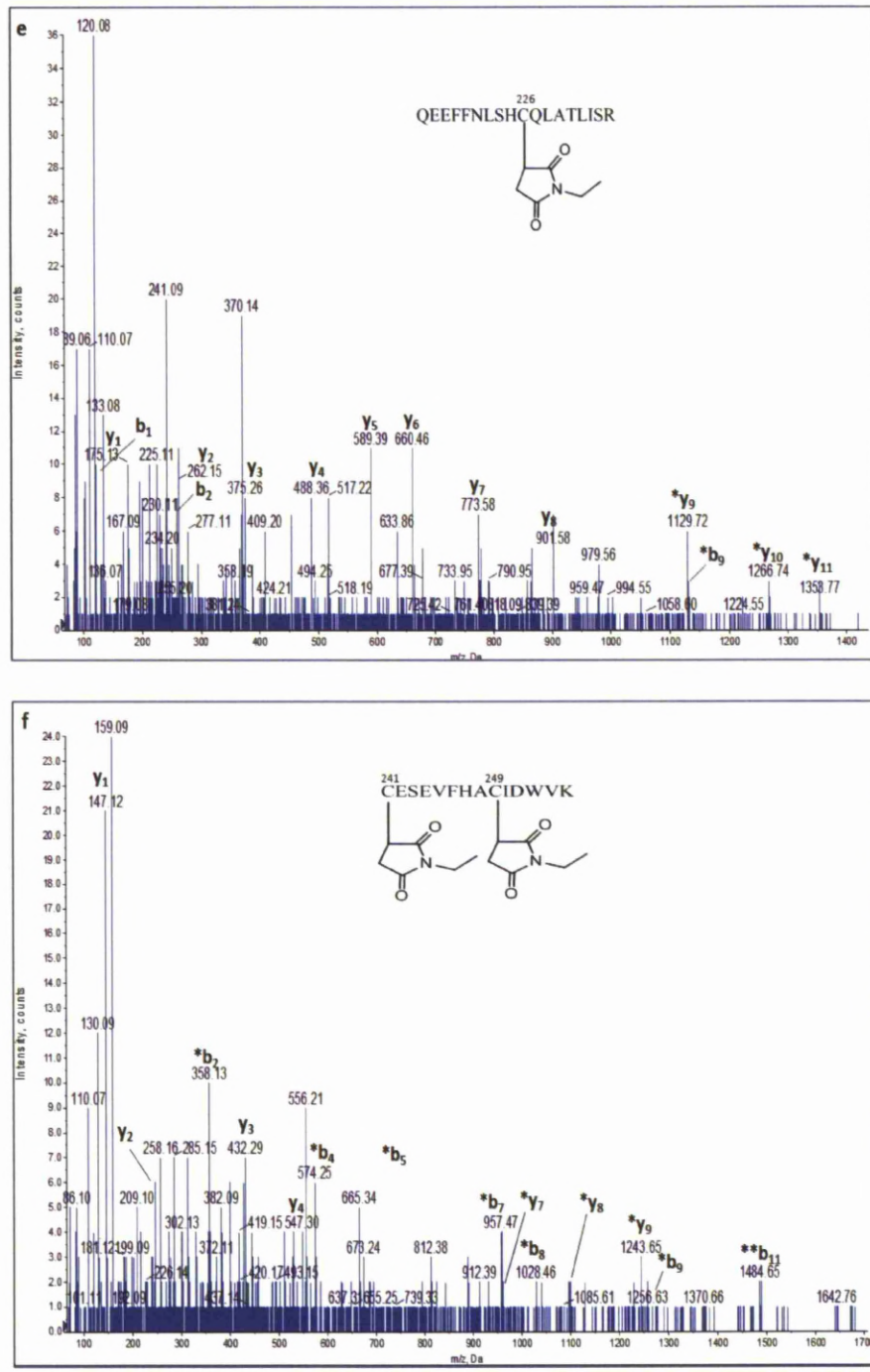

Figure 4.10: MS/MS spectrum indicating modification of Keap1-V5 (e) Cys-226 and (f) Cys-241/229 by NEM in HEK293T cells. y- and b-ions are labelled where present. * represents ions for which a mass shift of +126.0Da indicates modification by NEM.

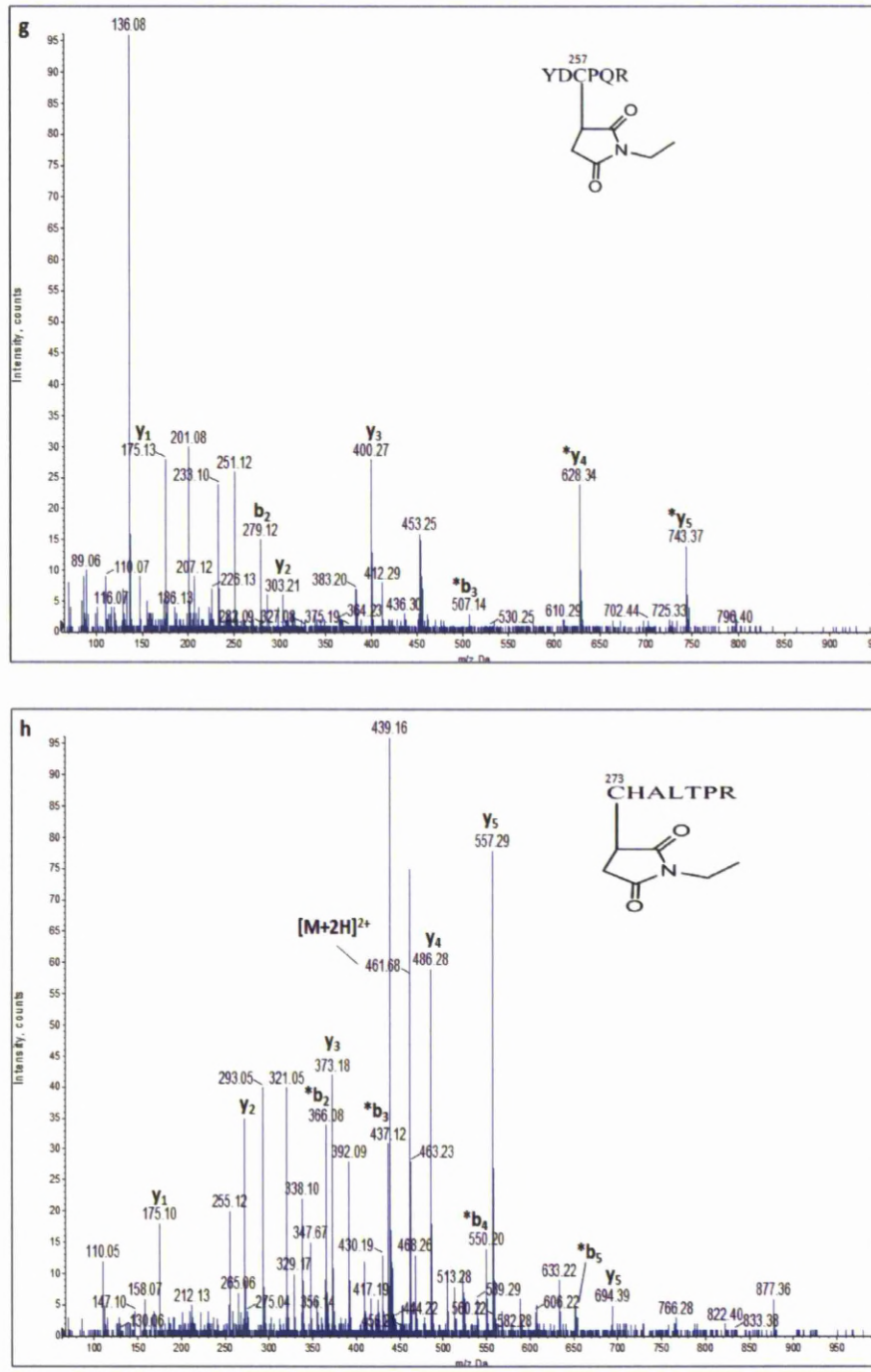

Figure 4.10: MS/MS spectrum indicating modification of Keap1-V5 (g) Cys-257 and (h) Cys-273 by NEM in HEK293T cells. y- and b-ions are labelled where present. * represents ions for which a mass shift of +126.0Da indicates modification by NEM.

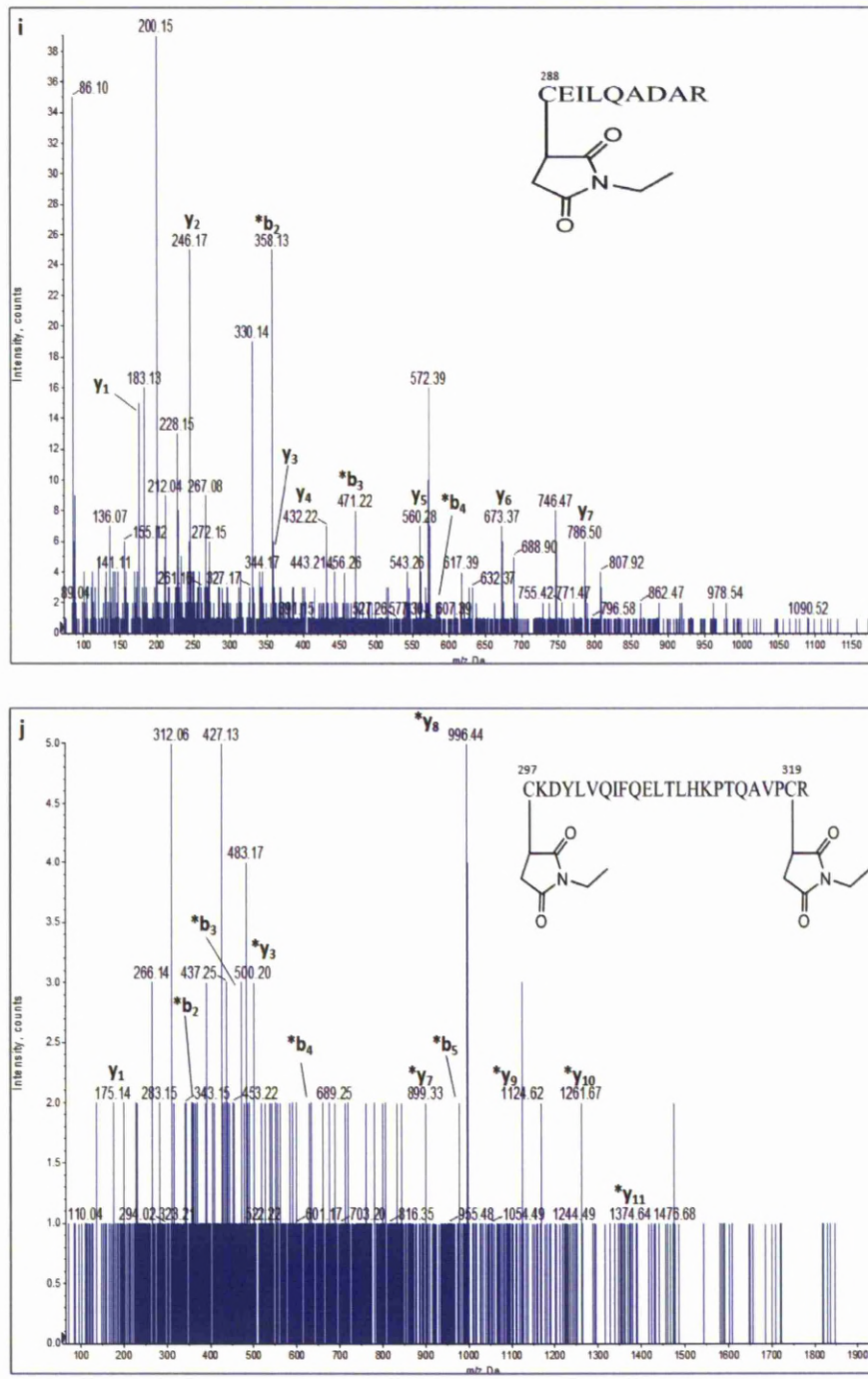

Figure 4.10: MS/MS spectrum indicating modification of Keap1-V5 (i) Cys-288 and (j) Cys-297/319 by NEM in HEK293T cells. y- and b-ions are labelled where present. * represents ions for which a mass shift of +126.0Da indicates modification by NEM.

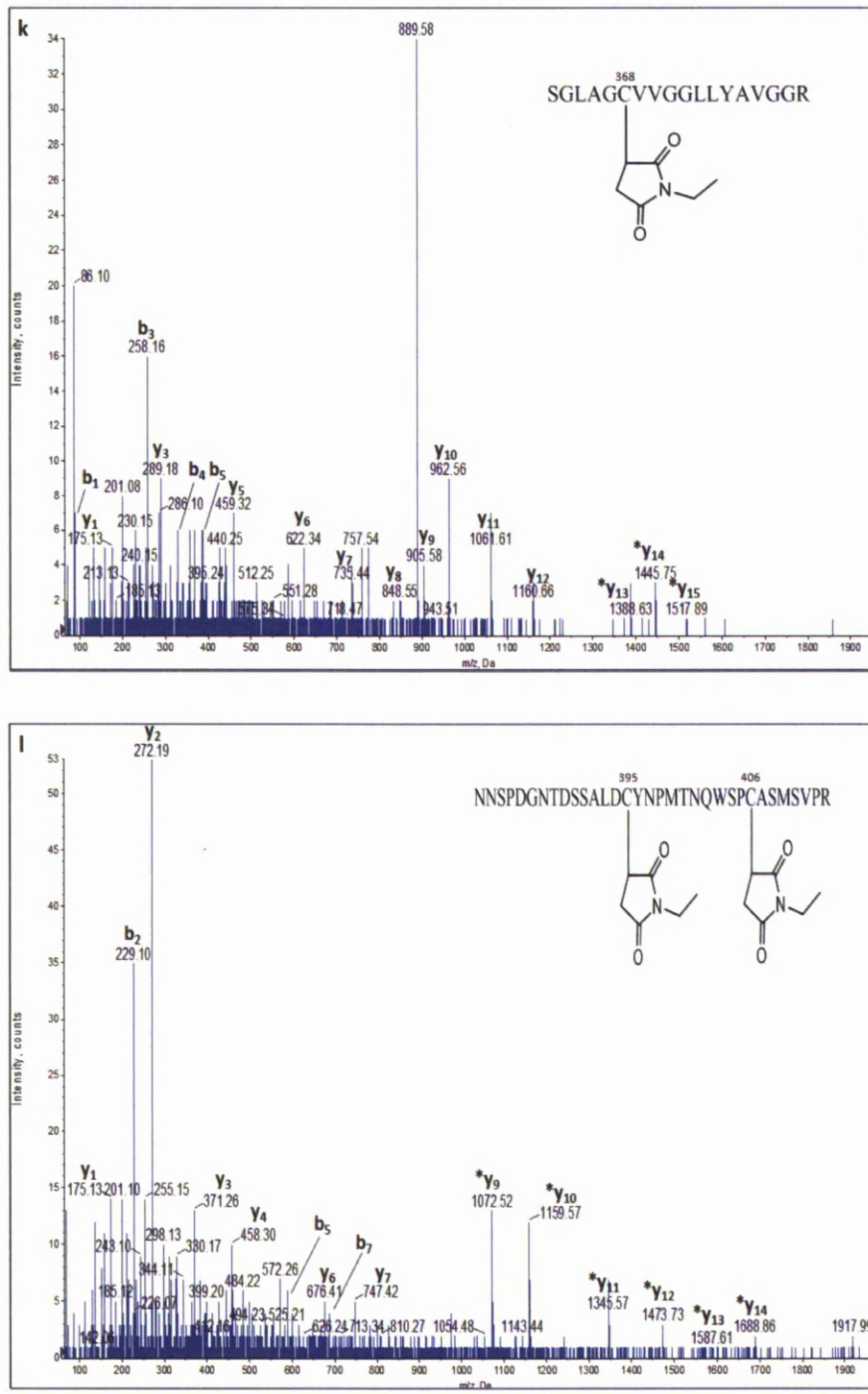

Figure 4.10: MS/MS spectrum indicating modification of Keap1-V5 (k) Cys-368 and (l) Cys-395/406 by NEM in HEK293T cells. y- and b-ions are labelled where present. * represents ions for which a mass shift of +126.0Da indicates modification by NEM.

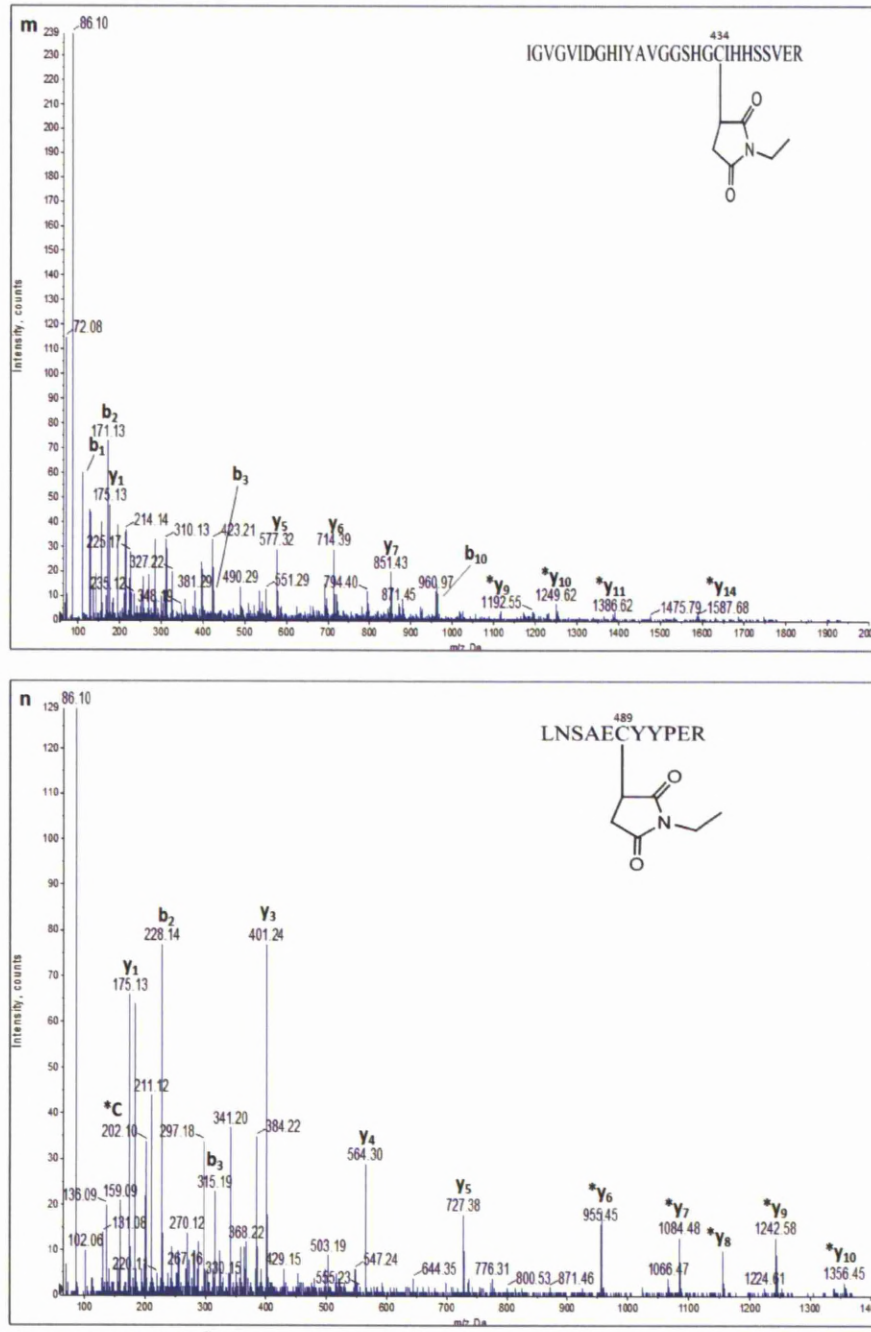

Figure 4.10: MS/MS spectrum indicating modification of Keap1-V5 (m) Cys-434 and (n) Cys-489 by NEM in HEK293T cells. y- and b-ions are labelled where present. * represents ions for which a mass shift of +126.0Da indicates modification by NEM. Immonium ions are labelled with C corresponding to cysteine.

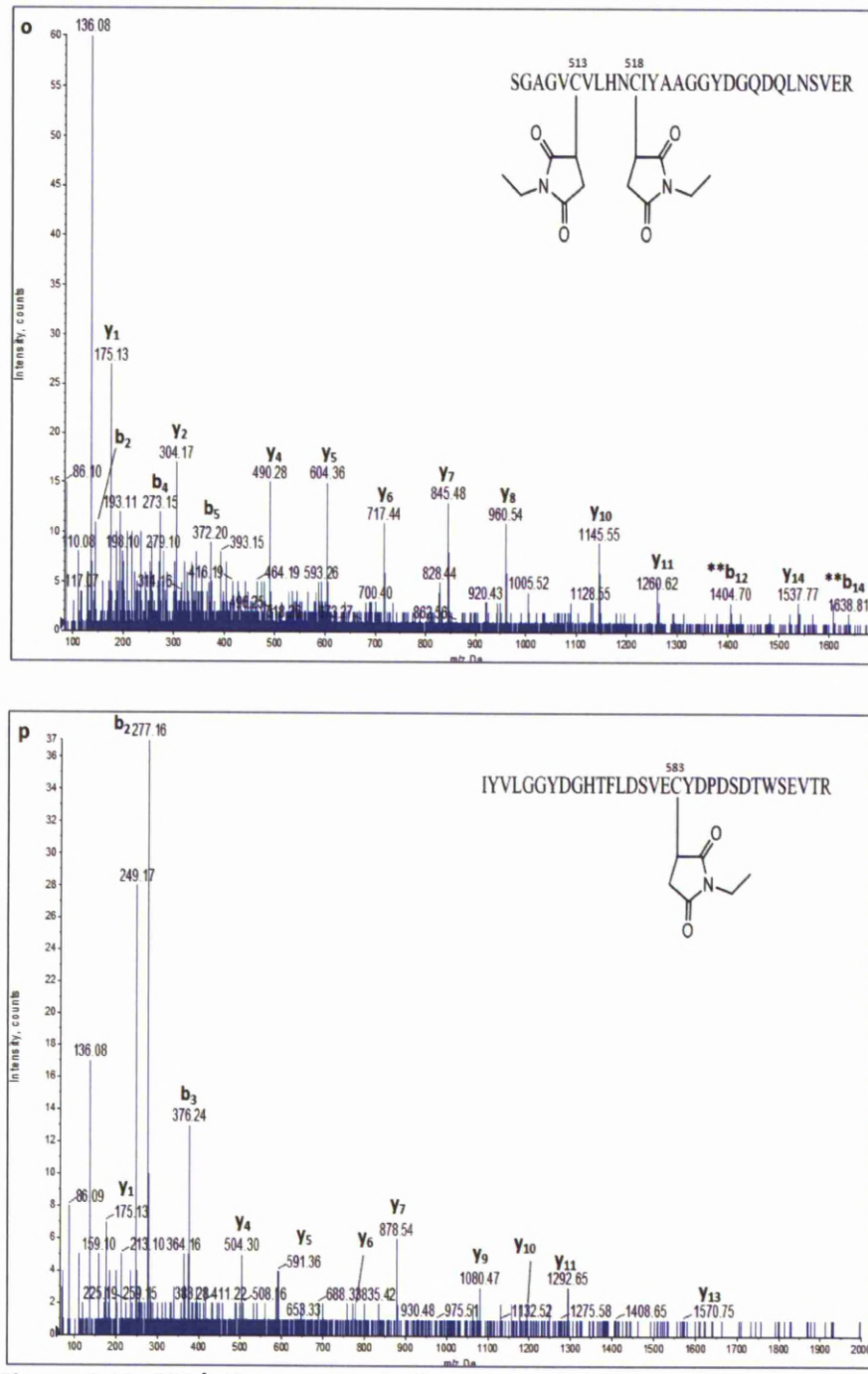

Figure 4.10: MS/MS spectrum indicating modification of Keap1-V5 (o) Cys-513/518 and (p) Cys-583 by NEM in HEK293T cells. y- and b-ions are labelled where present. * represents ions for which a mass shift of +126.0Da indicates modification by NEM.

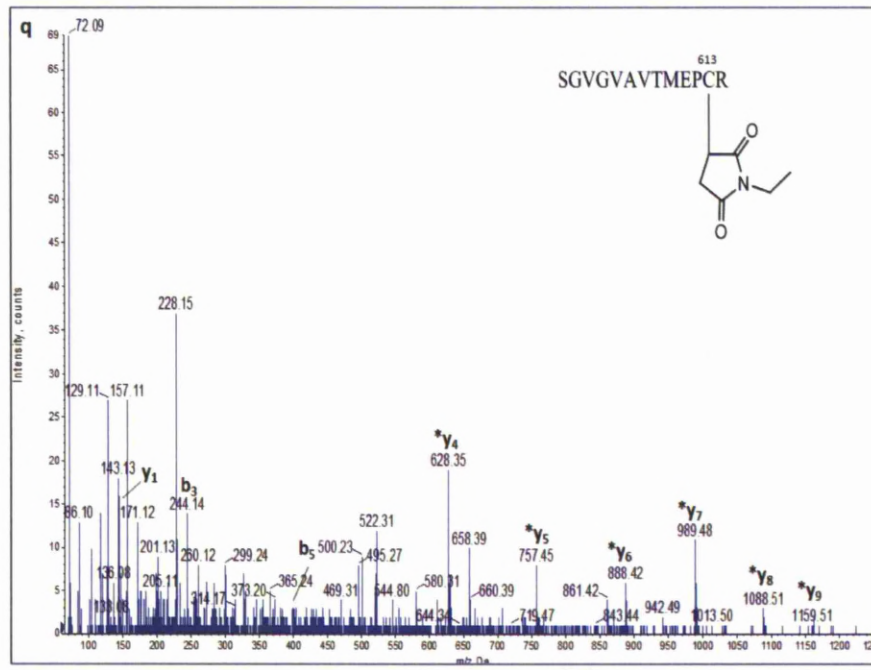

Figure 4.10: MS/MS spectrum indicating modification of Keap1-V5 (q) Cys-613 by NEM in HEK293T cells. y- and b-ions are labelled where present. * represents ions for which a mass shift of +126.0Da indicates modification by NEM.

HSA:NEM		1:0		1:1		1:10		1:100		1:500	
No	Pos	NEM	IA	NEM	IA	NEM	IA	NEM	IA	NEM	IA
1	34		x	x	x	x	x	x	x	x	x
2	53		x		x		x		x		x
3	62		x		x		x		x		x
4	75		x		x		x		x		x
5	90		x		x		x		x		x
6	91		x		x		x		x		x
7	101		x		x		x		x		x
8	124		x		x		x		x		x
9	168		x		x		x		x		x
10	169		x		x		x		x		x
11	177		x		x		x		x		x
12	200										
13	245		x		x		x		x		x
14	246		x		x		x		x		x
15	253		x		x		x		x		x
16	265		x		x		x		x		x
17	278		x		x		x		x		x
18	279		x		x		x		x		x
19	289		x		x		x		x		x
20	316										
21	360		x		x		x		x		x
22	361		x		x		x		x		x
23	369		x		x		x		x		x
24	392		x		x		x		x		x
25	437		x		x		x		x		x
26	438		x		x		x		x		x
27	448		x		x		x		x		x
28	461										
29	476										
30	477		x		x		x		x		x
31	487		x		x		x		x		x
32	514		x		x		x		x		x
33	558		x		x		x		x		x
34	559		x		x		x		x		x
35	567		x		x		x		x		x

Table 4.1: HSA cysteine residue 34 is selectively modified by NEM. HSA was incubated with NEM, or DMSO as a control at increasing molar ratios from 0 to 500 for 2mins under *in vitro* condition. HSA was washed several times and reduced with 10mM DTT. After further washes, 55mM of IA was added to adduct the newly reduced cysteines. HSA was digested with trypsin overnight and LC-ESI-MS/MS analysis was performed.

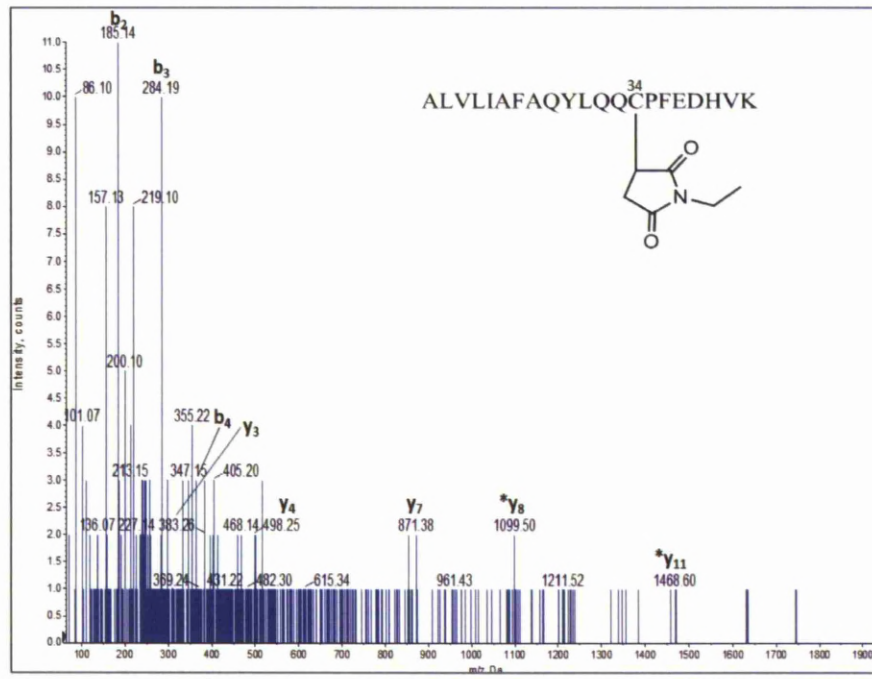

Figure 4.11: MS/MS spectrum indicating modification of HSA Cys-34 by NEM *in vitro*. y- and b-ions are labelled where present. * represents ions for which a mass shift of +126.0Da indicates modification by NEM.

4.3.4 Using deuterated-5-NEM as an alkylating agent

It has shown that, IA could not adduct Keap1-V5 cysteine residues as efficiently as NEM (Fig 4.9). Another alternative alkylating agent which has similar characteristics to NEM was therefore required to substitute IA. Dueterated-5-NEM (d_5NEM) (Fig 4.12) was selected as an alternative alkylating agent to IA as it has the same structure as NEM, although it is 5Da heavier. This mass difference can be detected by LC-ESI-MS/MS (Niwayama *et al.* 2001). Hence, NEM and d_5NEM were used as alkylating agents to investigate the basal thiol status of Keap1-V5. Here a lower concentration of NEM (1mM) was used to adduct Keap1-V5 cysteines for 5min. At this concentration of NEM, all of the Keap-V5 cysteines were modified by NEM, suggesting that the cysteines were available for NEM adduction (Fig 4.13). After DTT reduction, d_5NEM was able to adduct all of the remaining Keap1-V5 cysteines (Fig 4.14), except for cysteine 297 which must have been fully adducted by NEM (Fig 4.13). This is in line with what was observed previously; high concentrations of NEM were able to adduct virtually all of the Keap1-V5 cysteines.

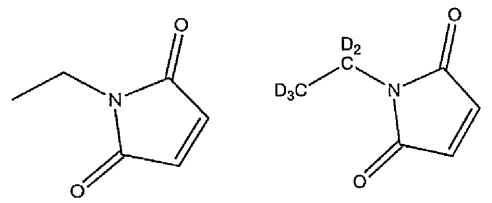

NEM
Molecular Weight:125.13

d_5NEM
Molecular Weight: 130.16

Figure 4.12: Chemical structure of NEM and d_5NEM. The d_5NEM is heavier than NEM by 5Da, due to the presence of deuterated hydrogen (D) instead of hydrogen on the ethyl group.

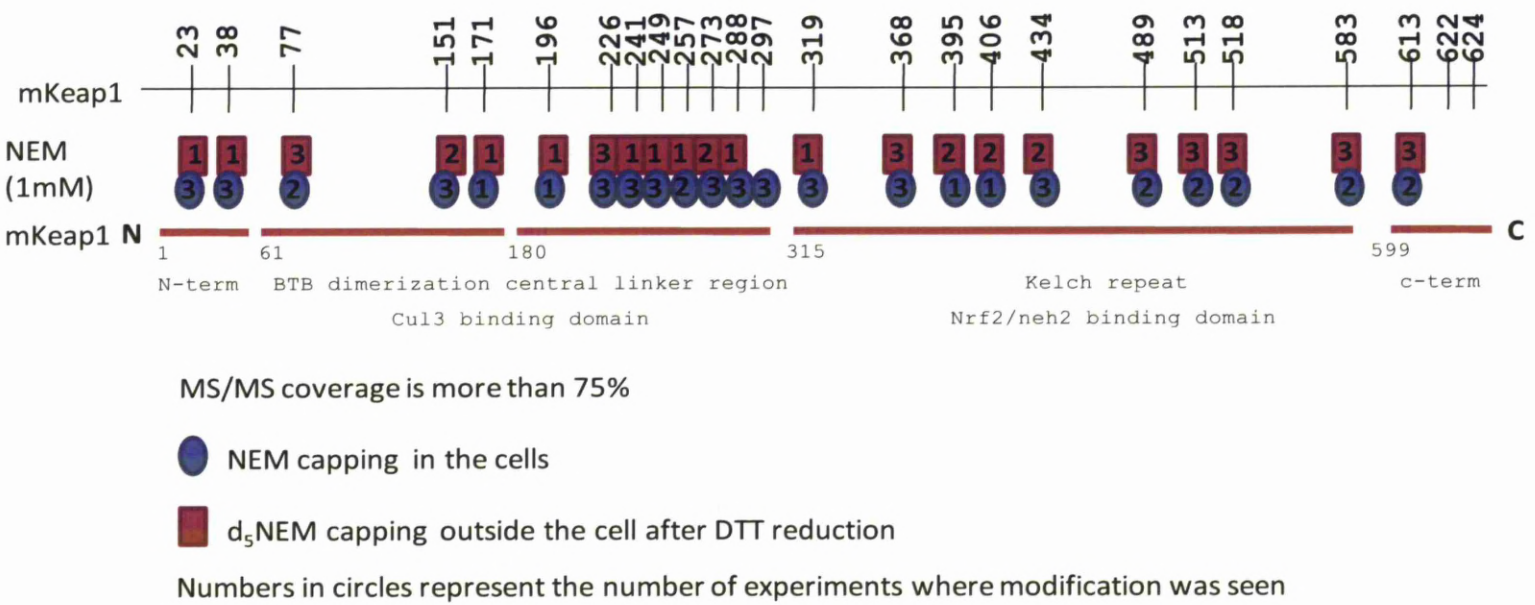

Figure 4.13: Schematic overview of mouse Keap1 cysteine residues and their modification by NEM and d_5NEM. Cysteines modified in the HEK293T cells by NEM are represented by blue circles. Red boxes represent cysteine modifications observed outside the cells after DTT reduction by d_5NEM respectively. Numbers in the circles and boxes represent the number of times modification was seen. Cysteines 622 and 624 were not detected as modified cysteines. NEM and d_5NEM modifications, n=3.

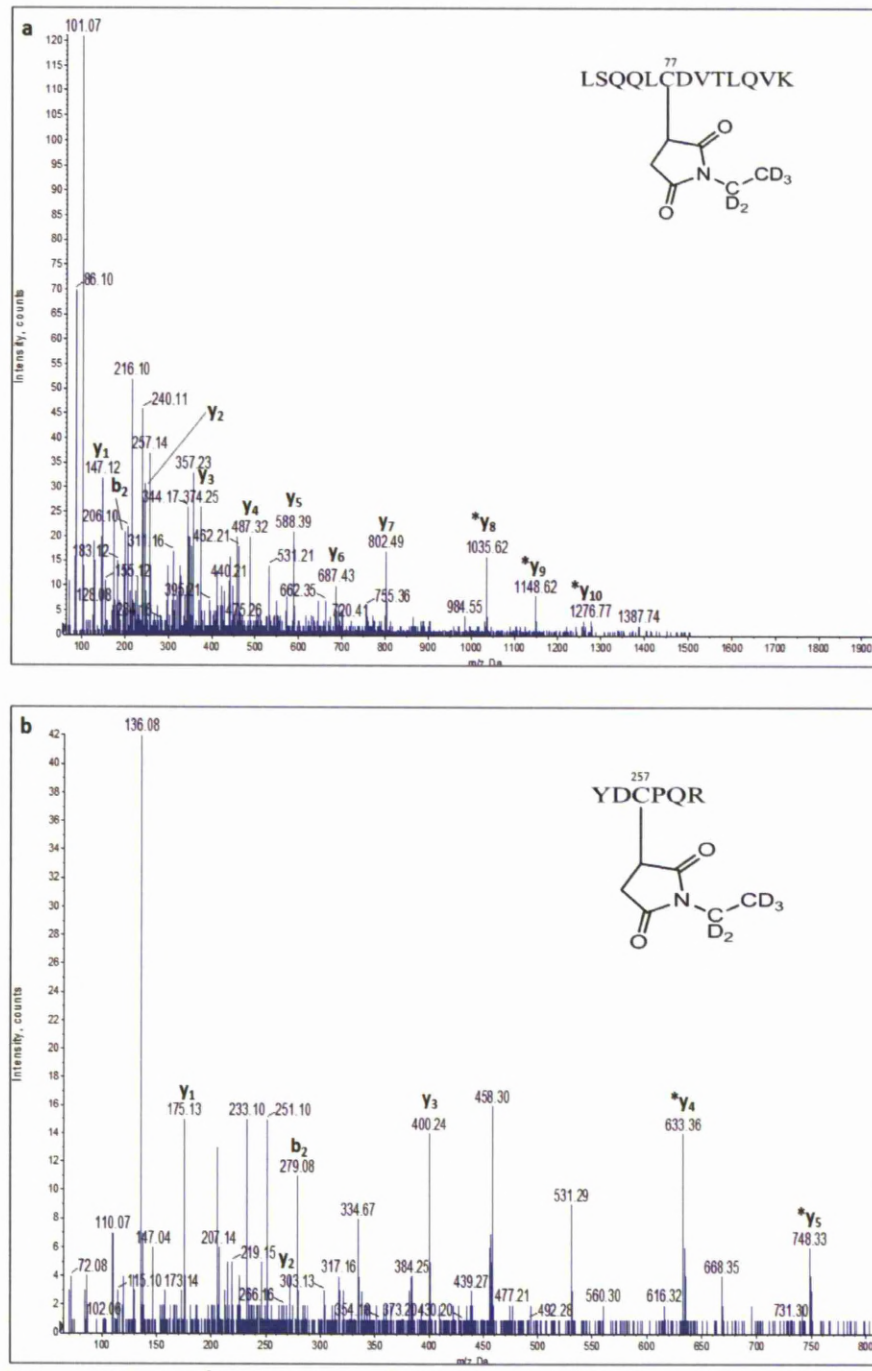

Figure 4.14: MS/MS spectrum indicating modification of Keap1-V5 (a) Cys-77 and (b) Cys-257 by d_5NEM in HEK293T cells. y- and b-ions are labelled where present. * represents ions for which a mass shift of +131.0Da indicates modification by d_5NEM.

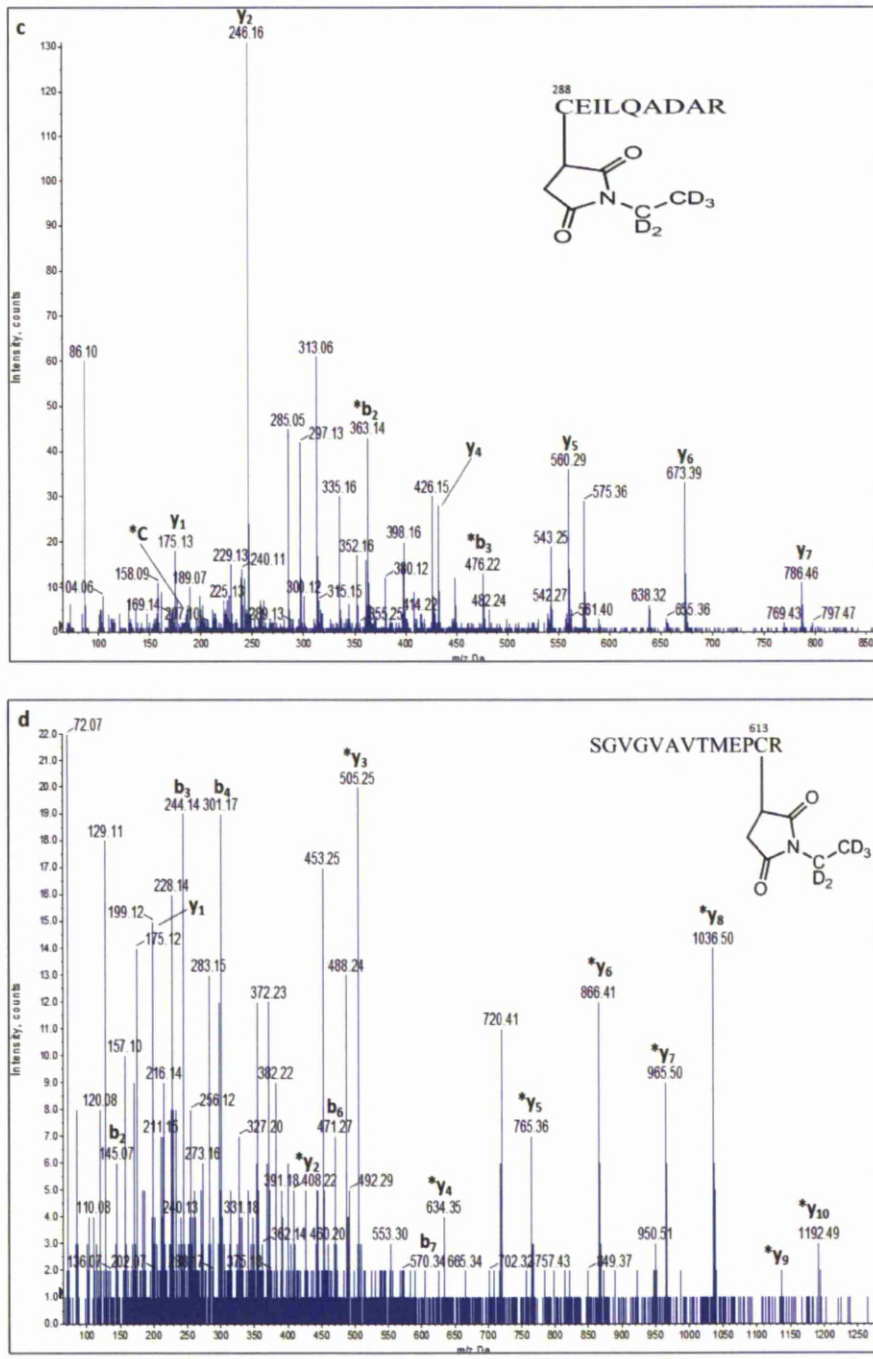

Figure 4.14: MS/MS spectrum indicating modification of Keap1-V5 (c) Cys-288 and (d) Cys-613 by d_5NEM in HEK293T cells. y- and b-ions are labelled where present. * represents ions for which a mass shift of +131.0Da indicates modification by d_5NEM. Immonium ions are labelled with C corresponding to cysteine.

4.3.5 Identification of S-glutathionylation of cysteine residues in Keap1-V5 under basal conditions and after cellular stress

Cysteine residues can undergo reversible oxidation to form disulphide bridges, S-glutathionylation or sulphenic acids. These oxidations are known as oxidative post-translational modifications (oxPTM). These oxPTM are known to control the activation or inactivation of proteins involved in many signalling pathways (Spickett *et al.* 2010). As previously shown, two forms of Keap1-V5 were identified on a CCB gel following immunoprecipitation with anti-V5 agarose beads from the cell lysates of HEK293T expressing Keap1-V5 (Fig 4.4). However, MALDI-TOF MS analysis did not identify any difference between the two forms. Figure 4.9 shows that all Keap1-V5 cysteine residues are present in a reduced form basally and are available to be alkylated by NEM, which suggests the absence of disulphide bridges. Following this observation, investigations were carried out to determine if there were other forms of reversible cysteine oxidation, such as s-glutathionylation, occurring on Keap1-V5 cysteine residues basally or after cellular stress.

HEK293T cells were transfected with Keap1-V5 overnight and treated with 100μM BSO or water as a control for 24hr. Following BSO treatment, cells were treated with high concentrations of IA, NEM or DMSO as a control for 2min. BSO, a known GSH depleting agent was employed (Griffith 1982) and has been shown in chapter 3 to activate Nrf2 when cellular GSH levels drop to 20% of the basal level. Under the current test conditions, BSO was found to deplete GSH to nearly 0% of control and this has also shown for IA and NEM treatment with or without prior BSO treatment in Keap1-V5 expressing HEK293T (Fig 4.15). Therefore, we attempted to determine if this GSH depletion was enough to induce S-glutathionylation on Keap1-V5 cysteine residues.

S-glutathionylation was determined by MALDI-TOF and GSH blotting analysis. Keap1-V5 was immunoprecipitated from HEK293T after treatment, resolved using SDS-PAGE under reducing and non-reducing conditions. The blots were probed with Keap1 and GSH antibodies. Immunoblotting showed the presence of S-glutathionylation on Keap1-V5 under non-reducing conditions (Fig 4.16a and c), which disappeared under reducing conditions (Fig 4.16b and d). From the immunoblotting analysis, S-glutathionylation was observed in the control, BSO, IA or NEM treated samples and in the BSO with IA or NEM treated samples (Fig 4.16).

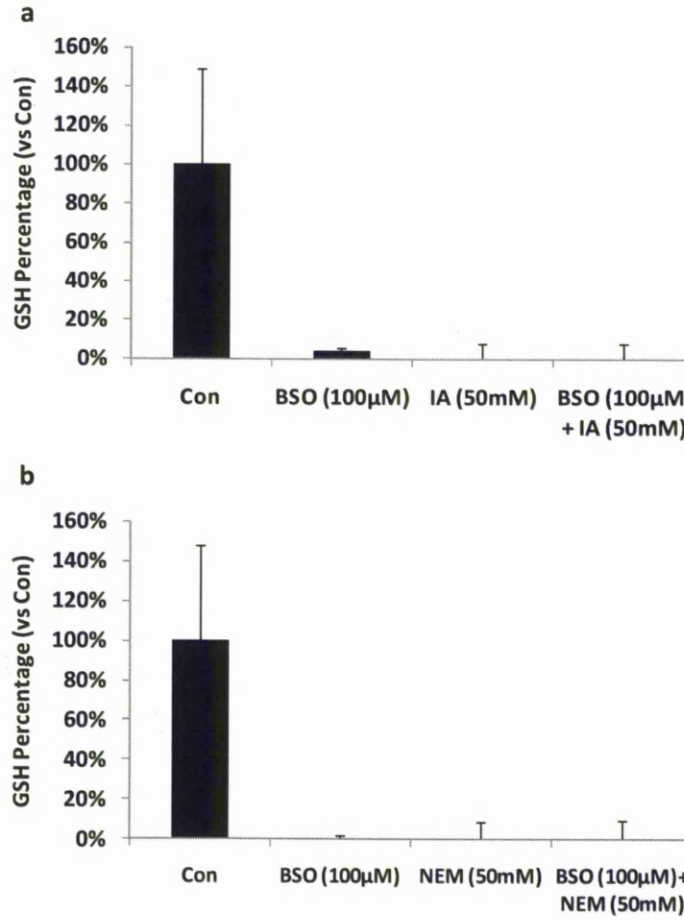

Figure 4.15: GSH depletion by BSO in HEK293T. HEK293T cells were transfected with Keap1-V5 overnight and treated with 100μM BSO or water as control for 24hrs. Following BSO or water treatment, cells were treated with IA and NEM for 2min and lysed with 10mM HCL. GSH was depleted by BSO with or without IA (a) and NEM (b). Total GSH was normalised to total protein content versus control. Error bars = average of two independent experiments of triplicate measurements, n=2.

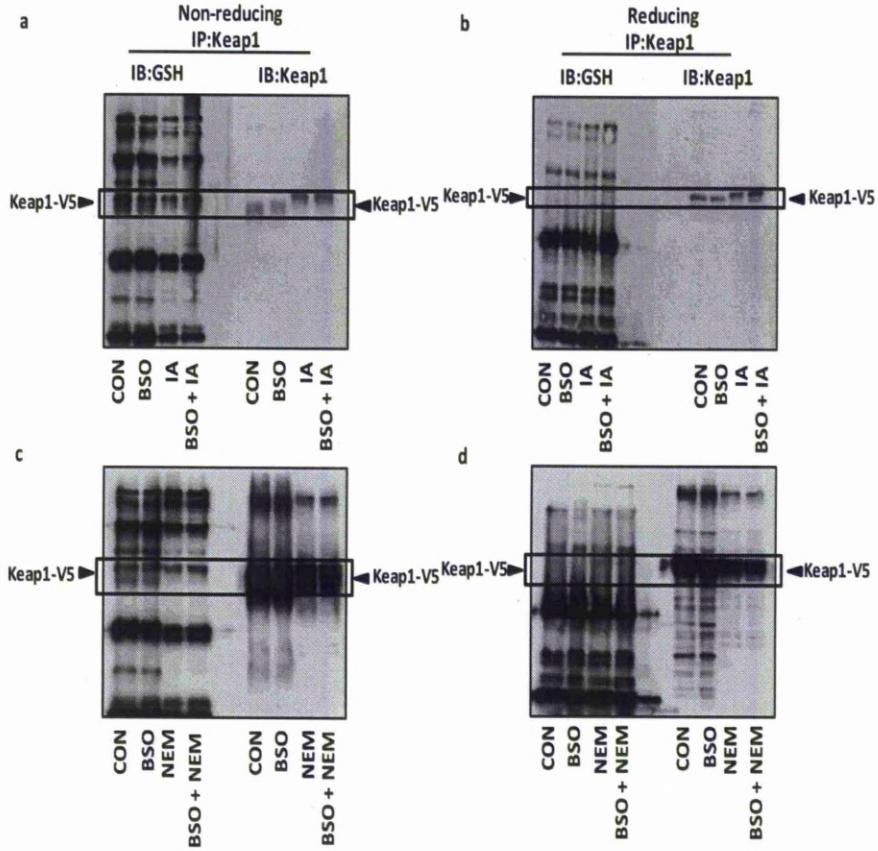

Figure 4.16: S-glutathionylation of Keap1-V5 in control and treated cells. HEK293T were transfected with Keap1-V5 overnight and treated with 100μM BSO and water as a control for 24hr. Cells were further treated with 50mM IA or NEM and DMSO as a control for 2min. Cells were lysed with RIPA buffer and Keap1-V5 was immunoprecipitated with anti-V5 agarose beads. Immunoprecipitated proteins were resolved by SDS-PAGE under non-reducing or reducing conditions, and probed with anti-Keap1 and anti-GSH antibodies. S-glutathionylation of Keap1 occurred in control and treated samples under non-reducing conditions (see ▭) (a and c). However, under reducing conditions S-glutathionylation of Keap1 is reversed the GSH immunoreactive signal disappeared from Keap1-V5 (see ▭) (b and d). IP; immunoprecipitation. IB; immunoblotting. Representative gel shown from n=2.

MALDI-TOF MS analysis was applied as a second method to look for GSH adduction of cysteine residues. Immunoprecipitated Keap1-V5 from HEK293T cells following treatment was resolved by SDS-PAGE and was stained with CCB. CCB-stained protein bands on the gel were excised and tryptically digested overnight for MALDI-TOF MS analysis (Fig 4.17). Bands excised from the CON and IA samples were identified as Keap1-V5 by MALDI-TOF MS. Keap1-V5 could not be identified in BSO-treated samples, as there might not have been enough peptides detected to cover the full amino acid sequencing of Keap1 by MALDI-TOF. The MALDI-TOF MS analysis identified S-glutathionylation on cysteine 273 in Keap1 in the control sample but it was a miscleaved peptide (Fig 4.18-4.20). The protein band excised in the IA sample was identified as Keap1-V5 and s-glutathionylation could be detected on cysteine 77 by MALDI-TOF MS analysis (Fig 4.21-4.23).

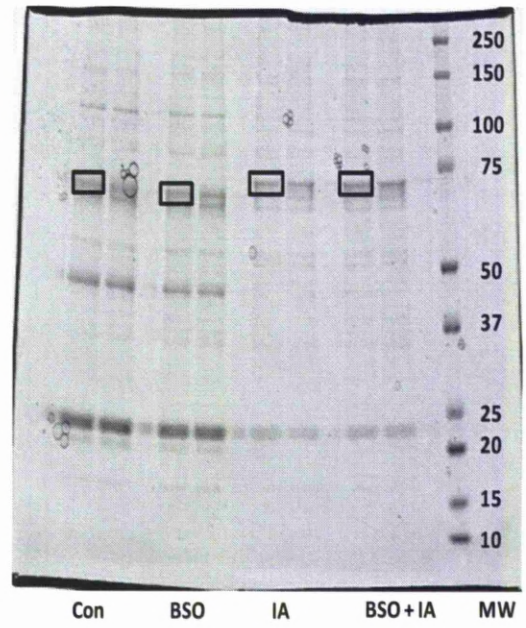

Figure 4.17: CCB staining of immunoprecipitated Keap1-V5 from over expressing HEK293T cells. HEK293T cells were transfected with Keap1-V5 and treated with 100μM BSO or water as a control for 24hr. Following BSO treatment, cells were further treated with 50mM IA or DMSO as a control. Whole cell lysates were prepared and incubated with anti-V5 agarose beads for 2hr at 4°C. Protein bound to anti-V5 agarose beads were loaded onto SDS-PAGE gels and CCB staining for protein was performed. Stained protein bands (▭) were excised, digested with trypsin and analysed by MALDI-TOF MS. The data obtained from MALDI-TOF MS spectra were used in a MASCOT protein database search to identify the major protein constituent(s) for each band, therefore giving protein identity with the highest degree of confidence for each band.

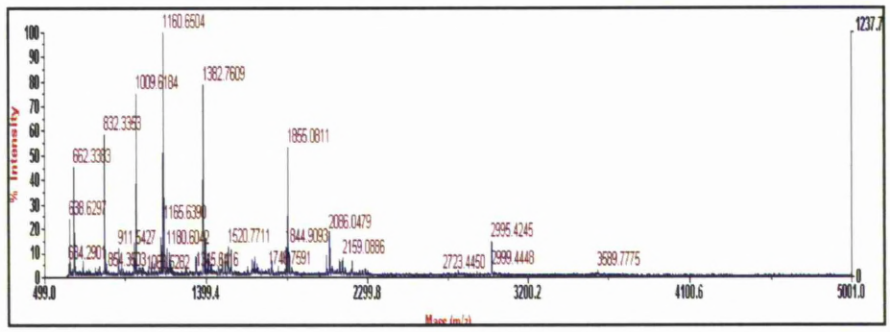

Figure 4.18: Representative MALDI-TOF mass spectrum of the tryptic digests of the Keap1 band from control samples. CCB staining of proteins bound anti-V5 agarose beads was performed. Stained protein bands were excised, digested with trypsin and analysed by MALDI-TOF. The resulting peptide mixture was visualised on a Voyager DE Pro MALDI-TOF Biospectrometry Workstation, in linear positive ion mode.

	Accession	Mass	Score	Description
1.	KEAP1_MOUSE	69508	176	Kelch-like ECH-associated protein 1 - Mus musculus (Mouse)
2.	KEAP1_RAT	69354	137	Kelch-like ECH-associated protein 1 - Rattus norvegicus (Rat)
3.	KEAP1_PIG	69771	86	Kelch-like ECH-associated protein 1 - Sus scrofa (Pig)
4.	SG269_MOUSE	191006	79	Tyrosine-protein kinase-protein kinase SgK269 - Mus musculus (Mouse)
5.	KEAP1_HUMAN	69621	79	Kelch-like ECH-associated protein 1 - Homo sapiens (Human)

Match to: **KEAP1_MOUSE Kelch-like ECH-associated protein 1 - Mus musculus (Mouse)**
Sequence Coverage: **46%**

1 MQPEPKLSGA PR**SSQFLPLW SK**CPEGAGDA VMYASTECK**A EVTPSQDGNR**
51 **TFSYTLEDHT KQAFGVMNEL R**LSQQLCDVT LQVK**YEDIPA AQFMAHK**VVL
101 ASSSPVFKAM FTNGLR**EQGM EVVSIEGIHP K**VMER**LIEFA YTASISVGEK**
151 CVLHVMNGAV MYQIDSVVRA CSDFLVQQLD PSNAIGIANF AEQIGCTELH
201 QRAR**EYIYMH FGEVAK**QEEF FNLSHCQLAT LISRDDLNVR CESEVFHACI
251 DWVKYDCPQR **RFYVQALLRA** VR**CHALTPRF LQTQLQKCEI LQADAR**CKDY
301 LVQIFQELTL HKPTQAVPCR APKVGR**LIYT AGGYFRQSLS YLEAYNPSNG**
351 **SWLRLADLQV PRSGLAGCVV GGLLYAVGGR** NNSPDGNTDS SALDCYNPMT
401 NQWSPCASMS VPRNRIGVGV IDGHIYAVGG SHGCIHHSSV E**RYEPERDEW**
451 **HLVAPMLTRR IGVGVAVLNR LLYAVGGFDG TNR**LNSAECY YPER**NEWRMI**
501 **TPMNTIR**SGA GVCVLHNCIY AAGGYDGQDQ LNSVER**YDVE TETWTFVAPM**
551 **R**HHR**SALGIT VHQGK**IYVLG GYDGHTFLDS VECYDPDSDT WSEVTR**MTSG**
601 **RSGVGVAVTM EPCR**KQIDQQ NCTC

Start - End	Observed	Mr(expt)	Mr(calc)	ppm	Miss	Sequence
13 - 22	1192.6670	1191.6597	1191.6288	26	0	R.SSQFLPLWSK.C
40 - 50	1173.6266	1172.6193	1172.5422	66	0	K.AEVTPSQDGNR.T
51 - 61	1341.6895	1340.6822	1340.6248	43	0	R.TFSYTLEDHTK.Q
62 - 71	1164.6172	1163.6099	1163.5757	29	0	K.QAFGVMNELR.L
85 - 97	1520.7686	1519.7613	1519.7129	32	0	K.YEDIPAAQFMAHK.V
117 - 131	1652.8959	1651.8886	1651.8239	39	0	R.EQGMEVVSIEGIHPK.V
136 - 150	1627.9120	1626.9048	1626.8505	33	0	R.LIEFAYTASISVGEK.C
205 - 216	1486.7467	1485.7394	1485.6962	29	0	R.EYIYMHFGEVAK.Q
261 - 269	1165.6384	1164.6311	1164.6767	-39	1	R.RFYVQALLR.A
262 - 269	1009.6185	1008.6112	1008.5756	35	0	R.FYVQALLR.A
273 - 279	797.4431	796.4358	796.4014	43	0	R.CHALTPR.F
280 - 287	1005.5999	1004.5926	1004.5655	27	0	R.FLQTQLQK.C
288 - 296	1018.5972	1017.5899	1017.4913	97	0	K.CEILQADAR.C
327 - 336	1160.6505	1159.6433	1159.6026	35	0	R.LIYTAGGYFR.Q
337 - 354	2085.0384	2084.0311	2083.9963	17	0	R.QSLSYLEAYNPSNGSWLR.L
355 - 362	911.5452	910.5379	910.5236	16	0	R.LADLQVPR.S
363 - 380	1648.9282	1647.9210	1647.8767	27	0	R.SGLAGCVVGGLLYAVGGR.N
443 - 447	693.3642	692.3569	692.3129	64	0	R.YEPER.D
443 - 459	2142.1085	2141.1012	2141.0364	30	1	R.YEPERDEWHLVAPMLTR.R
448 - 459	1467.7947	1466.7874	1466.7340	36	0	R.DEWHLVAPMLTR.R
460 - 470	1153.7613	1152.7541	1152.7091	39	1	R.RIGVGVAVLNR.L
461 - 470	997.6531	996.6458	996.6080	38	0	R.IGVGVAVLNR.L
471 - 483	1382.7608	1381.7535	1381.6990	39	0	R.LLYAVGGFDGTNR.L
495 - 507	1661.8642	1660.8569	1660.8177	24	1	R.NEWRMITPMNTIR.S
499 - 507	1076.5830	1075.5758	1075.5518	22	0	R.MITPMNTIR.S
537 - 551	1844.9069	1843.8996	1843.8451	30	0	R.YDVETETWTFVAPMR.H
555 - 565	1110.6336	1109.6263	1109.6193	6	0	R.SALGITVHQGK.I
597 - 614	1838.0091	1837.0018	1836.8645	75	1	R.MTSGRSGVGVAVTMEPCR.K
615 - 624	1180.6035	1179.5962	1179.5012	80	1	R.KQIDQQNCTC.-

Figure 4.19: MASCOT protein database search results for a peptide mass fingerprint obtained from the MALDI-TOF MS analysis of the Keap1 band from control samples. The peptide mass fingerprint shown was used in a MASCOT protein database search, which identified mouse Keap1 without any post-translational modification from the tryptic digest. The top five proteins identified with the highest score of confidence are shown. The amino acid sequence coverage for mouse Keap1 was 46% and specific peptides covered by the MALDI-TOF MS analysis are underlined and highlighted in bold.

	Accession	Mass	Score	Description
1.	KEAP1_MOUSE	69508	160	Kelch-like ECH-associated protein 1 - Mus musculus (Mouse)
2.	KEAP1_RAT	69354	123	Kelch-like ECH-associated protein 1 - Rattus norvegicus (Rat)
3.	KEAP1_PIG	69771	80	Kelch-like ECH-associated protein 1 - Sus scrofa (Pig)
4.	MRH4_LODEL	191006	77	ATP-dependent RNA helicase MRH4, mitochondrial - Lodderomyces elongisporus (Yeast)
5.	KEAP1_HUMAN	69621	68	Kelch-like ECH-associated protein 1 - Homo sapiens (Human)

Match to: **KEAP1_MOUSE Kelch-like ECH-associated protein 1 - Mus musculus (Mouse)**
Sequence Coverage: **47%**

1 MQPEPKLSGA PR**SSQFLPLW SK**CPEGAGDA VMYASTECK**A EVTPSQDGNR**
51 **TFSYTLEDHT KQAFGVMNEL R**LSQQLCDVT LQVK**YEDIPA AQFMAHK**VVL
101 ASSSPVFKAM FTNGLR**EQGM EVVSIEGIHP K**VMER**LIEFA YTASISVGEK**
151 CVLHVMNGAV MYQIDSVVRA CSDFLVQQLD PSNAIGIANF AEQIGCTELH
201 QRAR**EYIYMH FGEVAK**QEEF FNLSHCQLAT LISRDDLNVR CESEVFHACI
251 DWVKYDCPQR **RFYVQALLRA VRCHALTPRF LQTQLQKCEI LQADAR**CKDY
301 LVQIFQELTL HKPTQAVPCR APKVGR**LIYT AGGYFRQSLS YLEAYNPSNG**
351 **SWLRLADLQV PRSGLAGCVV GGLLYAVGGR** NNSPDGNTDS SALDCYNPMT
401 NQWSPCASMS VPRNRIGVGV IDGHIYAVGG SHGCIHHSSV ER**YEPERDEW**
451 **HLVAPMLTRR IGVGVAVLNR LLYAVGGFDG TNR**LNSAECY YPER**NEWRMI**
501 **TPMNTIR**SGA GVCVLHNCIY AAGGYDGQDQ LNSVER**YDVE TETWTFVAPM**
551 **R**HHR**SALGIT VHQGK**IYVLG GYDGHTFLDS VECYDPDSDT WSEVTR**MTSG**
601 **RSGVGVAVTM EPCRKQIDQQ NCTC**

Start - End	Observed	Mr(expt)	Mr(calc)	ppm	Miss	Sequence
13 - 22	1192.6670	1191.6597	1191.6288	26	0	R.SSQFLPLWSK.C
40 - 50	1173.6266	1172.6193	1172.5422	66	0	K.AEVTPSQDGNR.T
51 - 61	1341.6895	1340.6822	1340.6248	43	0	R.TFSYTLEDHTK.Q
62 - 71	1164.6172	1163.6099	1163.5757	29	0	K.QAFGVMNELR.L
85 - 97	1520.7686	1519.7613	1519.7129	32	0	K.YEDIPAAQFMAHK.V
117 - 131	1652.8959	1651.8886	1651.8239	39	0	R.EQGMEVVSIEGIHPK.V
136 - 150	1627.9120	1626.9048	1626.8505	33	0	R.LIEFAYTASISVGEK.C
205 - 216	1486.7467	1485.7394	1485.6962	29	0	R.EYIYMHFGEVAK.Q
261 - 269	1165.6384	1164.6311	1164.6767	-39	1	R.RFYVQALLR.A
262 - 269	1009.6185	1008.6112	1008.5756	35	0	R.FYVQALLR.A
270 - 279	1428.6727	1427.6654	1427.6762	-8	1	R.AVRCHALTPR.F Glutathione (C)
273 - 279	797.4431	796.4358	796.4014	43	0	R.CHALTPR.F
280 - 287	1005.5999	1004.5926	1004.5655	27	0	R.FLQTQLQK.C
288 - 296	1018.5972	1017.5899	1017.4913	97	0	K.CEILQADAR.C
327 - 336	1160.6505	1159.6433	1159.6026	35	0	R.LIYTAGGYFR.Q
337 - 354	2085.0384	2084.0311	2083.9963	17	0	R.QSLSYLEAYNPSNGSWLR.L
355 - 362	911.5452	910.5379	910.5236	16	0	R.LADLQVPR.S
363 - 380	1648.9282	1647.9210	1647.8767	27	0	R.SGLAGCVVGGLLYAVGGR.N
443 - 447	693.3642	692.3569	692.3129	64	0	R.YEPER.D
443 - 459	2142.1085	2141.1012	2141.0364	30	1	R.YEPERDEWHLVAPMLTR.R
448 - 459	1467.7947	1466.7874	1466.7340	36	0	R.DEWHLVAPMLTR.R
460 - 470	1153.7613	1152.7541	1152.7091	39	1	R.RIGVGVAVLNR.L
461 - 470	997.6531	996.6458	996.6080	38	0	R.IGVGVAVLNR.L
471 - 483	1382.7608	1381.7535	1381.6990	39	0	R.LLYAVGGFDGTNR.L
495 - 507	1661.8642	1660.8569	1660.8177	24	1	R.NEWRMITPMNTIR.S
499 - 507	1076.5830	1075.5758	1075.5518	22	0	R.MITPMNTIR.S
537 - 551	1844.9069	1843.8996	1843.8451	30	0	R.YDVETETWTFVAPMR.H
555 - 565	1110.6336	1109.6263	1109.6193	6	0	R.SALGITVHQGK.I
597 - 614	1838.0091	1837.0018	1836.8645	75	1	R.MTSGRSGVGVAVTMEPCR.K

Figure 4.20: MASCOT protein database search result for a peptide mass fingerprint obtained from the MALDI-TOF MS analysis of the Keap1 band from control samples. The peptide mass fingerprint shown was used in a MASCOT protein database search, which identified mouse Keap1 with S-glutathionylation on cysteine 273 but it was a miscleaved peptide. The top five proteins identified with the highest score of confidence are shown. The amino acid sequence coverage for mouse Keap1 was 47% and specific peptides covered by the MALDI-TOF MS analysis are underlined and highlighted in bold.

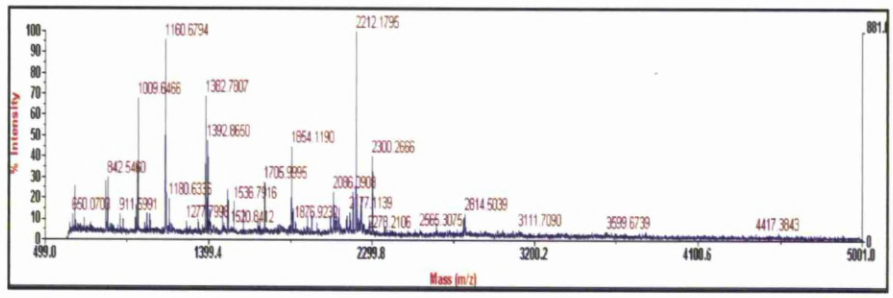

Figure 4.21: Representative MALDI-TOF mass spectrum of the trypsin digests of the Keap1 from the IA treated samples. CCB staining for protein bound to anti-V5 agarose beads was performed. Stained protein bands were excised, digested with trypsin and analysed by MALDI-TOF MS. The resulting peptide mixture was visualised on a Voyager DE Pro MALDI-TOF Biospectrometry Workstation, in linear positive ion mode.

	Accession	Mass	Score	Description
1.	Mixture 1		196	KEAP1_MOUSE + V010_FOWPV
2.	KEAP1_MOUSE	69508	126	Kelch-like ECH-associated protein 1 - Mus musculus (Mouse)
3.	KEAP1_RAT	69354	118	Kelch-like ECH-associated protein 1 - Rattus norvegicus (Rat)
4.	MY61F_DROME	69771	64	Myosin-IB - Drosophila melanogaster (Fruit Fly)
5.	UBIE_ZYMMO	191006	64	Ubiquinone/menaquinone biosynthesis methyltransferase ubiE - Zymomonas mobilis (bacterium)

Match to: **KEAP1_MOUSE Kelch-like ECH-associated protein 1 - Mus musculus (Mouse)**
Sequence Coverage: **50%**

1 MQPEPKLSGA PR**SSQFLPLW SK**CPEGAGDA VMYASTECKA EVTPSQDGNR
51 **TFSYTLEDHT K**QAFGVMNEL R**LSQQLCDVT LQVKYEDIPA AQFMAHK**VVL
101 ASSSPVFKAM FTNGLREQGM EVVSIEGIHP KVMERLIEFA YTASISVGEK
151 CVLHVMNGAV MYQIDSVVRA CSDFLVQQLD PSNAIGIANF AEQIGCTELH
201 QRAREYIYMH FGEVAK**QEEF FNLSHCQLAT LISR**DDLNVR **CESEVFHACI**
251 **DWVKYDCPQR RFYVQALLRA VRCHALTPRF LQTQLQKCEI LQADARCKDY**
301 **LVQIFQELTL HKPTQAVPCR** APKVGR**LIYT AGGYFRQSLS YLEAYNPSNG**
351 **SWLRLADLQV PRSGLAGCVV GGLLYAVGGR** NNSPDGNTDS SALDCYNPMT
401 NQWSPCASMS VPRNR**IGVGV IDGHIYAVGG SHGCIHHSSV ERYEPER**DEW
451 HLVAPMLTRR **IGVGVAVLNR LLYAVGGFDG TNRLNSAECY YPER**NEWRMI
501 TPMNTIRSGA GVCVLHNCIY AAGGYDGQDQ LNSVER**YDVE TETWTFVAPM**
551 **R**HHRSALGIT VHQGKIYVLG GYDGHTFLDS VECYDPDSDT WSEVTR**MTSG**
601 **RSGVGVAVTM EPCR**KQIDQQ NCTC

Start - End	Observed	Mr(expt)	Mr(calc)	ppm	Miss	Sequence
13 - 22	1192.6834	1191.6761	1191.6288	40	0	R.SSQFLPLWSK.C
51 - 61	1341.7008	1340.6936	1340.6248	51	0	R.TFSYTLEDHTK.Q
72 - 84	1531.9168	1530.9095	1530.8076	67	0	R.LSQQLCDVTLQVK.Y Carbamidomethyl (C)
85 - 97	1520.8501	1519.8428	1519.7129	85	0	K.YEDIPAAQFMAHK.V
151 - 169	2134.0169	2133.0097	2133.0533	-20	0	K.CVLHVMNGAVMYQIDSVVR.A
217 - 234	2193.1625	2192.1552	2192.0684	40	0	K.QEEFFNLSHCQLATLISR.D Carbamidomethyl (C)
241 - 254	1779.8743	1778.8670	1778.7756	51	0	R.CESEVFHACIDWVK.Y 2 Carbamidomethyl (C)
255 - 260	838.4151	837.4078	837.3439	76	0	K.YDCPQR.R Carbamidomethyl (C)
261 - 269	1165.6774	1164.6701	1164.6767	-6	1	R.RFYVQALLR.A
262 - 269	1009.6477	1008.6404	1008.5756	64	0	R.FYVQALLR.A
270 - 279	1180.6352	1179.6279	1179.6295	-1	1	R.AVRCHALTPR.F Carbamidomethyl (C)
273 - 279	797.4207	796.4135	796.4014	15	0	R.CHALTPR.F
273 - 279	854.3822	853.3749	853.4229	-56	0	R.CHALTPR.F Carbamidomethyl (C)
280 - 287	1005.6203	1004.6130	1004.5655	47	0	R.FLQTQLQK.C
288 - 296	1075.5885	1074.5812	1074.5128	64	0	K.CEILQADAR.C Carbamidomethyl (C)
288 - 298	1363.7160	1362.7087	1362.6384	52	1	K.CEILQADARCK.D 2 Carbamidomethyl (C)
299 - 320	2656.5108	2655.5036	2655.3843	45	0	K.DYLVQIFQELTLHKPTQAVPCR.A Carbamidomethyl (C)
327 - 336	1160.6803	1159.6730	1159.6026	61	0	R.LIYTAGGYFR.Q
337 - 354	2085.0691	2084.0618	2083.9963	31	0	R.QSLSYLEAYNPSNGSWLR.L
355 - 362	911.5953	910.5880	910.5236	71	0	R.LADLQVPR.S
363 - 380	1648.9063	1647.8990	1647.8767	14	0	R.SGLAGCVVGGLLYAVGGR.N
363 - 380	1706.0025	1704.9952	1704.8981	57	0	R.SGLAGCVVGGLLYAVGGR.N Carbamidomethyl (C)
416 - 442	2813.5068	2812.4996	2812.3828	42	0	R.IGVGVIDGHIYAVGGSHGCIHHSSVER.Y Carbamidomethyl (C)
443 - 447	693.3351	692.3278	692.3129	21	0	R.YEPER.D
461 - 470	997.6653	996.6580	996.6080	50	0	R.IGVGVAVLNR.L
471 - 483	1382.7813	1381.7740	1381.6990	54	0	R.LLYAVGGFDGTNR.L
484 - 494	1401.7074	1400.7001	1400.6030	69	0	R.LNSAECYYPER.N Carbamidomethyl (C)
537 - 551	1844.9609	1843.9536	1843.8451	59	0	R.YDVETETWTFVAPMR.H
597 - 614	1837.9836	1836.9764	1836.8645	61	1	R.MTSGRSGVGVAVTMEPCR.K

Figure 4.22: MASCOT protein database search results for a peptide mass fingerprint obtained from the MALDI-TOF MS analysis of the Keap1 from the IA treated samples. The peptide mass fingerprint shown was used in a MASCOT protein database search, which identified mouse Keap1 with cysteines adducted with carbamidomethy. The top five proteins identified with the highest score of confidence are shown. The amino acid sequence coverage for mouse Keap1 was 50% and specific peptides covered by the MALDI-TOF MS are analysis are underlined and highlighted in bold.

	Accession	Mass	Score	Description
1.	MURI_CLONN	28542	73	Glutamate racemase - Clostridium novyi (strain NT) (Bacterium)
2.	V010_FOWPV	40591	69	Uncharacterized serpin-like protein FPV010 - Fowlpox virus
3.	ANR53_MOUSE	56702	65	Ankyrin repeat domain-containing protein 53 - Mus musculus (Mouse)
4.	GADX_SHIFL	31432	62	HTH-type transcriptional regulator gadX - Shigella flexneri (Bacterium)
5.	KEAP1_MOUSE	69508	57	Kelch-like ECH-associated protein 1 - Mus musculus (Mouse)

Match to: **KEAP1_MOUSE Kelch-like ECH-associated protein 1 - Mus musculus (Mouse)**
Sequence Coverage: **32%**

1 MQPEPKLSGA PR**SSQFLPLW SK**CPEGAGDA VMYASTECKA EVTPSQDGNR
51 **TFSYTLEDHT K**QAFGVMNEL R**LSQQLCDVT LQVKYEDIPA AQFMAHK**VVL
101 ASSSPVFKAM FTNGLREQGM EVVSIEGIHP KVMERLIEFA YTASISVGEK
151 **CVLHVMNGAV MYQIDSVVR**A CSDFLVQQLD PSNAIGIANF AEQIGCTELH
201 QRAREYIYMH FGEVAKQEEF FNLSHCQLAT LISRDDLNVR CESEVFHACI
251 DWVKYDCPQR **RFYVQALLR**A VR**CHALTPRF LQTQLQK**CEI LQADARCKDY
301 LVQIFQELTL HKPTQAVPCR APKVGR**LIYT AGGYFRQSLS YLEAYNPSNG**
351 **SWLRLADLQV PRSGLAGCVV GGLLYAVGGR** NNSPDGNTDS SALDCYNPMT
401 NQWSPCASMS VPRNRIGVGV IDGHIYAVGG SHGCIHHSSV ER**YEPER**DEW
451 HLVAPMLTRR **IGVGVAVLNR LLYAVGGFDG TNR**LNSAECY YPERNEWRMI
501 TPMNTIRSGA GVCVLHNCIY AAGGYDGQDQ LNSVER**YDVE TETWTFVAPM**
551 **R**HHRSALGIT VHQGKIYVLG GYDGHTFLDS VECYDPDSDT WSEVTR**MTSG**
601 **RSGVGVAVTM EPCR**KQIDQQ NCTC

Start - End	Observed	Mr(expt)	Mr(calc)	ppm	Miss	Sequence
13 - 22	1192.6834	1191.6761	1191.6288	40	0	R.SSQFLPLWSK.C
51 - 61	1341.7008	1340.6936	1340.6248	51	0	R.TFSYTLEDHTK.Q
72 - 84	1779.8743	1778.8670	1778.8543	7	0	R.LSQQLCDVTLQVK.Y Glutathione (C)
85 - 97	1520.8501	1519.8428	1519.7129	85	0	K.YEDIPAAQFMAHK.V
151 - 169	2134.0169	2133.0097	2133.0533	-20	0	K.CVLHVMNGAVMYQIDSVVR.A
261 - 269	1165.6774	1164.6701	1164.6767	-6	1	R.RFYVQALLR.A
262 - 269	1009.6477	1008.6404	1008.5756	64	0	R.FYVQALLR.A
273 - 279	797.4207	796.4135	796.4014	15	0	R.CHALTPR.F
280 - 287	1005.6203	1004.6130	1004.5655	47	0	R.FLQTQLQK.C
327 - 336	1160.6803	1159.6730	1159.6026	61	0	R.LIYTAGGYFR.Q
337 - 354	2085.0691	2084.0618	2083.9963	31	0	R.QSLSYLEAYNPSNGSWLR.L
355 - 362	911.5953	910.5880	910.5236	71	0	R.LADLQVPR.S
363 - 380	1648.9063	1647.8990	1647.8767	14	0	R.SGLAGCVVGGLLYAVGGR.N
443 - 447	693.3351	692.3278	692.3129	21	0	R.YEPER.D
461 - 470	997.6653	996.6580	996.6080	50	0	R.IGVGVAVLNR.L
471 - 483	1382.7813	1381.7740	1381.6990	54	0	R.LLYAVGGFDGTNR.L
537 - 551	1844.9609	1843.9536	1843.8451	59	0	R.YDVETETWTFVAPMR.H

Figure 4.23: MASCOT protein database search results for a peptide mass fingerprint obtained from the MALDI-TOF MS analysis of the Keap1 from the IA treated samples. The peptide mass fingerprint shown was used in a MASCOT protein databased search, which identified mouse Keap1 GSH binding to cysteine 77. The top five proteins identified with the highest score of confidence are shown. The amino acid sequence coverage for mouse Keap1 was 50% and specific peptides covered by the MALDI-TOF MS analysis are underlined and highlighted in bold.

4.3.6 Determination of cysteine oxidation on Keap1-V5 after BSO treatment using LC-ESI-MS/MS

S-glutathionylation has been shown here to occur on Keap1 basally and after GSH depletion or chemical stress through immunoblotting. However, MADLI-TOF MS analysis could only identify S-glutathionylation on cysteine 273 and on cysteine 77 in the control and IA-treated samples, respectively. Next, cysteine oxidation on Keap1-V5 was investigated with LC ESI-MS/MS in order to determine if Keap1 cysteine oxidation is a possible mechanism for Nrf2 activation. The ability of BSO to deplete GSH (Fig 4.15) was used to model the effect of redox perturbation without any concomitant cysteine modification. NEM, which was previously shown to alkylate all Keap1-V5 cysteine residues, was used to determine if BSO induced any form of cysteine oxidation that might render Keap1-V5 cysteines less available for NEM adduction. DNCB, which selectively adducts one Keap1-V5 cysteine 257 (Copple *et al.* 2008a), was also used to determine if BSO induces oxidation of this residue and renders cysteine 257 unavailable for DNCB adduction. Therefore, HEK293T cells were pre-treated with 100μM of BSO for 24hr and then exposed to 50mM of NEM for 2min or 100μM of DNCB for 1hr. Keap1-V5 adduction by NEM and DNCB was then compared before and after BSO treatment.

Prior treatment of cells with BSO did not make any Keap1-V5 cysteine residues less available for NEM adduction. Every cysteine residues of a proportion of Keap1-V5 were available to be adducted with NEM after BSO treatment. This included the three critical cysteines (Cys151, Cys273 and Cys288) previously implicated in the role of Keap1 function (Zhang *et al.* 2003; Levonen *et al.* 2004; Wakabayashi *et al.* 2004; Kobayashi *et al.* 2006a; Yamamoto *et al.* 2008) (Fig 4.24a).

Furthermore, in the samples treated alone with BSO, all Keap1-V5 cysteines were available for IA adduction after DTT reduction (Fig 4.24b). This therefore, suggests that there was no cysteine oxidation (reversible or irreversible) detectable by LC ESI-MS/MS, caused by BSO. Nevertheless, BSO redox perturbation caused Keap1-V5 cysteine 257 to be less available for dinitrophenol (DNP) adduction on subsequent treatment with DNCB (Fig 4.25b and Fig 4.26b) when compared to DNCB treatment only (Fig 4.25a and 4.26a). DNP adduction on cysteine 257 was only observed in two out of five experiments when samples were pre-treated with BSO, while DNP-modification of cysteine 257 was observed in five out of five experiments when BSO pre-treatment was omitted.

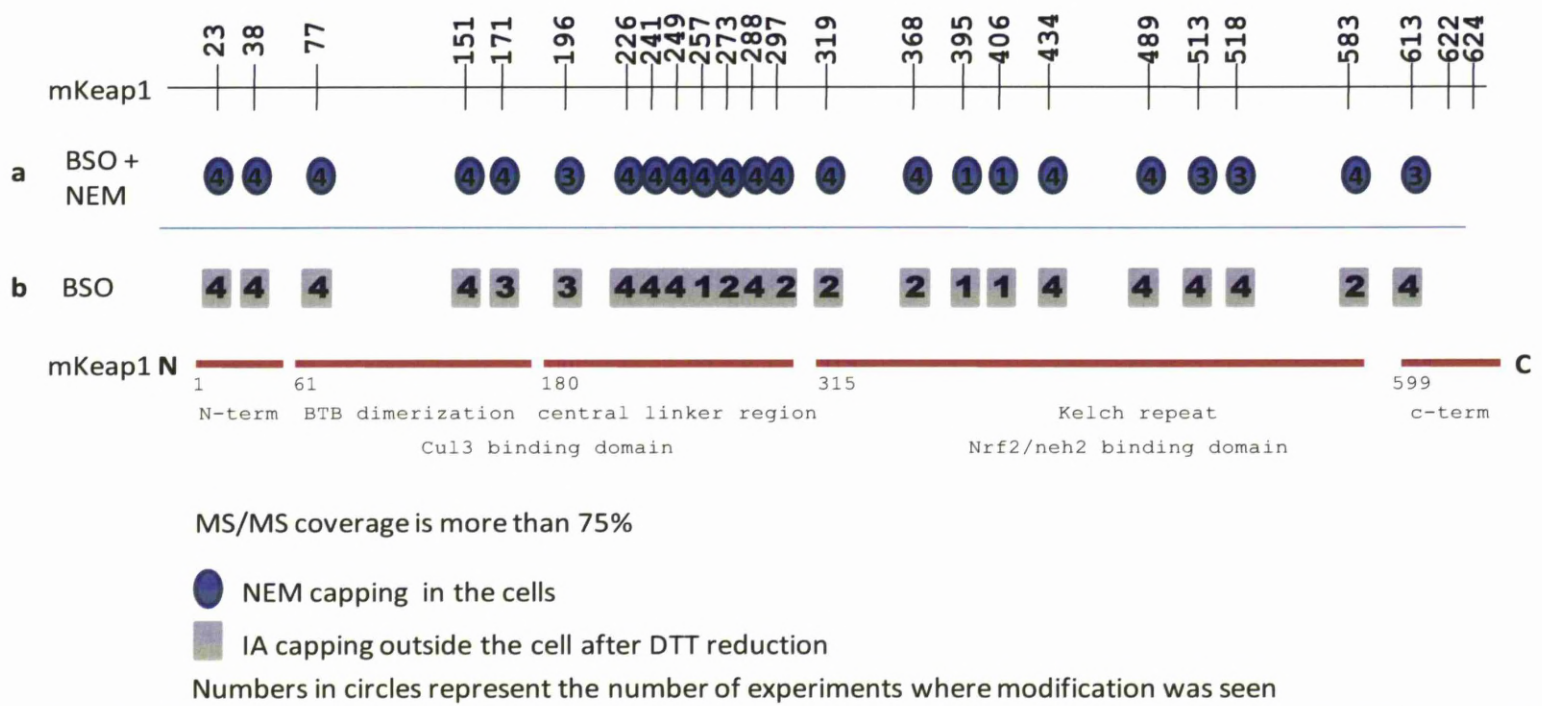

Figure 4.24: Schematic overview of mouse Keap1 cysteine residue modifications by NEM after BSO in overexpressing HEK293T cells. Cysteine residues in Keap1 modified in the HEK293T cells by NEM after BSO treatment are represented by blue circles (a). Grey boxes (b) represent cysteine modifications outside the cell following DTT reduction by IA. Numbers in the circles and boxes represent the number of experiments where the modification was observed. n=4.

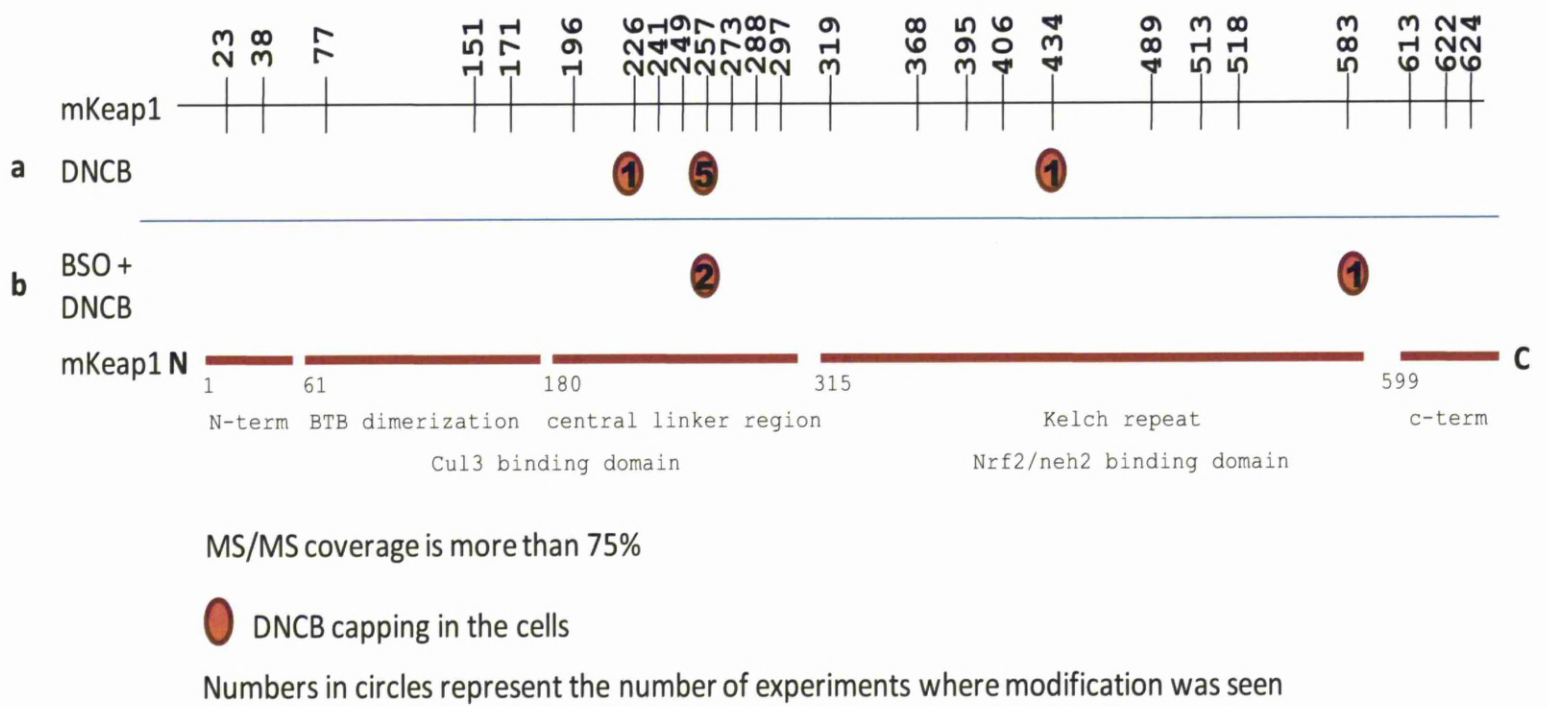

Figure 4.25: Schematic overview of mouse Keap1 cysteine residue modifications by DNCB after BSO treatment in overexpressing HEK293 cells. Cysteine residues in Keap1 modified in the HEK293T cells by DNCB are represented by yellow circles, DNCB treatment only (a) and BSO pre-treatment with DNCB treatment (b). Numbers in the circles and boxes represent the number of experiments where the modification was observed seen. n=5

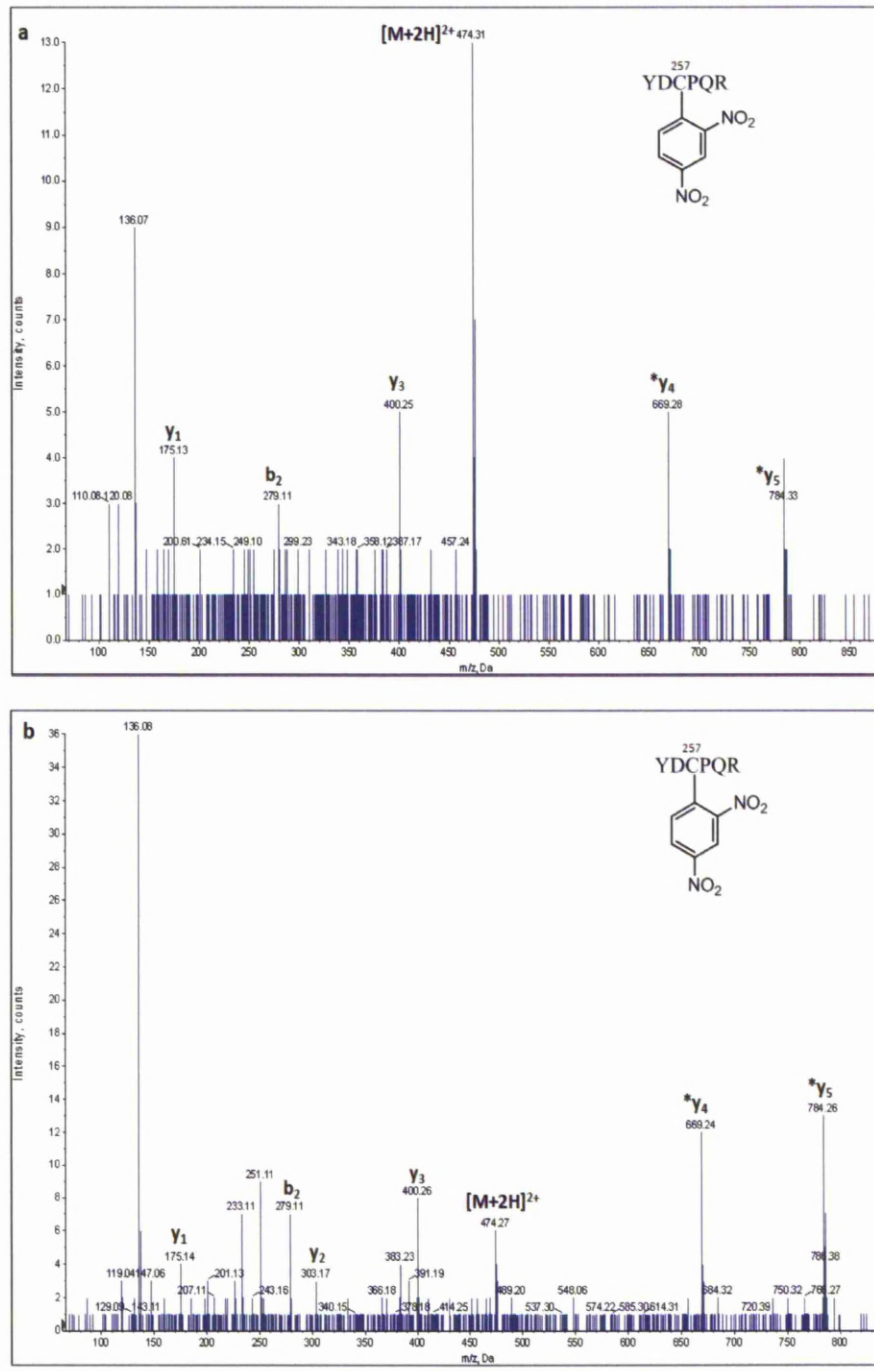

Figure 4.26: MS/MS spectrum indicating modification of Keap1-V5 Cys-257 by (a) DNCB and (b) BSO and DNCB in HEK293T cells. y- and b-ions are labelled where present. * represents ions for which a mass shift of +166.0Da indicates modification by DNCB.

4.3.7 Using diamide as an alternative oxidising agent to BSO, to induce cysteine oxidation on Keap1-V5

Diamide (Fig 4.27) is a known thiol oxidising agent that converts reduced GSH to GSH disulphide (GSSG). Use of diamide is a common approach to induce S-glutathionylation on proteins thiols in the presence of GSH (Dalle-Donne *et al.* 2003b; Hansen *et al.* 2009). The mechanism of diamide-induced S-glutathionylation is through modification of reactive protein thiols to diamide-activated protein species (1). The diamide activating protein species can then react with GSH to form a protein-GSH mixed disulphide and a hydrazine product (2) (Kosower *et al.* 1995).

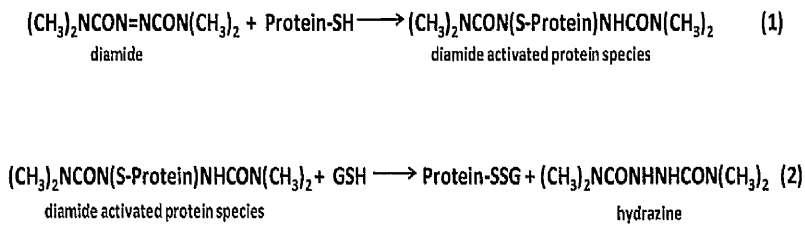

Figure 4.27: The chemical structure of diamide.

Diamide therefore was used as an alternative to BSO to model the effect of redox perturbation without any concomitant cysteine modification. Diamide was initially tested for Nrf2 activation and GSH depletion in Hepa-1c1c7 cells. Diamide induced Nrf2 dose-dependently in Hepa-1c1c7 cells after a 30min treatment (Fig 4.28a). No toxicity was observed during treatment after 30min (Fig 4.28b). The oxidation of GSH

to GSSG by diamide *in vitro* and in Hepa-1c1c7 cells was also determined. For *in vitro* GSH oxidation, 100μM diamide was added to 500μM of GSH in water and allowed to react for 30min at room temperature. For cellular oxidation, Hepa-1c1c7 cells were treated with diamide (300μM) for 30min at room temperature. Samples were analysed by LC-MS/MS. GSH was oxidised to GSSG by diamide *in vitro* and the production of hydrazine and GSSG was identified by MS/MS spectra (Fig 4.29a - e). Hepa-1c1c7 cells were treated with 300μM of diamide and led to the formation of GSSG. However, the presence of GSSG was not quantitatively measured in the cells.

After treatment with diamide, immunoprecipitated Keap1-V5 was resolved by SDS-PAGE under reducing and non-reducing conditions. Probing the blots with an anti-GSH antibody indicated that S-glutathionylation of Keap1-V5 had occurred (Fig 4.30). The observed formation of S-glutathionylation may have caused Keap1-V5 cysteines to be less available for cysteine modification, therefore, HEK293T cells were transfected with Keap1-V5 overnight and treated with 100μM diamide for 30min. Cells were then treated with 1mM of NEM for 5mins and Keap1-V5 was immunoprecipitated with anti-V5 agarose beads. Following immunoprecipitation, Keap1-V5 was reduced with DTT and treated with d_5NEM before tryptic digestion overnight for LC-ESI-MS/MS analysis. Prior treatment with diamide rendered NEM unable to alkylate cysteines 171 and 196, however the three critical cysteines 151, 273 and 288 were not affected (Fig 4.31b). This suggests that diamide may have oxidised both cysteine 171 and 196. However, there was no evidence to suggest that oxidation occured on the three critical cysteines 151, 273 and 288 within this investigation.

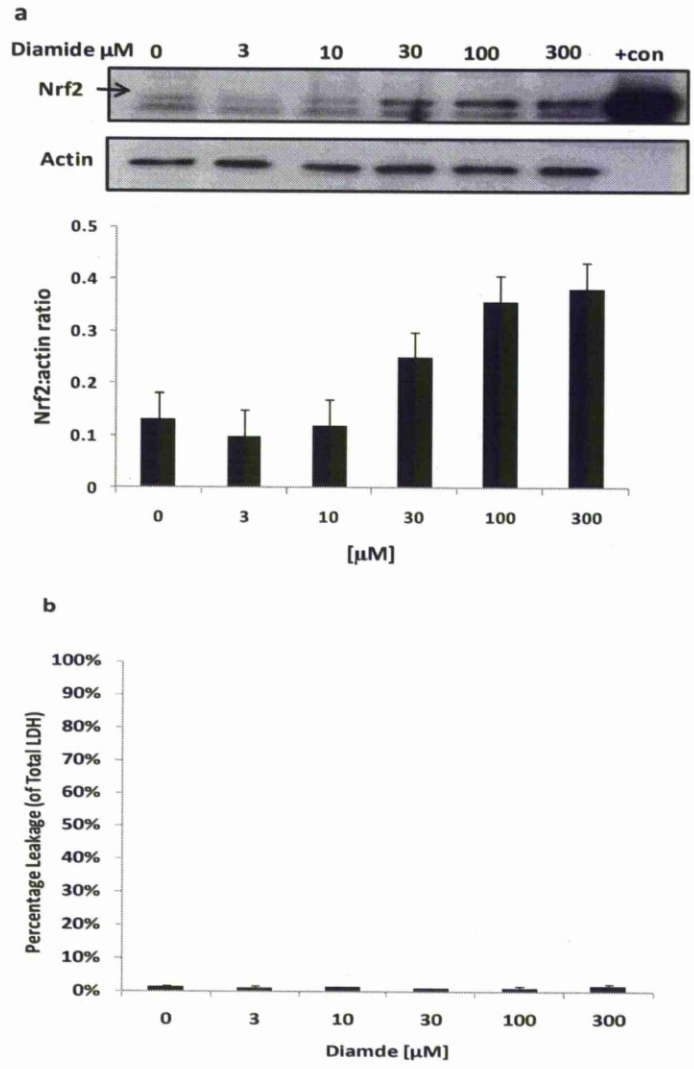

Figure 4.28: The effect of diamide on Nrf2 activation and cell toxicity. Hepa-1c1c7 cells were treated for 30min with diamide. Whole cell lysates were resolved by SDS-PAGE and probed for Nrf2. Diamide (a) activates Nrf2 dose-dependently. Actin is shown as a loading control. Recombinant mouse His-tagged Nrf2 was loaded as a positive control on the blot (+con). The bottom panel shows the densitometric anaylsis of Nrf2 positive bands normalised against actin. The LDH assay showed minimal leakage upon treatment with diamide which was not significant (b). Extracellular LDH release is expressed as a percentage of total (extracellular plus intracellular) LDH activity. In all experiments, the control cells were treated with water. Error bars = standard deviation of mean, n=3. Representative gel from n=3.

a) Diamide

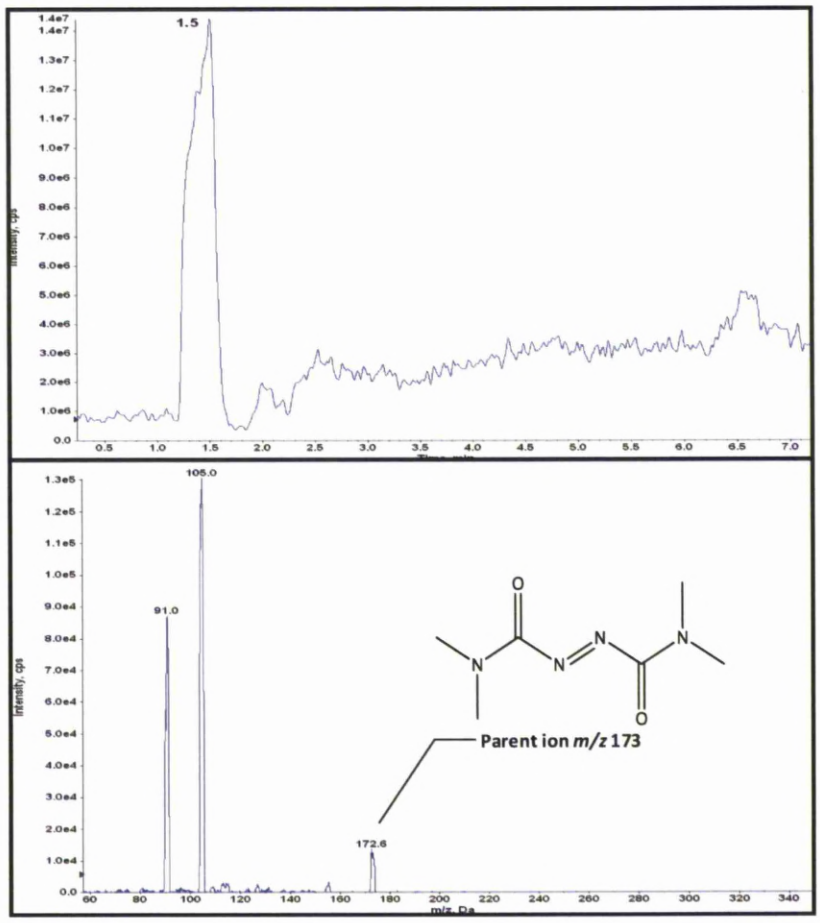

Figure 4.29: Representative Ion chromatogram and LC-MS/MS spectrum of (a) diamide *in vitro*. 100μM of diamide was reacted with 500μM of GSH in water at room temperature for 30min. Panel is a representative ion extracted chromatogram and MS/MS containing diamide, $(M+H)^+$ m/z 173.

b) Diamide + GSH

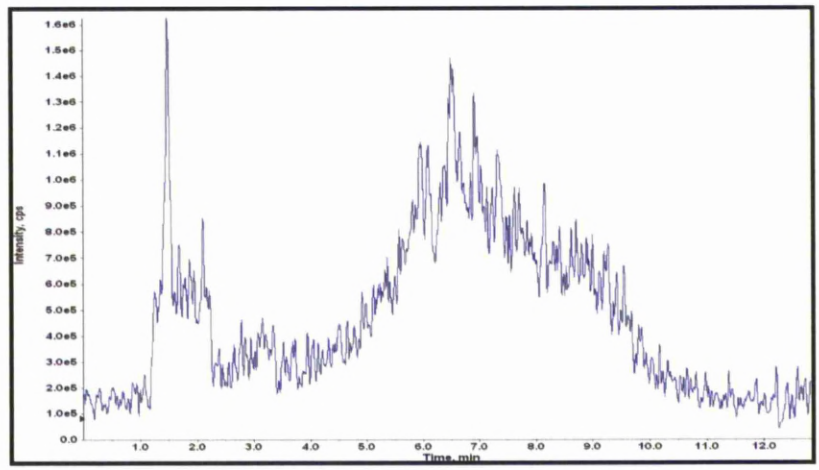

Figure 4.29: Representative Ion chromatogram and LC-MS/MS spectrum of (b) diamide and GSH conjugate *in vitro*. 100µM of diamide was reacted with 500µM of GSH in water at room temperature for 30min. Panel is a representative ion extracted chromatogram and MS/MS containing diamide and GSH, no conjugate formed.

c) GSH

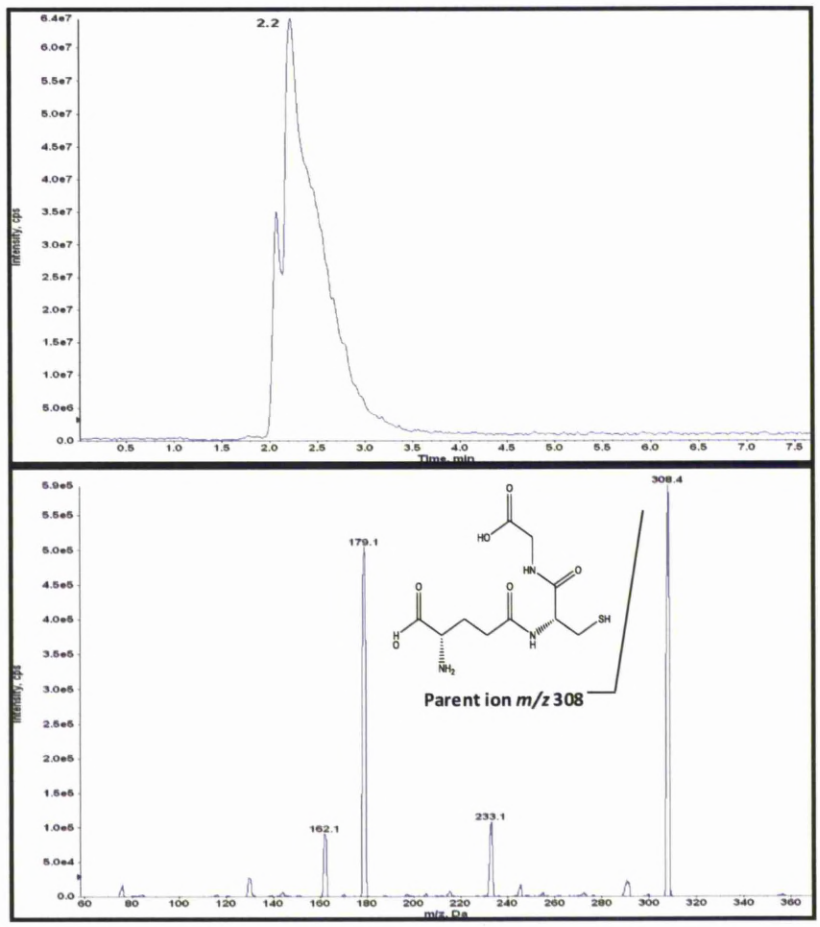

Figure 4.29: Representative Ion chromatogram and LC-MS/MS spectrum of (c) GSH *in vitro*. 100µM of diamide was reacted with 500µM of GSH in water at room temperature for 30min. Panel is a representative ion extracted chromatogram and MS/MS containing GSH, protonated molecular ion m/z 308.

d) GSSG

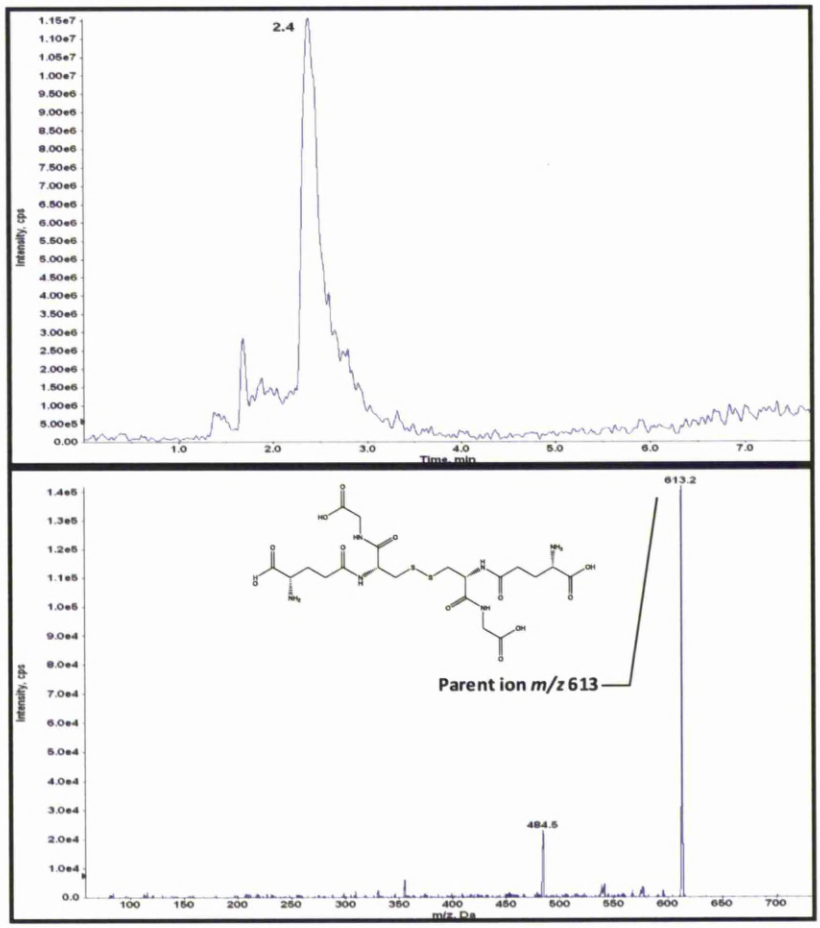

Figure 4.29: Representative Ion chromatogram and LC-MS/MS spectrum of (d) GSSG *in vitro*. 100µM of diamide was reacted with 500µM of GSH in water at room temperature for 30min. Panel is a representative ion extracted chromatogram and MS/MS containing GSSG, protonated molecular ion m/z 613.

e) Hydrazine

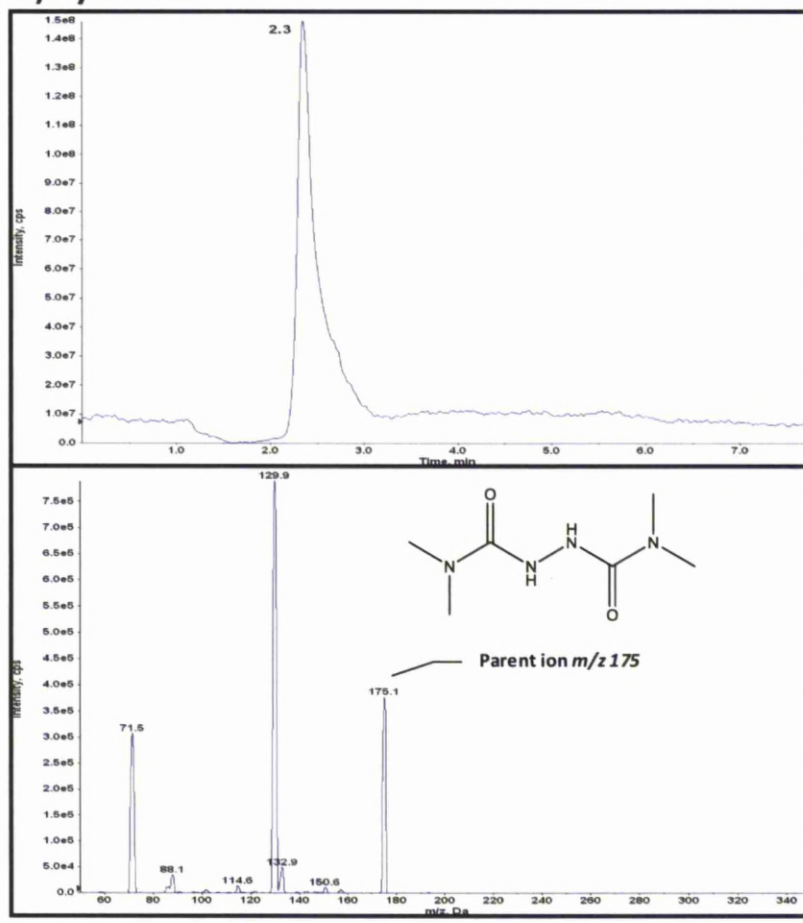

Figure 4.29: Representative Ion chromatogram and LC-MS/MS spectrum of (e) hydrazine *in vitro*. 100μM of diamide was reacted with 500μM of GSH in water at room temperature for 30min. Panel is a representative ion extracted chromatogram and MS/MS containing hydrazine, protonated molecular ion m/z 175.

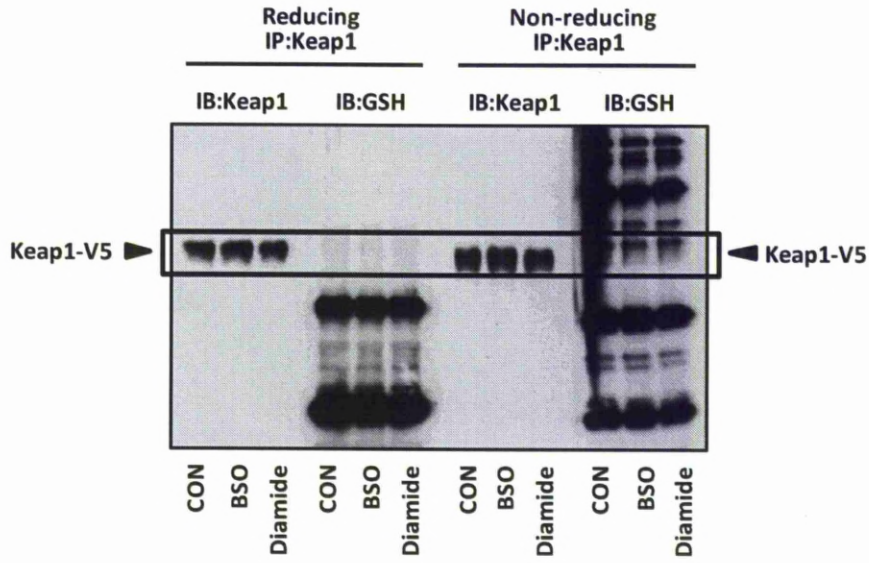

Figure 4.30: S-glutathionylation of Keap1-V5 in control and treated cells. HEK293T were transfected with Keap1-V5 overnight and treated with 100μM BSO and diamide for 24hr and 30min respectively using water as a control for 24hr. Cells were further treated with 50mM IA or NEM and DMSO as a control. Cells were lysed with RIPA buffer and Keap1-V5 was immunoprecipitated with anti-V5 agarose beads. Immunoprecipitated proteins were resolved by SDS-PAGE under non-reducing or reducing conditions, and probed with anti-Keap1 and anti-GSH antibodies. S-glutathionylation of Keap1 occurred in control, BSO and diamide treated samples under non-reducing conditions (see ▭). However, under reducing conditions s-glutathionylation of Keap1 was reversed and the GSH immunoreactive signal disappeared from Keap1-V5 (see ▭). Representative gel from n=1. IP; immunoprecipitation. IB; immunoblotting. Representative gel shown from n=1.

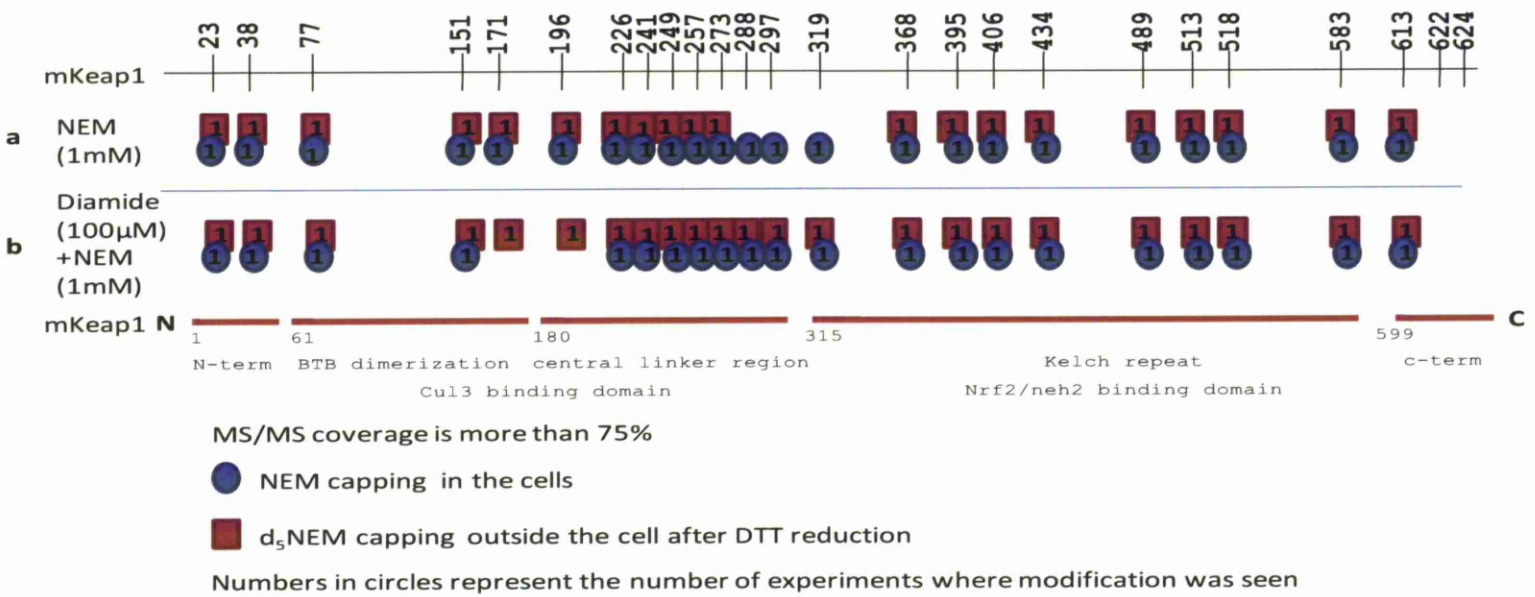

Figure 4.31: Schematic overview of mouse Keap1 cysteine residues after diamide treatment and their modification by NEM. Cysteine residues in Keap1 modified the HEK293T cells by diamide NEM were represented by blue circles, NEM treatment only (a) and diamide pre-treatment with NEM (b). Red boxes represent cysteine modifications outside the cell following DTT reduction by d_5NEM. Numbers in the circles and boxes represent the number of modifications seen. BSO treatment and DNCB modifications, n=1.

4.4 DISCUSSION

The Keap1/Nrf2 pathway plays an important role in cellular defence against endogenous and exogenous stress. The pathway controls the transcription of cytoprotective genes which enable the protection of cells against these stresses (Itoh *et al.* 1997). The currently accepted hypothesis is that Keap1, through covalent modification of its cysteine residues, mediates the up-regulation of cytoprotective genes by permitting Nrf2-dependent gene expression. Since cysteine is the most sensitive amino acid to covalent modification due to its chemical reactivity, it has been postulated to play a significant role as a 'sensor' to chemical and oxidative stress (Rudolph *et al.* 2009). Extensive studies have shown that three critical cysteines are involved in the functionality of Keap1. Cys151 maintains the binding of Cul3 ligase to Keap1. The adduction of Cys151 leads to the dissociation of Cul3 ligase from Keap1, which inhibits Nrf2 ubiquitination and subsequent degradation (Zhang *et al.* 2004; Gao *et al.* 2007; Rachakonda *et al.* 2008; Eggler *et al.* 2009; Kobayashi *et al.* 2009). The mutation of Cys151 to a larger partial molar volume of the amino acid side chain on Keap1 also increases the activation of Nrf2. However, this assumes that the modification of cysteine 151 which also increases the molar volume at this position will also be enough for Nrf2 activation (Eggler *et al.* 2009). Cysteines 273 and 288 maintain the ability of Keap1 to repress basal Nrf2 activation (Zhang *et al.* 2003; Levonen *et al.* 2004; Wakabayashi *et al.* 2004; Kobayashi *et al.* 2006a; Yamamoto *et al.* 2008). Adduction to these two cysteines simultaneously may suggest to cause the disruption of Nrf2 binding to Keap1 at the DLG motif (Tong *et al.* 2007) or the release of zinc (Dinkova-Kostova *et al.* 2005), leading to the disruption in Nrf2 ubquitination and proteosomal degradation. Other studies which report cysteine modifications have shown that cysteine adduction by

electrophiles or chemicals can lead to Nrf2 activation and induction of Nrf2-dependent proteins *in vitro* and in cell based assays (Dinkova-Kostova *et al.* 2002; Dietz *et al.* 2005; Eggler *et al.* 2005; Hong *et al.* 2005a; Hong *et al.* 2005b; Liu *et al.* 2005; Luo *et al.* 2007; Copple *et al.* 2008a; Dietz *et al.* 2008; Rachakonda *et al.* 2008; He *et al.* 2010). Hence, it is plausible that Keap1 cysteine residues play a significant role as 'sensors' to cellular stress. However, little is known about the basal thiol status of Keap1 in cells and how they actually serve as sensors to chemical and oxidative stress.

A cell based model system was previously described by us in the CDSS in which mouse Keap1-V5 was over-expressed in HEK293T cells (Copple *et al.* 2008a). Within this system, Keap1-V5 modifications on cysteine residues in a cellular context were detected. Initial investigations reported in this chapter were designed to transfect and over-express mouse Keap1-V5 in Hepa-1c1c7 cells. This cell did not express sufficient levels of Keap1 needed for experiments in this chapter. Thus, the HEK293T cell model was used for all subsequent experiments. The expression of Keap1-V5 in HEK293T cells as a model for the investigation of cellular modification of Keap1 cysteines remains an accepted model, but clearly it would have been more advantageous to investigate cellular modification of Keap1 in Hepa-1c1c7 with respect to liver cells. Immunoprecipitation of endogenous Keap1 from Hepa-1c1c7 cells was attempted previously within the department (Dr Ian Copple, thesis 2008). It was not possible to immunoprecipitate sufficient Keap1 for LC-ESI-MS/MS analysis within these investigations, probably because Keap1 cellular levels are known to be very low (McMahon *et al.* 2006). Therefore, a new method of transfection was tested to transfect Keap1-V5 into Hepa-1c1c7 within this investigation. Lipofectamine-

mediated transfection of Keap1-V5 into Hepa-1c1c7 was attempted previously in our department and showed a lower level of expression than HEK293T transfected cells by the same method. This is in line with the reported observations in this chapter, where expression of Keap1-V5 in Hepa-1c1c7 cells by Lipofectamine transfection and longer transfection did not improve Keap1-V5 expression (Fig 4.2a and 4.2b). A Nucleofection-mediated method was therefore attempted to improve expression of Keap1-V5 in the Hepa-1c1c7 cells. Using Nucleofection, an improvement in expression of Keap1-V5 was seen (Fig 4.3a) compared to lipofectamine. However, optimising the transfections conditions by increasing the number of cells and using a longer incubation period did not further improve Keap-V5 protein over expression (Fig 4.3b and c). Moreover, transfection of Hepa-1c1c7 using nucleofection gave an inconsistent level of Keap1 expression across experiments. Hence, HEK293T cells remained the most suitable cell type to use to express Keap1-V5 for the subsequent cysteine covalent modification studies.

Two common alkylating agents, IA and NEM, were used for detection of cysteine modification by LC-ESI-MS/MS. High concentrations of IA and NEM (50mM) over 2min were used to alkylate Keap1-V5 cysteine residues intracellularly. This is to achieve the maximum coverage of Keap1-V5 cysteines intracellularly with the shortest time without resulting in permanent damage to the cells. However, the full adduction of Keap1-V5 cysteines by carbamidomethyl was not detected in five experiments using a high concentration of IA (Fig 4.9a). Surprisingly, when high concentrations of NEM were used, the maximum adduction of Keap1-V5 was detected in four experiments (Fig 4.9b). Hence, the difference in Keap1-V5 cysteine modifications by IA and NEM suggested that there was a difference in the ability of these

chemicals to adduct cysteine residues. Indeed, it has been suggested that NEM has a faster reactivity in alkylating thiol groups compared to IA (Rogers *et al.* 2006). Therefore, the advantage of NEM in being a better and more efficient alkylating agent, allowing this compound to adduct every Keap1-V5 cysteine residues, resulted in it being utilised in subsequent investigations. Interestingly, this does suggests that all the cysteine residues in of Keap1-V5 cysteine residues are virtually available for NEM alkylation and that a proportion of them are all in a reduced form under basal conditions. Keap1 is a cysteine-rich protein, with highly reactive cysteine residues that can readily form intra- or inter- molecular disulphides bonds (Rudolph *et al.* 2009). Hence, to further confirm that Keap1 cysteines are all in a reduced form under basal conditions, NEM was tested for its ability to break disulphide linkages and react with cysteines in such a bond. HSA was used as a model protein for this purpose. HSA contains thirty-five cysteines, all of these except for Cys34 participate in disulphide linkage (Oettl *et al.* 2010). The MS/MS analysis showed that NEM was only able to bind to Cys34 even at increasing HSA to NEM molar ratios (Table 4.1). Therefore, this suggests that NEM was not able to break disulphide linkages. This further supports the observation that all Keap1-V5 cysteines are previously available for modification and that a proportion of them are reduced under basal conditions, without disulphide linkage.

NEM was found to be a more efficient alkylating agent compared to IA in the investigations described in this chapter. This was in line with what Rogers and colleagues have suggested previously (Rogers *et al.* 2006). Hence, an alternative alkylating agent which has similar chemical characteristics to NEM was required to replace IA in order to carry out differential labelling experiments. A heavy hydrogen labelled NEM,

d_5NEM, was selected as the alternative alkylator (Fig 4.12). d_5NEM has exactly the same structure as NEM but it is 5Da heavier than NEM, which can be easily identified on the LC ESI-MS/MS (Niwayama *et al.* 2001). It was shown within this chapter that d_5NEM was able to adduct Keap1-V5 cysteines (Fig 4.13). NEM (1mM) was able to adduct all Keap1-V5 cysteines in HEK293T cells and d_5NEM was able to adduct all Keap1-V5 cysteines after DTT reduction, except for cysteine 297 which might have been fully adducted by NEM. Hence, after intense and overwhelming chemical exposure, virtually a proportion of all the cysteines in Keap1 molecule in the cell are still in a reduced state.

Two bands which correspond to the molecular weight of Keap1-V5 were observed following the CCB staining of Keap1-V5 resolved by SDS-PAGE following V5-immunoprecipitation of from HEK293T cells (Fig 4.4). MALDI-TOF MS analysis identified both forms as mouse Keap1 but no forms of cysteine oxidation were detected within them (Fig 4.5-4.8). S-glutathionylation is one of the reversible forms of post-translational modification where cysteine is oxidised by GSH. The formation of S-glutathionylation on proteins can either be constitutive, serve as a storage mechanism of cellular GSH, serve to protect cysteine against irreversible oxidation, act in the regulation of protein function or be a form of cellular stress-induced oxidation (Dalle-Donne *et al.* 2007). Currently, there are a range of proteins that have been shown to be S-glutathionylated and whose function is regulated by S-glutathionylation. Proteins which can be inhibited by S-glutathionylation are NF-κB (Pineda-Molina *et al.* 2001; Qanungo *et al.* 2007), IKK (Reynaert *et al.* 2006; Chung *et al.* 2010), actin (Dalle-Donne *et al.* 2003a; Dalle-Donne *et al.* 2003b) and p53 (Velu *et al.* 2007; Yusuf *et al.* 2010). Examples of proteins which can be activated by S-glutathionylation include carbonic

anhydrase 3 (Kim *et al.* 2005), matrix metalloproteinase (Okamoto *et al.* 2001) and p21ras (Clavreul *et al.* 2006). Other than the regulation of protein function, S-glutathionylation has been shown to prevent the ubiquitination of IκB (Kil *et al.* 2008) and also to protect thiols from irreversible oxidation in metallothionein molecules (Casadei *et al.* 2008). Therefore, the oxidation of Keap1 cysteines by GSH was further investigated by using immunoblotting and MALDI-TOF analysis to determine S-glutathionylation of Keap1-V5.

The immunoblotting method showed that under non-reducing conditions, S-glutathionylation of Keap1-V5 was detected with an anti-GSH antibody in control and treated cells (Fig 4.16a and c). However, under reducing conditions S-glutathionylation was reversed from Keap1-V5 as it was not detected with anti-GSH antisera (Fig 4.16b and d). This is in line with a recent report that describes S-glutathionylation on endogenous Keap1 in Hepa-1c1c7 cells treated with an electrophilic thiophene compound (Zhang *et al.* 2010). The authors, however, did not observe S-glutathionylation in untreated cells, which was observed on Keap1-V5 in control HEK293T samples within this study. This difference in observations could be explained through the model used here which utilised the overexpression of Keap1-V5 whereas Zhang and colleagues looked at endogenous Keap1.

The MALDI-TOF MS analysis of protein bands excised from CCB-stained gels (Fig 4.17) identified control samples (Fig 4.18-4.20) and IA treated (Fig 4.21-4.23) bands as mouse Keap1. S-glutathionylation was also detected on both Control and IA bands by MALDI-TOF. However, the S-glutathionylation which was detected on Cys273 was present in a miscleaved peptide from the control band (Fig 4.20). From the IA band, S-glutathionylation was detected on Cys77 (Fig 4.23). This observation

on Cys77 has also been reported by Holland and colleagues who used recombinant Keap1 (Holland *et al.* 2008). Therefore, S-glutathionylation on Keap1 could have occurred from either constitutive or cellular stress oxidation.

The investigation of potential cysteine oxidation on Keap1 that may lead to Nrf2 activation was furthered explored by the use of LC ESI-MS/MS analysis. The same HEK293T cell Keap1-V5 model was used to look for cysteine modification by LC ESI-MS/MS. The ability of BSO to deplete GSH was used to model the effect of redox perturbation without any concomitant cysteine modification. BSO was observed to induce oxidative stress by cellular GSH depletion (Ito *et al.* 2006). The investigation of whether BSO can induce oxidation of Keap1-V5 in our model was measured indirectly by assaying the availability of adduction on the Keap1-V5 cysteines following BSO treatment. Prior treatment of cells with BSO did not hinder the ability of a high concentration of NEM to alkylate Keap1-V5 cysteines (Fig 4.24). Therefore, this suggested that depletion of GSH in our model did not induce oxidation of a sufficient proportion of the Keap1-V5 cysteines to be detected by LC-ESI-MS/MS analysis. We have shown previously that DNCB selectively alkylates cysteine 257 in Keap1 (Copple *et al.* 2008a) and that exposure to DNCB is associated with the induction of Nrf2 and GSH depletion (chapter 2). The treatment of cells with 100μM DNCB for 1hr after GSH depletion with BSO allows the cells to undergo further chemical or oxidative stress, and potentially, sufficient/further oxidation to be detected by LC-ESI-MS/MS. Indeed, DNCB exposure with BSO treatment did reduce the frequency of DNP adduction of cysteine 257 in comparison to DNCB treatment only (Fig 4.25). This suggests that cysteine oxidation of Keap1 may occur in a cellular context.

Diamide, a known oxidising agent, was used as an alternative to BSO to induce cysteine oxidation on Keap1-V5. It is commonly applied to induce s-glutathionylation on protein thiols (Dalle-Donne *et al.* 2003b; Casadei *et al.* 2008; Hansen *et al.* 2009; Yusuf *et al.* 2010). In Hepa-1c1c7 cells, diamide was able to induce Nrf2 activation from 30μM to 300μM after 30min exposure (Fig 4.28a) and cellular toxicity was not apparent (Fig 4.28b). Diamide, in the presence of GSH, could oxidise GSH to GSSG but did not form a GSH-conjugate. Using LC-MS/MS, GSSG was detected after treatment with diamide under *in vitro* conditions (Fig 4.29d) and also in Hepa-1c1c7 cells, where GSSG was formed in the presence of diamide but not in untreated cells. Using, immunoblotting of Keap1-V5 with anti-GSH antibodies, the data presented in this chapter show that S-glutathionylation can occur on Keap1-V5 following diamide treatment under non-reducing conditions, which is reversible under reducing conditions (Fig 4.30). Cysteine oxidation by diamide was further investigated using LC-ESI-MS/MS analysis. Keap1-V5 expressing HEK293T cells were treated with 100μM diamide, followed by 1mM of NEM. Immunoprecipitated Keap1-V5 was tryptically digested and analysed by MS/MS. Diamide treatment resulted in the Keap1-V5 cysteines, 171 and 196, to be unavailable for NEM alkylation. However the three critical cysteines (Cys151, Cys273 and Cys288) were not affected (Fig 4.31a). Therefore, this suggested that diamide may have caused the oxidation of Cys171 and Cys196 which could be adducted by d_5NEM after DTT reduction (Fig 4.31a).

Oxidising agents such as BSO and diamide, have been shown here to induce Nrf2 activation and deplete GSH through separate mechanisms. Both compounds induce cysteine oxidation of Keap1-V5 containing cysteines. Cysteine oxidation on Keap1-V5 was indirectly

measured through the modification of reduced cysteines by electrophiles after BSO or diamide treatment. S-glutathionylation could not be detected directly, due to the detection limits of LC-ESI-MS/MS. Reversible oxidation was difficult to detect on peptides which are not reduced as they do not ionise on the mass spectrometry; the amount of oxidised cysteine peptides may have been below the limit of MS/MS detection. Regardless of these limitations, using BSO and diamide and electrophiles to indirectly determine cellular Keap1 cysteine oxidation remains a novel method. Currently, the investigation of cellular Keap1 cysteine oxidation is restricted to 2D immunoblotting (Wakabayashi *et al.* 2004), non-reducing 1D immunoblotting (Fourquet *et al.* 2010) and biotinylated cysteines (Takagi *et al.* 2009). To date, LC-MS/MS analysis of Keap1 oxidation was only successfully carried out *in vitro* using bacteria expressing recombinant Keap1 (Holland *et al.* 2008).

Currently, there is no reported evidence that all Keap1 cysteine residues can all exist in the reduced form in living cells and are not involved in any disulphide linkage. The crystal structure of the Keap1 DGR domain indicates eight cysteines that are not involved in a disulphide linkage (Li *et al.* 2004). However, the data presented here show for the first time that the Keap1-V5 thiol status of all cysteine residues can exist in a reduced form under basal conditions in a cell, under conditions where the protein is functionally active in targeting Nrf2 (Ms Rym Megherbi thesis) and therefore that a proportion of all Keap1 cysteines are available for covalent modification. This represents an important finding considering that Keap1 is a very cysteine-rich protein (4.3% and 4% of the total amino acid content in human and mouse Keap1 protein are cysteine residues, which is above the average of 2.3% across human and mouse proteins). Other cysteine-rich protein

such as metallothionein, an antioxidant protein (30% of 61 amino acids are cysteines) (Messerle *et al.* 1990; Zangger *et al.* 1999), do contain disulphide bonds *in vivo* under physiological conditions unlike Keap1 (Feng *et al.* 2006). Furthermore, the detection of S-glutathionylation of Keap1-V5 in the HEK293T cell model used here suggests that S-glutathionylation can be found in Keap1-V5 basally and after cellular stress. This suggests that Keap1 can either be constitutively oxidised under basal conditions or oxidised under conditions of oxidative stress to prevent irreversible oxidation of Keap1 free thiols during cell stress. Therefore, the hypothesis that Keap1 cysteines play a significant role as "key sensors" that sense exogenous and endogenous stress is further supported by the observations made within this chapter, i.e. that all Keap1 cysteines are reduced and available.

Chapter 5

Use of click chemistry for the investigation of Nrf2 activation

CONTENTS

5.1 INTRODUCTION

The Keap1/Nrf2 pathway protects the cells against endogenous and exogenous stress. The nuclear accumulation and activation of Nrf2 leads to the transcription of many cytoprotective proteins, i.e. phase II enzymes, antioxidants, molecular chaperones and transport proteins (Prestera *et al.* 1995; Hayes *et al.* 1999; Itoh *et al.* 1999b; Kwak *et al.* 2003; Hu *et al.* 2006; Adachi *et al.* 2007; Aleksunes *et al.* 2009; Xu *et al.* 2010). The widely accepted model of Nrf2 activation centres on the covalent modification of Keap1 cysteines that could lead to the de-repression of Nrf2, through the abrogation of Nrf2 ubiquitination and subsequent proteosomal degradation. The investigation of the relationship between Nrf2 activation and Keap1 cysteine modification has been extensively investigated. Different classes of reactive compounds that covalently modify cysteines in both bacterially-expressed recombinant Keap1 and ectopically-expressed Keap1 cells have been found to induce Nrf2 activation (Dinkova-Kostova *et al.* 2002; Zhang *et al.* 2003; Levonen *et al.* 2004; Dietz *et al.* 2005; Dinkova-Kostova *et al.* 2005; Eggler *et al.* 2005; Hong *et al.* 2005a; Sakurai *et al.* 2006; Luo *et al.* 2007; Copple *et al.* 2008a; Rachakonda *et al.* 2008). These classes of reactive compounds can target cysteines found on different domains of Keap1 based on their chemistry with the targeted cysteines (Holland *et al.* 2008; Kobayashi *et al.* 2009; Holland *et al.* 2010). This combined with previous work further supports the hypothesis that Keap1 cysteine modification leads to activation of Nrf2, although this does not rule out the potential involvement of other triggers for activation

Click-Chemistry (CC) was first introduced into the field of activity-based protein profiling (ABPP) to determine the functional state of

proteins in their endogenous cellular environment (Cravatt *et al.* 2000; Adam *et al.* 2002; Speers *et al.* 2005). Until recently, ABPP experiments have been conducted only with cell or tissue homogenates. However, CC-ABPP enables profiling of living cells and organisms through CC probes which comprise two elements; a reactive group, which enables the binding and covalent labelling of the protein under investigation and secondly one or more reporter tags for detection and isolation of probe-labelled proteins (Speers *et al.* 2004; Speers *et al.* 2005). CC is a copper(I)-catalysed [3+2] cycloaddition reaction between alkyne and azide groups (Fig 5.1) (Kolb *et al.* 2001; Speers *et al.* 2004). The azide group can be labelled with either rhodamine (Speers *et al.* 2004) or biotin reporter tags (Speers *et al.* 2005) (Fig 5.1) for in-gel fluorescence screening or protein purification for proteomics analysis (Speers *et al.* 2004; Evans *et al.* 2005). Alkyne groups are rarely found *in vivo*, therefore CC can be used to monitor covalent modification of proteins in cells (Evans *et al.* 2005). A number of electrophiles can have an alkyne group incorporated and then utilised as CC probes for proteomics profiling and analysis of cysteine modifications (Macpherson *et al.* 2007; Vila *et al.* 2008; Weerapana *et al.* 2008). Iodoacetamide (IA) and maleimide reactive groups are common cysteine alkylating agents and have been extensively studied in proteomic investigations (Rogers *et al.* 2006; Shin *et al.* 2007; Zabet-Moghaddam *et al.* 2008). In addition, IA and N-ethylmaleimide (NEM) are also known to modify Keap1 cysteines and activate Nrf2 (Dinkova-Kostova *et al.* 2002; Eggler *et al.* 2005; Eggler *et al.* 2007; Copple *et al.* 2008a). Consequently, these compounds were utilised in CC experiments, incorporating an alkyne group in both to form the novel structures: IA-click and NEM-click for cysteine modification profiling during Nrf2 activation (Fig 5.2).

Investigations into the relationship between Keap1 cysteine modifications and Nrf2 activation have relied significantly on proteomic analysis. These investigations are commonly based on Keap1 cysteine modification by reactive compounds, detected on tandem liquid chromatography-mass spectrometry/mass spectrometry (LC-MS/MS) (Dinkova-Kostova *et al.* 2002; Hong *et al.* 2005a; Copple *et al.* 2008a; Rachakonda *et al.* 2008). This enables the identification of the site of cysteine modifications by reactive compounds. In this chapter, I have aimed to use these click compounds as novel alkylating agents in the investigation of Keap1 covalent modification and Nrf2 activation. The initial aim was to assess these novel click compounds in comparison with their parent compounds with regard to their ability to deplete GSH, activate Nrf2 by alkylating cysteines on Keap1 and their effect on cell viability. Ultimately, the goal of this work is to determine which novel click compound is suitable as a novel probe and for future investigations of Keap1 cysteine modification and Nrf2 activation.

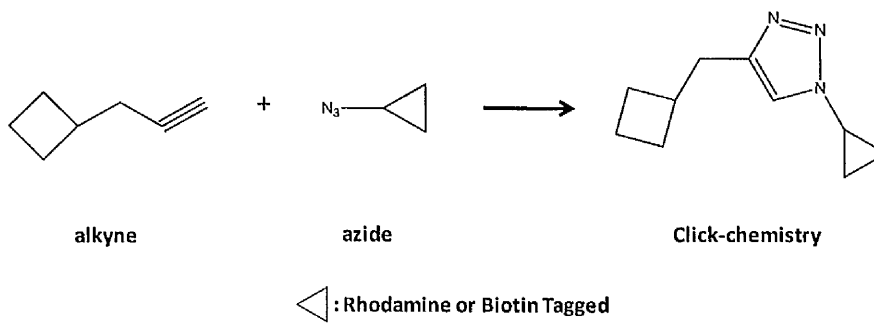

Figure 5.1: Schematic diagram of Click Chemistry. Cycloadditon reaction between alkyne and azide group.

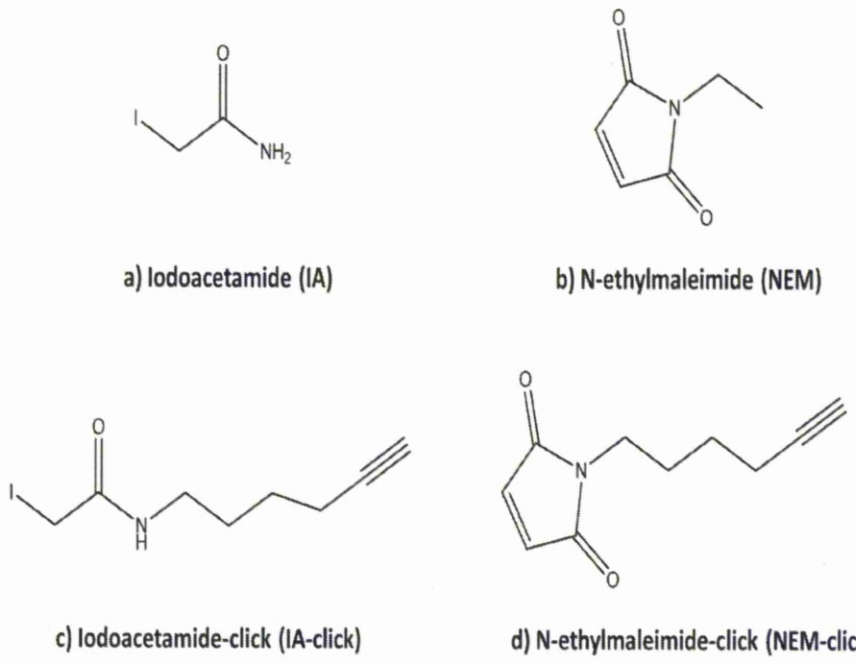

Figure 5.2 Chemical structure of parent compounds and their click derivatives. Iodoacetamide (a) and Iodoacetamide-click (c) and; N-ethylmaleimide (b) and N-ethylmaleimide-click (d).

5.2 MATERIALS AND METHODS

5.2.1 Materials

The Iodoacetamide-click and N-ethylmaleimide-click molecules were kind gifts of Professor Paul O'Neill (Department of Chemistry, University of Liverpool, UK). Iodoacetamide and N-ethylmaleimide were from Sigma-Aldrich (Poole, UK). All other reagents were of analytical or molecular grade and were purchased from Sigma-Aldrich.

5.2.2 Cell Culture and Cell Count

Hepa-1c1c7 cells were maintained and counted as detailed in section 2.2.2.

5.2.3 Cell Treatment

Hepa-1c1c7 cells were seeded onto 96-well plates and 24-well plates at 2 x 10^4 cells/well and 2 x 10^5 cells/well respectively on the previous day. IA, IA-click, NEM and NEM-clicks were dissolved in dimethyl sulfoxide (DMSO). Cells treatment was prepared as detailed in section 2.2.3.

5.2.4 Preparation of whole cell lysates

For whole cell lysate preparation was detailed as in section 2.2.4.

5.2.5 Measurement of protein content

The total protein content was determined as detailed in section 2.2.5.

5.2.6 Western immunoblotting

Nrf2 western immunoblotting was prepared as detailed in section 2.2.6.

5.2.7 Measurement of Lactate Dehydrogenase Leakage

Cellular cytotoxicity was determined by LDH measurements as detailed in section 2.2.10.

5.2.8 Measurement of Glutathione

Total GSH content was quantified as detailed in section 2.2.11.

5.2.9 LC-MS/MS method

Samples were prepared by adding together the following in a ratio of 1:1, NEM-Click:GSH, followed by a 1 in 25 dilution in phosphate buffered saline (PBS) (pH 7.4). The formation of conjugates was measured as described in 4.2.12. The gradient solvent system used to elute the sample was 95% H_2O + 0.1% formic acid (A) and 5% methanol (B) held for 4min, then increased to 95% (B) linearly over 15min. The flow rate was 0.2mL/min, and column temperature was set to 30°C. A total ion current chromatogram was acquired using the following conditions: positive ionisation mode, ionisation voltage 5500V, ion source temperature 350°C, selected mass range 100 to 550Da. Collision activated dissociation of parent ions was performed using nitrogen gas in the Q2 collision cell. Collision energy was 25V, and collision gas was maintained at a setting of 8. LC-MS/MS scans were operated in MRM mode and product ion mode. The mass transitions monitored were 485.5/356.5 (conjugated molecule) and 308.3/179.3 (GSH) $[[M+H]-129]^+$. The dwell time per transition was 100ms.

5.2.10 Data Analysis

Data are expressed as mean ± standard deviation of the mean. Normality was assessed by the Shapiro-Wilk Test. The significance of differences within the data was assessed by a one-way ANOVA for normally distributed data, and Kruskal-Wallis analysis of variance (ANOVA) for non-parametric data. A difference was considered significant at $p<0.05$.

5.3 RESULTS

5.3.1 A comparison of Nrf2 activation by IA-click and its parent compound, IA

Hepa-1c1c7 cells were exposed to IA and IA-click with the first aim to determine whether IA-click can activate Nrf2 and then to compare its Nrf2-inducing efficacy to its parent compound, IA. IA and IA-click both induce Nrf2 accumulation (Fig 5.3). IA-click can activate Nrf2 despite the addition of the alkyne group. In contrast, the potency of IA and IA-click at inducing Nrf2 activation varies between them. IA induced Nrf2 at 10μM and reached the highest induction at 100μM (Fig 5.3a). IA-click induced Nrf2 at 30μM, which was the highest level of induction for this compound (Fig 5.3b). Both compounds caused depletion of total GSH content dose-dependently (Fig 5.4a and b). Similar to Nrf2 activation, IA-click has a weaker potency in depletion of GSH (Fig 5.4b) compared to IA (Fig 5.4a). IA-click resulted in GSH depletion to 40% of the control (Fig 5.4b), whereas IA caused GSH depletion to undetectable levels (Fig 5.4a). Cytotoxicity was determined by LDH leakage and this indicated no clear toxicity after 1hr incubation with either compound up to the high concentration of 1000μM of IA-click (Fig 5.4c). However, after 24hr, toxicity was seen for IA and IA-click (10μM to 1000μM) (Fig 5.4d). Due to the difficulty in synthesising IA-click with consequent low yields, only a single sample test was carried out, therefore statistical analysis was not appropriate for this experiment.

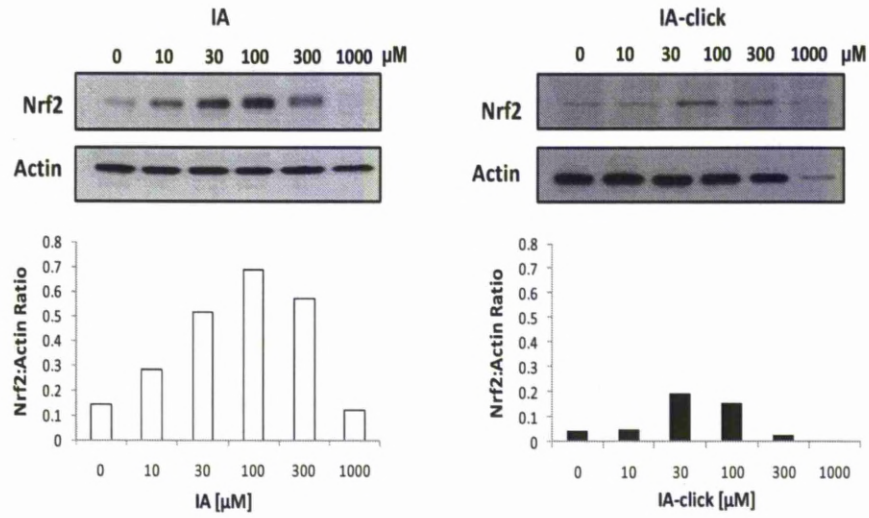

Figure 5.3: The effect of IA and IA-click on Nrf2 activation. Hepa-1c1c7 cells were treated for 1hr with IA (a) and IA-click (b) and RIPA whole cell lysates resolved using SDS-page gels and probed for Nrf2. Exposure to IA (a) and IA-click (b) results in Nrf2 accumulation. Actin is shown as a loading control. The bottom panel shows the densitometric analysis of Nrf2 positive bands normalised against actin. The control cells were treated with 0.1% DMSO. A representative gel for IA and IA-click n=1 is shown. Densitometric values shown for IA and IA-click, n=1.

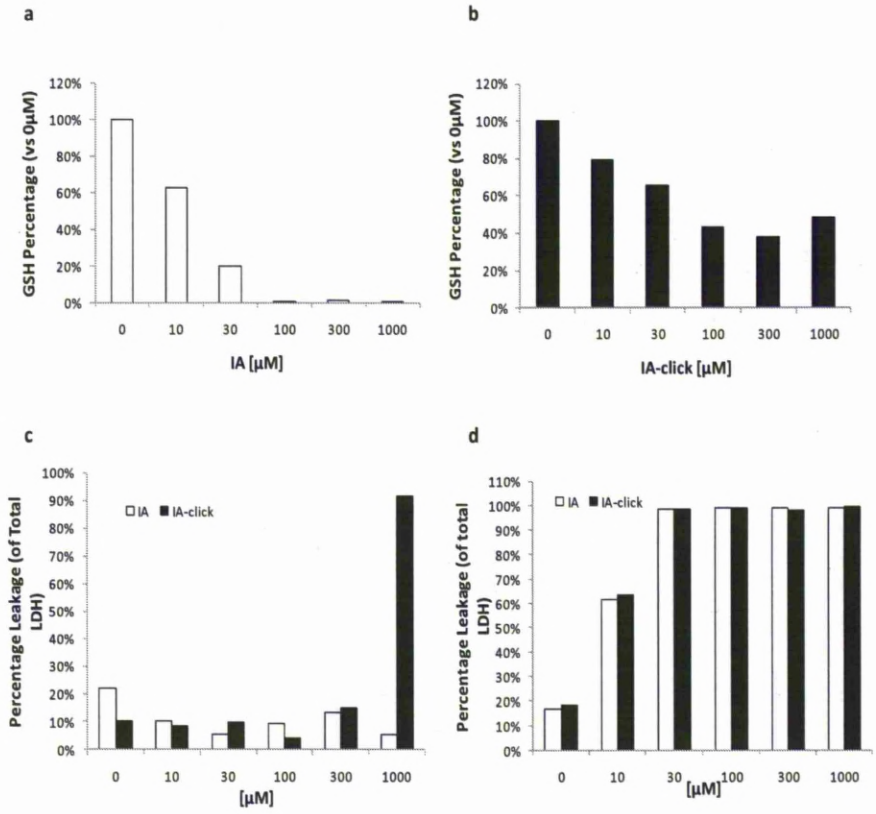

Figure 5.4: The effect of IA and IA-click on GSH and cell toxicity. Hepa-1c1c7 cells were treated for 1hr with IA (a) or IA-click (b) and lysed with 10mM HCl. GSH depletion reaches 100% of control with a high dose of IA (a) and 40% of control with 100μM of IA-click (b). Total GSH was normalised against total protein content. Cells were treated with IA or IA-click for 1hr (c) and 24hr (d). LDH assay shows minimal leakage upon treatment with IA or IA-click for 1hr, except for IA-click at 1000μM where substantial leakage was seen (c). The LDH assay shows substantial leakage upon treatment with IA or IA-click (d) after 24 hrs. Extracellular LDH activity is expressed as a percentage of total (extracellular plus intracellular) LDH activity. In all experiments, the control cells were treated with 0.1% DMSO. GSH percentage from triplicate measurements, n=1. Percentage leakage of total LDH from triplicate measurements, n=1.

5.3.2 Nrf2 activation by N-ethylmaleimide and N-ethylmaleimide-click

Hepa-1c1c7 cells were exposed to NEM and NEM-click with the aim to determine whether NEM-click resulted in Nrf2 activation, and then to compare this with NEM, the parent compound. NEM and NEM-click both induce Nrf2 accumulation (Fig 5.5). NEM-click can activate Nrf2 with similar potency as NEM, despite the addition of the alkyne group. Nrf2 activation by NEM and NEM-click is evident at 3μM (Fig 5.5). NEM-click induced the highest level of Nrf2 at 30μM (Fig 5.5a) and NEM (Fig 5.5b) induced the highest Nrf2 level at 100μM. Both compounds caused depletion of total GSH content dose-dependently (Fig 5.6a and b). Both NEM and NEM-click caused the depletion of GSH to undetectable levels at the highest dose of 100μM (Fig 5.6a and b). Following a 1hr exposure to both NEM and NEM-click, no cytotoxicity was seen (Fig 5.6c). However, after 24hr, neither NEM nor NEM-click resulted in toxicity at 100μM (Fig 5.6d), as determined by LDH leakage.

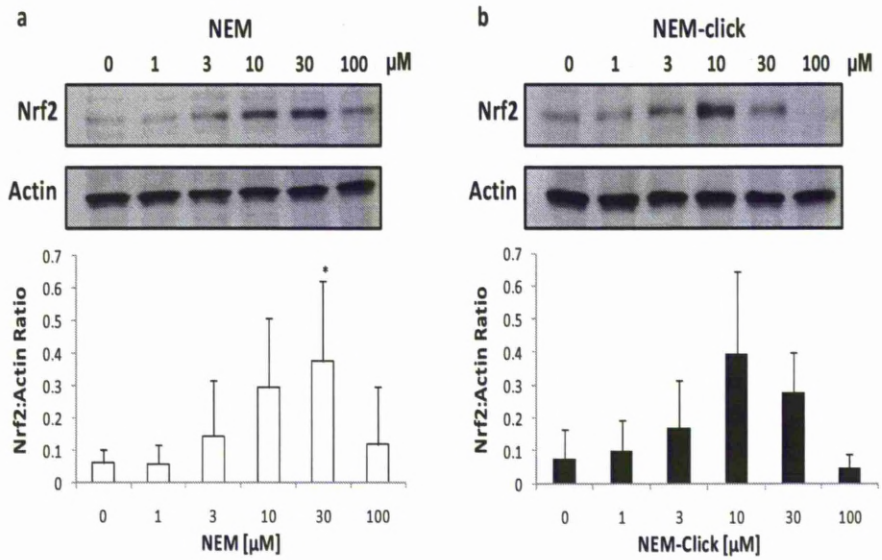

Figure 5.5: NEM and NEM-click activation of Nrf2. Hepa-1c1c7 cells were treated for 1hr with NEM (a) or NEM-click (b) and RIPA whole cell lysates were resolved using SDS-PAGE gel and probed for Nrf2. NEM (a) and NEM-click (b) activates Nrf2 accumulation. Actin is shown as loading control. The bottom panel shows the densitometric analysis of Nrf2 positive bands normalised against actin. Kruskal-Wallis, $*p<0.05$. The control cells were treated with 0.1% DMSO. A representative gel from n=3 is shown. Error bars = standard deviation of mean, n=3.

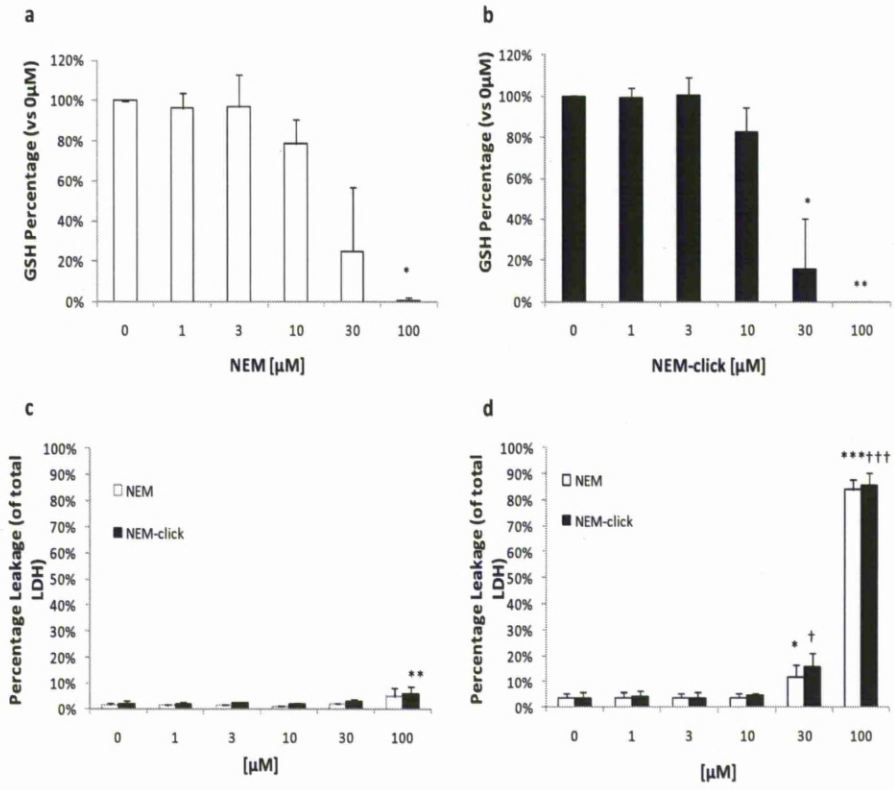

Fig 5.6: The effect of NEM and NEM-click on GSH and cell toxicity. Hepa-1c1c7 cells were treated for 1hr with NEM (a) or NEM-click (b) and lysed with 10mM HCL. GSH depletion reaches to 100% of control with high dose of NEM (a) and NEM-click (b). Total GSH normalised against total protein content. Cells were treated with NEM or NEM-click for 1hr (c) and 24hr (d). Kruskal-Wallis, *p<0.05, **p<0.01. LDH assay shows minimal leakage upon treatment with NEM or NEM-click for 1hr (c). The LDH assay shows substantial leakage upon treatment with NEM or NEM-click (d) after 24hr. Extracellular LDH activity is expressed as a percentage of total (extracellular plus intracellular) LDH activity. One-way ANOVA, *p<0.05, **p<0.01, ***p<0.001, †p<0.05, †††p<0.001. In all experiments, the control cells were treated with 0.1% DMSO. Error bars = standard deviation of mean, n=3.

5.3.3 Identification of a NEM-click-glutathione conjugate on LC-MS/MS

NEM-click was then assessed for its ability to bind to GSH and to form a GSH conjugate, using 100μM of NEM-click which was mixed with an eqimolar concentration of GSH in PBS. This mixture was allowed to react for 30min at room temperature. Samples were identified by LC-MS/MS analysis. A NEM-click-GSH conjugate was detected with a protonated molecular ion of *m/z* 485.52 (Fig 5.7a). Its identity was confirmed by a product ion scan (MS/MS) which produced fragment ions that corresponded to *m/z* 339.4, *m/z* 356.3 and *m/z* 410.28 (Fig 5.7b).

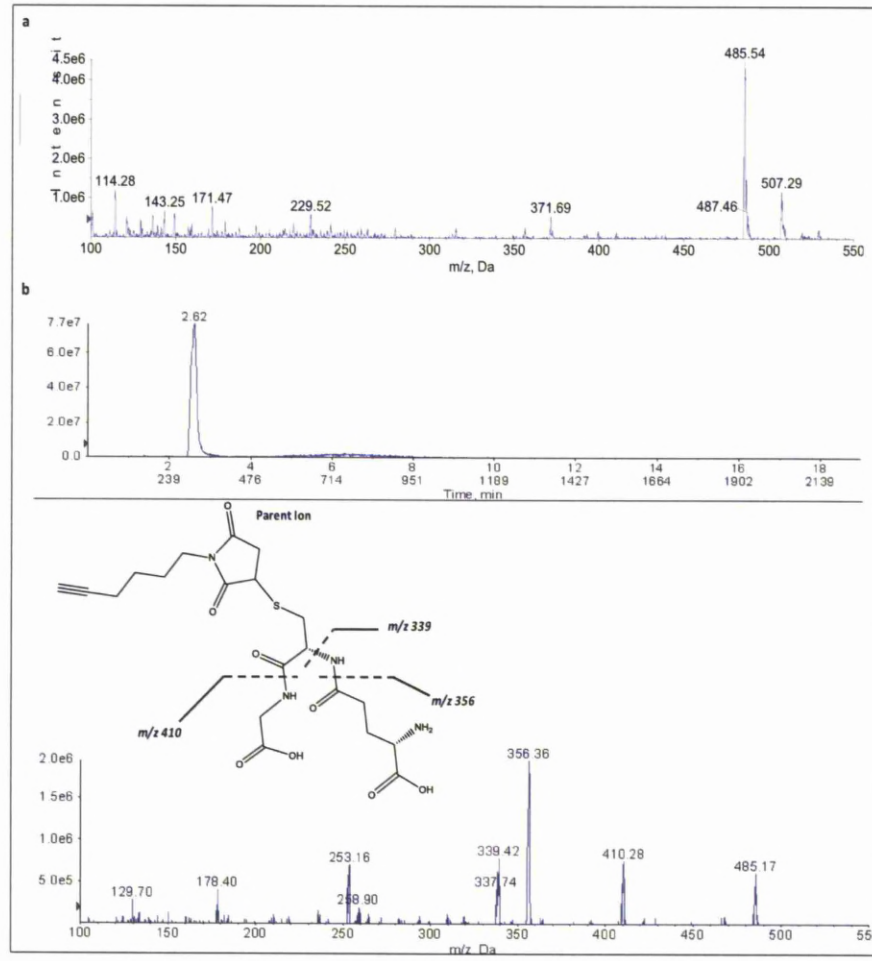

Figure 5.7: LC-MS/MS spectra of a NEM-click-GSH conjugate. An equimolar concentration of NEM-click (100µM) was reacted with GSH in PBS at room temperature for 30min. Samples were diluted for LC-MS/MS. A NEM-click-GSH conjugate was detected with a protonated molecular ion of 485.52Da (a). A product ion scan (MS/MS) which produced fragment ions that tentatively corresponded to the NEM-click-GSH conjugate is shown $[M-X]^+$ (b).

5.3.4 Comparison of Nrf2 activation and GSH depletion between the IA-click and NEM-click compounds

The effect of IA-click and NEM-click treatment on Nrf2 activity and GSH depletion can be seen clearly in double-y graphs (Fig 5.8). NEM-click had a more pronounced effect on both GSH and Nrf2 levels, resulting in greater GSH depletion and increased Nrf2 activation in comparison with IA-click. Consequently, it appears that NEM-click is a more potent Nrf2 inducer and cysteine alkylator.

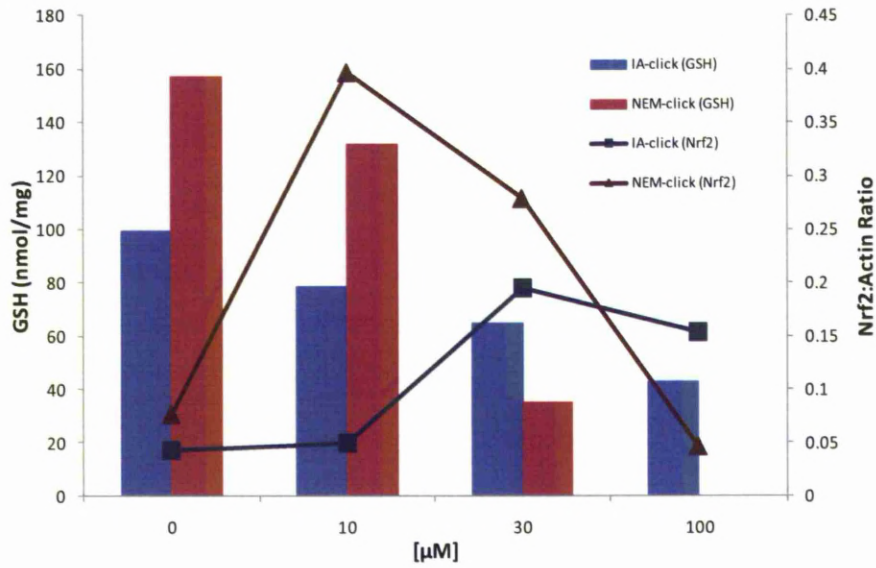

Figure 5.8: Effect on Nrf2 and GSH by treatment of cells with IA-click and NEM-click. NEM-click increased Nrf2 nuclear accumulation with GSH depletion more potently than IA-click. Error bars have been omitted from the graphs for clarity.

5.4 DISCUSSION

The hypothesis that Keap1 cysteine covalent modifications are key to the mechanism of Nrf2 activation is well described with compelling evidence to support it. Three cysteines, Cys151, Cys273 and Cys288 have been suggested to be critical in Keap1 ability to repress Nrf2 basally. The association of Cul3 ligase to Keap1 is disrupted when Cys151 is covalently modified by electrophiles, that could lead to the abrogation of Nrf2 ubquitination and proteasomal degradation (Zhang *et al.* 2003; Zhang *et al.* 2004; Gao *et al.* 2007; Rachakonda *et al.* 2008). The mutation of Cys273 and Cys288 render Keap1 unable to repress Nrf2 via the abrogation of Nrf2 ubiquitination and subsequent degradation (Zhang *et al.* 2003; Levonen *et al.* 2004; Wakabayashi *et al.* 2004; Kobayashi *et al.* 2006a) and also Nrf2 activation by Nrf2 inducers is attenuated or aboragated (Zhang *et al.* 2003; Levonen *et al.* 2004). However, it is not clear that the cysteines that are most important in covalent modifications in Nrf2 activation have been uncovered, despite the fact that many chemical compounds target cysteines on different domains of Keap1 [for a review, see (Holland *et al.* 2010)]. Since the Keap1/Nrf2 pathway can be activated concurrently with the covalent modification of Keap1 cysteines, the use of activity-based protein profiling to profile cysteines may be a useful tool to aid in improved understanding of the Keap1/Nrf2 pathway. Recently, ABPP has been applied to investigate the relation between covalent modifications of cysteine and the functionality of the proteins, such as the Transient Receptor Potential (TRP) A1 ion channel and the chloride intracellular channel (CLIC) family (Macpherson *et al.* 2007; Weerapana *et al.* 2008). Rhodamine labelling with click compounds by CC was used to show that TRPA1 ion channel can be activated by cysteine modification and also the cysteine modifications by click compound was investigated by mass

spectrometry analysis (Macpherson *et al.* 2007). The CLIC family members conserved cysteine residue has been shown to be bound by click compounds via fluorescent imaging (Weerapana *et al.* 2008). Hence, the application of electrophilic compounds coupled with an alkyne group (Fig 5.1) has been used to target those proteins. For that reason, the use of two novel cysteine alkylating compounds, IA-click (Fig 5.2c) and NEM-click (Fig 5.2d) in the Keap1/Nrf2 pathway were investigated in this chapter.

IA and NEM are common alkylating agents that were used to investigate Keap1 cysteine modification by proteomic analysis. Both IA and NEM were incorporated with an alkyne group to form the click compounds. The click compounds were used in comparison with their parent compounds, IA and NEM, to look at their Nrf2 induction efficacy. IA-click and NEM-click both activated Nrf2 and depleted GSH similar to their parent compounds. In addition, the Nrf2 responses to both click molecules and their parent compounds occur at concentrations where toxicity is not or has not yet become apparent, hence these factors appear to be able to sense and respond before toxicity emerges. Nevertheless, IA-click activates Nrf2 but it did not induce Nrf2 as effectively as IA (Fig 5.3). As shown in the results, IA-click did not induce Nrf2 or deplete GSH, and consequently toxicity emerges within 1hr after treatment with the highest dose of 1000μM. The addition of the alkyne group to IA was shown to reduce the effectiveness in cysteine modification seen from the decreased Nrf2 activation and GSH depletion. Macpherson *et al* noted the opposite effect on IA-click's cysteine-modifying properties; they reported that IA-click had a lower EC_{50} compared to IA (Macpherson *et al.* 2007). However, this difference can be explained through the investigation and the use of different

methods for determination of cysteine modification. In contrast, NEM-click was as efficient as NEM in activating Nrf2 (Fig. 5.5). In fact, the profiles of Nrf2 activation and GSH depletion by both compounds were very similar. NEM-click also reacted with GSH *in vitro*, to form a NEM-click-GSH adduct shown by LC-MS/MS (Fig 5.7). Unlike IA-click, the addition of the alkyne group to NEM did not reduce Nrf2 activation properties. Comparing both click compounds, NEM-click was shown to be a more efficient Nrf2 activator and depletes GSH, forming GSH adduct (Fig 5.8). Furthermore, NEM and NEM-click were less toxic compared to IA and IA-click at 10 and 30μM over 24hr. Therefore, NEM-click is clearly a more suitable alkylating agent than IA-click to use in Keap1/Nrf2 pathway experiments.

A novel proteomic analysis method using click compounds to investigate the role of cysteine modification on protein functions have been shown here. The used of CC to label cysteine residues of TRAP1 and CLIC protein with reactive compounds incorporated with an alkyne group have been shown (Macpherson *et al.* 2007; Vila *et al.* 2008; Weerapana *et al.* 2008). The role of cysteines in these proteins was measured by rhodamine fluorescence gel visualisation or identification of cysteine peptide adduction by mass spectrometry after protein purification from cells (Macpherson *et al.* 2007; Weerapana *et al.* 2008). The cysteine reactive compounds used against TRPA1; isothiocyanate, NEM and IA, not only binds to TRPA1 but can also bind to Keap1 (Wakabayashi *et al.* 2004; Eggler *et al.* 2005; Hong *et al.* 2005a; Macpherson *et al.* 2007; Salazar *et al.* 2008). Recently, 4-hydroxylnonenal (HNE), a known lipid oxidation product which can also modify Keap1, was reported to be incorporated with an alkyne group. The HNE-alkyne was used to modify cellular proteins and HNE-alkyne

modified proteins were reacted with an azide-biotin tag using CC. All HNE-alkyne modified biotin tagged proteins were isolated and purified using streptavidin beads and identified by mass spectrometry (Vila *et al.* 2008). Currently, all Keap1 cysteine modification experiments have been conducted through the purification of epitope-tagged Keap1, expressed either in bacteria or in over-expressed cell lines, utilising mass spectrometry for the identification of the isolated epitope-tag Keap1 (Dinkova-Kostova *et al.* 2002; Levonen *et al.* 2004; Copple *et al.* 2008a; Rachakonda *et al.* 2008). Based on the studies of Vila *et al*, overexpressed Keap1, without any epitope tag, or endogenous Keap1, can be modified by NEM-click for isolation and purification. This can serve as a novel method in the immunoprecipitation of Keap1 overexpressed as wild type or at endogenous levels in cells. Furthermore, this method can be used to isolate and purify endogenous Keap1 for mass spectrometry if the abundance of Keap1 is enough. NEM-click can also be used as an alternative alkylating agent to NEM for cysteine modification for mass spectrometry. This will help in differentiating from standard NEM modification during in cell treatment and should help to quantify the amount of Keap1 cysteines that are available to be modified by either NEM or NEM-click. NEM-click can provide a better understanding on how endogenous Keap1 senses chemical stress and how the role of cysteines residues plays in Nrf2 activation. Therefore, the novel compound NEM-click, which has similar properties as NEM shown here can be used as a novel method in the investigation of Keap1 cysteine modification and Nrf2 activation.

Chapter 6

Final Discussion

CONTENTS

6.1 INTRODUCTION

One of main contributors to patient morbidity and mortality during drug therapy are adverse drug reactions (ADRs). The liver is a major target organ for the occurrence of ADRs due to its physiological role in drug metabolism and clearance. Drug induced liver injury (DILI) is one of the most common causes of drug withdrawal and acetaminophen-induced liver injury accounts for nearly 50% of acute liver failure cases seen in the United States (Lee 2003). The critical protein hypothesis suggests that the binding of chemically reactive metabolites (CRMs) to cellular proteins caused impairment to their functionality and will elicit cellular toxicity. Hence, during the initiation of an ADR, the formation of CRMs from parent compounds may play a major part. Although the liver functions as a detoxification organ, it can also generate CRMs through the activity of the CYP450 enzymes. These enzymes can bioactivate parent drug compounds to CRMs which are rapidly quenched by glutathione (GSH). However, the binding and alteration of hepatic proteins by CRMs after the depletion of GSH may also induce a hepatocellular defence response. The various proteins involved in the hepatocellular defence response that were described in chapter 1 can trigger different tiers of defence, drug metabolism and an adaptive response, to achieve cellular defence responses to counter the toxic insults (Fig 1.3). The redox sensitive transcription factors namely, Nrf2 and NF-κB, play an important role in the cellular defence system. This is attributed to their ability to induce the transcription of cytoprotective proteins such as phase II enzymes, antioxidant and GSH synthesising proteins. Hence, the understanding of the molecular mechanisms behind the regulation and activation of these transcription factors will provide valuable insight on the events that occur during progression and consequence of drug induced liver injury (DILI).

Therefore, the main aims of this thesis were to further the understanding of how these transcription factors can regulate cellular defence responses to cellular stress, especially by the involvement of the Keap1/Nrf2 pathway.

6.2 THE SIMULTANEOUS REGULATION OF THE KEAP1/NRF2 AND NF-KB PATHWAYS UNDER CELLULAR STRESS

Paracetamol (APAP), a commonly used analgesic and antipyretic drug, is associated with DILI following overdose. In fact, DILI caused by an overdose of APAP is the main cause of acute liver failure in both the UK (Davern *et al.* 2006) and USA (Larson *et al.* 2005). The APAP induced toxicity is associated with the formation of its reactive metabolite, NAPQI, which is able to bind to cellular proteins and also elicits cellular adaptive response (Zhou et al, 2005 and Copple et al, 2008). Hence, NAPQI along with two other molecules, DNCB and BSO have been used to investigate the cellular adaptive response to cellular stress. The results presented in chapter 2 suggested that NAPQI, DNCB and BSO can induced a differential cellular response, by triggering different cellular stresses, chemical or oxidative, that can bring about a different response from both transcription factors (Nrf2 and NF-κB). Chemical stress from NAPQI and DNCB activates Nrf2 but inhibits NF-κB, while oxidative stress from GSH depletion mediated by BSO activates both Nrf2 and NF-κB simultaneously in the cell based model. These findings are in line with what the laboratory here has previously published regarding the induction of Nrf2 by NAPQI (Goldring *et al.* 2004; Copple *et al.* 2008a) and BSO (Copple *et al.* 2008a), and also the inhibition of NF-κB by NAPQI (Blazka *et al.* 1995) or induction of NF-κB by BSO (D'Alessio *et al.* 2004; Filomeni *et al.* 2005) shown by others. However, it should be emphasised that the Nrf2 and NF-κB mediated cellular stress responses

observed previously were based on the investigation of individual proteins. The observations made in chapter 2 were based on the simultaneous response of both Nrf2 and NF-κB towards cellular stress, as such co-regulation has not been shown before in the published literature.

Based on the difference in response by Nrf2 and NF-κB to chemical and oxidative stress, RNAi modulation of the transcription factors was used to mimic activation and inhibition of Nrf2 and NF-κB by cellular stress. Using with RNAi modulation and DNCB as a model electrophile, the results suggested that there is crosstalk between the Nrf2 and NF-κB pathways. From the observations seen in chapter 2, the RNAi modulation of p65 attenuates Nrf2 protein expression and the induction of GSH by Keap1 RNAi modulation suggests a possible crosstalk mechanism between the Nrf2 and NF-κB pathways. However, the mechanism remains unknown and further investigations are required but this is consistent with evidence shown by others that crosstalk between Nrf2 and NF-κB may occur. Nrf2 has been shown to regulate GCLC indirectly via NF-κB in rat (Yang *et al.* 2005a; Yang *et al.* 2005b). The transcriptional role of Nrf2 can be repressed directly by the activity of NF-κB competing for the transcription co-activator CREB binding protein (CBP) (Liu *et al.* 2008). Recently, evidence suggests that NF-κB activity can be regulated by the Keap1/Nrf2 pathway and this is thought to occur via the direct regulation of IKKβ by Keap1 (Lee *et al.* 2009; Kim *et al.* 2010a). This evidence further suggests that the presence of co-regulation between Nrf2 and NF-κB exists. Furthermore, the Keap1/Nrf2 and NF-κB pathways have been shown to be involved in crosstalk with other transcription factors and proteins. Evidence has shown that both pathways are involved in crosstalk with the p53

pathway. The NF-κB pathway has been shown to negatively regulate p53 by either controlling the expression of the p53 inhibitory E3 ubiquitin ligase Mdm2 (Tergaonkar *et al.* 2002), or competing for the binding of CBP with p53 by phosphorylated p65 in stimulated cells (Huang *et al.* 2007). The Keap1/Nrf2 pathway has been shown to be positively regulated by the cyclin-dependent kinase (CDK) inhibitor p21, a p53 dependent protein, via the binding of p21 to Keap1 which results in the accumulation of Nrf2 during cellular stress (Chen *et al.* 2009). In addition, Keap1/Nrf2 and NF-κB pathways have been reported to interact with sequestosome 1/p62 protein. In recent reports, it has been observed that p62 regulates the Keap1/Nrf2 pathway by directly binding to Keap1 (Lau *et al.* 2010), this direct interaction has been postulated to target Keap1 for degradation via autophagy which can inhibit the ubiquitination and degradation of Nrf2 by Keap1 during Nrf2 activation (Copple *et al.* 2010b). Crosstalk interaction between p62 and NF-κB pathway has also been observed, whereby p62 has been suggested to serve as a scaffolding protein to facilitate the activation of NF-κB pathway. This is through the ubiquitination of tumor necrosis factor receptor-associated factor 6 (TRAF6) which leads to the phosphorylation of IKKβ and initiation of NF-κB activating pathway (Wooten *et al.* 2005; Nakamura *et al.* 2010). Therefore, these crosstalk interactions amongst transcription factors and proteins may suggest the complexity of cell defence and survival response during cellular stress, and are schematically represented in figure 6.1. This demonstrates the complexity of how a cell initiates its defence response against the progression and onset of cellular damaged. Nevertheless, in order to improve the understanding of the role of Nrf2 and NF-κB in cellular stress, further work is required to fully elucidate these crosstalk mechanisms.

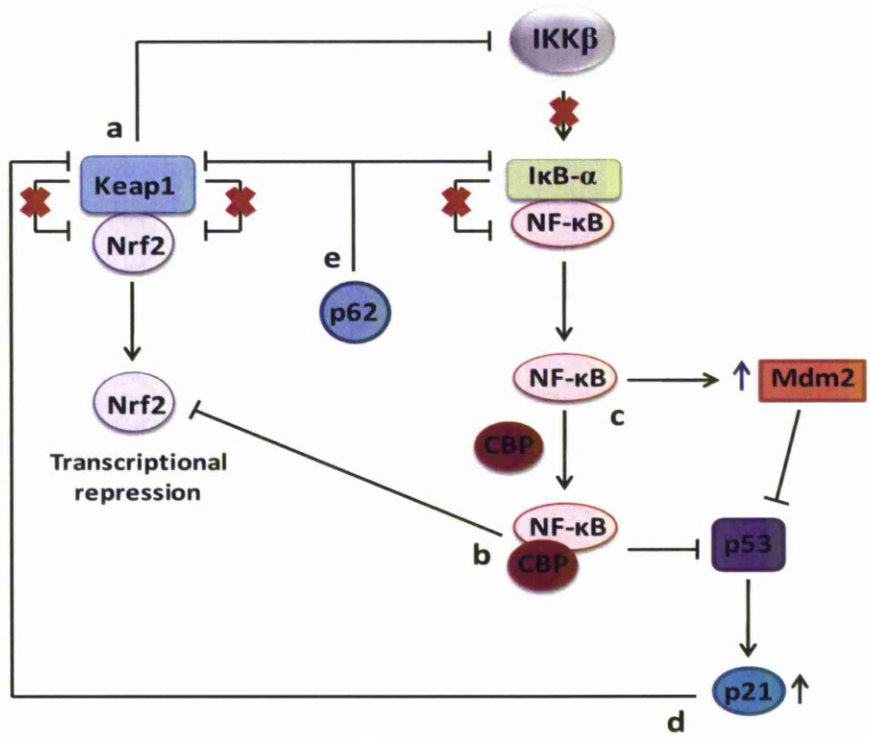

Fig 6.1: Schematic overview of crosstalk interactions between Keap1/Nrf2 and NF-κB pathways, and their interactions with p53 and other proteins. (a) Keap1 negatively regulate NF-κB pathway via promoting IKKβ ubiquitination and proteosomal or autophagic degradations (Lee *et al.* 2009; Kim *et al.* 2010a). (b) NF-κB represses Nrf2 transcriptional role by competing for CBP (Liu *et al.* 2008). (c) NF-κB can negatively regulate p53 by competing for CBP (Huang *et al.* 2007) or increasing p53 inhibitory protein Mdm2 (Tergaonkar *et al.* 2002). (d) p53 can positively regulate Keap1/Nrf2 pathway by the direct binding of p21, p53 dependent protein, to Keap1 (Chen *et al.* 2009). (e) p62 interacts with Keap1/Nrf2 and NF-κB pathways by regulating Keap1 degradation via autophagy (Copple *et al.* 2010b) and facilitating the activation of NF-κB pathway (Wooten *et al.* 2005; Nakamura *et al.* 2010), respectively.

6.3 THE ROLE OF KEAP1 CYSTEINE MODIFICATION IN THE MECHANISM OF NRF2 ACTIVATION

The mechanism behind the role of Keap1 in sensing cellular stress and allowing Nrf2 nuclear accumulation remains unclear. However, mutagenesis studies from cultured cells overexpressing

mutant Keap1 and transgenic mouse models have identified three critical cysteines (Cys151, Cys273 and Cys288) that play an important role in the ability of Keap1 to repress Nrf2. These three critical cysteines, which serve as key sensors, are originally suggested from previous reports highlighting four highly sensitive cysteines (Cys257, Cys273, Cys288 and Cys297) found within the IVR domain (Dinkova-Kostova *et al.* 2002). Therefore, the consequence of the modification of these critical cysteines has been postulated to result in the conformational change of Keap1, which will in turn result in the abrogation of Nrf2 ubiquitination and degradation. This is supported by the observations from circular dichroism spectroscopy experiments which show that the covalent modification of Cys151 leads to a structural change in Keap1, which results in the dissociation of Cul3 ligase from Keap1 (Gao *et al.* 2007; Rachakonda *et al.* 2008). However, it has yet to be demonstrated conclusively that the modification of Keap1 can antagonises the interaction between Keap1 and Nrf2 via the DLG and ETGE motifs.

Despite the focus on the three critical cysteines of Keap1 (Cys151, Cys273 and Cys288), a large range of Nrf2 inducing molecules still target Keap1 cysteines randomly (Fig 4.1). In addition, recent work by Hayes and colleagues proposed that endogenous molecules, nitric oxide (NO), zinc and alkenals target Keap1 cysteines too and these molecules modify Keap1 cysteines during cellular stress leading to Nrf2 activation (McMahon *et al.* 2010). This is attributed to the fact that Keap1 is a cysteine-rich protein and that the other Keap1 cysteine residues can also play a role in the Keap1 mediation of Nrf2 activation and control of cellular defence. Therefore, the molecular mechanisms of how Keap1 senses cellular stress which can lead to the activation of Nrf2 is further investigated in this thesis.

6.3.1 Role of cysteine modification and GSH depletion in Nrf2 activation

The mechanism of Nrf2 activation by cysteine modification and GSH depletion was addressed in chapter 3. The chemical modification of Keap1 cysteines with or without GSH depletion has been shown to induce Nrf2 nuclear accumulation (chapter 3). Alkylating agents such as dinitrochlorobenzene (DNCB) and iodoacetamide (IA) can activate Nrf2 by covalently modifying Keap1 cysteine residues and depleting GSH. On the other hand, alkylating agents such as 15d-PGJ_2 and dexamethasone 21—mesylate (Dex-mes) that only covalently modify Keap1 cysteine residues but does not deplete GSH can also activate Nrf2. This is in agreement with the hypothesis thst chemical modification of key Keap1 cysteines can initiate Nrf2 activation (Dinkova-Kostova *et al.* 2002). However, GSH depletion without concomitant chemical modification by buthionine sulfoximine (BSO), a known GSH depleting agent, can also instigate the nuclear accumulation of Nrf2. The GSH depletion mechanism of BSO, which can cause redox perturbation in the cell (Hansen *et al.* 2004; Ito *et al.* 2006), results in an increase in the susceptibility of Keap1 cysteines to oxidation. This may then lead to Nrf2 activation. The oxidation of Keap1 was first observed following the formation of intermolecular disulphide bonds between Keap1 subunits after treatment with an Nrf2 inducing agent (Wakabayashi *et al.* 2004). Moreover, others have also observed that Nrf2 activation can be initiated by the formation of disulphide bonds between Keap1 cysteines and by other forms of cysteine oxidations (Fig 1.5), which will now be highlighted. Hydrogen peroxide, hypochlorous acid and NO have all been shown to oxidise Keap1 by the formation of disulphide bonds (Fourquet *et al.* 2010). A similar response is seen by increasing the amount of GSSG to GSH ratio (Holland *et al.* 2008). The cysteines on Keap1 have also

been found to be s-oxidised by a proton pump inhibitor, Lansoprazole (Takagi *et al.* 2009). S-glutathionylation was also observed on Keap1 cysteine residues in the presence of high GSSG concentrations (Holland *et al.* 2008) and also after treatment with a thiophene compound (Zhang *et al.* 2010). NO and NO donating compounds such as spermine NONOate and s-nitrosocysteine have been suggested to induce nitrosylation on Keap1 cysteines (Buckley *et al.* 2008; Li *et al.* 2009). Therefore, these observations strongly support the postulation that Nrf2 activation can occur through Keap1 cysteine oxidation. Furthermore, S-glutathionylation was also observed on Keap1-V5 proteins after treatment with BSO, IA or NEM in chapter 4. To further support this postulation, an investigation into the potential of BSO treatment to induce cysteine oxidation was carried out by MS analysis in chapter 4. Following prior treatment with BSO, the ability of DNCB to alkylate cysteine 257 on Keap1 was reduced compared to treatment without BSO. This suggests that the oxidation of cysteine 257 can inhibit DNCB modification. Therefore, the evidence presented in chapters 3 and 4 supports the mechanism of Nrf2 activation by Keap1 cysteine modification, either by covalent modification directly with chemicals or via oxidation through the indirect mechanism of GSH depletion.

6.3.2 An investigation into the basal thiol status of Keap1

Despite the weight of evidence that supports the role played by the sensing of chemical and oxidative stress by Keap1 which can lead to the activation of Nrf2, little is known about the basal status of the cysteines in Keap1 within living cells. To date, only the DGR domain of mouse and human Keap1 has been structurally classified by crystallisation (Li *et al.* 2004; Padmanabhan *et al.* 2006). In addition, the eight cysteine residues in the DGR domain have been observed to be

basally reduced (Li *et al.* 2004). Therefore, by establishing the basal thiol status of Keap1, a greater understanding of the molecular basis of how Keap1 cysteines serve as sensor to chemical and oxidative stress can be gained. In chapter 4, using a cell-based method, all of the cysteine residues in Keap1 were found to be potentially available to be alkylated or oxidised and a proportion of them are all in a reduced form under basal conditions. This observation supports the hypothesis that Keap1 cysteine modification is a key mechanism for Nrf2 activation in cell defence. The modification of a single cysteine can lead to conformational changes in the Keap1 structure. This therefore disrupts the binding between Keap1 and Nrf2 and/or Cul3 ligase, resulting ultimately in the abrogation of Nrf2 ubquitination. Hence, the presence of reduced and available cysteine residues may allow Keap1 to serve as the universal 'sensor' for chemical and oxidative stress.

Recently, the structure of Keap1 was reconstructed by electron microscopy (Ogura *et al.* 2010). The authors suggested that Keap1 is a forked-stem structure connecting to two linkers made up of the BTB domain, which is further connected to the IVR and DGR domains which are enclosed in a large globular structure. Based on the reconstructed Keap1 structure, the following suggestions are made on the role of Keap1 as a sensor for Nrf2 activation; 1) the modification of the IVR cysteines can affect the structural integrity of the DGR domain leading to the disruption of Nrf2 DLG binding to the DGR domain (hinge and latch model); 2) the modification of the BTB cysteines, especially cysteine 151, can disrupt the association of the Cul3 ligase and Keap1 (Ogura *et al.* 2010). However, there is no concrete evidence that confirms that covalent modification of IVR domain can disrupt Nrf2 through the 'hinge and latch model', but there is some evidence that suggest the covalent

modification of cysteine 151 on BTB domain can lead to the disassociation of Cul3 ligase from Keap1 (Gao *et al.* 2007; Rachakonda *et al.* 2008). Moreover, increasing the molar volume of cysteine 151 by substituting it for a larger residue can also affect the interaction between Cul3 ligase and Keap1 (Eggler *et al.* 2009). Nevertheless, it is the first time that Keap1 cysteine residues have been suggested to be available and reduced basally. This clearly suggests that all cysteines are partially important in sensing cellular stress and implies the importance of the role of Keap1 in activating cellular protection.

6.4 FUTURE DIRECTIONS

Since the discovery of NF-κB (Sen *et al.* 1986) and Nrf2 (Moi *et al.* 1994), huge advances have been made with regards to the understanding of the chemical, biochemical and molecular events that regulate the NF-κB and Keap1/Nrf2 pathways. This thesis has sought to address the importance of the co-regulation or crosstalk between the NF-κB and Keap1/Nrf2 pathways. The availability of both pathways to be activated or inhibited by cysteine modification, via chemical stress, can lead to a perturbation balance between cell protection and cell death. Therefore, the identification of cysteine modifications on NF-κB should be considered for future investigations. This is to determine whether or not the potential of a chemical to modify cysteine residues within Keap1 which results in Nrf2 activation can also inhibit NF-κB. As well as key cysteines within IKK, the p65 and p50 subunits have been shown to be covalently modified; the position of covalent cysteine modifications should be identified to verify which part of the NF-κB pathway is being inhibited, and this should be done in cells which overexpressed the Nrf2 and NF-κB pathways to look for dose-response relationships, before

attempting to examine them at endogenous level with the technology allowing this to be done.

Cells are also constantly exposed to redox perturbation under physiological conditions and this perturbation can cause GSH depletion, which results in the activation of both Nrf2 and NF-κB. Hence, the use of GSH modulators should also be considered for future research to determine exactly how GSH depletion can induce the activation of both Nrf2 and NF-κB. The use of BSO and phorone to deplete GSH and a measurement of oxidative stress using chemical probes such as 2'-7'-dichlorofluorescene diacetate (DCF-DA) may be performed. This would provide an indication as to the level of oxidative stress from GSH depletion that is require for the induction of Nrf2 and NF-κB. This in turn will further support the notion that oxidative stress without concomitant modification can also activate the cellular defence response. Antioxidants such as N-acetylcysteine (NAC) and GSH ester can be used to replenish the depleted GSH. The use of these agents will determine if the presence of NAC or the GSH ester can attenuate the activation of Nrf2 and the inhibition of NF-κB in cells undergoing chemical stress. Furthermore, the attenuation of the activation of Nrf2 and NF-κB in cells undergoing oxidative stress can also be investigated in this system.

Thus, these future investigations will provide a better understanding about how chemical or oxidative stresses can lead to the activation of cellular protection via Nrf2 or NF-κB activation or cell death via NF-κB inhibition. In addition, both the Keap1/Nrf2 and NF-κB pathways have been suggested to be in crosstalk with other transcription factor, p53 (Tergaonkar *et al.* 2002; Huang *et al.* 2007; Chen *et al.* 2009) or p62 protein (Wooten *et al.* 2005; Copple *et al.* 2010b; Lau *et al.* 2010; Nakamura *et al.* 2010). Hence, the effect of direct

chemical cysteine modification or modification via oxidation as a consequence of GSH depletion on Nrf2 and NF-κB with regards to their interaction with p53 or p62 needs to be further examined. This will provide a higher level of understanding of how the cells respond to different forms of cellular stresses by the adaptive response from the co-regulation of different transcription pathways; 1) cellular protection via Keap1/Nrf2; and 2) cell survival via NF-κB.

Despite having strong evidence to suggest that the direct cysteine modification of Keap1 (Dinkova-Kostova *et al.* 2002; Hong *et al.* 2005a; Copple *et al.* 2008a; Kobayashi *et al.* 2009) by Nrf2-inducing molecules results in the activation of Nrf2, it has yet to be defined how GSH depletion, without direct cysteine modification, by BSO and diamide, can trigger Nrf2 activation. However, both BSO and diamide can alter the GSH:GSSG ratio or the GSH:GSSG redox potential in cells (Hansen *et al.* 2004; Hansen *et al.* 2009). In fact, the alteration of the GSH:GSSG ratio or the redox potential by BSO have been suggested to induce Nrf2 nuclear translocation (Hansen *et al.* 2004). A recent report by Holland and colleagues, has shown that by altering the GSH:GSSG ratio *in vitro*, this can induce cysteine oxidation in bacterially-expressed recombinant Keap1 (Holland *et al.* 2008). Therefore, the use of BSO and particularly diamide, which can increase the intracellular GSSG concentration (Hansen *et al.* 2009), to alter the GSH:GSSG ratio in living cells is a worthwhile experiment. This will allow the investigation of cysteine oxidation on Keap1 in a more physiologically relevant environment. The constraint that further hampers the investigation of protein oxidation is that oxidation of Keap1 cysteine might occur only on a small proportion of the total sum of Keap1 proteins, which is beyond the limit of detection of the current mass spectrometry method (MS)

used within this investigation. This is despite the use of a cell model which overexpresses Keap1 at relatively high levels. Therefore, future investigations should be considered to improve the methods used to determine the oxidation status of Keap1 cysteines. A more sensitive MS analysis system such as the QTRAP™, which is a combination of a triple quadrupole scan mode and ion-trap mass spectrometer, can be used. The QTRAP triple quadrupole scan modes such as precursor ion and constant neutral loss scans which are not available on other types of mass spectrometer makes QTRAP more efficient in detecting peptides with posttranslational modifications and the QTRAP ion-trap mass spectrometer which can trap more fragment ions yielding higher sensitivity, may contribute to a lower limit of detection during MS scanning (Hager 2004).

The investigations carried out in chapter 4 revealed that the MS-based method used was not sensitive enough to detect potential oxidation modifications by BSO. However, with regards to DNCB treatment, the availability of cysteine 257 to be modified by DNCB is hindered by the pre-treatment with BSO. Hence, this suggests that the treatment with BSO coupled with DNCB further increased the redox perturbation of the cell which may have caused the oxidation of cysteine 257. In this regard, the investigation of cysteine oxidation by an indirect measurement of cysteine modification by NEM should be considered for future research. These proposals are based on the observations from previous work from within this laboratory which has shown that cysteine 257 is selectively modified by other dinitrophenyl (DNP) compounds such as DNCB (Copple *et al.* 2008a), dinitrobromobenzene, dinitroiodobenzene and dinitrofluorobenzene (Megherbi Thesis 2010). This suggests that Cys257 may be important for the sensing of chemical

insults from DNP compounds via direct DNP modification or oxidation from DNP-induced cellular stress. Therefore, for future research, the use of the differential chemical approach developed in section 4.3.4 of chapter 4 to identify indirectly which cysteines are oxidised should be employed (Fig 6.2). Hence, this method may also facilitate the investigation into Keap1 cysteines, especially Cys151, Cys273 and Cys288, and the role of oxidation during Nrf2 activation.

With regards to the investigation of cysteine modification within Keap1, experiments conducted currently rely on using cell-based models that can express proteins from transfected genes at high levels that are incorporated with an epitope tag. This methodology is useful for gaining a chemical insight into the modification of intracellular Keap1. However, the overexpression of the protein and the incorporation of the epitope tag do not reflect the expression of endogenous proteins in cells in cultured or *in vivo*. Therefore, the enrichment of endogenous Keap1 or the overexpression of Keap1 without an epitope tag is required in order to facilitate the true analysis of cysteines modification in cells. The enrichment of endogenous Keap1 can be assisted with the use of the NEM-click methodologies described in chapter 5. NEM-click can be used to target Keap1 via cysteine modification and NEM-click modified Keap1 can be immunoprecipitated by click chemistry. This can allow the enrichment of endogenous Keap1 to be sufficient for MS analysis. Furthermore, Keap1 without an epitope tag can be expressed in cells and immunoprecipitated using NEM-click. Therefore, Keap1 expression can be maintained in cells similarly to the endogenous protein. This would facilitate a more accurate analysis of the role of Keap1 in cellular stress and protection. Therefore, for future investigation the use of click chemistry described in chapter 5 should be considered.

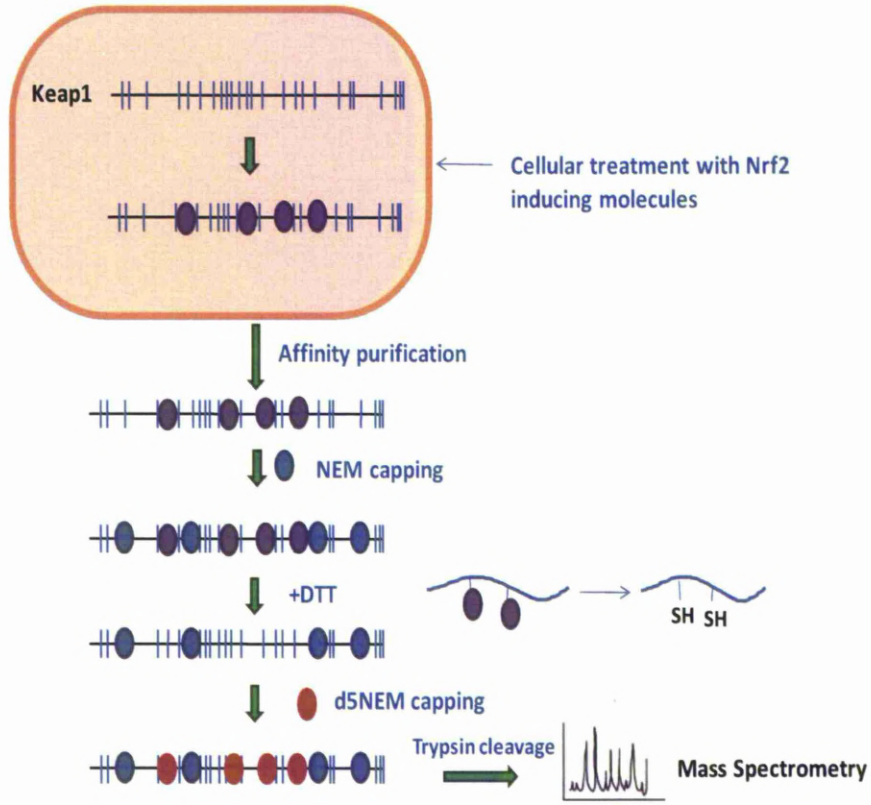

Figure 6.2: Schematic overview covering the use of a differential chemical approach to identify cysteine oxidation. Following the treatment of Keap1 which is overexpressed in HEK293T cells with Nrf2 inducing molecules, modified Keap1 is immunoprecipitated by agarose V5 beads and treated with NEM. DTT is used to reduce Keap1 oxidised cysteines to free cysteines and d5NEM is added to modify all the free cysteines. Keap1 is then tryptically disgested overnight prior to MS analysis. The purple circles represent oxidised cysteines induced by Nrf2 inducing molecules. Blue circles represent cysteines modified by NEM which are not oxidised. Red circles represent cysteines modified by d5NEM after DTT reduction.

6.5 CONCLUDING DISCUSSION

The studies presented in this thesis were designed to further address our understanding of how redox transcription factors are regulated and to elucidate their role in cellular protection against chemical-induced damage. In particular, the aims of the investigations have been carried out to elucidate the simultaneous regulation of the Keap1/Nrf2 and NF-κB pathways in response to chemical or oxidative stresses, and to explore how these two forms of stresses can trigger the mechanism of Nrf2 activation. The results presented from these investigations have demonstrated that Keap1/Nrf2 and NF-κB respond differently to these stresses. Chemical stress can activate Keap1/Nrf2 but inhibit NF-κB, whereas GSH depletion can activate both pathways. In addition, chemical stress involving molecules that can alkylate cysteine residues can initiate the Nrf2 activation regardless of GSH depletion. Also, oxidative stress from molecules that deplete GSH without modifying cysteine residues can also initiate Nrf2 activation. Based on these findings, an investigation into the basal status of Keap1 thiols was undertaken with regards to investigating the role of Keap1 cysteine residues serving as a site for chemical or oxidative modification in the molecular mechanism during the activation of Nrf2 (Dinkova-Kostova *et al.* 2002; Wakabayashi *et al.* 2004; Copple *et al.* 2008a). The observation that a proportion of the Keap1 cysteine residues are all present in the thiol reduced state and available for modification under basal conditions further supports the hypothesis that Keap1 cysteines are perhaps the universal sensor for Nrf2 activation. Hence, the better understanding of co-regulation of transcription factors involved in cellular defence and the molecular mechanisms of activating Nrf2 can further improve on the understanding of how cells adapt to cellular environmental stress and perturbation, and also determine the baseline or threshold level of

chemical defence. Moreover, this new knowledge may improve pre-clinical screens for novel therapeutic drugs against diseases such as cancer, where resistance to treatments are on the rise.

The roles of the Nrf2 and NF-κB pathways in regulating cellular defence and survival may also play an important role not only in DILI but also in cancer. In this thesis, my work has shown that exogenous molecules can have a differential effect on the regulation of both Nrf2 and NF-κB pathways. The Keap1/Nrf2 (Lau *et al.* 2008) and NF-κB (Li *et al.* 2010) pathways have been shown to play an important roles in chemoresistance during cancer treatment. Increases in Nrf2 levels, the loss of Keap1 (Singh *et al.* 2008; Wang *et al.* 2008; Zhang *et al.* 2010) and increased levels of NF-κB (Zatelli *et al.* 2009; Cherfils-Vicini *et al.* 2010; Kong *et al.* 2010) all confer chemoresistance in cancer cells. Therefore, it will be important to determine if a chemotherapeutic agent used in the treatment of cancer does have a differential effect on both pathways. This understanding is important as chemotherapeutic drugs which target components of the NF-κB pathway may also activate Nrf2 which could ultimately confer the induction of resistance to treatment in cancer cells. Hence, future research focussed on the design of safe and effective therapeutic agents and anti-cancer therapeutics is dependent on a comprehensive understanding of the biochemical and molecular mechanisms that result in the simultaneous regulation of transcription factors during adaptive response in cellular defence.

BIBLIOGRAPHY

Abate, C., D. Luk and T. Curran (1991). "Transcriptional regulation by Fos and Jun in vitro: interaction among multiple activator and regulatory domains." Mol Cell Biol **11**(7): 3624-3632.

Adachi, T., H. Nakagawa, I. Chung, Y. Hagiya, K. Hoshijima, N. Noguchi, M. T. Kuo and T. Ishikawa (2007). "Nrf2-dependent and -independent induction of ABC transporters ABCC1, ABCC2, and ABCG2 in HepG2 cells under oxidative stress." J Exp Ther Oncol **6**(4): 335-348.

Adam, G. C., E. J. Sorensen and B. F. Cravatt (2002). "Chemical strategies for functional proteomics." Mol Cell Proteomics **1**(10): 781-790.

Ahmad, R., D. Raina, C. Meyer, S. Kharbanda and D. Kufe (2006). "Triterpenoid CDDO-Me blocks the NF-kappaB pathway by direct inhibition of IKKbeta on Cys-179." J Biol Chem **281**(47): 35764-35769.

Alam, J., E. Killeen, P. Gong, R. Naquin, B. Hu, D. Stewart, J. R. Ingelfinger and K. A. Nath (2003). "Heme activates the heme oxygenase-1 gene in renal epithelial cells by stabilizing Nrf2." Am J Physiol Renal Physiol **284**(4): F743-752.

Alam, J., D. Stewart, C. Touchard, S. Boinapally, A. M. Choi and J. L. Cook (1999). "Nrf2, a Cap'n'Collar transcription factor, regulates induction of the heme oxygenase-1 gene." J Biol Chem **274**(37): 26071-26078.

Aleksic, M., C. K. Pease, D. A. Basketter, M. Panico, H. R. Morris and A. Dell (2007). "Investigating protein haptenation mechanisms of skin sensitisers using human serum albumin as a model protein." Toxicol In Vitro **21**(4): 723-733.

Aleksunes, L. M., A. L. Slitt, J. M. Maher, L. M. Augustine, M. J. Goedken, J. Y. Chan, N. J. Cherrington, C. D. Klaassen and J. E. Manautou (2008). "Induction of Mrp3 and Mrp4 transporters during acetaminophen hepatotoxicity is dependent on Nrf2." Toxicol Appl Pharmacol **226**(1): 74-83.

Aleksunes, L. M., R. L. Yeager and C. D. Klaassen (2009). "Application of multivariate statistical procedures to identify transcription factors that correlate with MRP2, 3, and 4 mRNA in adult human livers." Xenobiotica **39**(7): 514-522.

Andrews, N. C., K. J. Kotkow, P. A. Ney, H. Erdjument-Bromage, P. Tempst and S. H. Orkin (1993). "The ubiquitous subunit of erythroid transcription factor NF-E2 is a small basic-leucine zipper protein related to the v-maf oncogene." Proc Natl Acad Sci U S A **90**(24): 11488-11492.

Antoine, D. J., D. P. Williams and B. K. Park (2008). "Understanding the role of reactive metabolites in drug-induced hepatotoxicity: state of the science." Expert Opin Drug Metab Toxicol **4**(11): 1415-1427.

Apopa, P. L., X. He and Q. Ma (2008). "Phosphorylation of Nrf2 in the transcription activation domain by casein kinase 2 (CK2) is critical for the nuclear translocation and transcription activation function of Nrf2 in IMR-32 neuroblastoma cells." J Biochem Mol Toxicol **22**(1): 63-76.

Arisawa, T., T. Tahara, T. Shibata, M. Nagasaka, M. Nakamura, Y. Kamiya, H. Fujita, D. Yoshioka, Y. Arima, M. Okubo, I. Hirata and H. Nakano (2007). "Association between promoter polymorphisms of nuclear factor-erythroid 2-related factor 2 gene and peptic ulcer diseases." Int J Mol Med **20**(6): 849-853.

Arisawa, T., T. Tahara, T. Shibata, M. Nagasaka, M. Nakamura, Y. Kamiya, H. Fujita, D. Yoshioka, Y. Arima, M. Okubo, I. Hirata and H. Nakano (2008). "The influence of promoter polymorphism of nuclear factor-erythroid 2-related factor 2 gene on the aberrant DNA methylation in gastric epithelium." Oncol Rep **19**(1): 211-216.

Baek, S. H., J. N. Min, E. M. Park, M. Y. Han, Y. S. Lee, Y. J. Lee and Y. M. Park (2000). "Role of small heat shock protein HSP25 in radioresistance and glutathione-redox cycle." J Cell Physiol **183**(1): 100-107.

Bains, N. and D. Hunter (1999). "Adverse reporting on adverse reactions." CMAJ **160**(3): 350-351.

Bartolone, J. B., R. B. Birge, K. Sparks, S. D. Cohen and E. A. Khairallah (1988). "Immunochemical analysis of acetaminophen covalent binding to proteins. Partial characterization of the major acetaminophen-binding liver proteins." Biochem Pharmacol **37**(24): 4763-4774.

Beckmann, R. P., M. Lovett and W. J. Welch (1992). "Examining the function and regulation of hsp 70 in cells subjected to metabolic stress." J Cell Biol **117**(6): 1137-1150.

Ben-Neriah, Y. (2002). "Regulatory functions of ubiquitination in the immune system." Nat Immunol **3**(1): 20-26.

Bessems, J. G. and N. P. Vermeulen (2001). "Paracetamol (acetaminophen)-induced toxicity: molecular and biochemical mechanisms, analogues and protective approaches." Crit Rev Toxicol **31**(1): 55-138.

Blank, V. and N. C. Andrews (1997). "The Maf transcription factors: regulators of differentiation." Trends Biochem Sci **22**(11): 437-441.

Blazka, M. E., D. R. Germolec, P. Simeonova, A. Bruccoleri, K. R. Pennypacker and M. I. Luster (1995). "Acetaminophen-induced hepatotoxicity is associated with early changes in NF-kB and NF-IL6 DNA binding activity." J Inflamm **47**(3): 138-150.

Bloom, D., S. Dhakshinamoorthy and A. K. Jaiswal (2002). "Site-directed mutagenesis of cysteine to serine in the DNA binding region of Nrf2 decreases its capacity to upregulate antioxidant response element-mediated expression and antioxidant induction of NAD(P)H:quinone oxidoreductase1 gene." Oncogene **21**(14): 2191-2200.

Bloom, D. A. and A. K. Jaiswal (2003). "Phosphorylation of Nrf2 at Ser40 by protein kinase C in response to antioxidants leads to the release of Nrf2 from INrf2, but is not required for Nrf2 stabilization/accumulation in the nucleus and transcriptional activation of antioxidant response element-mediated NAD(P)H:quinone oxidoreductase-1 gene expression." J Biol Chem **278**(45): 44675-44682.

Bonizzi, G. and M. Karin (2004). "The two NF-kappaB activation pathways and their role in innate and adaptive immunity." Trends Immunol **25**(6): 280-288.

Borst, P. and R. O. Elferink (2002). "Mammalian ABC transporters in health and disease." Annu Rev Biochem **71**: 537-592.

Boulares, H. A., C. Giardina, C. L. Navarro, E. A. Khairallah and S. D. Cohen (1999). "Modulation of serum growth factor signal transduction in Hepa 1-6 cells by acetaminophen: an inhibition of c-myc expression, NF-kappaB activation, and Raf-1 kinase activity." Toxicol Sci **48**(2): 264-274.

Bradford, M. M. (1976). "A rapid and sensitive method for the quantitation of microgram quantities of protein utilizing the principle of protein-dye binding." Anal Biochem **72**: 248-254.

Braeuer, S. J., C. Buneker, A. Mohr and R. M. Zwacka (2006). "Constitutively activated nuclear factor-kappaB, but not induced NF-kappaB, leads to TRAIL resistance by up-regulation of X-linked inhibitor of apoptosis protein in human cancer cells." Mol Cancer Res **4**(10): 715-728.

Brockman, J. A., D. C. Scherer, T. A. McKinsey, S. M. Hall, X. Qi, W. Y. Lee and D. W. Ballard (1995). "Coupling of a signal response domain in I kappa B alpha to multiple pathways for NF-kappa B activation." Mol Cell Biol **15**(5): 2809-2818.

Brown, K., S. Gerstberger, L. Carlson, G. Franzoso and U. Siebenlist (1995). "Control of I kappa B-alpha proteolysis by site-specific, signal-induced phosphorylation." Science **267**(5203): 1485-1488.

Buckley, B. J., S. Li and A. R. Whorton (2008). "Keap1 modification and nuclear accumulation in response to S-nitrosocysteine." Free Radic Biol Med **44**(4): 692-698.

Casadei, M., T. Persichini, F. Polticelli, G. Musci and M. Colasanti (2008). "S-glutathionylation of metallothioneins by nitrosative/oxidative stress." Exp Gerontol **43**(5): 415-422.

Cernuda-Morollon, E., E. Pineda-Molina, F. J. Canada and D. Perez-Sala (2001). "15-Deoxy-Delta 12,14-prostaglandin J2 inhibition of NF-kappaB-DNA binding through covalent modification of the p50 subunit." J Biol Chem **276**(38): 35530-35536.

Chan, J. Y., X. L. Han and Y. W. Kan (1993). "Cloning of Nrf1, an NF-E2-related transcription factor, by genetic selection in yeast." Proc Natl Acad Sci U S A **90**(23): 11371-11375.

Chan, J. Y. and M. Kwong (2000). "Impaired expression of glutathione synthetic enzyme genes in mice with targeted deletion of the Nrf2 basic-leucine zipper protein." Biochim Biophys Acta **1517**(1): 19-26.

Chan, J. Y., M. Kwong, R. Lu, J. Chang, B. Wang, T. S. Yen and Y. W. Kan (1998). "Targeted disruption of the ubiquitous CNC-bZIP transcription factor, Nrf-1, results in anemia and embryonic lethality in mice." EMBO J **17**(6): 1779-1787.

Chanas, S. A., Q. Jiang, M. McMahon, G. K. McWalter, L. I. McLellan, C. R. Elcombe, C. J. Henderson, C. R. Wolf, G. J. Moffat, K. Itoh, M. Yamamoto and J. D. Hayes (2002). "Loss of the Nrf2 transcription factor causes a marked reduction in constitutive and inducible expression of the glutathione S-transferase Gsta1, Gsta2, Gstm1, Gstm2, Gstm3 and Gstm4 genes in the livers of male and female mice." Biochem J **365**(Pt 2): 405-416.

Chen, C., L. C. Edelstein and C. Gelinas (2000). "The Rel/NF-kappaB family directly activates expression of the apoptosis inhibitor Bcl-x(L)." Mol Cell Biol **20**(8): 2687-2695.

Chen, F. E. and G. Ghosh (1999). "Regulation of DNA binding by Rel/NF-kappaB transcription factors: structural views." Oncogene **18**(49): 6845-6852.

Chen, K. M., T. E. Spratt, B. A. Stanley, D. A. De Cotiis, M. C. Bewley, J. M. Flanagan, D. Desai, A. Das, E. S. Fiala, S. Amin and K. El-Bayoumy (2007). "Inhibition of nuclear factor-kappaB DNA binding by organoselenocyanates through covalent modification of the p50 subunit." Cancer Res **67**(21): 10475-10483.

Chen, L., M. Kwong, R. Lu, D. Ginzinger, C. Lee, L. Leung and J. Y. Chan (2003). "Nrf1 is critical for redox balance and survival of liver cells during development." Mol Cell Biol **23**(13): 4673-4686.

Chen, L. F. and W. C. Greene (2004). "Shaping the nuclear action of NF-kappaB." Nat Rev Mol Cell Biol **5**(5): 392-401.

Chen, W., Z. Sun, X. J. Wang, T. Jiang, Z. Huang, D. Fang and D. D. Zhang (2009). "Direct interaction between Nrf2 and p21(Cip1/WAF1) upregulates the Nrf2-mediated antioxidant response." Mol Cell **34**(6): 663-673.

Cheng, P. Y., M. Wang and E. T. Morgan (2003). "Rapid transcriptional suppression of rat cytochrome P450 genes by endotoxin treatment and its inhibition by curcumin." J Pharmacol Exp Ther **307**(3): 1205-1212.

Cherfils-Vicini, J., S. Platonova, M. Gillard, L. Laurans, P. Validire, R. Caliandro, P. Magdeleinat, F. Mami-Chouaib, M. C. Dieu-Nosjean, W. H. Fridman, D. Damotte, C. Sautes-Fridman and I. Cremer (2010). "Triggering of TLR7 and TLR8 expressed by human lung cancer cells induces cell survival and chemoresistance." J Clin Invest **120**(4): 1285-1297.

Chiu, H., C. R. Gardner, D. M. Dambach, J. A. Brittingham, S. K. Durham, J. D. Laskin and D. L. Laskin (2003). "Role of p55 tumor necrosis factor receptor 1 in acetaminophen-induced antioxidant defense." Am J Physiol Gastrointest Liver Physiol **285**(5): G959-966.

Cho, H. Y., A. E. Jedlicka, S. P. Reddy, L. Y. Zhang, T. W. Kensler and S. R. Kleeberger (2002). "Linkage analysis of susceptibility to hyperoxia. Nrf2 is a candidate gene." Am J Respir Cell Mol Biol **26**(1): 42-51.

Chu, Z. L., T. A. McKinsey, L. Liu, J. J. Gentry, M. H. Malim and D. W. Ballard (1997). "Suppression of tumor necrosis factor-induced cell death by inhibitor of apoptosis c-IAP2 is under NF-kappaB control." Proc Natl Acad Sci U S A **94**(19): 10057-10062.

Chung, S., I. K. Sundar, H. Yao, Y. S. Ho and I. Rahman (2010). "Glutaredoxin 1 regulates cigarette smoke-mediated lung inflammation through differential modulation of I{kappa}B kinases in mice: impact on histone acetylation." Am J Physiol Lung Cell Mol Physiol **299**(2): L192-203.

Ciocca, D. R., S. Oesterreich, G. C. Chamness, W. L. McGuire and S. A. Fuqua (1993). "Biological and clinical implications of heat shock protein 27,000 (Hsp27): a review." J Natl Cancer Inst **85**(19): 1558-1570.

Claiborne, A., J. I. Yeh, T. C. Mallett, J. Luba, E. J. Crane, 3rd, V. Charrier and D. Parsonage (1999). "Protein-sulfenic acids: diverse roles for an unlikely player in enzyme catalysis and redox regulation." Biochemistry **38**(47): 15407-15416.

Clavreul, N., M. M. Bachschmid, X. Hou, C. Shi, A. Idrizovic, Y. Ido, D. Pimentel and R. A. Cohen (2006). "S-glutathiolation of p21ras by peroxynitrite mediates endothelial insulin resistance caused by oxidized low-density lipoprotein." Arterioscler Thromb Vasc Biol **26**(11): 2454-2461.

Cooper, C. E., R. P. Patel, P. S. Brookes and V. M. Darley-Usmar (2002). "Nanotransducers in cellular redox signaling: modification of thiols by reactive oxygen and nitrogen species." Trends Biochem Sci **27**(10): 489-492.

Copple, I. M., C. E. Goldring, R. E. Jenkins, A. J. Chia, L. E. Randle, J. D. Hayes, N. R. Kitteringham and B. K. Park (2008a). "The hepatotoxic metabolite of acetaminophen directly activates the Keap1-Nrf2 cell defense system." Hepatology **48**(4): 1292-1301.

Copple, I. M., C. E. Goldring, N. R. Kitteringham and B. K. Park (2008b). "The Nrf2-Keap1 defence pathway: role in protection against drug-induced toxicity." Toxicology **246**(1): 24-33.

Copple, I. M., C. E. Goldring, N. R. Kitteringham and B. K. Park (2010a). "The keap1-nrf2 cellular defense pathway: mechanisms of regulation and role in protection against drug-induced toxicity." Handb Exp Pharmacol(196): 233-266.

Copple, I. M., A. Lister, A. D. Obeng, N. R. Kitteringham, R. E. Jenkins, R. Layfield, B. J. Foster, C. E. Goldring and B. K. Park (2010b). "Physical and functional interaction of sequestosome 1 with Keap1 regulates the Keap1-Nrf2 cell defense pathway." J Biol Chem **285**(22): 16782-16788.

Cravatt, B. F. and E. J. Sorensen (2000). "Chemical strategies for the global analysis of protein function." Curr Opin Chem Biol **4**(6): 663-668.

Cristofanon, S., F. Morceau, A. I. Scovassi, M. Dicato, L. Ghibelli and M. Diederich (2009). "Oxidative, multistep activation of the noncanonical NF-kappaB pathway via disulfide Bcl-3/p50 complex." FASEB J **23**(1): 45-57.

Cullinan, S. B. and J. A. Diehl (2004a). "PERK-dependent activation of Nrf2 contributes to redox homeostasis and cell survival following endoplasmic reticulum stress." J Biol Chem **279**(19): 20108-20117.

Cullinan, S. B., J. D. Gordan, J. Jin, J. W. Harper and J. A. Diehl (2004b). "The Keap1-BTB protein is an adaptor that bridges Nrf2 to a Cul3-based E3 ligase: oxidative stress sensing by a Cul3-Keap1 ligase." Mol Cell Biol **24**(19): 8477-8486.

Cullinan, S. B., D. Zhang, M. Hannink, E. Arvisais, R. J. Kaufman and J. A. Diehl (2003). "Nrf2 is a direct PERK substrate and effector of PERK-dependent cell survival." Mol Cell Biol **23**(20): 7198-7209.

D'Alessio, M., C. Cerella, C. Amici, C. Pesce, S. Coppola, C. Fanelli, M. De Nicola, S. Cristofanon, G. Clavarino, A. Bergamaschi, A. Magrini, G. Gualandi and L. Ghibelli (2004). "Glutathione depletion up-regulates Bcl-2 in BSO-resistant cells." FASEB J **18**(13): 1609-1611.

Dahlin, D. C., G. T. Miwa, A. Y. Lu and S. D. Nelson (1984). "N-acetyl-p-benzoquinone imine: a cytochrome P-450-mediated oxidation product of acetaminophen." Proc Natl Acad Sci U S A **81**(5): 1327-1331.

Dalle-Donne, I., D. Giustarini, R. Rossi, R. Colombo and A. Milzani (2003a). "Reversible S-glutathionylation of Cys 374 regulates actin filament formation by inducing structural changes in the actin molecule." Free Radic Biol Med **34**(1): 23-32.

Dalle-Donne, I., R. Rossi, D. Giustarini, R. Colombo and A. Milzani (2003b). "Actin S-glutathionylation: evidence against a thiol-disulphide exchange mechanism." Free Radic Biol Med **35**(10): 1185-1193.

Dalle-Donne, I., R. Rossi, D. Giustarini, R. Colombo and A. Milzani (2007). "S-glutathionylation in protein redox regulation." Free Radic Biol Med **43**(6): 883-898.

Davern, T. J., 2nd, L. P. James, J. A. Hinson, J. Polson, A. M. Larson, R. J. Fontana, E. Lalani, S. Munoz, A. O. Shakil and W. M. Lee (2006). "Measurement of serum acetaminophen-protein adducts in patients with acute liver failure." Gastroenterology **130**(3): 687-694.

David Josephy, P. (2005). "The molecular toxicology of acetaminophen." Drug Metab Rev **37**(4): 581-594.

Davies, E. C., C. F. Green, S. Taylor, P. R. Williamson, D. R. Mottram and M. Pirmohamed (2009). "Adverse drug reactions in hospital in-patients: a prospective analysis of 3695 patient-episodes." PLoS One **4**(2): e4439.

Davies, M. J. (2005). "The oxidative environment and protein damage." Biochim Biophys Acta **1703**(2): 93-109.

Davis, D. C., W. Z. Potter, D. J. Jollow and J. R. Mitchell (1974). "Species differences in hepatic glutathione depletion, covalent binding and hepatic necrosis after acetaminophen." Life Sci **14**(11): 2099-2109.

DeLeve, L. D. and N. Kaplowitz (1991). "Glutathione metabolism and its role in hepatotoxicity." Pharmacol Ther **52**(3): 287-305.

Delhalle, S., V. Deregowski, V. Benoit, M. P. Merville and V. Bours (2002). "NF-kappaB-dependent MnSOD expression protects adenocarcinoma cells from TNF-alpha-induced apoptosis." Oncogene **21**(24): 3917-3924.

Derjuga, A., T. S. Gourley, T. M. Holm, H. H. Heng, R. A. Shivdasani, R. Ahmed, N. C. Andrews and V. Blank (2004). "Complexity of CNC transcription factors as revealed by gene targeting of the Nrf3 locus." Mol Cell Biol **24**(8): 3286-3294.

Dhakshinamoorthy, S. and A. K. Jaiswal (2000). "Small maf (MafG and MafK) proteins negatively regulate antioxidant response element-mediated expression and antioxidant induction of the NAD(P)H:Quinone oxidoreductase1 gene." J Biol Chem **275**(51): 40134-40141.

Dhakshinamoorthy, S. and A. K. Jaiswal (2001). "Functional characterization and role of INrf2 in antioxidant response element-mediated expression and antioxidant induction of NAD(P)H:quinone oxidoreductase1 gene." Oncogene **20**(29): 3906-3917.

DiDonato, J. A., M. Hayakawa, D. M. Rothwarf, E. Zandi and M. Karin (1997). "A cytokine-responsive IkappaB kinase that activates the transcription factor NF-kappaB." Nature **388**(6642): 548-554.

Dietz, B. M., Y. H. Kang, G. Liu, A. L. Eggler, P. Yao, L. R. Chadwick, G. F. Pauli, N. R. Farnsworth, A. D. Mesecar, R. B. van Breemen and J. L. Bolton (2005). "Xanthohumol isolated from Humulus lupulus Inhibits menadione-induced DNA damage through induction of quinone reductase." Chem Res Toxicol **18**(8): 1296-1305.

Dietz, B. M., D. Liu, G. K. Hagos, P. Yao, A. Schinkovitz, S. M. Pro, S. Deng, N. R. Farnsworth, G. F. Pauli, R. B. van Breemen and J. L. Bolton (2008). "Angelica sinensis and its alkylphthalides induce the detoxification enzyme NAD(P)H: quinone oxidoreductase 1 by alkylating Keap1." Chem Res Toxicol **21**(10): 1939-1948.

Dignam, J. D., R. M. Lebovitz and R. G. Roeder (1983). "Accurate transcription initiation by RNA polymerase II in a soluble extract from isolated mammalian nuclei." Nucleic Acids Res **11**(5): 1475-1489.

Dinkova-Kostova, A. T., W. D. Holtzclaw, R. N. Cole, K. Itoh, N. Wakabayashi, Y. Katoh, M. Yamamoto and P. Talalay (2002). "Direct evidence that sulfhydryl groups of Keap1 are the sensors regulating induction of phase 2 enzymes that protect against carcinogens and oxidants." Proc Natl Acad Sci U S A **99**(18): 11908-11913.

Dinkova-Kostova, A. T., W. D. Holtzclaw and N. Wakabayashi (2005). "Keap1, the sensor for electrophiles and oxidants that regulates the phase 2 response, is a zinc metalloprotein." Biochemistry **44**(18): 6889-6899.

Djavaheri-Mergny, M., D. Javelaud, J. Wietzerbin and F. Besancon (2004). "NF-kappaB activation prevents apoptotic oxidative stress via an increase of both thioredoxin and MnSOD levels in TNFalpha-treated Ewing sarcoma cells." FEBS Lett **578**(1-2): 111-115.

Droge, W., K. Schulze-Osthoff, S. Mihm, D. Galter, H. Schenk, H. P. Eck, S. Roth and H. Gmunder (1994). "Functions of glutathione and glutathione disulfide in immunology and immunopathology." FASEB J **8**(14): 1131-1138.

DuBridge, R. B., P. Tang, H. C. Hsia, P. M. Leong, J. H. Miller and M. P. Calos (1987). "Analysis of mutation in human cells by using an Epstein-Barr virus shuttle system." Mol Cell Biol **7**(1): 379-387.

Dykxhoorn, D. M. and J. Lieberman (2005). "The silent revolution: RNA interference as basic biology, research tool, and therapeutic." Annu Rev Med **56**: 401-423.

Eggler, A. L., G. Liu, J. M. Pezzuto, R. B. van Breemen and A. D. Mesecar (2005). "Modifying specific cysteines of the electrophile-sensing human Keap1 protein is insufficient to disrupt binding to the Nrf2 domain Neh2." Proc Natl Acad Sci U S A **102**(29): 10070-10075.

Eggler, A. L., Y. Luo, R. B. van Breemen and A. D. Mesecar (2007). "Identification of the highly reactive cysteine 151 in the chemopreventive agent-sensor Keap1 protein is method-dependent." Chem Res Toxicol **20**(12): 1878-1884.

Eggler, A. L., E. Small, M. Hannink and A. D. Mesecar (2009). "Cul3-mediated Nrf2 ubiquitination and antioxidant response element (ARE) activation are dependent on the partial molar volume at position 151 of Keap1." Biochem J **422**(1): 171-180.

El Gazzar, M. A., R. El Mezayen, M. R. Nicolls and S. C. Dreskin (2007). "Thymoquinone attenuates proinflammatory responses in lipopolysaccharide-activated mast cells by modulating NF-kappaB nuclear transactivation." Biochim Biophys Acta **1770**(4): 556-564.

Elbashir, S. M., J. Harborth, W. Lendeckel, A. Yalcin, K. Weber and T. Tuschl (2001). "Duplexes of 21-nucleotide RNAs mediate RNA interference in cultured mammalian cells." Nature **411**(6836): 494-498.

Enomoto, A., K. Itoh, E. Nagayoshi, J. Haruta, T. Kimura, T. O'Connor, T. Harada and M. Yamamoto (2001). "High sensitivity of Nrf2 knockout mice to acetaminophen hepatotoxicity associated with decreased expression of ARE-regulated drug metabolizing enzymes and antioxidant genes." Toxicol Sci **59**(1): 169-177.

Evans, M. J., A. Saghatelian, E. J. Sorensen and B. F. Cravatt (2005). "Target discovery in small-molecule cell-based screens by in situ proteome reactivity profiling." Nat Biotechnol **23**(10): 1303-1307.

Ewing, J. F. and M. D. Maines (1993). "Glutathione depletion induces heme oxygenase-1 (HSP32) mRNA and protein in rat brain." J Neurochem **60**(4): 1512-1519.

Feng, W., F. W. Benz, J. Cai, W. M. Pierce and Y. J. Kang (2006). "Metallothionein disulfides are present in metallothionein-overexpressing transgenic mouse heart and increase under conditions of oxidative stress." J Biol Chem **281**(2): 681-687.

Filomeni, G., K. Aquilano, G. Rotilio and M. R. Ciriolo (2005). "Antiapoptotic response to induced GSH depletion: involvement of heat shock proteins and NF-kappaB activation." Antioxid Redox Signal **7**(3-4): 446-455.

Fire, A., S. Xu, M. K. Montgomery, S. A. Kostas, S. E. Driver and C. C. Mello (1998). "Potent and specific genetic interference by double-stranded RNA in Caenorhabditis elegans." Nature **391**(6669): 806-811.

Fourquet, S., R. Guerois, D. Biard and M. B. Toledano (2010). "Activation of NRF2 by nitrosative agents and H2O2 involves KEAP1 disulfide formation." J Biol Chem **285**(11): 8463-8471.

Freeman, B. C. and R. I. Morimoto (1996). "The human cytosolic molecular chaperones hsp90, hsp70 (hsc70) and hdj-1 have distinct roles in recognition of a non-native protein and protein refolding." EMBO J **15**(12): 2969-2979.

Furukawa, M. and Y. Xiong (2005). "BTB protein Keap1 targets antioxidant transcription factor Nrf2 for ubiquitination by the Cullin 3-Roc1 ligase." Mol Cell Biol **25**(1): 162-171.

Gao, L., J. Wang, K. R. Sekhar, H. Yin, N. F. Yared, S. N. Schneider, S. Sasi, T. P. Dalton, M. E. Anderson, J. Y. Chan, J. D. Morrow and M. L. Freeman (2007). "Novel n-3 fatty acid oxidation products activate Nrf2 by destabilizing the association between Keap1 and Cullin3." J Biol Chem **282**(4): 2529-2537.

Gharavi, N., S. Haggarty and A. O. El-Kadi (2007). "Chemoprotective and carcinogenic effects of tert-butylhydroquinone and its metabolites." Curr Drug Metab **8**(1): 1-7.

Ghezzi, P. and V. Bonetto (2003). "Redox proteomics: identification of oxidatively modified proteins." Proteomics **3**(7): 1145-1153.

Ghosh, A. and P. C. Sil (2009). "Protection of acetaminophen induced mitochondrial dysfunctions and hepatic necrosis via Akt-NF-kappaB pathway: role of a novel plant protein." Chem Biol Interact **177**(2): 96-106.

Gibson, G. G., P. Skett and MyiLibrary (2001). Introduction to drug metabolism. Cheltenham, Nelson Thornes.

Giudice, A., C. Arra and M. C. Turco (2010). "Review of molecular mechanisms involved in the activation of the Nrf2-ARE signaling pathway by chemopreventive agents." Methods Mol Biol **647**: 37-74.

Giudice, A. and M. Montella (2006). "Activation of the Nrf2-ARE signaling pathway: a promising strategy in cancer prevention." Bioessays **28**(2): 169-181.

Gloire, G., S. Legrand-Poels and J. Piette (2006). "NF-kappaB activation by reactive oxygen species: fifteen years later." Biochem Pharmacol **72**(11): 1493-1505.

Gloire, G. and J. Piette (2009). "Redox regulation of nuclear post-translational modifications during NF-kappaB activation." Antioxid Redox Signal **11**(9): 2209-2222.

Goldring, C. E., N. R. Kitteringham, R. Elsby, L. E. Randle, Y. N. Clement, D. P. Williams, M. McMahon, J. D. Hayes, K. Itoh, M. Yamamoto and B. K. Park (2004). "Activation of hepatic Nrf2 in vivo by acetaminophen in CD-1 mice." Hepatology **39**(5): 1267-1276.

Griffith, O. W. (1982). "Mechanism of action, metabolism, and toxicity of buthionine sulfoximine and its higher homologs, potent inhibitors of glutathione synthesis." J Biol Chem **257**(22): 13704-13712.

Gu, X., S. Ke, D. Liu, T. Sheng, P. E. Thomas, A. B. Rabson, M. A. Gallo, W. Xie and Y. Tian (2006). "Role of NF-kappaB in regulation of PXR-mediated gene expression: a mechanism for the suppression of cytochrome P-450 3A4 by proinflammatory agents." J Biol Chem **281**(26): 17882-17889.

Guengerich, F. P. (2003). "Cytochromes P450, drugs, and diseases." Mol Interv **3**(4): 194-204.

Ha, K. H., M. S. Byun, J. Choi, J. Jeong, K. J. Lee and D. M. Jue (2009). "N-tosyl-L-phenylalanine chloromethyl ketone inhibits NF-kappaB activation by blocking specific cysteine residues of IkappaB kinase beta and p65/RelA." Biochemistry **48**(30): 7271-7278.

Hager, J. W. (2004). "Q TRAP(TM) mass spectrometer technology for proteomics applications." Drug Discovery Today: TARGETS **3**(2, Supplement 1): 31-36.

Hamann, M., T. Zhang, S. Hendrich and J. A. Thomas (2002). "Quantitation of protein sulfinic and sulfonic acid, irreversibly oxidized protein cysteine sites in cellular proteins." Methods Enzymol **348**: 146-156.

Han, Y., J. A. Englert, R. Yang, R. L. Delude and M. P. Fink (2005). "Ethyl pyruvate inhibits nuclear factor-kappaB-dependent signaling by directly targeting p65." J Pharmacol Exp Ther **312**(3): 1097-1105.

Hansen, J. M., W. H. Watson and D. P. Jones (2004). "Compartmentation of Nrf-2 redox control: regulation of cytoplasmic activation by glutathione and DNA binding by thioredoxin-1." Toxicol Sci **82**(1): 308-317.

Hansen, R. E., D. Roth and J. R. Winther (2009). "Quantifying the global cellular thiol-disulfide status." Proc Natl Acad Sci U S A **106**(2): 422-427.

Harikumar, K. B., A. B. Kunnumakkara, K. S. Ahn, P. Anand, S. Krishnan, S. Guha and B. B. Aggarwal (2009). "Modification of the cysteine residues in IkappaBalpha kinase and NF-kappaB (p65) by xanthohumol leads to suppression of NF-kappaB-regulated gene products and potentiation of apoptosis in leukemia cells." Blood **113**(9): 2003-2013.

Hayden, M. S. and S. Ghosh (2004). "Signaling to NF-kappaB." Genes Dev **18**(18): 2195-2224.

Hayes, J. D., S. A. Chanas, C. J. Henderson, M. McMahon, C. Sun, G. J. Moffat, C. R. Wolf and M. Yamamoto (2000). "The Nrf2 transcription factor contributes both to the basal expression of glutathione S-transferases in mouse liver and to their induction by the chemopreventive synthetic antioxidants, butylated hydroxyanisole and ethoxyquin." Biochem Soc Trans **28**(2): 33-41.

Hayes, J. D. and L. I. McLellan (1999). "Glutathione and glutathione-dependent enzymes represent a co-ordinately regulated defence against oxidative stress." Free Radic Res **31**(4): 273-300.

Hayes, J. D. and M. McMahon (2009). "NRF2 and KEAP1 mutations: permanent activation of an adaptive response in cancer." Trends Biochem Sci **34**(4): 176-188.

He, X. and Q. Ma (2009). "NRF2 cysteine residues are critical for oxidant/electrophile-sensing, Kelch-like ECH-associated protein-1-dependent ubiquitination-proteasomal degradation, and transcription activation." Mol Pharmacol **76**(6): 1265-1278.

He, X. and Q. Ma (2010). "Critical cysteine residues of Kelch-like ECH-associated protein 1 in arsenic sensing and suppression of nuclear factor erythroid 2-related factor 2." J Pharmacol Exp Ther **332**(1): 66-75.

Hess, J., P. Angel and M. Schorpp-Kistner (2004). "AP-1 subunits: quarrel and harmony among siblings." J Cell Sci **117**(Pt 25): 5965-5973.

Hinson, J. A., L. R. Pohl, T. J. Monks and J. R. Gillette (1981). "Acetaminophen-induced hepatotoxicity." Life Sci **29**(2): 107-116.

Hinz, B., O. Cheremina and K. Brune (2008). "Acetaminophen (paracetamol) is a selective cyclooxygenase-2 inhibitor in man." FASEB J **22**(2): 383-390.

Holland, R. and J. C. Fishbein (2010). "Chemistry of the cysteine sensors in Kelch-like ECH-associated protein 1." Antioxid Redox Signal **13**(11): 1749-1761.

Holland, R., A. E. Hawkins, A. L. Eggler, A. D. Mesecar, D. Fabris and J. C. Fishbein (2008). "Prospective type 1 and type 2 disulfides of Keap1 protein." Chem Res Toxicol **21**(10): 2051-2060.

Holt, M. and C. Ju (2010). "Drug-induced liver injury." Handb Exp Pharmacol(196): 3-27.

Holtzclaw, W. D., A. T. Dinkova-Kostova and P. Talalay (2004). "Protection against electrophile and oxidative stress by induction of phase 2 genes: the quest for the elusive sensor that responds to inducers." Adv Enzyme Regul **44**: 335-367.

Hong, F., M. L. Freeman and D. C. Liebler (2005a). "Identification of sensor cysteines in human Keap1 modified by the cancer chemopreventive agent sulforaphane." Chem Res Toxicol **18**(12): 1917-1926.

Hong, F., K. R. Sekhar, M. L. Freeman and D. C. Liebler (2005b). "Specific patterns of electrophile adduction trigger Keap1 ubiquitination and Nrf2 activation." J Biol Chem **280**(36): 31768-31775.

Hosoya, T., A. Maruyama, M. I. Kang, Y. Kawatani, T. Shibata, K. Uchida, E. Warabi, N. Noguchi, K. Itoh and M. Yamamoto (2005). "Differential responses of the Nrf2-Keap1 system to laminar and oscillatory shear stresses in endothelial cells." J Biol Chem **280**(29): 27244-27250.

Howie, D., P. I. Adriaenssens and L. F. Prescott (1977). "Paracetamol metabolism following overdosage: application of high performance liquid chromatography." J Pharm Pharmacol **29**(4): 235-237.

Hu, R., C. Xu, G. Shen, M. R. Jain, T. O. Khor, A. Gopalkrishnan, W. Lin, B. Reddy, J. Y. Chan and A. N. Kong (2006). "Gene expression profiles induced by cancer chemopreventive isothiocyanate sulforaphane in the liver of C57BL/6J mice and C57BL/6J/Nrf2 (-/-) mice." Cancer Lett **243**(2): 170-192.

Hua, C. C., L. C. Chang, J. C. Tseng, C. M. Chu, Y. C. Liu and W. B. Shieh (2010). "Functional haplotypes in the promoter region of transcription factor Nrf2 in chronic obstructive pulmonary disease." Dis Markers **28**(3): 185-193.

Huang, A., H. Xiao, J. M. Samii, J. A. Vita and J. F. Keaney, Jr. (2001). "Contrasting effects of thiol-modulating agents on endothelial NO bioactivity." Am J Physiol Cell Physiol **281**(2): C719-725.

Huang, H. C., T. Nguyen and C. B. Pickett (2000a). "Regulation of the antioxidant response element by protein kinase C-mediated phosphorylation of NF-E2-related factor 2." Proc Natl Acad Sci U S A **97**(23): 12475-12480.

Huang, H. C., T. Nguyen and C. B. Pickett (2002). "Phosphorylation of Nrf2 at Ser-40 by protein kinase C regulates antioxidant response element-mediated transcription." J Biol Chem **277**(45): 42769-42774.

Huang, T. T., N. Kudo, M. Yoshida and S. Miyamoto (2000b). "A nuclear export signal in the N-terminal regulatory domain of IkappaBalpha controls cytoplasmic localization of inactive NF-kappaB/IkappaBalpha complexes." Proc Natl Acad Sci U S A **97**(3): 1014-1019.

Huang, W. C., T. K. Ju, M. C. Hung and C. C. Chen (2007). "Phosphorylation of CBP by IKKalpha promotes cell growth by switching the binding preference of CBP from p53 to NF-kappaB." Mol Cell **26**(1): 75-87.

Iida, K., K. Itoh, Y. Kumagai, R. Oyasu, K. Hattori, K. Kawai, T. Shimazui, H. Akaza and M. Yamamoto (2004). "Nrf2 is essential for the chemopreventive efficacy of oltipraz against urinary bladder carcinogenesis." Cancer Res **64**(18): 6424-6431.

Ishibe, T., A. Kimura, Y. Ishida, T. Takayasu, T. Hayashi, K. Tsuneyama, K. Matsushima, I. Sakata, N. Mukaida and T. Kondo (2009). "Reduced acetaminophen-induced liver injury in mice by genetic disruption of IL-1 receptor antagonist." Lab Invest **89**(1): 68-79.

Ishii, T., K. Itoh, S. Takahashi, H. Sato, T. Yanagawa, Y. Katoh, S. Bannai and M. Yamamoto (2000). "Transcription factor Nrf2 coordinately regulates a group of oxidative stress-inducible genes in macrophages." J Biol Chem **275**(21): 16023-16029.

Ishii, T., K. Itoh and M. Yamamoto (2002). "Roles of Nrf2 in activation of antioxidant enzyme genes via antioxidant responsive elements." Methods Enzymol **348**: 182-190.

Ito, K., A. Hirao, F. Arai, K. Takubo, S. Matsuoka, K. Miyamoto, M. Ohmura, K. Naka, K. Hosokawa, Y. Ikeda and T. Suda (2006). "Reactive oxygen species act through p38 MAPK to limit the lifespan of hematopoietic stem cells." Nat Med **12**(4): 446-451.

Itoh, K., T. Chiba, S. Takahashi, T. Ishii, K. Igarashi, Y. Katoh, T. Oyake, N. Hayashi, K. Satoh, I. Hatayama, M. Yamamoto and Y. Nabeshima (1997). "An Nrf2/small Maf heterodimer mediates the induction of phase II detoxifying enzyme genes through antioxidant response elements." Biochem Biophys Res Commun **236**(2): 313-322.

Itoh, K., T. Ishii, N. Wakabayashi and M. Yamamoto (1999a). "Regulatory mechanisms of cellular response to oxidative stress." Free Radic Res **31**(4): 319-324.

Itoh, K., M. Mochizuki, Y. Ishii, T. Ishii, T. Shibata, Y. Kawamoto, V. Kelly, K. Sekizawa, K. Uchida and M. Yamamoto (2004). "Transcription factor Nrf2 regulates inflammation by mediating the effect of 15-deoxy-Delta(12,14)-prostaglandin j(2)." Mol Cell Biol **24**(1): 36-45.

Itoh, K., N. Wakabayashi, Y. Katoh, T. Ishii, K. Igarashi, J. D. Engel and M. Yamamoto (1999b). "Keap1 represses nuclear activation of antioxidant responsive elements by Nrf2 through binding to the amino-terminal Neh2 domain." Genes Dev **13**(1): 76-86.

Itoh, K., N. Wakabayashi, Y. Katoh, T. Ishii, T. O'Connor and M. Yamamoto (2003). "Keap1 regulates both cytoplasmic-nuclear shuttling and degradation of Nrf2 in response to electrophiles." Genes Cells **8**(4): 379-391.

Jacobs, M. D. and S. C. Harrison (1998). "Structure of an IkappaBalpha/NF-kappaB complex." Cell **95**(6): 749-758.

Jaeschke, H. and M. L. Bajt (2006). "Intracellular signaling mechanisms of acetaminophen-induced liver cell death." Toxicol Sci **89**(1): 31-41.

Jaeschke, H., G. J. Gores, A. I. Cederbaum, J. A. Hinson, D. Pessayre and J. J. Lemasters (2002). "Mechanisms of hepatotoxicity." Toxicol Sci **65**(2): 166-176.

Jain, A. K., D. A. Bloom and A. K. Jaiswal (2005). "Nuclear import and export signals in control of Nrf2." J Biol Chem **280**(32): 29158-29168.

Jenkins, R. E., N. R. Kitteringham, C. E. Goldring, S. M. Dowdall, J. Hamlett, C. S. Lane, J. S. Boerma, N. P. Vermeulen and B. K. Park (2008). "Glutathione-S-transferase pi as a model protein for the characterisation of chemically reactive metabolites." Proteomics **8**(2): 301-315.

Ji, C., K. R. Kozak and L. J. Marnett (2001). "IkappaB kinase, a molecular target for inhibition by 4-hydroxy-2-nonenal." J Biol Chem **276**(21): 18223-18228.

Johnson, C., D. Van Antwerp and T. J. Hope (1999). "An N-terminal nuclear export signal is required for the nucleocytoplasmic shuttling of IkappaBalpha." EMBO J **18**(23): 6682-6693.

Johnson, D. A., G. K. Andrews, W. Xu and J. A. Johnson (2002). "Activation of the antioxidant response element in primary cortical neuronal cultures derived from transgenic reporter mice." J Neurochem **81**(6): 1233-1241.

Jollow, D. J., J. R. Mitchell, N. Zampaglione and J. R. Gillette (1974). "Bromobenzene-induced liver necrosis. Protective role of glutathione and evidence for 3,4-bromobenzene oxide as the hepatotoxic metabolite." Pharmacology **11**(3): 151-169.

Jowsey, I. R., Q. Jiang, K. Itoh, M. Yamamoto and J. D. Hayes (2003). "Expression of the aflatoxin B1-8,9-epoxide-metabolizing murine glutathione S-transferase A3 subunit is regulated by the Nrf2 transcription factor through an antioxidant response element." Mol Pharmacol **64**(5): 1018-1028.

Kairisalo, M., L. Korhonen, K. Blomgren and D. Lindholm (2007). "X-linked inhibitor of apoptosis protein increases mitochondrial antioxidants through NF-kappaB activation." Biochem Biophys Res Commun **364**(1): 138-144.

Kalmar, B. and L. Greensmith (2009). "Induction of heat shock proteins for protection against oxidative stress." Adv Drug Deliv Rev **61**(4): 310-318.

Kang, K. W., S. J. Lee, J. W. Park and S. G. Kim (2002). "Phosphatidylinositol 3-kinase regulates nuclear translocation of NF-E2-related factor 2 through actin rearrangement in response to oxidative stress." Mol Pharmacol **62**(5): 1001-1010.

Kang, M. I., A. Kobayashi, N. Wakabayashi, S. G. Kim and M. Yamamoto (2004). "Scaffolding of Keap1 to the actin cytoskeleton controls the function of Nrf2 as key regulator of cytoprotective phase 2 genes." Proc Natl Acad Sci U S A **101**(7): 2046-2051.

Kaplowitz, N., T. Y. Aw and M. Ookhtens (1985). "The regulation of hepatic glutathione." Annu Rev Pharmacol Toxicol **25**: 715-744.

Karin, M. (1995). "The regulation of AP-1 activity by mitogen-activated protein kinases." J Biol Chem **270**(28): 16483-16486.

Karin, M., Z. Liu and E. Zandi (1997). "AP-1 function and regulation." Curr Opin Cell Biol **9**(2): 240-246.

Kato, T., Jr., M. Delhase, A. Hoffmann and M. Karin (2003). "CK2 Is a C-Terminal IkappaB Kinase Responsible for NF-kappaB Activation during the UV Response." Mol Cell **12**(4): 829-839.

Katoh, Y., K. Iida, M. I. Kang, A. Kobayashi, M. Mizukami, K. I. Tong, M. McMahon, J. D. Hayes, K. Itoh and M. Yamamoto (2005). "Evolutionary conserved N-terminal domain of Nrf2 is essential for the Keap1-mediated degradation of the protein by proteasome." Arch Biochem Biophys **433**(2): 342-350.

Katoh, Y., K. Itoh, E. Yoshida, M. Miyagishi, A. Fukamizu and M. Yamamoto (2001). "Two domains of Nrf2 cooperatively bind CBP, a CREB binding protein, and synergistically activate transcription." Genes Cells **6**(10): 857-868.

Ke, S., A. B. Rabson, J. F. Germino, M. A. Gallo and Y. Tian (2001). "Mechanism of suppression of cytochrome P-450 1A1 expression by tumor necrosis factor-alpha and lipopolysaccharide." J Biol Chem **276**(43): 39638-39644.

Keum, Y. S., E. D. Owuor, B. R. Kim, R. Hu and A. N. Kong (2003). "Involvement of Nrf2 and JNK1 in the activation of antioxidant responsive element (ARE) by chemopreventive agent phenethyl isothiocyanate (PEITC)." Pharm Res **20**(9): 1351-1356.

Keum, Y. S., S. Yu, P. P. Chang, X. Yuan, J. H. Kim, C. Xu, J. Han, A. Agarwal and A. N. Kong (2006). "Mechanism of action of sulforaphane: inhibition of p38 mitogen-activated protein kinase isoforms contributing to the induction of antioxidant response element-mediated heme oxygenase-1 in human hepatoma HepG2 cells." Cancer Res **66**(17): 8804-8813.

Kil, I. S., S. Y. Kim and J. W. Park (2008). "Glutathionylation regulates IkappaB." Biochem Biophys Res Commun **373**(1): 169-173.

Kim, G. and R. L. Levine (2005). "Molecular determinants of S-glutathionylation of carbonic anhydrase 3." Antioxid Redox Signal **7**(7-8): 849-854.

Kim, J. E., D. J. You, C. Lee, C. Ahn, J. Y. Seong and J. I. Hwang (2010a). "Suppression of NF-kappaB signaling by KEAP1 regulation of IKKbeta activity through autophagic degradation and inhibition of phosphorylation." Cell Signal **22**(11): 1645-1654.

Kim, Y. R., J. E. Oh, M. S. Kim, M. R. Kang, S. W. Park, J. Y. Han, H. S. Eom, N. J. Yoo and S. H. Lee (2010b). "Oncogenic NRF2 mutations in squamous cell carcinomas of oesophagus and skin." J Pathol **220**(4): 446-451.

Kimura, T., Y. Kawasaki, F. Okumura, T. Sone, R. Natsuki and M. Isobe (2009). "Ethanol-induced expression of glutamate-cysteine ligase catalytic subunit gene is mediated by NF-kappaB." Toxicol Lett **185**(2): 110-115.

Kitteringham, N. R., H. Powell, Y. N. Clement, C. C. Dodd, J. N. Tettey, M. Pirmohamed, D. A. Smith, L. I. McLellan and B. Kevin Park (2000). "Hepatocellular response to chemical stress in CD-1 mice: induction of early genes and gamma-glutamylcysteine synthetase." Hepatology **32**(2): 321-333.

Klaassen, C. D. and L. M. Aleksunes (2010). "Xenobiotic, bile acid, and cholesterol transporters: function and regulation." Pharmacol Rev **62**(1): 1-96.

Kobayashi, A., E. Ito, T. Toki, K. Kogame, S. Takahashi, K. Igarashi, N. Hayashi and M. Yamamoto (1999). "Molecular cloning and functional characterization of a new Cap'n' collar family transcription factor Nrf3." J Biol Chem **274**(10): 6443-6452.

Kobayashi, A., M. I. Kang, H. Okawa, M. Ohtsuji, Y. Zenke, T. Chiba, K. Igarashi and M. Yamamoto (2004a). "Oxidative stress sensor Keap1 functions as an adaptor for Cul3-based E3 ligase to regulate proteasomal degradation of Nrf2." Mol Cell Biol **24**(16): 7130-7139.

Kobayashi, A., M. I. Kang, Y. Watai, K. I. Tong, T. Shibata, K. Uchida and M. Yamamoto (2006a). "Oxidative and electrophilic stresses activate Nrf2 through inhibition of ubiquitination activity of Keap1." Mol Cell Biol **26**(1): 221-229.

Kobayashi, A., T. Ohta and M. Yamamoto (2004b). "Unique function of the Nrf2-Keap1 pathway in the inducible expression of antioxidant and detoxifying enzymes." Methods Enzymol **378**: 273-286.

Kobayashi, M., K. Itoh, T. Suzuki, H. Osanai, K. Nishikawa, Y. Katoh, Y. Takagi and M. Yamamoto (2002). "Identification of the interactive interface and phylogenic conservation of the Nrf2-Keap1 system." Genes Cells **7**(8): 807-820.

Kobayashi, M., L. Li, N. Iwamoto, Y. Nakajima-Takagi, H. Kaneko, Y. Nakayama, M. Eguchi, Y. Wada, Y. Kumagai and M. Yamamoto (2009). "The antioxidant defense system Keap1-Nrf2 comprises a multiple sensing mechanism for responding to a wide range of chemical compounds." Mol Cell Biol **29**(2): 493-502.

Kobayashi, M. and M. Yamamoto (2006b). "Nrf2-Keap1 regulation of cellular defense mechanisms against electrophiles and reactive oxygen species." Adv Enzyme Regul **46**: 113-140.

Kolb, H. C., M. G. Finn and K. B. Sharpless (2001). "Click Chemistry: Diverse Chemical Function from a Few Good Reactions." Angew Chem Int Ed Engl **40**(11): 2004-2021.

Kong, R., B. Sun, H. Jiang, S. Pan, H. Chen, S. Wang, G. W. Krissansen and X. Sun (2010). "Downregulation of nuclear factor-kappaB p65 subunit by small interfering RNA synergizes with gemcitabine to inhibit the growth of pancreatic cancer." Cancer Lett **291**(1): 90-98.

Korashy, H. M. and A. O. El-Kadi (2008). "NF-kappaB and AP-1 are key signaling pathways in the modulation of NAD(P)H:quinone oxidoreductase 1 gene by mercury, lead, and copper." J Biochem Mol Toxicol **22**(4): 274-283.

Kosower, N. S. and E. M. Kosower (1995). "Diamide: an oxidant probe for thiols." Methods Enzymol **251**: 123-133.

Kreuz, S., D. Siegmund, P. Scheurich and H. Wajant (2001). "NF-kappaB inducers upregulate cFLIP, a cycloheximide-sensitive inhibitor of death receptor signaling." Mol Cell Biol **21**(12): 3964-3973.

Kucharczak, J., M. J. Simmons, Y. Fan and C. Gelinas (2003). "To be, or not to be: NF-kappaB is the answer--role of Rel/NF-kappaB in the regulation of apoptosis." Oncogene **22**(56): 8961-8982.

Kwak, M. K., K. Itoh, M. Yamamoto, T. R. Sutter and T. W. Kensler (2001). "Role of transcription factor Nrf2 in the induction of hepatic phase 2 and antioxidative enzymes in vivo by the cancer chemoprotective agent, 3H-1, 2-dimethiole-3-thione." Mol Med **7**(2): 135-145.

Kwak, M. K., N. Wakabayashi, K. Itoh, H. Motohashi, M. Yamamoto and T. W. Kensler (2003). "Modulation of gene expression by cancer chemopreventive dithiolethiones through the Keap1-Nrf2 pathway. Identification of novel gene clusters for cell survival." J Biol Chem **278**(10): 8135-8145.

Kwong, M., Y. W. Kan and J. Y. Chan (1999). "The CNC basic leucine zipper factor, Nrf1, is essential for cell survival in response to oxidative stress-inducing agents. Role for Nrf1 in gamma-gcs(l) and gss expression in mouse fibroblasts." J Biol Chem **274**(52): 37491-37498.

Lammert, C., E. Bjornsson, A. Niklasson and N. Chalasani (2010). "Oral medications with significant hepatic metabolism at higher risk for hepatic adverse events." Hepatology **51**(2): 615-620.

Larson, A. M., J. Polson, R. J. Fontana, T. J. Davern, E. Lalani, L. S. Hynan, J. S. Reisch, F. V. Schiodt, G. Ostapowicz, A. O. Shakil and W. M. Lee (2005). "Acetaminophen-induced acute liver failure: results of a United States multicenter, prospective study." Hepatology **42**(6): 1364-1372.

Lau, A., N. F. Villeneuve, Z. Sun, P. K. Wong and D. D. Zhang (2008). "Dual roles of Nrf2 in cancer." Pharmacol Res **58**(5-6): 262-270.

Lau, A., X. J. Wang, F. Zhao, N. F. Villeneuve, T. Wu, T. Jiang, Z. Sun, E. White and D. D. Zhang (2010). "A noncanonical mechanism of Nrf2 activation by autophagy deficiency: direct interaction between Keap1 and p62." Mol Cell Biol **30**(13): 3275-3285.

Lazarou, J., B. H. Pomeranz and P. N. Corey (1998). "Incidence of adverse drug reactions in hospitalized patients: a meta-analysis of prospective studies." JAMA **279**(15): 1200-1205.

Lee-Hilz, Y. Y., A. M. Boerboom, A. H. Westphal, W. J. Berkel, J. M. Aarts and I. M. Rietjens (2006). "Pro-oxidant activity of flavonoids induces EpRE-mediated gene expression." Chem Res Toxicol **19**(11): 1499-1505.

Lee, D. F., H. P. Kuo, M. Liu, C. K. Chou, W. Xia, Y. Du, J. Shen, C. T. Chen, L. Huo, M. C. Hsu, C. W. Li, Q. Ding, T. L. Liao, C. C. Lai, A. C. Lin, Y. H. Chang, S. F. Tsai, L. Y. Li and M. C. Hung (2009). "KEAP1 E3 ligase-mediated downregulation of NF-kappaB signaling by targeting IKKbeta." Mol Cell **36**(1): 131-140.

Lee, H. R., J. M. Cho, D. H. Shin, C. S. Yong, H. G. Choi, N. Wakabayashi and M. K. Kwak (2008). "Adaptive response to GSH depletion and resistance to L-buthionine-(S,R)-sulfoximine: involvement of Nrf2 activation." Mol Cell Biochem **318**(1-2): 23-31.

Lee, J. M., J. M. Hanson, W. A. Chu and J. A. Johnson (2001). "Phosphatidylinositol 3-kinase, not extracellular signal-regulated kinase, regulates activation of the antioxidant-responsive element in IMR-32 human neuroblastoma cells." J Biol Chem **276**(23): 20011-20016.

Lee, W. M. (2003). "Drug-induced hepatotoxicity." N Engl J Med **349**(5): 474-485.

Lee, W. M. (2004). "Acetaminophen and the U.S. Acute Liver Failure Study Group: lowering the risks of hepatic failure." Hepatology **40**(1): 6-9.

Lee, W. M. and J. R. Senior (2005). "Recognizing drug-induced liver injury: current problems, possible solutions." Toxicol Pathol **33**(1): 155-164.

Lenardo, M. J. and D. Baltimore (1989). "NF-kappa B: a pleiotropic mediator of inducible and tissue-specific gene control." Cell **58**(2): 227-229.

Leung, R. K. and P. A. Whittaker (2005). "RNA interference: from gene silencing to gene-specific therapeutics." Pharmacol Ther **107**(2): 222-239.

Levonen, A. L., A. Landar, A. Ramachandran, E. K. Ceaser, D. A. Dickinson, G. Zanoni, J. D. Morrow and V. M. Darley-Usmar (2004). "Cellular mechanisms of redox cell signalling: role of cysteine modification in controlling antioxidant defences in response to electrophilic lipid oxidation products." Biochem J **378**(Pt 2): 373-382.

Li, C. Q., M. Y. Kim, L. C. Godoy, A. Thiantanawat, L. J. Trudel and G. N. Wogan (2009). "Nitric oxide activation of Keap1/Nrf2 signaling in human colon carcinoma cells." Proc Natl Acad Sci U S A **106**(34): 14547-14551.

Li, F. and G. Sethi (2010). "Targeting transcription factor NF-kappaB to overcome chemoresistance and radioresistance in cancer therapy." Biochim Biophys Acta **1805**(2): 167-180.

Li, W., S. W. Yu and A. N. Kong (2006). "Nrf2 possesses a redox-sensitive nuclear exporting signal in the Neh5 transactivation domain." J Biol Chem **281**(37): 27251-27263.

Li, X., D. Zhang, M. Hannink and L. J. Beamer (2004). "Crystallization and initial crystallographic analysis of the Kelch domain from human Keap1." Acta Crystallogr D Biol Crystallogr **60**(Pt 12 Pt 2): 2346-2348.

Liebler, D. C., F. Hong, K. R. Sekhar, M. L. Freeman and C. F. James (2006). Chapter 3 Site-Specific Modification of the Electrophile Sensor Protein Keap1 and Activation of Nrf2-Dependent Gene Expression. Advances in Molecular Toxicology, Elsevier. **Volume 1:** 65-83.

Lindquist, S. (1986). "The heat-shock response." Annu Rev Biochem **55**: 1151-1191.

Liu, G., A. L. Eggler, B. M. Dietz, A. D. Mesecar, J. L. Bolton, J. M. Pezzuto and R. B. van Breemen (2005). "Screening method for the discovery of potential cancer chemoprevention agents based on mass spectrometric detection of alkylated Keap1." Anal Chem **77**(19): 6407-6414.

Liu, G. H., J. Qu and X. Shen (2008). "NF-kappaB/p65 antagonizes Nrf2-ARE pathway by depriving CBP from Nrf2 and facilitating recruitment of HDAC3 to MafK." Biochim Biophys Acta **1783**(5): 713-727.

Lluis, J. M., F. Buricchi, P. Chiarugi, A. Morales and J. C. Fernandez-Checa (2007). "Dual role of mitochondrial reactive oxygen species in hypoxia signaling: activation of nuclear factor-{kappa}B via c-SRC and oxidant-dependent cell death." Cancer Res **67**(15): 7368-7377.

Lo, S. C., X. Li, M. T. Henzl, L. J. Beamer and M. Hannink (2006). "Structure of the Keap1:Nrf2 interface provides mechanistic insight into Nrf2 signaling." EMBO J **25**(15): 3605-3617.

Lou, H., S. Du, Q. Ji and A. Stolz (2006). "Induction of AKR1C2 by phase II inducers: identification of a distal consensus antioxidant response element regulated by NRF2." Mol Pharmacol **69**(5): 1662-1672.

Lowney, E. D. (1971). "Tolerance of dinitrochlorobenzene, a contact sensitizer, in man." J Allergy Clin Immunol **48**(1): 28-35.

Luo, Y., A. L. Eggler, D. Liu, G. Liu, A. D. Mesecar and R. B. van Breemen (2007). "Sites of alkylation of human Keap1 by natural chemoprevention agents." J Am Soc Mass Spectrom **18**(12): 2226-2232.

Macpherson, L. J., A. E. Dubin, M. J. Evans, F. Marr, P. G. Schultz, B. F. Cravatt and A. Patapoutian (2007). "Noxious compounds activate TRPA1 ion channels through covalent modification of cysteines." Nature **445**(7127): 541-545.

Maher, J. M., M. Z. Dieter, L. M. Aleksunes, A. L. Slitt, G. Guo, Y. Tanaka, G. L. Scheffer, J. Y. Chan, J. E. Manautou, Y. Chen, T. P. Dalton, M. Yamamoto and C. D. Klaassen (2007). "Oxidative and electrophilic stress induces multidrug resistance-associated protein transporters via the nuclear factor-E2-related factor-2 transcriptional pathway." Hepatology **46**(5): 1597-1610.

Malewicz, M., N. Zeller, Z. B. Yilmaz and F. Weih (2003). "NF kappa B controls the balance between Fas and tumor necrosis factor cell death pathways during T cell receptor-induced apoptosis via the expression of its target gene A20." J Biol Chem **278**(35): 32825-32833.

Mallet, C., D. A. Barriere, A. Ermund, B. A. Jonsson, A. Eschalier, P. M. Zygmunt and E. D. Hogestatt (2010). "TRPV1 in brain is involved in acetaminophen-induced antinociception." PLoS One **5**(9).

Marini, M. G., K. Chan, L. Casula, Y. W. Kan, A. Cao and P. Moi (1997). "hMAF, a small human transcription factor that heterodimerizes specifically with Nrf1 and Nrf2." J Biol Chem **272**(26): 16490-16497.

Marnett, L. J., J. N. Riggins and J. D. West (2003). "Endogenous generation of reactive oxidants and electrophiles and their reactions with DNA and protein." J Clin Invest **111**(5): 583-593.

Marzec, J. M., J. D. Christie, S. P. Reddy, A. E. Jedlicka, H. Vuong, P. N. Lanken, R. Aplenc, T. Yamamoto, M. Yamamoto, H. Y. Cho and S. R. Kleeberger (2007). "Functional polymorphisms in the transcription factor NRF2 in humans increase the risk of acute lung injury." FASEB J **21**(9): 2237-2246.

Matsumaru, K., C. Ji and N. Kaplowitz (2003). "Mechanisms for sensitization to TNF-induced apoptosis by acute glutathione depletion in murine hepatocytes." Hepatology **37**(6): 1425-1434.

May, M. J. and S. Ghosh (1998). "Signal transduction through NF-kappa B." Immunol Today **19**(2): 80-88.

McMahon, M., K. Itoh, M. Yamamoto, S. A. Chanas, C. J. Henderson, L. I. McLellan, C. R. Wolf, C. Cavin and J. D. Hayes (2001). "The Cap'n'Collar basic leucine zipper transcription factor Nrf2 (NF-E2 p45-related factor 2) controls both constitutive and inducible expression of intestinal detoxification and glutathione biosynthetic enzymes." Cancer Res **61**(8): 3299-3307.

McMahon, M., K. Itoh, M. Yamamoto and J. D. Hayes (2003). "Keap1-dependent proteasomal degradation of transcription factor Nrf2 contributes to the negative regulation of antioxidant response element-driven gene expression." J Biol Chem **278**(24): 21592-21600.

McMahon, M., D. J. Lamont, K. A. Beattie and J. D. Hayes (2010). "Keap1 perceives stress via three sensors for the endogenous signaling molecules nitric oxide, zinc, and alkenals." Proc Natl Acad Sci U S A **107**(44): 18838-18843.

McMahon, M., N. Thomas, K. Itoh, M. Yamamoto and J. D. Hayes (2004). "Redox-regulated turnover of Nrf2 is determined by at least two separate protein domains, the redox-sensitive Neh2 degron and the redox-insensitive Neh6 degron." J Biol Chem **279**(30): 31556-31567.

McMahon, M., N. Thomas, K. Itoh, M. Yamamoto and J. D. Hayes (2006). "Dimerization of substrate adaptors can facilitate cullin-mediated ubiquitylation of proteins by a "tethering" mechanism: a two-site interaction model for the Nrf2-Keap1 complex." J Biol Chem **281**(34): 24756-24768.

Megherbi, R. (Thesis 2010). "The role of protein haptenation in signalling pathway and cell activation " Division of Molecular and Clinical Pharmacology, Institute of Translational Medicine, The University of Liverpool

Meister, A. (1988). "On the discovery of glutathione." Trends Biochem Sci **13**(5): 185-188.

Mercurio, F., B. W. Murray, A. Shevchenko, B. L. Bennett, D. B. Young, J. W. Li, G. Pascual, A. Motiwala, H. Zhu, M. Mann and A. M. Manning (1999). "IkappaB kinase (IKK)-associated protein 1, a common component of the heterogeneous IKK complex." Mol Cell Biol **19**(2): 1526-1538.

Mercurio, F., H. Zhu, B. W. Murray, A. Shevchenko, B. L. Bennett, J. Li, D. B. Young, M. Barbosa, M. Mann, A. Manning and A. Rao (1997). "IKK-1 and IKK-2: cytokine-activated IkappaB kinases essential for NF-kappaB activation." Science **278**(5339): 860-866.

Messerle, B. A., A. Schaffer, M. Vasak, J. H. Kagi and K. Wuthrich (1990). "Three-dimensional structure of human [113Cd7]metallothionein-2 in solution determined by nuclear magnetic resonance spectroscopy." J Mol Biol **214**(3): 765-779.

Meyer, U. A. (1996). "Overview of enzymes of drug metabolism." J Pharmacokinet Biopharm **24**(5): 449-459.

Micheau, O., S. Lens, O. Gaide, K. Alevizopoulos and J. Tschopp (2001). "NF-kappaB signals induce the expression of c-FLIP." Mol Cell Biol **21**(16): 5299-5305.

Miseta, A. and P. Csutora (2000). "Relationship between the occurrence of cysteine in proteins and the complexity of organisms." Mol Biol Evol **17**(8): 1232-1239.

Mitchell, J. R., D. J. Jollow, W. Z. Potter, D. C. Davis, J. R. Gillette and B. B. Brodie (1973). "Acetaminophen-induced hepatic necrosis. I. Role of drug metabolism." J Pharmacol Exp Ther **187**(1): 185-194.

Moi, P., K. Chan, I. Asunis, A. Cao and Y. W. Kan (1994). "Isolation of NF-E2-related factor 2 (Nrf2), a NF-E2-like basic leucine zipper transcriptional activator that binds to the tandem NF-E2/AP1 repeat of the beta-globin locus control region." Proc Natl Acad Sci U S A **91**(21): 9926-9930.

Motohashi, H., T. O'Connor, F. Katsuoka, J. D. Engel and M. Yamamoto (2002). "Integration and diversity of the regulatory network composed of Maf and CNC families of transcription factors." Gene **294**(1-2): 1-12.

Motterlini, R., R. Foresti, M. Intaglietta and R. M. Winslow (1996). "NO-mediated activation of heme oxygenase: endogenous cytoprotection against oxidative stress to endothelium." Am J Physiol **270**(1 Pt 2): H107-114.

Nakamura, K., A. J. Kimple, D. P. Siderovski and G. L. Johnson (2010). "PB1 domain interaction of p62/sequestosome 1 and MEKK3 regulates NF-kappaB activation." J Biol Chem **285**(3): 2077-2089.

Nakamura, Y., T. Kumagai, C. Yoshida, Y. Naito, M. Miyamoto, H. Ohigashi, T. Osawa and K. Uchida (2003). "Pivotal role of electrophilicity in glutathione S-transferase induction by tert-butylhydroquinone." Biochemistry **42**(14): 4300-4309.

Natsch, A. and R. Emter (2008). "Skin sensitizers induce antioxidant response element dependent genes: application to the in vitro testing of the sensitization potential of chemicals." Toxicol Sci **102**(1): 110-119.

Nguyen, P. M., M. S. Park, M. Chow, J. H. Chang, L. Wrischnik and W. K. Chan (2010). "Benzo[a]pyrene increases the Nrf2 content by downregulating the Keap1 message." Toxicol Sci **116**(2): 549-561.

Nguyen, T., H. C. Huang and C. B. Pickett (2000). "Transcriptional regulation of the antioxidant response element. Activation by Nrf2 and repression by MafK." J Biol Chem **275**(20): 15466-15473.

Nguyen, T., P. J. Sherratt, H. C. Huang, C. S. Yang and C. B. Pickett (2003). "Increased protein stability as a mechanism that enhances Nrf2-mediated transcriptional activation of the antioxidant response element. Degradation of Nrf2 by the 26 S proteasome." J Biol Chem **278**(7): 4536-4541.

Nioi, P., M. McMahon, K. Itoh, M. Yamamoto and J. D. Hayes (2003). "Identification of a novel Nrf2-regulated antioxidant response element (ARE) in the mouse NAD(P)H:quinone oxidoreductase 1 gene: reassessment of the ARE consensus sequence." Biochem J **374**(Pt 2): 337-348.

Nioi, P. and T. Nguyen (2007). "A mutation of Keap1 found in breast cancer impairs its ability to repress Nrf2 activity." Biochem Biophys Res Commun **362**(4): 816-821.

Nioi, P., T. Nguyen, P. J. Sherratt and C. B. Pickett (2005). "The carboxy-terminal Neh3 domain of Nrf2 is required for transcriptional activation." Mol Cell Biol **25**(24): 10895-10906.

Nishinaka, T. and C. Yabe-Nishimura (2005). "Transcription factor Nrf2 regulates promoter activity of mouse aldose reductase (AKR1B3) gene." J Pharmacol Sci **97**(1): 43-51.

Niture, S. K., A. K. Jain and A. K. Jaiswal (2009). "Antioxidant-induced modification of INrf2 cysteine 151 and PKC-delta-mediated phosphorylation of Nrf2 serine 40 are both required for stabilization and nuclear translocation of Nrf2 and increased drug resistance." J Cell Sci **122**(Pt 24): 4452-4464.

Niwayama, S., S. Kurono and H. Matsumoto (2001). "Synthesis of d-labeled N-alkylmaleimides and application to quantitative peptide analysis by isotope differential mass spectrometry." Bioorg Med Chem Lett **11**(17): 2257-2261.

Nouhi, Z., G. Chevillard, A. Derjuga and V. Blank (2007). "Endoplasmic reticulum association and N-linked glycosylation of the human Nrf3 transcription factor." FEBS Lett **581**(28): 5401-5406.

Novina, C. D. and P. A. Sharp (2004). "The RNAi revolution." Nature **430**(6996): 161-164.

Numazawa, S., M. Ishikawa, A. Yoshida, S. Tanaka and T. Yoshida (2003). "Atypical protein kinase C mediates activation of NF-E2-related factor 2 in response to oxidative stress." Am J Physiol Cell Physiol **285**(2): C334-342.

Oettl, K. and G. Marsche (2010). "Redox state of human serum albumin in terms of cysteine-34 in health and disease." Methods Enzymol **474**: 181-195.

Ogura, T., K. I. Tong, K. Mio, Y. Maruyama, H. Kurokawa, C. Sato and M. Yamamoto (2010). "Keap1 is a forked-stem dimer structure with two large spheres enclosing the intervening, double glycine repeat, and C-terminal domains." Proc Natl Acad Sci U S A **107**(7): 2842-2847.

Ohtsuji, M., F. Katsuoka, A. Kobayashi, H. Aburatani, J. D. Hayes and M. Yamamoto (2008). "Nrf1 and Nrf2 play distinct roles in activation of antioxidant response element-dependent genes." J Biol Chem **283**(48): 33554-33562.

Okamoto, T., T. Akaike, T. Sawa, Y. Miyamoto, A. van der Vliet and H. Maeda (2001). "Activation of matrix metalloproteinases by peroxynitrite-induced protein S-glutathiolation via disulfide S-oxide formation." J Biol Chem **276**(31): 29596-29602.

Ostapowicz, G., R. J. Fontana, F. V. Schiodt, A. Larson, T. J. Davern, S. H. Han, T. M. McCashland, A. O. Shakil, J. E. Hay, L. Hynan, J. S. Crippin, A. T. Blei, G. Samuel, J. Reisch and W. M. Lee (2002). "Results of a prospective study of acute liver failure at 17 tertiary care centers in the United States." Ann Intern Med **137**(12): 947-954.

Ottani, A., S. Leone, M. Sandrini, A. Ferrari and A. Bertolini (2006). "The analgesic activity of paracetamol is prevented by the blockade of cannabinoid CB1 receptors." Eur J Pharmacol **531**(1-3): 280-281.

Padmanabhan, B., K. I. Tong, T. Ohta, Y. Nakamura, M. Scharlock, M. Ohtsuji, M. I. Kang, A. Kobayashi, S. Yokoyama and M. Yamamoto (2006). "Structural basis for defects of Keap1 activity provoked by its point mutations in lung cancer." Mol Cell **21**(5): 689-700.

Pahl, H. L. (1999). "Activators and target genes of Rel/NF-kappaB transcription factors." Oncogene **18**(49): 6853-6866.

Papaiahgari, S., Q. Zhang, S. R. Kleeberger, H. Y. Cho and S. P. Reddy (2006). "Hyperoxia stimulates an Nrf2-ARE transcriptional response via ROS-EGFR-PI3K-Akt/ERK MAP kinase signaling in pulmonary epithelial cells." Antioxid Redox Signal **8**(1-2): 43-52.

Park, B. K., N. R. Kitteringham, J. L. Maggs, M. Pirmohamed and D. P. Williams (2005a). "The role of metabolic activation in drug-induced hepatotoxicity." Annu Rev Pharmacol Toxicol **45**: 177-202.

Park, B. K., M. Pirmohamed and N. R. Kitteringham (1995). "The role of cytochrome P450 enzymes in hepatic and extrahepatic human drug toxicity." Pharmacol Ther **68**(3): 385-424.

Park, B. K., M. Pirmohamed and N. R. Kitteringham (1998). "Role of drug disposition in drug hypersensitivity: a chemical, molecular, and clinical perspective." Chem Res Toxicol **11**(9): 969-988.

Park, K., D. P. Williams, D. J. Naisbitt, N. R. Kitteringham and M. Pirmohamed (2005b). "Investigation of toxic metabolites during drug development." Toxicol Appl Pharmacol **207**(2 Suppl): 425-434.

Paulsen, C. E. and K. S. Carroll (2010). "Orchestrating redox signaling networks through regulatory cysteine switches." ACS Chem Biol **5**(1): 47-62.

Pepe, A. E., Q. Xiao, A. Zampetaki, Z. Zhang, A. Kobayashi, Y. Hu and Q. Xu (2010). "Crucial role of nrf3 in smooth muscle cell differentiation from stem cells." Circ Res **106**(5): 870-879.

Perkins, N. D. (2006). "Post-translational modifications regulating the activity and function of the nuclear factor kappa B pathway." Oncogene **25**(51): 6717-6730.

Perkins, N. D. (2007). "Integrating cell-signalling pathways with NF-kappaB and IKK function." Nat Rev Mol Cell Biol **8**(1): 49-62.

Pham, C. G., C. Bubici, F. Zazzeroni, S. Papa, J. Jones, K. Alvarez, S. Jayawardena, E. De Smaele, R. Cong, C. Beaumont, F. M. Torti, S. V. Torti and G. Franzoso (2004). "Ferritin heavy chain upregulation by NF-kappaB inhibits TNFalpha-induced apoptosis by suppressing reactive oxygen species." Cell **119**(4): 529-542.

Pi, J., Y. Bai, J. M. Reece, J. Williams, D. Liu, M. L. Freeman, W. E. Fahl, D. Shugar, J. Liu, W. Qu, S. Collins and M. P. Waalkes (2007). "Molecular mechanism of human Nrf2 activation and degradation: role of sequential phosphorylation by protein kinase CK2." Free Radic Biol Med **42**(12): 1797-1806.

Pineda-Molina, E. and S. Lamas (2001). "Nitric oxide as a regulator of gene expression: studies with the transcription factor proteins cJun and p50." Biofactors **15**(2-4): 113-115.

Pirkkala, L., P. Nykanen and L. Sistonen (2001). "Roles of the heat shock transcription factors in regulation of the heat shock response and beyond." FASEB J **15**(7): 1118-1131.

Pirmohamed, M., A. M. Breckenridge, N. R. Kitteringham and B. K. Park (1998). "Adverse drug reactions." BMJ **316**(7140): 1295-1298.

Pirmohamed, M., S. James, S. Meakin, C. Green, A. K. Scott, T. J. Walley, K. Farrar, B. K. Park and A. M. Breckenridge (2004). "Adverse drug reactions as cause of admission to hospital: prospective analysis of 18 820 patients." BMJ **329**(7456): 15-19.

Potter, D. W. and J. A. Hinson (1986). "Reactions of N-acetyl-p-benzoquinone imine with reduced glutathione, acetaminophen, and NADPH." Mol Pharmacol **30**(1): 33-41.

Potter, W. Z., S. S. Thorgeirsson, D. J. Jollow and J. R. Mitchell (1974). "Acetaminophen-induced hepatic necrosis. V. Correlation of hepatic necrosis, covalent binding and glutathione depletion in hamsters." Pharmacology **12**(3): 129-143.

Preall, J. B. and E. J. Sontheimer (2005). "RNAi: RISC gets loaded." Cell **123**(4): 543-545.

Prestera, T., W. D. Holtzclaw, Y. Zhang and P. Talalay (1993a). "Chemical and molecular regulation of enzymes that detoxify carcinogens." Proc Natl Acad Sci U S A **90**(7): 2965-2969.

Prestera, T., P. Talalay, J. Alam, Y. I. Ahn, P. J. Lee and A. M. Choi (1995). "Parallel induction of heme oxygenase-1 and chemoprotective phase 2 enzymes by electrophiles and antioxidants: regulation by upstream antioxidant-responsive elements (ARE)." Mol Med **1**(7): 827-837.

Prestera, T., Y. Zhang, S. R. Spencer, C. A. Wilczak and P. Talalay (1993b). "The electrophile counterattack response: protection against neoplasia and toxicity." Adv Enzyme Regul **33**: 281-296.

Primiano, T., T. R. Sutter and T. W. Kensler (1997). "Redox regulation of genes that protect against carcinogens." Comp Biochem Physiol B Biochem Mol Biol **118**(3): 487-497.

Qanungo, S., D. W. Starke, H. V. Pai, J. J. Mieyal and A. L. Nieminen (2007). "Glutathione supplementation potentiates hypoxic apoptosis by S-glutathionylation of p65-NFkappaB." J Biol Chem **282**(25): 18427-18436.

Rachakonda, G., Y. Xiong, K. R. Sekhar, S. L. Stamer, D. C. Liebler and M. L. Freeman (2008). "Covalent modification at Cys151 dissociates the electrophile sensor Keap1 from the ubiquitin ligase CUL3." Chem Res Toxicol **21**(3): 705-710.

Rahman, I. and W. MacNee (2000). "Regulation of redox glutathione levels and gene transcription in lung inflammation: therapeutic approaches." Free Radic Biol Med **28**(9): 1405-1420.

Ramos-Gomez, M., M. K. Kwak, P. M. Dolan, K. Itoh, M. Yamamoto, P. Talalay and T. W. Kensler (2001). "Sensitivity to carcinogenesis is increased and chemoprotective efficacy of enzyme inducers is lost in nrf2 transcription factor-deficient mice." Proc Natl Acad Sci U S A **98**(6): 3410-3415.

Randle, L. E., C. E. Goldring, C. A. Benson, P. N. Metcalfe, N. R. Kitteringham, B. K. Park and D. P. Williams (2008). "Investigation of the effect of a panel of model hepatotoxins on the Nrf2-Keap1 defence response pathway in CD-1 mice." Toxicology **243**(3): 249-260.

Raucy, J. L., J. M. Lasker, C. S. Lieber and M. Black (1989). "Acetaminophen activation by human liver cytochromes P450IIE1 and P450IA2." Arch Biochem Biophys **271**(2): 270-283.

Recknagel, R. O., E. A. Glende, Jr., J. A. Dolak and R. L. Waller (1989). "Mechanisms of carbon tetrachloride toxicity." Pharmacol Ther **43**(1): 139-154.

Reisman, S. A., I. L. Csanaky, L. M. Aleksunes and C. D. Klaassen (2009). "Altered disposition of acetaminophen in Nrf2-null and Keap1-knockdown mice." Toxicol Sci **109**(1): 31-40.

Reynaert, N. L., A. van der Vliet, A. S. Guala, T. McGovern, M. Hristova, C. Pantano, N. H. Heintz, J. Heim, Y. S. Ho, D. E. Matthews, E. F. Wouters and Y. M. Janssen-Heininger (2006). "Dynamic redox control of NF-kappaB through glutaredoxin-regulated S-glutathionylation of inhibitory kappaB kinase beta." Proc Natl Acad Sci U S A **103**(35): 13086-13091.

Roberts, D. W., N. R. Pumford, D. W. Potter, R. W. Benson and J. A. Hinson (1987). "A sensitive immunochemical assay for acetaminophen-protein adducts." J Pharmacol Exp Ther **241**(2): 527-533.

Rogers, L. K., B. L. Leinweber and C. V. Smith (2006). "Detection of reversible protein thiol modifications in tissues." Anal Biochem **358**(2): 171-184.

Rossi, A., P. Kapahi, G. Natoli, T. Takahashi, Y. Chen, M. Karin and M. G. Santoro (2000). "Anti-inflammatory cyclopentenone prostaglandins are direct inhibitors of IkappaB kinase." Nature **403**(6765): 103-108.

Rudolph, T. K. and B. A. Freeman (2009). "Transduction of redox signaling by electrophile-protein reactions." Sci Signal **2**(90): re7.

Rushmore, T. H., M. R. Morton and C. B. Pickett (1991). "The antioxidant responsive element. Activation by oxidative stress and identification of the DNA consensus sequence required for functional activity." J Biol Chem **266**(18): 11632-11639.

Sakurai, T., M. Kanayama, T. Shibata, K. Itoh, A. Kobayashi, M. Yamamoto and K. Uchida (2006). "Ebselen, a seleno-organic antioxidant, as an electrophile." Chem Res Toxicol **19**(9): 1196-1204.

Salazar, H., I. Llorente, A. Jara-Oseguera, R. Garcia-Villegas, M. Munari, S. E. Gordon, L. D. Islas and T. Rosenbaum (2008). "A single N-terminal cysteine in TRPV1 determines activation by pungent compounds from onion and garlic." Nat Neurosci **11**(3): 255-261.

Salazar, M., A. I. Rojo, D. Velasco, R. M. de Sagarra and A. Cuadrado (2006). "Glycogen synthase kinase-3beta inhibits the xenobiotic and antioxidant cell response by direct phosphorylation and nuclear exclusion of the transcription factor Nrf2." J Biol Chem **281**(21): 14841-14851.

Salminen, W. F., Jr., R. Voellmy and S. M. Roberts (1996). "Induction of hsp 70 in HepG2 cells in response to hepatotoxicants." Toxicol Appl Pharmacol **141**(1): 117-123.

Salminen, W. F., Jr., R. Voellmy and S. M. Roberts (1997a). "Differential heat shock protein induction by acetaminophen and a nonhepatotoxic regioisomer, 3'-hydroxyacetanilide, in mouse liver." J Pharmacol Exp Ther **282**(3): 1533-1540.

Salminen, W. F., Jr., R. Voellmy and S. M. Roberts (1997b). "Protection against hepatotoxicity by a single dose of amphetamine: the potential role of heat shock protein induction." Toxicol Appl Pharmacol **147**(2): 247-258.

Sankaranarayanan, K. and A. K. Jaiswal (2004). "Nrf3 negatively regulates antioxidant-response element-mediated expression and antioxidant induction of NAD(P)H:quinone oxidoreductase1 gene." J Biol Chem **279**(49): 50810-50817.

Scherer, D. C., J. A. Brockman, Z. Chen, T. Maniatis and D. W. Ballard (1995). "Signal-induced degradation of I kappa B alpha requires site-specific ubiquitination." Proc Natl Acad Sci U S A **92**(24): 11259-11263.

Schoonbroodt, S., V. Ferreira, M. Best-Belpomme, J. R. Boelaert, S. Legrand-Poels, M. Korner and J. Piette (2000). "Crucial role of the amino-terminal tyrosine residue 42 and the carboxyl-terminal PEST domain of I kappa B alpha in NF-kappa B activation by an oxidative stress." J Immunol **164**(8): 4292-4300.

Sen, R. and D. Baltimore (1986). "Multiple nuclear factors interact with the immunoglobulin enhancer sequences." Cell **46**(5): 705-716.

Sewer, M. B., D. R. Koop and E. T. Morgan (1996). "Endotoxemia in rats is associated with induction of the P4504A subfamily and suppression of several other forms of cytochrome P450." Drug Metab Dispos **24**(4): 401-407.

Shelby, M. K. and C. D. Klaassen (2006). "Induction of rat UDP-glucuronosyltransferases in liver and duodenum by microsomal enzyme inducers that activate various transcriptional pathways." Drug Metab Dispos **34**(10): 1772-1778.

Shertzer, H. G., V. Vasiliou, R. M. Liu, M. W. Tabor and D. W. Nebert (1995). "Enzyme induction by L-buthionine (S,R)-sulfoximine in cultured mouse hepatoma cells." Chem Res Toxicol **8**(3): 431-436.

Shibata, T., A. Kokubu, M. Gotoh, H. Ojima, T. Ohta, M. Yamamoto and S. Hirohashi (2008). "Genetic alteration of Keap1 confers constitutive Nrf2 activation and resistance to chemotherapy in gallbladder cancer." Gastroenterology **135**(4): 1358-1368, 1368 e1351-1354.

Shin, N. Y., Q. Liu, S. L. Stamer and D. C. Liebler (2007). "Protein targets of reactive electrophiles in human liver microsomes." Chem Res Toxicol **20**(6): 859-867.

Singh, A., S. Boldin-Adamsky, R. K. Thimmulappa, S. K. Rath, H. Ashush, J. Coulter, A. Blackford, S. N. Goodman, F. Bunz, W. H. Watson, E. Gabrielson, E. Feinstein and S. Biswal (2008). "RNAi-mediated silencing of nuclear factor erythroid-2-related factor 2 gene expression in non-small cell lung cancer inhibits tumor growth and increases efficacy of chemotherapy." Cancer Res **68**(19): 7975-7984.

Singh, A., V. Misra, R. K. Thimmulappa, H. Lee, S. Ames, M. O. Hoque, J. G. Herman, S. B. Baylin, D. Sidransky, E. Gabrielson, M. V. Brock and S. Biswal (2006). "Dysfunctional KEAP1-NRF2 interaction in non-small-cell lung cancer." PLoS Med **3**(10): e420.

Snyder, G. H., M. J. Cennerazzo, A. J. Karalis and D. Field (1981). "Electrostatic influence of local cysteine environments on disulfide exchange kinetics." Biochemistry **20**(23): 6509-6519.

Speers, A. E. and B. F. Cravatt (2004). "Profiling enzyme activities in vivo using click chemistry methods." Chem Biol **11**(4): 535-546.

Speers, A. E. and B. F. Cravatt (2005). "A tandem orthogonal proteolysis strategy for high-content chemical proteomics." J Am Chem Soc **127**(28): 10018-10019.

Spickett, C. M. and A. R. Pitt (2010). "Protein oxidation: role in signalling and detection by mass spectrometry." Amino Acids.

Stehlik, C., R. de Martin, I. Kumabashiri, J. A. Schmid, B. R. Binder and J. Lipp (1998). "Nuclear factor (NF)-kappaB-regulated X-chromosome-linked iap gene expression protects endothelial cells from tumor necrosis factor alpha-induced apoptosis." J Exp Med **188**(1): 211-216.

Stewart, D., E. Killeen, R. Naquin, S. Alam and J. Alam (2003). "Degradation of transcription factor Nrf2 via the ubiquitin-proteasome pathway and stabilization by cadmium." J Biol Chem **278**(4): 2396-2402.

Straus, D. S., G. Pascual, M. Li, J. S. Welch, M. Ricote, C. H. Hsiang, L. L. Sengchanthalangsy, G. Ghosh and C. K. Glass (2000). "15-deoxy-delta 12,14-prostaglandin J2 inhibits multiple steps in the NF-kappa B signaling pathway." Proc Natl Acad Sci U S A **97**(9): 4844-4849.

Sumioka, I., T. Matsura, M. Kai and K. Yamada (2004). "Potential roles of hepatic heat shock protein 25 and 70i in protection of mice against acetaminophen-induced liver injury." Life Sci **74**(20): 2551-2561.

Takagi, T., Y. Naito, H. Okada, T. Ishii, K. Mizushima, S. Akagiri, S. Adachi, O. Handa, S. Kokura, H. Ichikawa, K. Itoh, M. Yamamoto, H. Matsui and T. Yoshikawa (2009). "Lansoprazole, a proton pump inhibitor, mediates anti-inflammatory effect in gastric mucosal cells through the induction of heme oxygenase-1 via activation of NF-E2-related factor 2 and oxidation of kelch-like ECH-associating protein 1." J Pharmacol Exp Ther **331**(1): 255-264.

Talalay, P., J. W. Fahey, W. D. Holtzclaw, T. Prestera and Y. Zhang (1995). "Chemoprotection against cancer by phase 2 enzyme induction." Toxicol Lett **82-83**: 173-179.

Tanaka, H., I. Matsumura, S. Ezoe, Y. Satoh, T. Sakamaki, C. Albanese, T. Machii, R. G. Pestell and Y. Kanakura (2002). "E2F1 and c-Myc potentiate apoptosis through inhibition of NF-kappaB activity that facilitates MnSOD-mediated ROS elimination." Mol Cell **9**(5): 1017-1029.

Tergaonkar, V., M. Pando, O. Vafa, G. Wahl and I. Verma (2002). "p53 stabilization is decreased upon NFkappaB activation: a role for NFkappaB in acquisition of resistance to chemotherapy." Cancer Cell **1**(5): 493-503.

Theodore, M., Y. Kawai, J. Yang, Y. Kleshchenko, S. P. Reddy, F. Villalta and I. J. Arinze (2008). "Multiple nuclear localization signals function in the nuclear import of the transcription factor Nrf2." J Biol Chem **283**(14): 8984-8994.

Thimmulappa, R. K., K. H. Mai, S. Srisuma, T. W. Kensler, M. Yamamoto and S. Biswal (2002). "Identification of Nrf2-regulated genes induced by the chemopreventive agent sulforaphane by oligonucleotide microarray." Cancer Res **62**(18): 5196-5203.

Thummel, K. E., C. A. Lee, K. L. Kunze, S. D. Nelson and J. T. Slattery (1993). "Oxidation of acetaminophen to N-acetyl-p-aminobenzoquinone imine by human CYP3A4." Biochem Pharmacol **45**(8): 1563-1569.

Tian, Y., S. Ke, M. S. Denison, A. B. Rabson and M. A. Gallo (1999). "Ah receptor and NF-kappaB interactions, a potential mechanism for dioxin toxicity." J Biol Chem **274**(1): 510-515.

Timbrell, J. A. and I. ebrary (2000). Principles of biochemical toxicology. London, Taylor & Francis.

Tolson, J. K., D. J. Dix, R. W. Voellmy and S. M. Roberts (2006). "Increased hepatotoxicity of acetaminophen in Hsp70i knockout mice." Toxicol Appl Pharmacol **210**(1-2): 157-162.

Tong, K. I., Y. Katoh, H. Kusunoki, K. Itoh, T. Tanaka and M. Yamamoto (2006a). "Keap1 recruits Neh2 through binding to ETGE and DLG motifs: characterization of the two-site molecular recognition model." Mol Cell Biol **26**(8): 2887-2900.

Tong, K. I., A. Kobayashi, F. Katsuoka and M. Yamamoto (2006b). "Two-site substrate recognition model for the Keap1-Nrf2 system: a hinge and latch mechanism." Biol Chem **387**(10-11): 1311-1320.

Tong, K. I., B. Padmanabhan, A. Kobayashi, C. Shang, Y. Hirotsu, S. Yokoyama and M. Yamamoto (2007). "Different electrostatic potentials define ETGE and DLG motifs as hinge and latch in oxidative stress response." Mol Cell Biol **27**(21): 7511-7521.

Vandeputte, C., I. Guizon, I. Genestie-Denis, B. Vannier and G. Lorenzon (1994). "A microtiter plate assay for total glutathione and glutathione disulfide contents in cultured/isolated cells: performance study of a new miniaturized protocol." Cell Biol Toxicol **10**(5-6): 415-421.

Velu, C. S., S. K. Niture, C. E. Doneanu, N. Pattabiraman and K. S. Srivenugopal (2007). "Human p53 is inhibited by glutathionylation of cysteines present in the proximal DNA-binding domain during oxidative stress." Biochemistry **46**(26): 7765-7780.

Venugopal, R. and A. K. Jaiswal (1996). "Nrf1 and Nrf2 positively and c-Fos and Fra1 negatively regulate the human antioxidant response element-mediated expression of NAD(P)H:quinone oxidoreductase1 gene." Proc Natl Acad Sci U S A **93**(25): 14960-14965.

Vila, A., K. A. Tallman, A. T. Jacobs, D. C. Liebler, N. A. Porter and L. J. Marnett (2008). "Identification of protein targets of 4-hydroxynonenal using click chemistry for ex vivo biotinylation of azido and alkynyl derivatives." Chem Res Toxicol **21**(2): 432-444.

Wakabayashi, N., A. T. Dinkova-Kostova, W. D. Holtzclaw, M. I. Kang, A. Kobayashi, M. Yamamoto, T. W. Kensler and P. Talalay (2004). "Protection against electrophile and oxidant stress by induction of the phase 2 response: fate of cysteines of the Keap1 sensor modified by inducers." Proc Natl Acad Sci U S A **101**(7): 2040-2045.

Wang, C. Y., M. W. Mayo, R. G. Korneluk, D. V. Goeddel and A. S. Baldwin, Jr. (1998). "NF-kappaB antiapoptosis: induction of TRAF1 and TRAF2 and c-IAP1 and c-IAP2 to suppress caspase-8 activation." Science **281**(5383): 1680-1683.

Wang, W. and J. Y. Chan (2006). "Nrf1 is targeted to the endoplasmic reticulum membrane by an N-terminal transmembrane domain. Inhibition of nuclear translocation and transacting function." J Biol Chem **281**(28): 19676-19687.

Wang, W., A. M. Kwok and J. Y. Chan (2007). "The p65 isoform of Nrf1 is a dominant negative inhibitor of ARE-mediated transcription." J Biol Chem **282**(34): 24670-24678.

Wang, X. J., Z. Sun, N. F. Villeneuve, S. Zhang, F. Zhao, Y. Li, W. Chen, X. Yi, W. Zheng, G. T. Wondrak, P. K. Wong and D. D. Zhang (2008). "Nrf2 enhances resistance of cancer cells to chemotherapeutic drugs, the dark side of Nrf2." Carcinogenesis **29**(6): 1235-1243.

Wang, Y., S. Vivekananda, L. Men and Q. Zhang (2004). "Fragmentation of protonated ions of peptides containing cysteine, cysteine sulfinic acid, and cysteine sulfonic acid." J Am Soc Mass Spectrom **15**(5): 697-702.

Weerapana, E., G. M. Simon and B. F. Cravatt (2008). "Disparate proteome reactivity profiles of carbon electrophiles." Nat Chem Biol **4**(7): 405-407.

Wester, K., A. K. Jonsson, O. Spigset, H. Druid and S. Hagg (2008). "Incidence of fatal adverse drug reactions: a population based study." Br J Clin Pharmacol **65**(4): 573-579.

Whitesell, L. and S. Lindquist (2009). "Inhibiting the transcription factor HSF1 as an anticancer strategy." Expert Opin Ther Targets **13**(4): 469-478.

Williams, D. P., D. J. Antoine, P. J. Butler, R. Jones, L. Randle, A. Payne, M. Howard, I. Gardner, J. Blagg and B. K. Park (2007). "The metabolism and toxicity of furosemide in the Wistar rat and CD-1 mouse: a chemical and biochemical definition of the toxicophore." J Pharmacol Exp Ther **322**(3): 1208-1220.

Wooten, M. W., T. Geetha, M. L. Seibenhener, J. R. Babu, M. T. Diaz-Meco and J. Moscat (2005). "The p62 scaffold regulates nerve growth factor-induced NF-kappaB activation by influencing TRAF6 polyubiquitination." J Biol Chem **280**(42): 35625-35629.

Wrighton, S. A., M. VandenBranden and B. J. Ring (1996). "The human drug metabolizing cytochromes P450." J Pharmacokinet Biopharm **24**(5): 461-473.

Xu, C., C. Y. Li and A. N. Kong (2005). "Induction of phase I, II and III drug metabolism/transport by xenobiotics." Arch Pharm Res **28**(3): 249-268.

Xu, S., J. Weerachayaphorn, S. Y. Cai, C. J. Soroka and J. L. Boyer (2010). "Aryl hydrocarbon receptor and NF-E2-related factor 2 are key regulators of human MRP4 expression." Am J Physiol Gastrointest Liver Physiol **299**(1): G126-135.

Xue, F. and L. Cooley (1993). "kelch encodes a component of intercellular bridges in Drosophila egg chambers." Cell **72**(5): 681-693.

Yamamoto, N., H. Sawada, Y. Izumi, T. Kume, H. Katsuki, S. Shimohama and A. Akaike (2007). "Proteasome inhibition induces glutathione synthesis and protects cells from oxidative stress: relevance to Parkinson disease." J Biol Chem **282**(7): 4364-4372.

Yamamoto, T., T. Suzuki, A. Kobayashi, J. Wakabayashi, J. Maher, H. Motohashi and M. Yamamoto (2008). "Physiological significance of reactive cysteine residues of Keap1 in determining Nrf2 activity." Mol Cell Biol **28**(8): 2758-2770.

Yamamoto, T., K. Yoh, A. Kobayashi, Y. Ishii, S. Kure, A. Koyama, T. Sakamoto, K. Sekizawa, H. Motohashi and M. Yamamoto (2004). "Identification of polymorphisms in the promoter region of the human NRF2 gene." Biochem Biophys Res Commun **321**(1): 72-79.

Yang, H., N. Magilnick, C. Lee, D. Kalmaz, X. Ou, J. Y. Chan and S. C. Lu (2005a). "Nrf1 and Nrf2 regulate rat glutamate-cysteine ligase catalytic subunit transcription indirectly via NF-kappaB and AP-1." Mol Cell Biol **25**(14): 5933-5946.

Yang, H., N. Magilnick, X. Ou and S. C. Lu (2005b). "Tumour necrosis factor alpha induces co-ordinated activation of rat GSH synthetic enzymes via nuclear factor kappaB and activator protein-1." Biochem J **391**(Pt 2): 399-408.

Yore, M. M., K. T. Liby, T. Honda, G. W. Gribble and M. B. Sporn (2006). "The synthetic triterpenoid 1-[2-cyano-3,12-dioxooleana-1,9(11)-dien-28-oyl]imidazole blocks nuclear factor-kappaB activation through direct inhibition of IkappaB kinase beta." Mol Cancer Ther **5**(12): 3232-3239.

Yueh, M. F. and R. H. Tukey (2007). "Nrf2-Keap1 signaling pathway regulates human UGT1A1 expression in vitro and in transgenic UGT1 mice." J Biol Chem **282**(12): 8749-8758.

Yusuf, M. A., T. Chuang, G. J. Bhat and K. S. Srivenugopal (2010). "Cys-141 glutathionylation of human p53: Studies using specific polyclonal antibodies in cancer samples and cell lines." Free Radic Biol Med **49**(5): 908-917.

Zabet-Moghaddam, M., T. Kawamura, E. Yatagai and S. Niwayama (2008). "Electrospray ionization mass spectroscopic analysis of peptides modified with N-ethylmaleimide or iodoacetanilide." Bioorg Med Chem Lett **18**(17): 4891-4895.

Zangger, K., G. Oz, J. D. Otvos and I. M. Armitage (1999). "Three-dimensional solution structure of mouse [Cd7]-metallothionein-1 by homonuclear and heteronuclear NMR spectroscopy." Protein Sci **8**(12): 2630-2638.

Zatelli, M. C., D. Mole, F. Tagliati, M. Minoia, M. R. Ambrosio and E. degli Uberti (2009). "Cyclo-oxygenase 2 modulates chemoresistance in breast cancer cells involving NF-kappaB." Cell Oncol **31**(6): 457-465.

Zhang, D. D. and M. Hannink (2003). "Distinct cysteine residues in Keap1 are required for Keap1-dependent ubiquitination of Nrf2 and for stabilization of Nrf2 by chemopreventive agents and oxidative stress." Mol Cell Biol **23**(22): 8137-8151.

Zhang, D. D., S. C. Lo, J. V. Cross, D. J. Templeton and M. Hannink (2004). "Keap1 is a redox-regulated substrate adaptor protein for a Cul3-dependent ubiquitin ligase complex." Mol Cell Biol **24**(24): 10941-10953.

Zhang, J., T. Hosoya, A. Maruyama, K. Nishikawa, J. M. Maher, T. Ohta, H. Motohashi, A. Fukamizu, S. Shibahara, K. Itoh and M. Yamamoto (2007a). "Nrf2 Neh5 domain is differentially utilized in the transactivation of cytoprotective genes." Biochem J **404**(3): 459-466.

Zhang, X., X. Zhao and Z. Ma (2010). "PYDDT, a novel phase 2 enzymes inducer, activates Keap1-Nrf2 pathway via depleting the cellular level of glutathione." Toxicol Lett **199**(1): 93-101.

Zhang, Y., D. H. Crouch, M. Yamamoto and J. D. Hayes (2006). "Negative regulation of the Nrf1 transcription factor by its N-terminal domain is independent of Keap1: Nrf1, but not Nrf2, is targeted to the endoplasmic reticulum." Biochem J **399**(3): 373-385.

Zhang, Y., A. Kobayashi, M. Yamamoto and J. D. Hayes (2009a). "The Nrf3 transcription factor is a membrane-bound glycoprotein targeted to the endoplasmic reticulum through its N-terminal homology box 1 sequence." J Biol Chem **284**(5): 3195-3210.

Zhang, Y., J. M. Lucocq and J. D. Hayes (2009b). "The Nrf1 CNC/bZIP protein is a nuclear envelope-bound transcription factor that is activated by t-butyl hydroquinone but not by endoplasmic reticulum stressors." Biochem J **418**(2): 293-310.

Zhang, Y., J. M. Lucocq, M. Yamamoto and J. D. Hayes (2007b). "The NHB1 (N-terminal homology box 1) sequence in transcription factor Nrf1 is required to anchor it to the endoplasmic reticulum and also to enable its asparagine-glycosylation." Biochem J **408**(2): 161-172.

Zhao, R., Y. Hou, P. Xue, C. G. Woods, J. Fu, B. Feng, D. Guan, G. Sun, J. Y. Chan, M. P. Waalkes, M. E. Andersen and J. Pi (2010). "Long Isoforms of NRF1 Contribute to Arsenic-induced Antioxidant Response in Human Keratinocytes." Environ Health Perspect.

Zhong, H., M. J. May, E. Jimi and S. Ghosh (2002). "The phosphorylation status of nuclear NF-kappa B determines its association with CBP/p300 or HDAC-1." Mol Cell **9**(3): 625-636.

Zhou, C., M. M. Tabb, E. L. Nelson, F. Grun, S. Verma, A. Sadatrafiei, M. Lin, S. Mallick, B. M. Forman, K. E. Thummel and B. Blumberg (2006). "Mutual repression between steroid and xenobiotic receptor and NF-kappaB signaling pathways links xenobiotic metabolism and inflammation." J Clin Invest **116**(8): 2280-2289.

Zhou, S., E. Chan, W. Duan, M. Huang and Y. Z. Chen (2005). "Drug bioactivation, covalent binding to target proteins and toxicity relevance." Drug Metab Rev **37**(1): 41-213.

Zipper, L. M. and R. T. Mulcahy (2002). "The Keap1 BTB/POZ dimerization function is required to sequester Nrf2 in cytoplasm." J Biol Chem **277**(39): 36544-36552.

Zipper, L. M. and R. T. Mulcahy (2003). "Erk activation is required for Nrf2 nuclear localization during pyrrolidine dithiocarbamate induction of glutamate cysteine ligase modulatory gene expression in HepG2 cells." Toxicol Sci **73**(1): 124-134.

Zong, W. X., L. C. Edelstein, C. Chen, J. Bash and C. Gelinas (1999). "The prosurvival Bcl-2 homolog Bfl-1/A1 is a direct transcriptional target of NF-kappaB that blocks TNFalpha-induced apoptosis." Genes Dev **13**(4): 382-387.

Zygmunt, P. M., H. Chuang, P. Movahed, D. Julius and E. D. Hogestatt (2000). "The anandamide transport inhibitor AM404 activates vanilloid receptors." Eur J Pharmacol **396**(1): 39-42.